SPACE SCIENCES LABORATORY

AN INTEGRATED STUDY OF EARTH RESOURCES IN THE STATE OF CALIFORNIA BASED ON ERTS-1 AND SUPPORTING AIRCRAFT DATA

A report of work done by scientists on 5 campuses of the University of California (Davis, Berkeley, Santa Barbara, Los Angeles and Riverside) under NASA Contract No. NAS 5-21827

Progress Report
31 July 1973

UNIVERSITY OF CALIFORNIA

Vol. 2 of 2

TABLE OF CONTENTS

Chapter 5

ANALYSIS OF RIVER MEANDERS FROM ERTS-1 IMAGERY (UN644)

Co-investigator: Gerald Schubert
Contributor: Richard Lingenfelter

Department of Planetary and Space Science, Los Angeles Campus

TABLE OF CONTENTS

5.1 INTRODUCTION

During the period covered by this report we have continued to investigate the possibility that significant information on stream flow rates can be obtained from aerial and satellite imagery of river meander patterns by seeking a correlation between the meander and discharge spectra of rivers. Such a correlation could provide the basis for a simple and inexpensive technique for remote sensing of the water resources of large geographical areas, eliminating the need for much hydrologic recording. The investigation of the nature of the meander and discharge spectra and their interrelationship can also contribute to a more fundamental understanding of the processes of both river meander formation and drainage of large basins.

A large number of correlations which we and others have already made clearly suggest that there is a relationship between meander wavelength and discharge but its quantitative form is not yet clear. We believe that this disagreement may result primarily from the oversimplification inherent in using a single meander wavelength and a single discharge to characterize the river rather than using the complete spectrum of wavelengths and discharges.

The idea of using a spectral analysis of the reach of a river as the basis of a correlation rather than a subjective estimate of an assumed single length scale is a necessary generalization in decribing the connection between a river's meander pattern and its discharge. However, a single discharge can perhaps be correlated with the multiple length scales. Just as there is an essential difficulty in attempting to characterize a meander pattern by a single length scale, there is a fundamental problem in trying to choose the dominant discharge, i.e. that discharge most effective in establishing the system of meanders. With the aid of ERTS-1 imagery we are testing the further generalization of the correlation to include the time-behavior of the discharge in the belief that it may bring an order to the relationship between the total meander pattern and the complete record of the discharge. Hopefully this more general correlation will be sufficiently reliable to quantitatively assess a river's flow rate from a spectrum of its meanders, thus making the knowledge of a region's water resources accessible from aerial or satellite imagery of the area.

As a basis for this study we have developed a fully automated system for obtaining both the discharge and meander wavelength spectra. Discharge spectra (probability of discharge per unit discharge vs. discharge) are constructed from historical records of daily stream discharge. Generation of meander power spectra involves three elements: digitization by photoelectric optical tracking of stream banks on each frame of imagery; collation and matching of successive frames into a single data record for each stream; and a Fourier transform analysis of the data. This system has been developed to facilitate the analysis of the large number of rivers required to assure the statistical reliability of the correlation.

Rivers have been selected on the basis of availability of both historical hydrologic data and aerial or satellite imagery, and on the absence of obvious geologic control of the river meander pattern. The statistical reliability of any correlation between the meander spectrum and the discharge frequency distribution depends upon the study of a large number of rivers whose discharges cover as great a range as possible. Infrared satellite imagery from ERTS-1 as provided by the NASA Data Processing Facility is being used in our study because it shows the best tone contrast between the stream and its surroundings. Historical streamflow data in machine readable format have been obtained from the Water Resources Division of the U.S. Department of the Interior.

From the imagery of a selected river reach, we determine the positions of the curve with respect to a cartesian coordinate system. This description of the river's course is transformed to a (θ,s) representation, where θ measures the angle that the curve makes with a reference direction as a function of distance travelled along the curve s. The (θ,s) description is preferred since the meander pattern of a river may be represented by a multi-valued function of position in a cartesian representation. The meander power spectrum which we calculate is the power spectral density of $\theta(s)$.

5.2 DIGITIZATION

The digitization of river meander patterns from satellite imagery is most accurately and economically accomplished through photoelectric optical scanning. We have developed a program for digitizing river meanders, using commercially available machines employing this technique. An important condition on the digitization procedure is that data points be located at equal increments of distance along the meander curve. This condition follows from the fact that local meander direction, θ, is a function of distance along the meander and the algorithm used for constructing the power spectrum requires that we know this quantity at equal increments of distance.

The fact that ERTS-1 imagery taken on one date is overlapped laterally by that taken at about the same time on the following day is being exploited in our study. Specifically, if the imagery of the river consists of two or more laterally overlapping "frames", the digitization procedure is repeated for each frame. The data for adjacent frames must then be matched to give a continuous digitized record of the meander pattern. We have developed a computer program which finds the appropriate coordinate transformation, i.e. includes both translation and rotation of one frame with respect to the other. This is accomplished by considering a length of river half the length of the overlap region on one frame and effectively sliding this portion of the data along the overlap portion of the adjacent frame, finding that transformation within the overlap region which minimizes the sum of the squares of the distances between matched points. Once the appropriate coordinate transformation is determined all of the data points on the second frame are transformed to the coordinate system of the first frame. The process

is then repeated to match successive frames until the entire record is transformed into a single coordinate system.

5.3 RIVER MEANDER POWER SPECTRA

The digitization and matching procedures described above produce a set of data points (x,y coordinates) which are equally spaced along the course of the river. A power spectral analysis of the river cannot be made directly from the x versus y data since the river may double back upon itself making x a double valued function of y. An equivalent representation of the river, which is single valued and thus amenable to power spectral analysis is its local direction θ, as a function of the distance, s, along the river's course. The power spectral density (deg^2 10^3 foot) for the direction θ is computed using standard techniques for determining the auto-correlation function, smoothing, and taking the Fourier transform.

5.4 DISCHARGE SPECTRA

From historical records of daily river discharge, we have constructed the frequency distributions from the fraction of time the discharge lies within a prescribed interval per unit interval. A remarkable property of most of these discharge frequency distributions is their nearly linear character on log-log plots for values of discharge larger than the mode. The daily discharge data on which each distribution was based extends over the indicated time interval for the particular gauging station identified by number according to the convention adopted by the USGS (1964). The slopes of the linear portions of these distributions vary from river to river and even from station to station on the same river over the range from less than -1 to -5. Flow duration curves have previously been interpreted as representing a random process described, for example, by a log-normal distribution. Our results, however, show that such an interpretation is not appropriate for a large number of rivers, since it is inconsistent with the clearly lineal character of the log-log frequency distribution plots. Instead, we suggest that the distribution for discharges greater than the mode must be essentially deterministic in nature, reflecting the decay phase of the flood hydrograph. We have not found any previous suggestion of a direct relationship between the form of the flow duration curve and the flood hydrograph.

5.5 MEANDER SPECTRA BASED ON ERTS-1 IMAGERY

Using the techniques and imagery already discussed, we have begun constructing meander power spectra of the local river direction as a function of distance along its course. These spectra are plots of power spectral density (deg^2 10^3 ft.) versus wave number (per 10^3 ft.). The range of wave number is limited at the high end (short wavelength) by the interval between data points and at the low end (long wavelength) by the length of the reach Fourier analyzed and the number of degrees of freedom. The maximum wave number is given by the Nyquist

criterion to be $N/2\ell$ where N is the number of data points and ℓ is the length of the reach. The minimum wave number at which spectral information is obtained is $N/2\ell m$ where m is the number of spectral estimates, or alternatively $n/4\ell$ where $n=2N/m$ is the number of degrees of freedom, a measure of the uncertainty in the power spectral density.

Most of the meander spectra which we had previously constructed were rather simple, broad spectra having significant power over a wave number range of approximately one decade. One value of ERTS-1 imagery is to be found in the increased wave number range per "frame" which it provides because of the tremendously broad synoptic view provided by such imagery.

5.6 WORK PERFORMED DURING PERIOD COVERED BY THIS REPORT

ERTS-1 infrared (Band 7) imagery of the Mississippi River obtained on orbits 975 and 989 on October 1 and October 2, respectively, (frames 1070 -- 16070, 16073 and 1071 -- 16113, 16120, 16122, 16125) have been digitized to produce power spectra for a 779 mile reach of the river from 36° 30' N to 30° N. Figures 5.1 and 5.2 show computer plots of the individual digitized frames which have been matched (overlapped) to produce continuous records of the river bank. The fundamental digitization step size is 0.786 thousand feet, but for the purpose of power spectral analysis we have used two larger step sizes to represent the river reach. The spacing between the 524 data points in Figure 5.1 is 7.86 thousand feet while for Figure 5.2 1057 points spaced 3.93 thousand feet apart were used. The river reach has been digitally represented at two different step sizes to determine to what extent the power spectra are dependent on step size.

Spectra determined from these two representations of the river are shown in Figures 5.3 and 5.4, which show the power spectral densities (deg^2 per thousand feet) versus wavelength (thousand feet). Both spectra show a broad peak in power between wavelengths of 50-100 thousand feet which is significantly above the noise level at lower wavelengths. The individual spectra are in close agreement over the significant part of the spectra and differ only slightly in the noise region (wavelengths $\lesssim$ 40 thousand feet). This shows that the spectra do not have a significant dependence on the step size used in the representation.

There is however a variation in power spectral density with position along the river reach as can be seen in Figures 5.3 through 5.7, covering the upper, middle and lower portions of the river. Even so, the maximum power is to be found at wavelengths of 50-100 thousand feet.

The discharge spectrum for this reach of river at station 7/320 (Memphis, Tennessee) based on thirty-seven years of continuous hydrologic recording (1933-1970) is shown in Figure 5.8. This shows a broad peak between between 10^5 and 10^6 c.f.s. with a mode at 2×10^5 c.f.s. and 3.5×10^5 c.f.s. From the modal flow rate to 10^6 c.f.s. the spectrum shows an inverse power law dependence on flow rate with an exponent of

-1.2 (Power Law Time Dependence of River Flood Decay and Its Relationship to Long Term Discharge Frequency Distribution, G. Schubert and R.E. Lingenfelter, submitted to Water Resources Research).

The relationship between the peaks in the meander power spectra and the discharge frequency spectrum for this reach of the Mississippi is consistent with a linear dependence of discharge on the square root of meander wavelength when considered together with similar analyses based on non-ERTS data which we have made of other rivers with smaller wavelengths and lower discharges.

5.7 CONCLUSION

Based on the rivers which we have studied so far we believe that there is significant structure in a meander power spectrum, namely the slopes and magnitudes of the power law segments and the wave numbers at which breaks in these segments occur. It is these characteristic parameters of the meander spectra which we will attempt to correlate with such characteristics of the discharge spectra as the modal discharge and the exponent of the flood recession. Before this can be attempted, however, we must first generate a significantly large number of corresponding meander and discharge spectra on which to base a correlation. This we are in the process of doing.

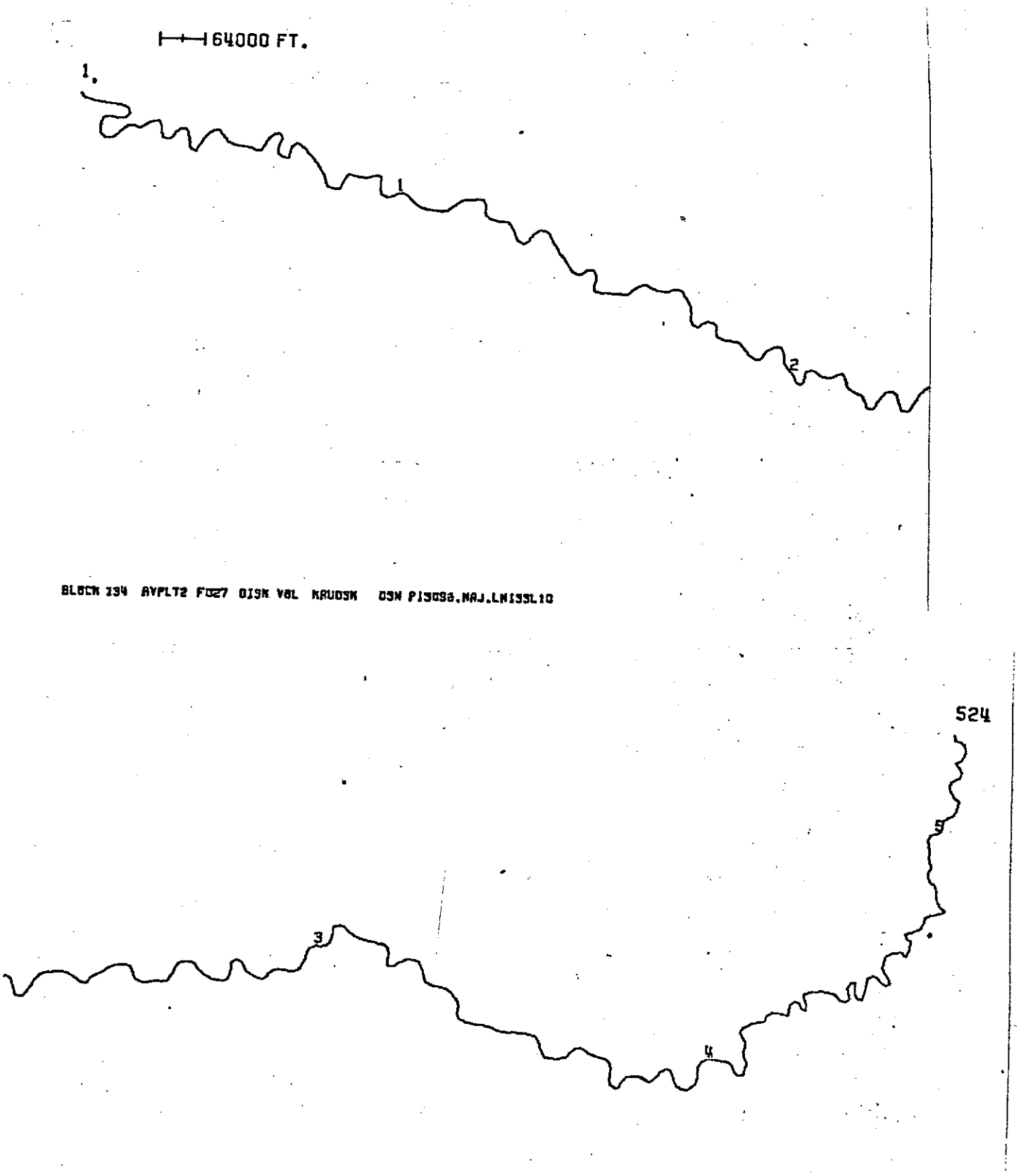

Figure 5.1. Computer plot of individual digitized frames of ERTS-1 Band 7 imagery of our Mississippi River study area obtained on October 1 and 2, 1972. The spacing between the 524 data points used in constructing this plot was 7.86 thousand feet.

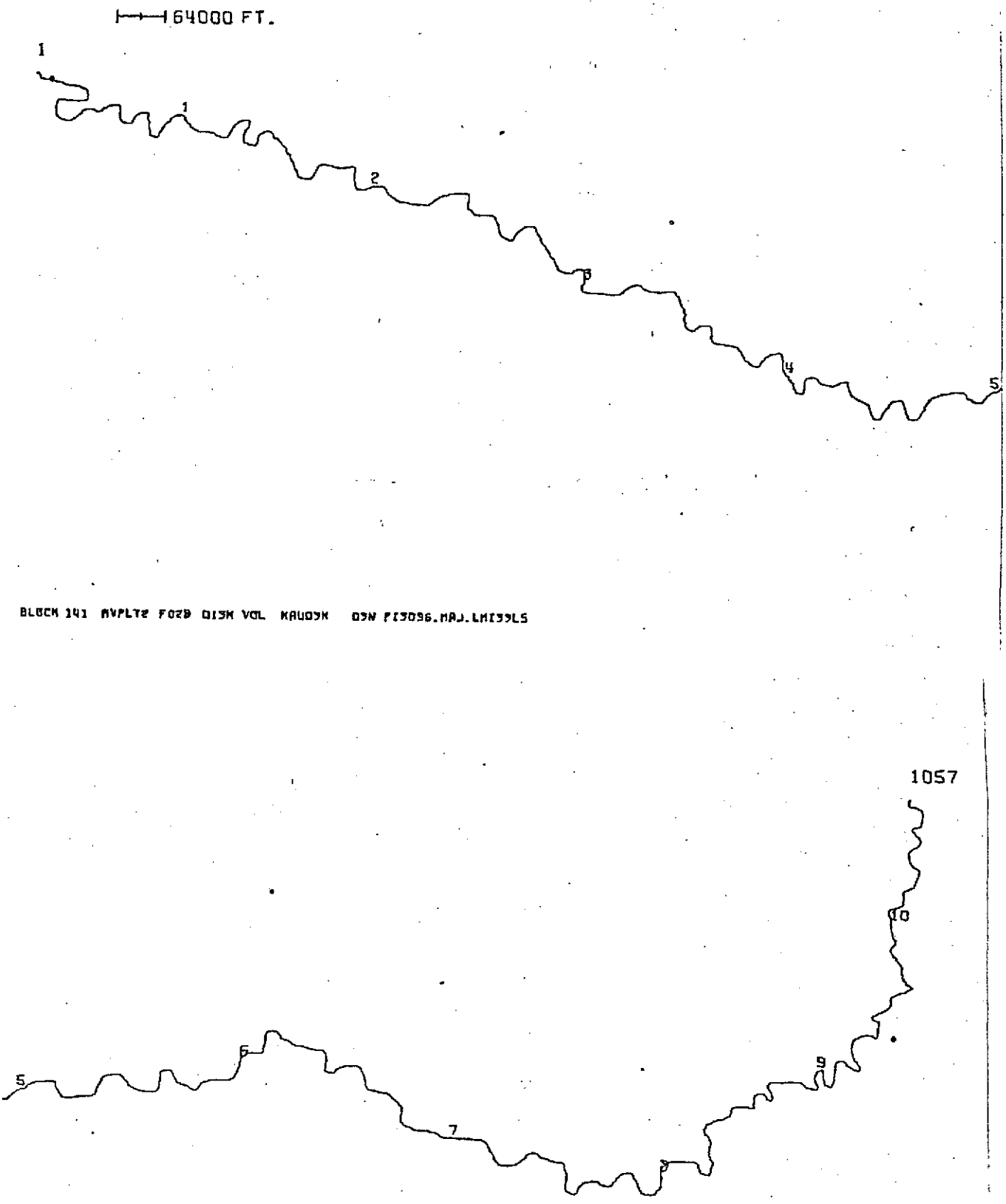

Figure 5.2. A second computer plot of the individual digitized frames of ERTS-1 Band 7 imagery of our Mississippi River study area obtained on October 1 and 2, 1972. The spacing between the 1057 data points used in constructing this plot was 3.93 thousand feet.

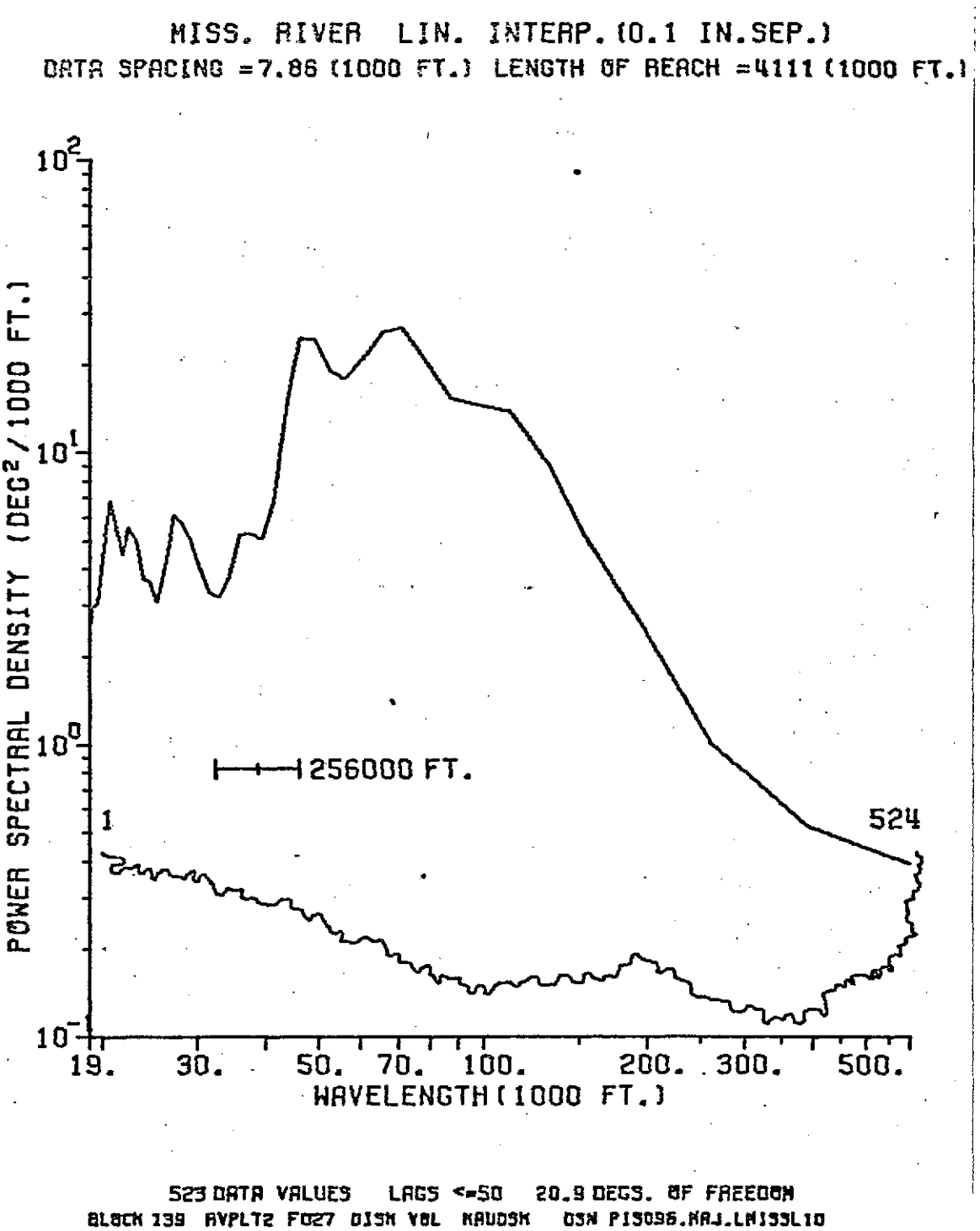

Figure 5.3. Power spectrum of Mississippi River meanders, based on Figure 5.1.

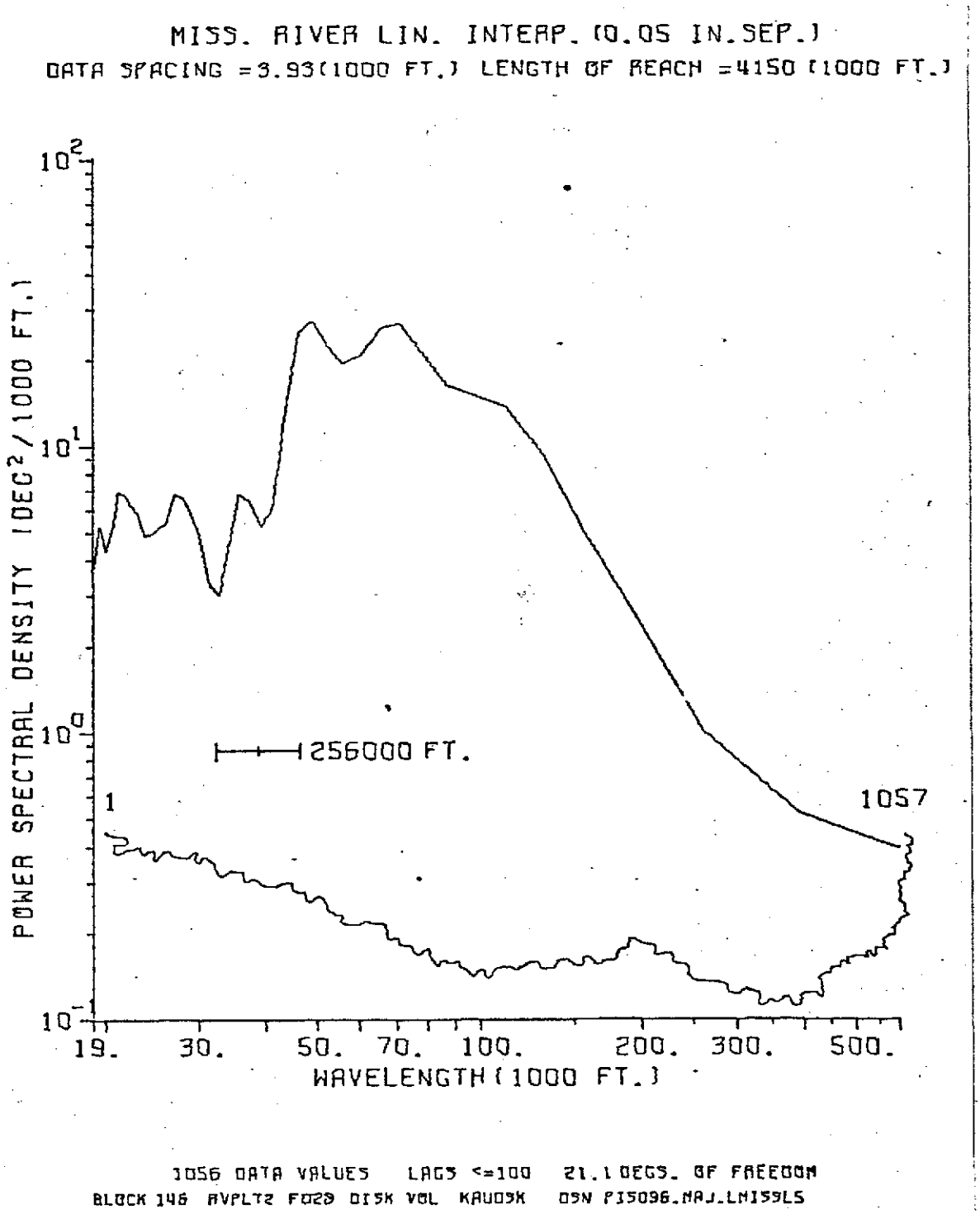

Figure 5.4. Power spectrum of Mississippi River meanders, based on Figure 5.2.

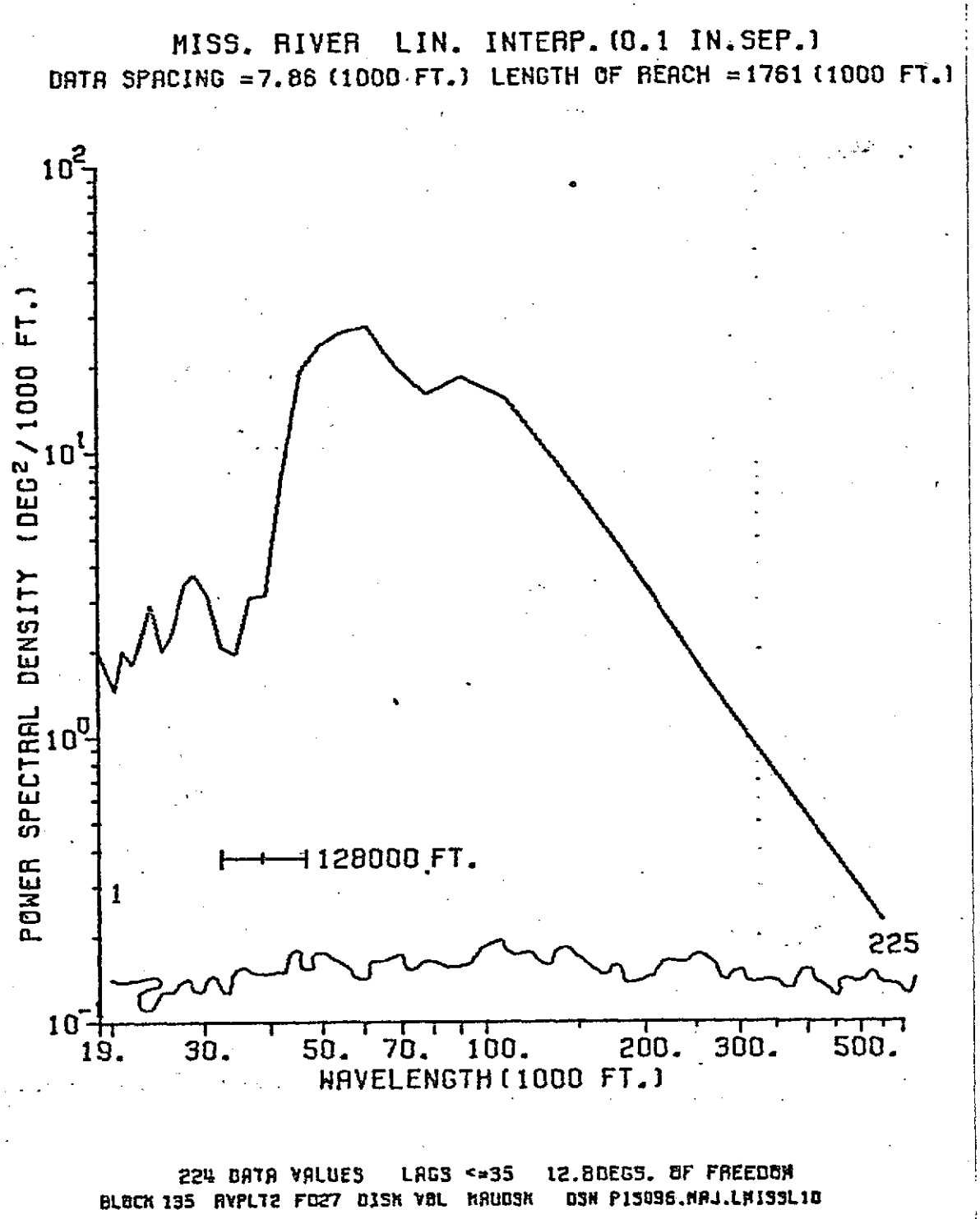

Figure 5.5. Graphical representation of Power Spectral Density for the upper portion of our Mississippi River study area.

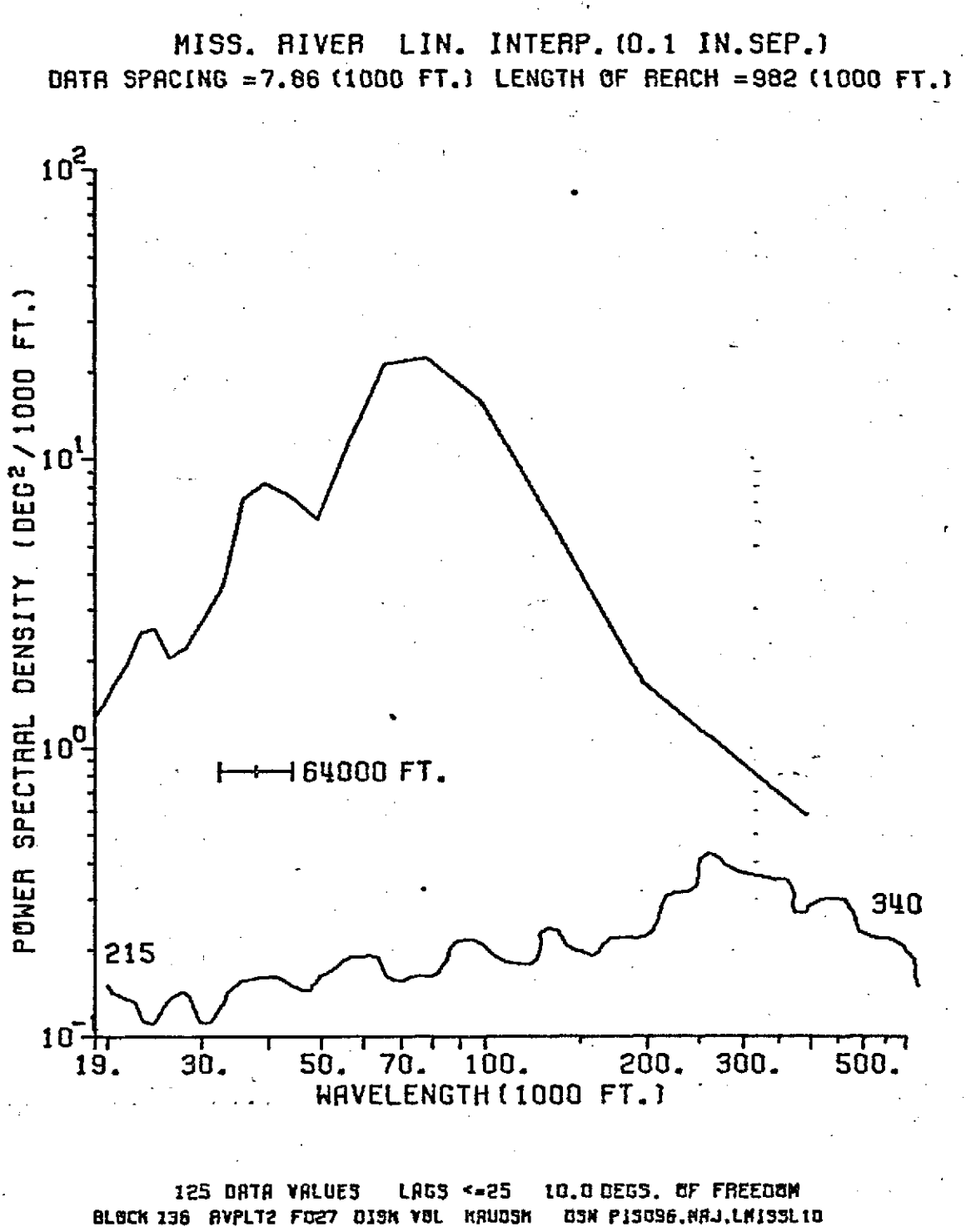

Figure 5.6. Graphical representation of Power Spectral Density for the middle portion of our Mississippi River study area.

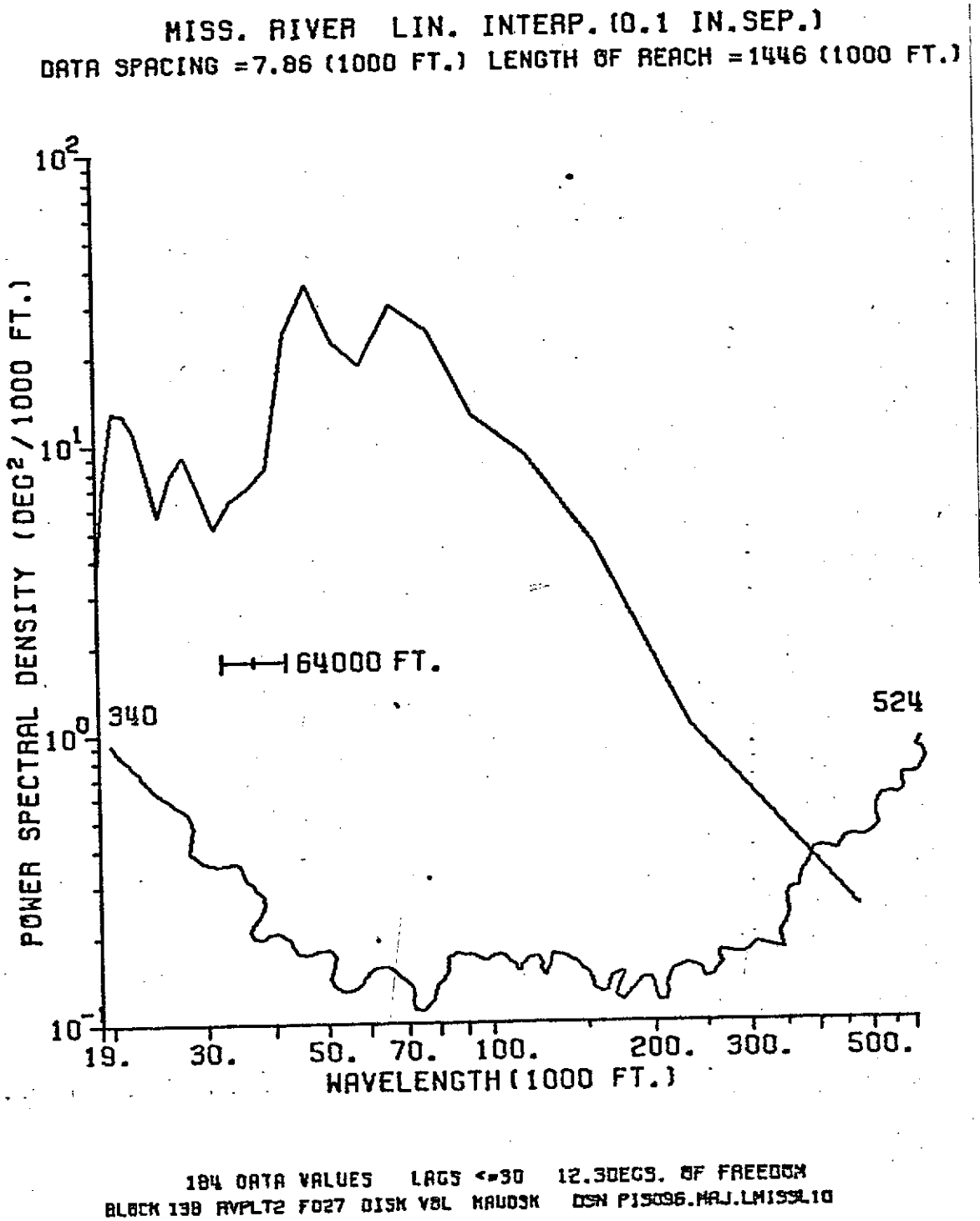

Figure 5.7. Graphical representation of Power Spectral Density for the lower portion of our Mississippi River study area.

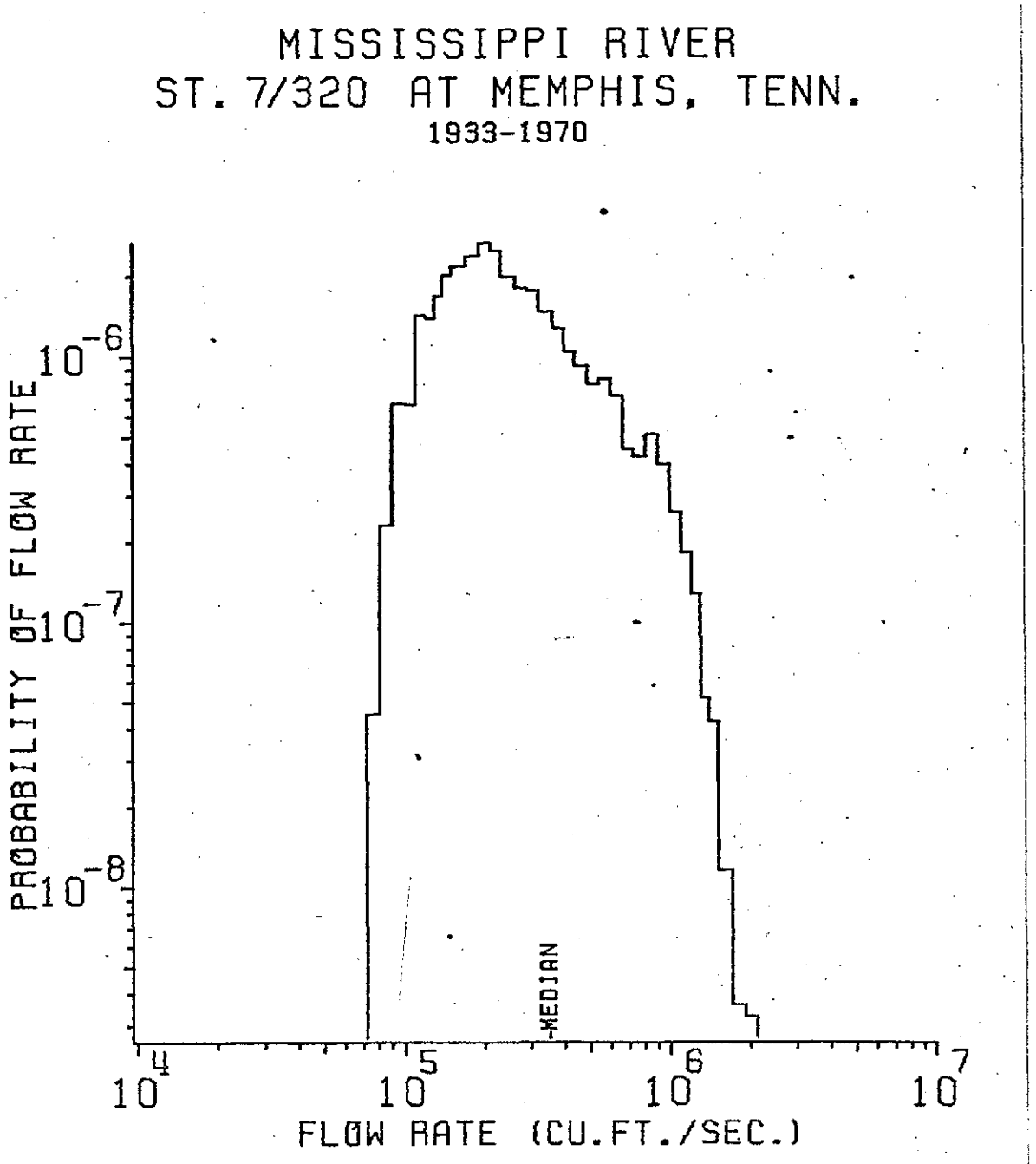

Figure 5.8. Discharge spectrum for our Mississippi River study area based on thirty-seven years of continuous hydrologic recording at Memphis, Tennessee.

Chapter 6

USE OF ERTS-1 DATA TO ASSESS AND MONITOR CHANGE IN THE WEST SIDE OF THE SAN JOAQUIN VALLEY AND CENTRAL COASTAL ZONE OF CALIFORNIA (UNO70)

Co-Investigator: John E. Estes

Contributors: L.W. Senger, R.R. Thaman, D. Brunelle, D. Cottrell, F. Evanisko, S.P. Kraus, B. Palmer, J.M. Ryerson, T. Soper, K. Thaman

Department of Geography, Santa Barbara Campus

TABLE OF CONTENTS

6.0 INTRODUCTION

The Geography Remote Sensing Unit (GRSU) at the University of California, Santa Barbara was responsible for investigations with ERTS-1 data in the Central Coastal Zone and West Side of the San Joaquin Valley. The nature of these investigations concerned the inventory, monitoring, and assessment of selected parameters that characterize the natural and cultural resources of the two areas. The determination of land use and the identification of agricultural crops, drainage networks and basins, landforms, and natural vegetation with the aid of ERTS-1 images were the principal subjects for investigation. These parameters are the key indicators of the dynamically changing character of the two areas. Monitoring of such parameters with ERTS-1 data provides the techniques and methodologies required to generate the information needed by federal, state, county, and local agencies to assess change-related phenomena and plan for management and development.

Progress reports submitted during the course of the ERTS-1 investigation primarily emphasized an analysis of ERTS-1 data for specific environmental information in selected sites. The purpose of this approach was to identify and develop workable solutions to interpretation and classification problems, in order that "set" methodologies and techniques could be defined preparatory to the construction of finalized data base maps for the selected resource parameters under investigation.

The construction of the various data bases required that two decisions be made: (1)where the boundaries should be drawn to define the area for which mapping would be accomplished; and (2) what specific ERTS-1 images should be used as the data sources for mapping. The mapping area, designated as the Central Region, was finally determined on the basis of including a wide range of environmental habitats, encompassing a sufficiently large area to demonstrate the significance of ERTS-1 type data, and having high quality ERTS-1 coverage. The resultant Central Region test site covers approximately 52,213 square kilometers of land area, with boundaries extending from Monterey in the extreme northwest; east through Hanford to the Sierra Nevada foothills; south along the Sierra Nevada foothills and across the Tehachapi Mountains to the western end of the San Fernando Valley; west to Point Concepcion, along coastal portions of Los Angeles, Ventura, and Santa Barbara counties; and finally, north-northwest along the coastline to Monterey. Included within the site are several million people and ten counties (all of Kings, San Luis Obispo, Santa Barbara and Ventura counties; and portions of Fresno, Kern, Los Angeles, Monterey, San Benito, and Tulare counties). The selection of ERTS-1 images to be used for mapping was based on cloud cover, image quality, and seasonal enhancement of environmental phenomena. The images from which interpretations were performed included the following frame numbers/dates: E1002-18140/25 Jul 72; E1018-18010/10 Aug 72; E1019-18062/11 Aug 72;

E1073-18064/04 Oct 72; E 1074-18123/05 Oct 72; E 1234-18021/14 Mar 73; E 1235-18073/15 Mar 73; E 1235-18075/15 Mar 73; and E 1255-18190/04 Apr 73.

The remainder of this final report, sections 6.1 - 6.7, is concerned with an evaluation of the utility of ERTS-1 data for inventorying, monitoring, and assessing specific resource parameters. Discussion centers on methodologies, data analysis, problems encountered, and detailed results. Section 6.1 presents the findings of land use investigations. ERTS-1 data were effective for general land use mapping, delineating transportation networks, and delimiting boundaries of cropped agricultural land; difficulty was encountered in consistently identifying urban boundaries. Section 6.2 discusses a method for crop identification from ERTS-1 data based on the presence or absence of vegetation in a given field, which may have significant implications for the development of computerized crop surveys. Section 6.3 deals with drainage and landform mapping. Drainage networks and basins can be accurately determined from ERTS-1 data, while only macro-level landform features could be consistently identified. Section 6.4 documents the capability to identify and measure kelp beds on ERTS-1 imagery, with important implications for routinely inventorying kelp resources.

In similar fashion, the feasibility of determining forest fire damage with high accuracy from ERTS-1 data is treated in section 6.5. Section 6.6 is concerned with natural vegetation mapping. It was possible to map vegetation at the association level with reasonable accuracy, using only limited ground truth information.

Conclusions regarding the utility of the ERTS-1 system as a data source for resource information are presented in section 6.7, based on significant results achieved in the investigations conducted by GRSU. ERTS Image Descriptors are also included. The key words used to describe the itemized ERTS-1 images represent a preliminary evaluation of information content by GRSU personnel.

6.1 LAND USE

This section represents a final evaluation of ERTS-1 as a source for a land use data base for the entire Central Region test area. The Central Region Land Use Data Base Map (see Figure 6.1), operational Land Use Classification Key (see Table 6.2), and analysis of the ERTS system presented herein are the result of both extensive and concentrated research conducted during previous reporting periods. This final evaluation, however, differs from earlier ones in that: (1) the region is mapped in its entirety; and, (2) an overall evaluation of the usefulness of ERTS as a land use identification tool is presented. The sections which follow are concerned with: (1) a brief review of earlier research methodologies and goals; (2) a description of the final construction of the complete test region land use map and operational data base

CENTRAL REGION LAND USE DATA BASE

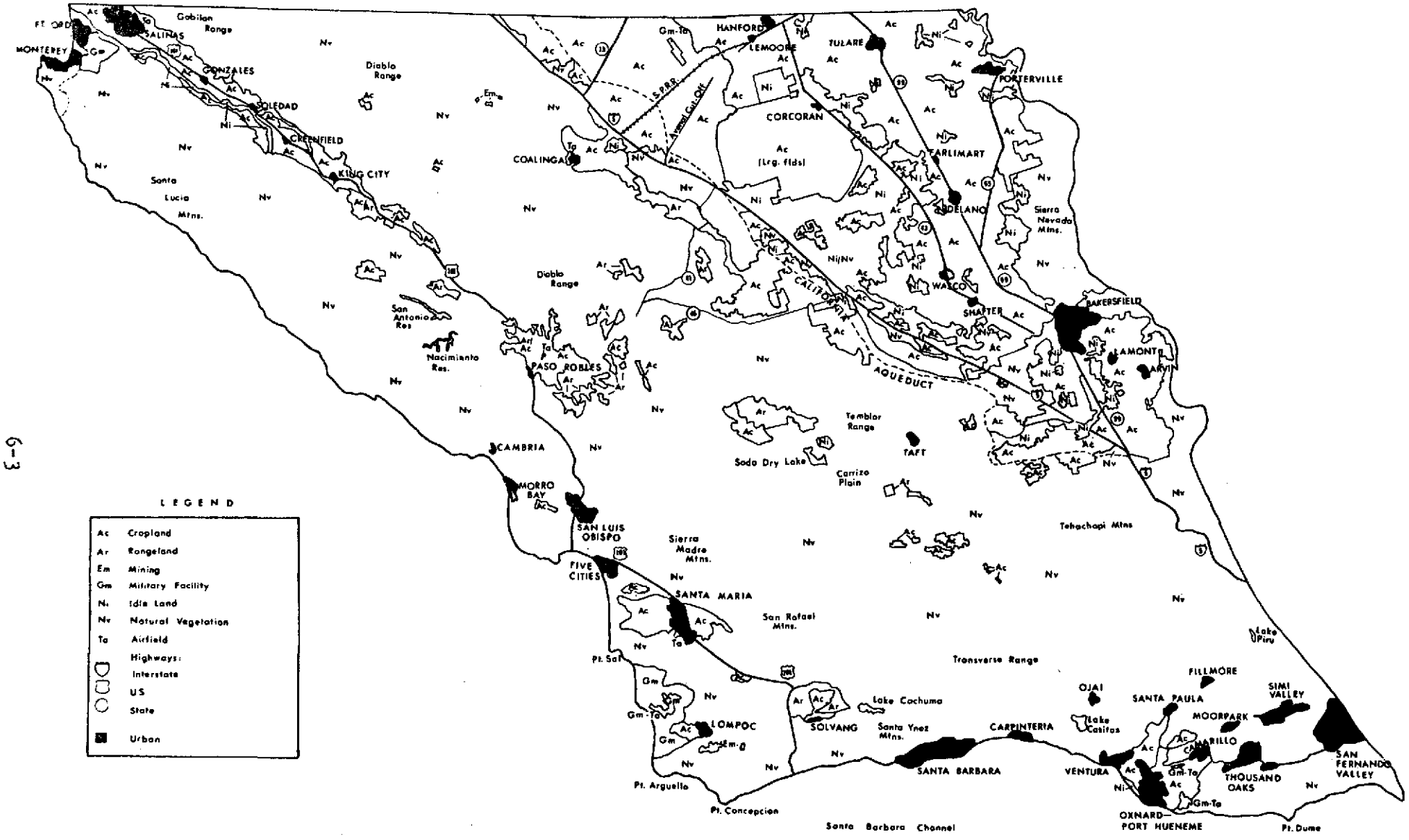

Figure 6.1. ERTS-1 central region land use map.

classification key; and (3) an overall analysis of earlier research and the utility and application of ERTS for future land use mapping.

6.1.1 Earlier Research Methodologies and Goals

During previous reporting periods our evaluation of land use features, using ERTS-1 imagery concentrated on determining the feasibility of ERTS as a data source for land use analysis. The methodology employed involved the use of individual 9.5 x 9.5-inch black-and-white transparencies (MSS bands 4-7), of selected areas within the Central Region test site, as source imagery for the identification, delimitation, evaluation, and mapping of various type land uses. In order to assess the capability of ERTS-1 as a data source for providing meaningful land use information within a working data base context, the investigations focused on identifying specific land use parameters within diversified cultural and environmental (physical) settings. The cultural features examined were: (1) spatial extent and location (both absolute and relative) of urbanized areas; (2) transportation routes and networks; and (3) agricultural development and extent.

Three sets of ERTS-1 MSS band positive transparencies (frame numbers: 1002-18140, North Central Coastal Region; 1073-18064, South Central Coastal Region; and 1019-18062 Central Valley Region) were used initially to evaluate specific land use information potential of ERTS data for diverse environments. For each of the three (3) ERTS-1 frame numbers utilized, MSS bands 4-7 were evaluated for total information content and application to land use studies. The results of these evaluations were summarized in the first three progress reports in the form of individual maps and comprehensive tables.

6.1.2 Land Use Map and Data Base Classification Methodology

The basic methodology employed in constructing a land use map and data base key for the entire Central Region test site involved: (1) determining the boundaries of the area; (2) selecting the optimal imagery for evaluation of land use features; and (3) examining and revising the land use classification scheme developed at the beginning of the project to reflect the interpretability of ERTS-1 imagery.

To insure compatibility of the land use data base map with other environmental maps presented in this report (e.g., natural vegetation, hydrology, etc.), a uniform boundary for the test area was defined. In addition to the previously mentioned North Central Coastal, South Central Coastal, and Central Valley Regions mapped earlier, portions of Ventura and Los Angeles counties, not previously mapped, were included. In order to effectively evaluate the suitability of ERTS-1 as a land use resource identification tool, it was deemed advisable to have a wide range of optimal test area imagery, flown during several periods. Therefore, nine 9.5 x 9.5-inch black-and-white transparencies imaged

on various dates were selected. This was done to insure overlapping of multiple frames at any point in the test area, and to allow for analysis of possible seasonal tonal signature differences.

Before actual mapping commenced, each band of each numbered image was evaluated for tone, texture and contrast, and those affording the best potential for land use analysis (usually bands 5 and 7) were used in preparation of the final map. Once the broad Central Region test area boundary had been outlined on clear mylar (acetate), actual land use mapping from the selected 9.5 x 9.5-inch transparencies began.

The procedure involved first examining each image for recognizable land use features. Once these features were identified, their extent was traced onto clear mylar placed over the image. To provide verification of an initial analysis, or further delimit land use features, overlapping images of different dates were then examined. Where additional land use signatures were discovered, this information was traced onto the acetate. In this manner (i.e. through the use of overlapping images), a detailed and comprehensive Central Region Land use data base map was constructed. Whereas earlier maps relied on imagery from a single date only, the final map made use of multiple date, overlapping imagery.

Preparatory to the commencement of the ERTS-1 program in July, 1972, GRSU devised a classification key for use in land use mapping (see Table 6.1). The key was purposely designed with built-in flexibility. Once actual analysis and interpretation of the imagery began, modifications to expand it (i.e., make it more specific), or collapse it (i.e., make it more general) could then be made. After extensive evaluation of various ERTS images, using both 9.5 x 9.5-inch transparencies and contact print enlargements from these transparencies, a considerably "collapsed" operational classification key (see Table 6.2) was devised to replace the earlier one.

6.1.3 Overall Analysis of the Utility and Application of ERTS for Land Use Evaluation

This section deals with an overall analysis of the utility and application of ERTS for land use mapping. The discussions which follow are concerned with use and applications in: (1) determining extent and location (both absolute and relative) of urbanized areas; (2) locating and tracing transportation routes and networks; (3) delimiting agricultural extent and development; and (4) measuring land use change.

It should be pointed out at this time that the ability to identify and delimit land use features is very dependent on several major factors, including: (1) ERTS image resolution and quality; (2) seasonal variations, and (3) the location of the particular feature in relation to

TABLE 6.1. INITIAL LAND USE CLASSIFICATION (JULY, 1972)

KEY:
General Category, ex. A (Agriculture)
Type within Category, ex. t (tree crops)
Specific Type, ex. c (citrus)
Total Code: Atc

Note: The more specific notation depends upon ability to identify, and additional types and specific types can be added to the system as they are encountered.

	CODE
AGRICULTURE	A
Grain Crops	Ag - (type)
Horticulture	Ah - (type)
Pasture (improved)	Api
Pasture (unimproved)	Apu
Row Crops	Ar - (type)
Stock farming (beef)	Asb
Stock farming (sheep)	Ass
Stock farming (dairy)	Asd
Tree Crops	At - (type)
EXTRACTIVE	E
Seawater mineral recovery	Es - (type)
Petroleum production fields	Ep - (type)
Construction materials	Ec - (type)
Mining Operations	Em - (type)
PUBLIC FACILITIES	G
Governmental - administrative	Ga - (type)
Governmental - Military	Gm - (type)
Cemeteries	Gc
Protection - Police & Fire	Gf - (type)
Hospitals	Gh
Prisons	Gp
Waste disposal (solid & liquid)	Gd - (type)
Education	Ge - (type)

TABLE 6.1. (Continued)

	Code
PARKS & RECREATION	P
Campground	Pc
Golf Course	Pg
Park	Pp
Stadium	Ps
Marinas	Pm
Resort	Pr
INDUSTRIAL	I
Power Plant (fossil, hydro,nuclear)	Ib - (type)
Warehousing	Id - (type)
Commercial fishing (docking & canneries)	If - (type)
Port facilities	Ip
Shipbuilding & repairs	Is
Heavy manufacturing	Ih - (type)
Light manufacturing	Il - (type)
Saw mills (or pulp)	Iw
Power substation & transmission	It
TRANSPORTATION	T
Airports	Ta - (type)
Highways (roads, etc.)	Th - (type)
Railroads & yards	Tr - (type)
Canals	Tc - (type)
COMMERCIAL	C
Clustered	Cc - (type)
Strip	Cs - (type)
RESIDENTIAL	R
Single family	Rs
Multi-family	Rm - (type)
NON-DEVELOPED	N
Natural vegetation	Nv - (type)
Idle land	Ni - (type)
Barren land	Nb - (type)
Water bodies	Nw - (type)

TABLE 6.2. OPERATIONAL LAND USE CLASSIFICATION (MAY, 1973)

KEY:
General Category, ex. A (Agriculture)
Type within Category, ex. c (crops)
Specific Type, ex. g (grain)
Total Code: Acg

General Category	Code	Comments
AGRICULTURE	A	
Field Crops	Ac - (type)	may include row type (r); grain type (g); and tree/ orchard (t). Additional sub-types could be added.
Range Areas	Ar - (type)	grasslands differentiated from surrounding vegetation and often showing signs of fencing (square borders). May include improved (i) or unimproved (u).
EXTRACTIVE	E	
Mining Operations	Em - (type)	may include open pit (o) etc., and additional sub-types.
Petroleum Production Fields	Ep	usually identified by maze of crossing access roads.
PUBLIC FACILITIES	G	
Governmental-military	Gm - (type)	may include air bases (ta), army installations (indicated by Fort _____), etc.
PARKS AND RECREATION	P	
Golf Course	Pg	readily identifiable on MSS Band 7 if of eighteen hole variety.
Marinas	Pm	identifiable due to geometrical signature along coastlines.
INDUSTRIAL	I	
Port Facilities	Ip	as Pm, but larger.
TRANSPORTATION	T	
Airports	Ta	signature depends on locational context to other features and runway material.

TABLE 6.2. (Continued)

General Category	Code	Comments
Highways (roads, etc.)	Th*	*roads are normally mapped using their federal, state or county number (e.g., 101 rather than the code).
Railroads	Tr*	*railroads are usually mapped using the abbreviations for their operating company (e.g., S.P.R.R. - Southern Pacific Railroad Co.).
Canals	Tc*	*canals are normally identified by name (e.g., California Aqueduct).
URBAN	U*	*urban areas, undifferentiated commercial Residential areas normally identified by the city name (e.g., OJAI) in bold type and their extent shaded in.
NON-DEVELOPED	N	
Barren Land	Nb	includes extensive sand or bare rock areas.
Idle Land	Ni	land within or bordering agricultural or urban areas which has been cleared but not used for commercial purposes.
Natural Vegetation	Nv	see natural vegetation data key and map for specific vegetation associations.
Water Bodies	Nw* - (type)	*normally indicated by lake (l), river (r), or ocean (o) name on map.

others. Often a land use feature exhibits a slightly different tonal or textural signature when one or more of the above factors changes. For instance, U.S. 101, a major four-lane highway, was inconspicuous and difficult to trace between Santa Barbara and Santa Maria on ERTS image number E1073-18064 for October, 1972. However, five months later, using ERTS image number E 1235-18075 for March 1973, the highway was easily traced. The reason for the variation between the two frames of the same area, was that the October 1972 image was taken at the end of the Southern California dry season, while the March 1973 image was taken after unseasonably heavy rainfall. Thus U.S. 101, with its light tonal signature, blended completely with the light toned surrounding grassland during the earlier period, but contrasted sharply against the dark, even textured, moist grassland in the latter period. Therefore, the following analysis, while applicable to the ERTS imagery used, may be subject to further modification in the future.

Urban Areas

In addition to extensive macro-scale evaluations made of individual urban concentrations in the three regional sectors analyzed earlier (see Table 6.3. "Evaluation of MSS Bands 4-7: Urban Concentrations"), a micro-scale analysis of the application of ERTS imagery to accurately delimit and measure urban areal extent was also conducted.

The results of both the macro- and micro-scale analysis would seem to indicate that ERTS is an excellent general purpose data source for the identification of urban area location. This is with particular reference to populated areas of over 4,000 inhabitants. The final map (see Figure 6.1) includes forty-two urban areas (see Table 6.4), with Atascadero (pop. 10,290) and Carmel (pop. 4,525), the only cities/areas over 4,000 pop., which were not identified on the imagery used. In part, this was due to inadequate tonal contrast in the former and constant cloud cover over the latter. Identification, in most cases, was facilitated by locating the characteristic light grey tonal signature and mottled texture of the urban area, as contrasted with the different signatures of surrounding non-urban areas. The contrast was best defined in areas of extensive agricultural production (e.g., San Luis Obispo). Also, location along transportation (road) networks further aided in identification. While ERTS-1 has proven a useful tool in the identification of urban area location, its value in determining actual urban areal extent is still to be proven. The previously mentioned micro-scale analysis, conducted in an earlier reporting period, compared known area figures from 1972 NASA High Flight (scale 1:120,000) and predicted area measurements from enlarged ERTS imagery (approx. scale 1:150,000). The results showed the latter to be relatively inaccurate, with an error of at least $\pm$ ten percent for ten sites that were sampled. The major source of error on ERTS occurred at the boundaries of the study areas, where urban and non-urban features merge as a result of population/building density

TABLE 6.3. EVALUATION OF MSS BANDS 4-7: URBAN CONCENTRATIONS

Location/City	Band 4	Band 5	Band 6	Band 7
Salinas Valley (U.S. 101)	Good to excellent. All five cities are well defined (vary from white to light grey) against dark background.	Fair to good. Urban response not as clear as Band 4. While Greenfield and Gonzales are identifiable by shape and tone/texture (white-light grey and slight mottling), Soledad and King City blend with surrounding agricultural land. Salinas easily located by white signature of CBD. However, boundaries tend to fade at interface with non-urban.	Poor to fair. None of 4 smaller cities south of Salinas defined. Salinas, however, has strong signature.	Poor to fair. Four smaller cities again are undifferentiable, owing to lack of tonal contrast. Salinas, with light to medium grey tone and mottled texture, also shows some street patterning. Border between urban and non-urban is well defined owing to tonal differences.

TABLE 6.3. (Continued)

Location/City	Band 4	Band 5	Band 6	Band 7
U.S. 99 Area - including cities east of 99: Arvin, Bakersfield, Delano, Earlimart, Lamont, McFarland, Porterville, Tulare, and Visalia	Fair to good delineation; Dark grey mottled appearance. Contrast well with surrounding agricultural land and/or linear patterns of the highways.	Good to excellent. Dark grey mottled tone/texture stands out against agri-cultural surroundings.	Poor to fair. Urban areas show a light spectral response against light signature of surrounding agri-cultural land. Bakersfield, Porterville, Tulare and Visalia give fair response including lightly defined street patterns.	Poor to good. Definition same as Band 6. Street patterns have better (darker) contrast.
Calif. 43/198: Hanford, Lemoore, Shafter, Wasco	Fair response, as above.	Same as Band 4.	Poor to fair. Same as above. Hanford is only city to give fair response (as Bakersfield, etc.)	Same as Band 6.
Coalinga	Poor definition; area of limited agriculture; urban grey spectral response blends with surrounding signatures.	Fair identification; dark, mottled against lighter toned surrounding area.	Poor.	Same as Band 6.
Taft	Not visible.	Poor - dark response against light toned idle land response.	Poor.	Same as Band 6.
San Luis Obispo	Poor to fair. Tends to blend with surrounding grassland lighter tone and mottled texture are evident but not obvious.	Fair. Urban area is evident as mottled texture contrasts strongly with uniform texture of surrounding land.	Poor. Urban blends with surrounding grassland.	Poor to fair - CBD displays medium grey signature, which con-trasts well with light grey of radiating urban area.

TABLE 6.3. (Continued)

Location/City	Band 4	Band 5	Band 6	Band 7
Lompoc, Santa Maria, and Vandenberg AFB	Fair to good. Lompoc and Vandenberg are well defined. In Lompoc area light grey tone contrasts well with surrounding mixed agricultural signatures. Vandenberg's urban strip contrasts well with surrounding scrubland and the large adjacent concrete flight ramp and runways. Santa Maria elicits a fair tonal signature with the light grey response contrasting well with the agricultural field patterns to the west. However, the response fades in other directions where it blends with extensive grassland.	Good. Lompoc and Vandenberg as in Band 4. Santa Maria gives a strong response due to a mottled textural signature and dark grey tones which contrast with both the regular field boundaries and irregular grassland/ rangeland.	Poor to good. Lompoc and Vandenberg as in Band 4. However both tend to lose some clarity where adjacent grasslands blend with the urban response. still possible to distinguish the distinctive mottled urban texture in most cases. Santa Maria, for an unknown reason, gives a very poor response with a general blending of tone and texture between urban, field agriculture and grassland.	Fair to good. As in Band 4. In addition, the main street linear networks are visible in Lompoc and Santa Maria.
NEW CUYAMA	Poor. Very small, urban settlement, mainly an agricultural and oil extractive area. Sparse population.	Poor.	Poor.	Poor.

TABLE 6.3. (Continued)

Location/City	Band 4	Band 5	Band 6	Band 7
VENTURA COUNTY - Camarillo, Ojai, Oxnard-Pt. Hueneme, Santa Paula, and Ventura	Fair to good response. Except for Ojai, all cities are in an area of extensive agriculture. Light grey spectral response of urban areas contrasts well with linear pattern and dark response of surrounding fields.	Good. Urban areas show a dark grey, distinctively mottled response which is easily differentiated from surrounding agricultural land.	Poor to fair. Difficult to determine juncture of urban and agricultural boundaries due to a wide variety of light and dark grey tonal signatures. Areas tend to merge.	Poor to fair Same as band 6.
SANTA BARBARA COUNTY - Santa Barbara and Carpinteria	Fair to good. Santa Barbara's tonal signature fair but tends to blend with lower elevation foothill slopes. Both urban response and foothill/ grassland have light grey tone with similar pictures. Carpinteria gives a good response with light grey urban spectral signature contrasting well be between the coast and mountains.	Good for both cities. Still a slight problem in differentiating urban and foothill boundaries in some instances.	Poor to good. Santa Barbara shows good response with dark grey tonal signature and a mottled texture These aid in distinguishing urban-grassland boundaries. However, on this band Carpinteria tends to blend with the grassland and scrub vegetation of its adjacent hillsides making identification poor.	Fair. Same problem as in Band 5.
SANTA YNEZ VALLEY	Poor. Small urban settlements of Santa Ynez, Solvang and Buellton with dispersed population densities make identification nearly impossible. No positive response, either textural or tonal.	Poor.	Poor.	Poor.

TABLE 6.4. URBAN AREA POPULATION DATA

CITY	COUNTY	AREA POPULATION*
Arvin	Kern	5,199
Bakersfield	Kern	69,515
Camarillo	Ventura	19,219
Cambria	San Luis Obispo	1,716
Carpenteria	Santa Barbara	6,982
Coalinga	Fresno	6,161
Corcoran	Kings	5,249
Delano	Kern	14,559
Earlimart	Tulare	3,080
Fillmore	Ventura	6,285
Five Cities (including Arroyo Grande, Grover city, Nipomo, Oceano and Pismo Beach)	San Luis Obispo	27,840
Fort Ord	Monterey	26,128
Gonzales	Monterey	2,575
Greenfield	Monterey	2,608
Hanford	Kings	15,179
King City	Monterey	3,717
Lamont	Kern	7,007
Lemoore	Kings	4,219
Lompoc	Santa Barbara	25,284
McFarland	Kern	4,177
Monterey (including Seaside and Pacific Grove)	Monterey	77,819 (est.)
Moorpark	Ventura	3,380
Morro Bay	San Luis Obispo	7,109
Ojai	Ventura	5,591
Oxnard-Pt. Hueneme	Ventura	85,520 (est.)
Paso Robles	San Luis Obispo	7,168

TABLE 6.4. (Continued)

CITY	COUNTY	AREA POPULATION*
Porterville	Tulare	12,602
Salinas	Monterey	58,896
San Luis Obispo	San Luis Obispo	28,036
Santa Barbara (including Goleta and Montecito)	Santa Barbara	128,215 (est.)
Santa Maria	Santa Barbara	32,749
Santa Paula	Ventura	18,001
Shafter	Kern	5,327
Simi Valley	Ventura	61,327
Soledad	Monterey	6,843
Solvang	Santa Barbara	2,004
Taft	Kern	4,285
Thousand Oaks	Ventura	36,334
Tulare	Tulare	16,235
Ventura	Ventura	57,964
Visalia	Tulare	27,482
Wasco	Kern	8,269

* 1970 U.S. Census Bureau figures

decreasing towards the perimeter. However, this may have been the result of resolution and seasonal variation, as August 1972 imagery was used. Initial examination of March 1973 imagery, following an extensive rainy season, shows differences both in urban signature and extent, with boundaries of the test areas better defined. A re-evaluation of ERTS as a data source for urban extent analysis, using the improved March 1973 imagery, may yield more accurate results.

ERTS-1, then, is a valuable data source for urban area identification, and a possible tool for accurate delimitation of urban areal extent. Unfortunately, attempts to identify smaller land use features (e.g., commercial and residential structures) within urbanized areas using ERTS have proved unsuccessful. Regardless, there are significant planning implications of applying the ERTS synoptic view as a monitoring tool for gross urban expansion and development.

Transportation Routes and Networks

An extensive evaluation of individual transportation features (e.g., highways, secondary roads, canals, airports, railroads, etc.) for the various test region sectors is contained in Table 6.5. "Evaluation of MSS Bands 4-7: Transportation Features." In general, ERTS has proven an accurate tool in locating, identifying, and tracing various transportation features, especially in those areas of extensive agricultural production where contrasts are greater. Thus, two lane and four lane highways are clearly traced in the agriculturally rich San Joaquin and Salinas Valleys, as are other transportation features such as the California Aqueduct (especially on bands 6 and 7.) However, as with urbanization, in locations with extensive grassland or natural vegetation regime characteristics (e.g., most of the Coastal Central Region), the typical light tonal, linear signature of highways and railroads readily blends with the similar light-toned, mottled texture of surrounding features. In addition, the relatively narrow width of transportation features such as roads and railroads, renders their identification even more difficult given the resolution capabilities of ERTS. Furthermore, seasonality has a marked effect on signature response, especially, where tonal contrasts between vegetative features and transportation arteries are highlighted. The earlier example of U.S. 101 between Santa Barbara and Santa Maria illustrates this point.

Regarding other transportation features (e.g., airports and railroads), the results have been less encouraging. In the case of airports, the main factors seem to be runway construction material, size of the facility, and contrast with surrounding land uses. The extensive concrete runway surfaces of Vandenburg and Oxnard Air Force Bases and Lemoore and Pt. Magu Naval Air Stations, were easily identified and mapped. However, the only civilian airports delimited were at Salinas, Paso Robles, Santa Maria and Coalinga where, for still undetermined reasons, there was good contrast between them and their surrounding environments. Unidentified

TABLE 6.5. EVALUATION OF MSS BANDS 4-7; TRANSPORTATION FEATURES

LOCATION	BAND 4	BAND 5	BAND 6	BAND 7
U.S.99-4 lane	Good response along entire route except when passing thru urban areas, where road signature blends with urban. Stands out well in areas of intensive agriculture, as well as areas of low-lying, sparse natural vegetation. Linear regularity aids in identification as does light signature.	Fair to good. Same as for Band 4, except that signature fades to the Northwest in an area of small fields and bare soil (highway and fields both display light tone).	Poor to fair. Road shows dark response which tends to blend very subtly with surroundings.	Fair to good. Dark, linear response against lighter agriculture signature. Also, unlike Band 5, it is well defined along entire ERTS-1 image.
Interstate 5-4 lane	Poor to good. Major portion of route well defined. However, as much of the surrounding land remains undeveloped, the signature tends to fade when this occurs on both sides of Interstate 5. Light response of road good against agriculture (dark), but poor against open land (also light).	Poor to fair. Generally same as Band 4. However more fade out in undeveloped areas.	Poor. Tends to blend with light signature of surrounding land along majority of route.	Poor. Light signature against light background--majority of route traced on Figure 1 not visible.
Calif. 43-2 lane	Poor to fair. Irregular response. Visible in areas of agriculture where regular field patterns lend good contrast. However, in several large sections identified as Ni areas or Ac with bare soil, the road tends to blend.	Same as Band 4	Not visible.	Fair. Dark response is well defined against agricultural regular patterned background. Slight loss of resolution in bare soil and idle land areas.
Calif. 198-2-4 lanes	Poor. Visible thru Hanford although small field patterns tend to disrupt signature. Contrast is poor. Cannot be traced thru the idle land east of Hanford and west of U.S. 99.	Same as Band 4.	Not visible.	Poor. Dark tone only visible against agricultural background with great difficulty.
Avenal cut-off-2 lane.	Poor to fair. Light pattern contrasts in areas of varying toned agriculture. Fades when encountering homogeneous light responses of bare soil, etc.	Same as Band 4.	Poor to fair, due to dark, linear pattern against lighter signature of agriculture.	Good. Dark linear response against regular agricultural patterns.

TABLE 6.5. (Continued)

LOCATION	BAND 4	BAND 5	BAND 6	BAND 7
U.S. 101	Poor to good. White linear signature appears best against dark grey or near black, especially in agricultural region of Salinas Valley and Mountain region north of San Luis Obispo. Tends to fade and blend with light grey in San Luis Obispo area and disappear into Salinas. Most of the highway is not visible from Santa Barbara to San Luis Obispo except where it transverses agricultural fields.	Poor to good. Tend toward a light grey response. Not evident in San Luis Obispo Area nor within Salinas. Also, tends to blend into Salinas River signature. Not visible from Santa Barbara to San Luis Obispo except where it transverses agricultural fields.	Very Poor to poor. Very poor except in the Salinas Valley from Salinas-Soledad. Even here the grey signature tends to merge with other greys around it. Not visible at all from Soledad to Santa Barbara.	Poor to good. Good through the Salinas Valley- presents a dark tone in contrast to lighter agricultural areas. Response fairly good south of King City but again fades. Visible through mountains north of San Luis Obispo, but fades from San Luis Obispo to Santa Barbara.
U.S. 1	Poor. Tends to blend with light grey tones of San Luis Obispo-Morro Bay. Invisible along most of the coast from Morro Bay northward and from Santa Maria southward.	Poor to fair. Along coast, portions are visible. Bend at Cambria especially apparent as are portions along raised sea platform to the north between Monterey-Cambria.	Very Poor.	Poor to excellent. Excellent through Morro Bay proper. Fair from Morro Bay-San Luis Obispo, through grassland. Not well defined along rest of coast.

TABLE 6.5. (Continued)

LOCATION	BAND 4	BAND 5	BAND 6	BAND 7
Calif. 126- 2-4 lanes	Good. Linear pattern and light tonal signature contrast well with surrounding pattern of fields.	Poor to good. Good contrast and response from Ventura to Santa Paula through area of agriculture. From NE of Santa Paula where agriculture is more irregular the contrast and response of the road are quite poor (especially as it borders the Santa Clara River).	Not visible	Not visible
Calif. 154- 2 lanes	Poor to good. Highway connects Santa Barbara with the Santa Ynez Valley via the Santa Ynez Mountains and Lake Cachuma. Response is nonexistent except for a small portion bisecting an agricultural area, which contrasts well (mainly due to the linear nature of the Highway response against the field patterns).	Same as Band 4	Not visible	Not visible

TABLE 6.5. (Continued)

LOCATION	BAND 4	BAND 5	BAND 6	BAND 7
Other Roads	Poorly defined.	Road patterns visible in some urban areas and some field boundaries.	Poor to fair. Street patterns visible in large cities.	Good to excellent. Street patterns in large cities detectable as dark linear response against mottled grey urban.
S.P.R.R.-Southern Pacific Railroad Line	Poor to fair between Interstate 5 and Hanford. Fair definition when crossing vegetated fields-contrast evident. Poor response between NAS Lemoore and Hanford, due to small fields and poor contrast. Not visible from Hanford to U.S. 99 or Interstate 5 to Coalinga.	Same as Band 4.	Same as Band 4.	Poor to good. Good east of the California Aqueduct. Contrasts well with agricultural land. Poor contrast to the west.
Canals-California Aqueduct	Fair to good along entire route. White tone and linear pattern. Water visible.	Same as Band 4.	Good to excellent. Water gives very dark response and contrasts with lighter agricultural land.	Same as Band 6.
Other Canals	Poor to fair located between Interstate 5 and U.S. 99 for main part. Light tone and linear pattern visible. Difficult to differentiate from roads.	Same as Band 4.	Same as above.	Same as Band 6.

TABLE 6.5. (Continued)

LOCATION	BAND 4	BAND 5	BAND 6	BAND 7
Airports	Poor to good-NAS Lemoore. Runways show white signature and good contrast with surrounding agriculture. Wasco-poor but visible. Light response. Coalinga- poor, dark signature. Vandenberg AFB, in an area of homogenous natural vegetation gives a good, light response.	Fair to good-NAS Lemoore. Wasco- same as Band 4. Coalinga- Poor to air. Shows dark against light signature of surrounding land. Shafter- poor but visible. Vandenberg and Santa Maria exhibit good tonal responses. NAS Pt. Mugu and Oxnard AFB (SE of Camarillo) give a fair response, tending to blend periodically with surrounding agriculture.	NAS Lemoore- good. Coalinga- good. Others are not visible.	NAS Lemoore- good. Coalinga- poor. Others are not visible.
Harbors	Poor to fair. Several harbors along the coast at Santa Barbara, Ventura and Oxnard to Pt. Hueneme are visible due to distinctive patterns. However, it is not possible to discern much detail.	Same as Band 4.	Same as Band 4.	Same as Band 4.

were several airports with 4,000'+ runways, including San Luis Obispo, Santa Barbara, Monterey, King City, Oxnard-Ventura, Shafter, and Bakersfield-Meadows.

Railroads proved even more difficult than airports. The only trackbed identified was a S.P.R.R. Spurline from Coalinga toward Hanford, through extensive agricultural land. Here contrasts with the surrounding environment facilitated identification. The main reasons for the inability to identify other tracks, including coastal and Central Valley mainlines, are: (1) the narrowness of the trackbed; and, (2) the common procedure of highway and railroad right of ways running adjacent to one another, so that the latter's trace blends with the former's.

In summary, ERTS has utility and applications as a resource tool to accurately identify, locate, and trace transportation networks. It should prove particularly relevant for highway planning and spatial network inventory analysis by federal, state, and county agencies. Furthermore, in conjunction with urban area uses, it could substantially aid not only in identifying existing networks, but in locating and evaluating future routes.

Agriculture

One of the most successful applications of ERTS-1 to land use identification in the Central Region test area was in agriculture. Results were achieved in: (1) identifying agricultural areas; and, (2) accurately measuring their extent. It was possible to recognize land now in agricultural use owing to rectangular field signatures and/or the presence of extensive, regular vegetation tone/texture. Ni land was identified on the basis of the absence of field boundaries and the presence of uniform vegetation/soil tonal responses. However, it should be noted that it is possible that small areas of fallow land may have been included in the classification, where field boundaries blended with the similar light signature of the bare soil. Table 6.6 "Evaluation of MSS Bands 4-7: Agricultural Features" illustrates these results.

Regardless, a high degree of mapping accuracy is possible, and the following specific example is an indication of the reliability of the rest of the mapped data for the study area. During the summer, 1972, an agricultural land use map of a portion of Kern County (radiating from Bakersfield N, W, and S) was constructed from 1971 NASA High Flight 70 mm black-and-white negatives (enlarged to a scale of 1:290,000), and crosschecked with 1:120,000 scale CIR imagery. This was sent to the Kern County Water Agency (K.C.W.A.) for verification of agriculture acreage estimates. When K.C.W.A. figures were received, the same area was mapped from ERTS-1 with the following results:

TABLE 6.6. EVALUATION OF MSS BANDS 4-7; AGRICULTURAL FEATURES

Location	Band 4	Band 5	Band 6	Band 7
Throughout Test Region	Poor to excellent. Depends on field size, distribution of crop types (tones), etc. Where crops show a homogeneous tone (e.g., light or dark grey), field boundaries are poorly defined and individual fields tend to blend together. Also, occurs in areas of small, compact fields. Larger field patterns result in better boundary definition, although heterogeneity of crop types (giving different tonal responses in adjacent fields) seems to be more important in determining contrast.	Poor to excellent. Field definition depends on contrast. Light response of perimeter roads (normally dirt) gives good contrast to generally darker tone of field crops. Only exception (poor) is when fallow, bare soil, or other light response situations tend to blend with the individual fields.	Poor to fair field definition. Very irregular in quality and difficult to discern when small fields exist. Ability to define boundaries improves with tonal contrasts.	Poor to good field definition. Same basic comments as Band 6. However, tonal signature of perimeter roads is better. Dark grey response tends to delimit borders rather well. However, homogeneous field responses tend to present similar problems as those experienced with Band 4.

Source	Agriculture Acreage Estimate (acres)
1. NASA High Flight (70mm) - 1971	753,369
2. K.C.W.A. - 1971	795,280 (including fallow)
3. 1969 Crop Survey (Kern County)	746,104 (excluding fallow)
4. ERTS-1	748,050

For future agricultural land use feature investigation, ERTS shows excellent possibilities as a relatively inexpensive, highly accurate tool for delimiting and measuring agricultural development in the Central Region test site. Particularly relevant would be its use by Federal, State and County agriculture officials to measure changes in agricultural extent, both on a regional and local basis.

Land Use Change

In order to evaluate the potential of ERTS-1 imagery as a tool for land use change identification and mapping, land use maps of the West Side of the San Joaquin Valley were constructed for 1971 and 1972. This particular section of the Central Region test site was selected for study since it has been an area of continuing land use transformation. This is primarily related to the mitigating effects of better quality water (available since 1968 via the California Aqueduct) and the construction of a major transportation link along its entire length (interstate Highway 5, completed in 1972). Furthermore, excellent quality high altitude photography, flown in 1971, was available of the West Side and afforded an opportunity for a detailed comparison with 1972 ERTS-1 imagery.

For mapping purposes, four general land use categories were selected as land use change indicators. These were considered compatible with ERTS-1 imagery resolution, and included: (1) cropland; (2) grazing (including pasture); (3) oil extraction; and, (4) non-productive. Urban area change, which was insignificant for the period, was excluded.

Using the four gross land use classifications listed above, two types of maps were produced to measure the nature and degree of land use change. The first type consisted of a pair of maps showing total West Side land utilization for the years 1971 and 1972. The second type comprised a pair of maps depicting the specific areas that had undergone change during the same one year period (1971 - 1972). Of this latter pair, the first map showed the areas that had changed and their land use in 1971, while the second map delimited the same areas, but indicated their new land use for 1972. In determining land use type, where multiple use was evident (e.g., oil extraction and grazing occurring together), the highest economic utilization (in dollars)

served as the basis for final classification. Oil extraction was considered the highest economic use, followed by cropland, grazing, and non-productive.

Once the mapping had been completed, the total acreage of the mapped area was computed, using a compensating polar planimeter, and a quantitative estimate was then made of the acreage within each land use category. Thus, by using the two sets of maps, and the resulting quantitative measures derived from them, it was possible to evaluate the changes that had occurred in the West Side between the years 1971 and 1972.

The actual 1971 and 1972 gross land use patterns for the West Side are illustrated by the two maps in Figure 6.2. A quantitative estimate of land use acreage, by category, was obtained using a compensating polar planimeter, and the results appear in Table 6.7. For both years (1971 and 1972), the predominant land uses were grazing and cropland. In 1971, 90.09 percent (2,572,452.8 acres) of all land use types occurred in these categories, while in 1972 the total had increased slightly to 90.39 percent (2,580,793.8 acres). Oil extraction, as a primary land use, had declined slightly during the one year period, from 6.11 percent (174,352.6 acres) to 6.03 percent (172,278.6 acres). This was to be expected in an area where long term production had finally begun to deplete an exhaustible economic resource. Non-productive land also declined, from 3.80 percent (108,619.8 acres) to 3.58 percent (102,352.8 acres) of the total.

In terms of net change, grazing land alone increased in areal extent, by some 2.0 percent (26,894 acres) over the period 1971 - 1972, while cropland decreased 1.5 percent (18,553 acres), non-productive 5.8 percent (6,267 acres), and oil extraction 1.2 percent (2,074 acres). Approximately 3 percent (81,543 acres) of the total area (2,855,425 acres) underwent a conversion from one land use category to another.

In terms of actual change, Figure 6.3 and Table 6.8 present comprehensive breakdown of the changes, by category and areal distribution, from 1971 - 1972. The dominant trend was a conversion of marginal cropland to grazing (49,152 acres), while grazing to cropland, the other major change, accounted for another 22,258 acres. Non-productive to cropland (7,163 acres), oil extraction to cropland (2,074 acres), and cropland to non-productive (896 acres), were the only other changes.

This trend of converting sections of existing cropland to grazing, as well as the lesser trend of converting grazing to cropland, is probably attributable to water availability. While the California Water Plan (via the California Aqueduct) has significantly increased the volume and quality of water in the West Side, it has not brought in unlimited supplies. With restrictions enforced on the amount available to individual property owners, and the tenuous cost/benefit of

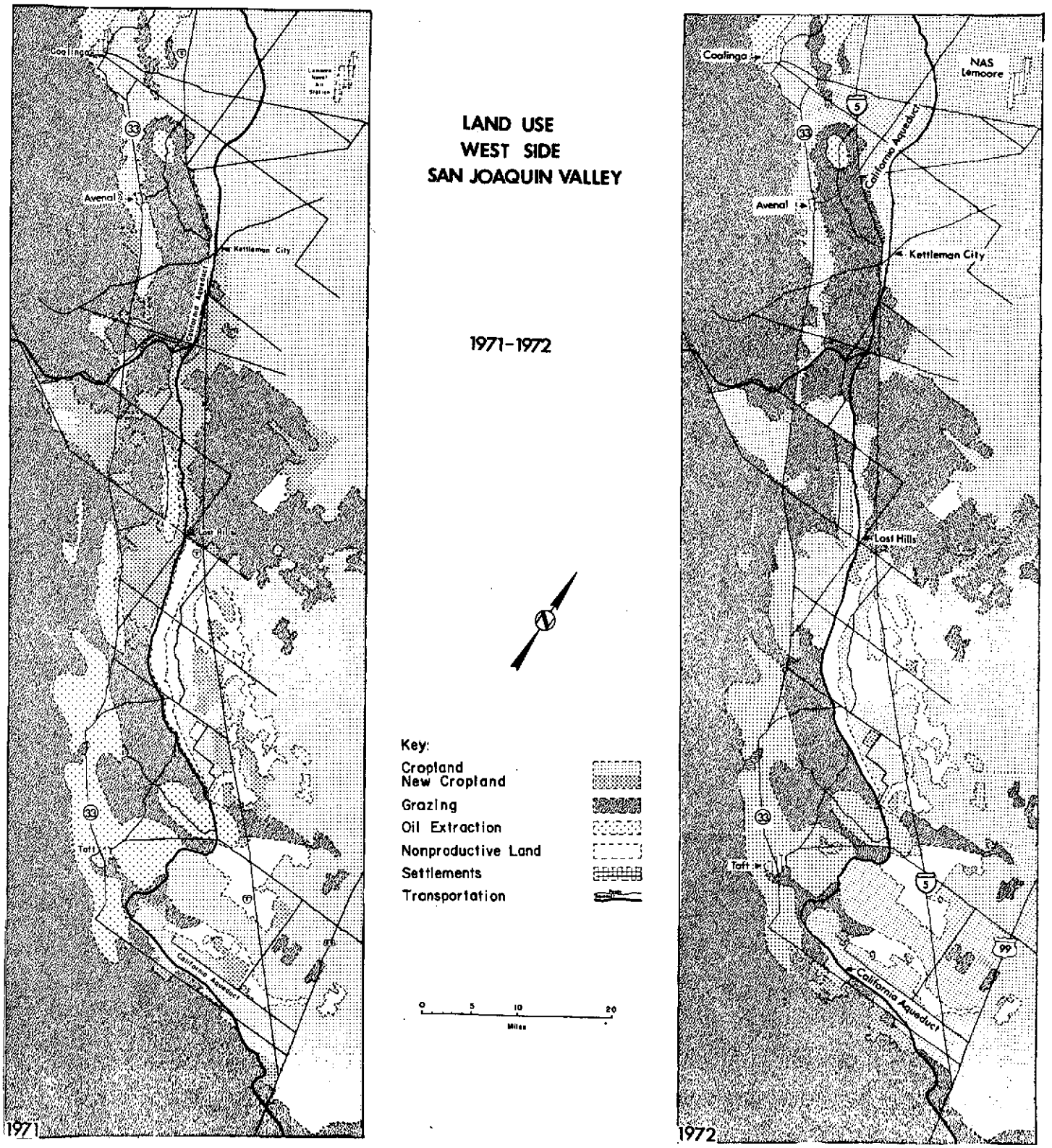

Figure 6.2. Land Use maps for the West Side of the San Joaquin Valley, California constructed from high altitude photography (1971) and ERTS-1 data (1972).

TABLE 6.7. NON-URBAN LAND USE 1971 AND 1972, WEST SIDE SAN JOAQUIN VALLEY

LAND USE CATEGORY	1971 (ACRES)	1972 (ACRES)	NET CHANGE (ACRES)
CROPLAND	1,233,063.9	1,214,510.9	-18,553.0
GRAZING	1,339,388.9	1,366,282.9	+26,894.0
OIL EXTRACTION	174,352.6	172,278.6	- 2,074.0
NON-PRODUCTIVE	108,619.8	102,352.8	- 6,267.0
TOTAL	2,855,425.2	2,855,425.2	

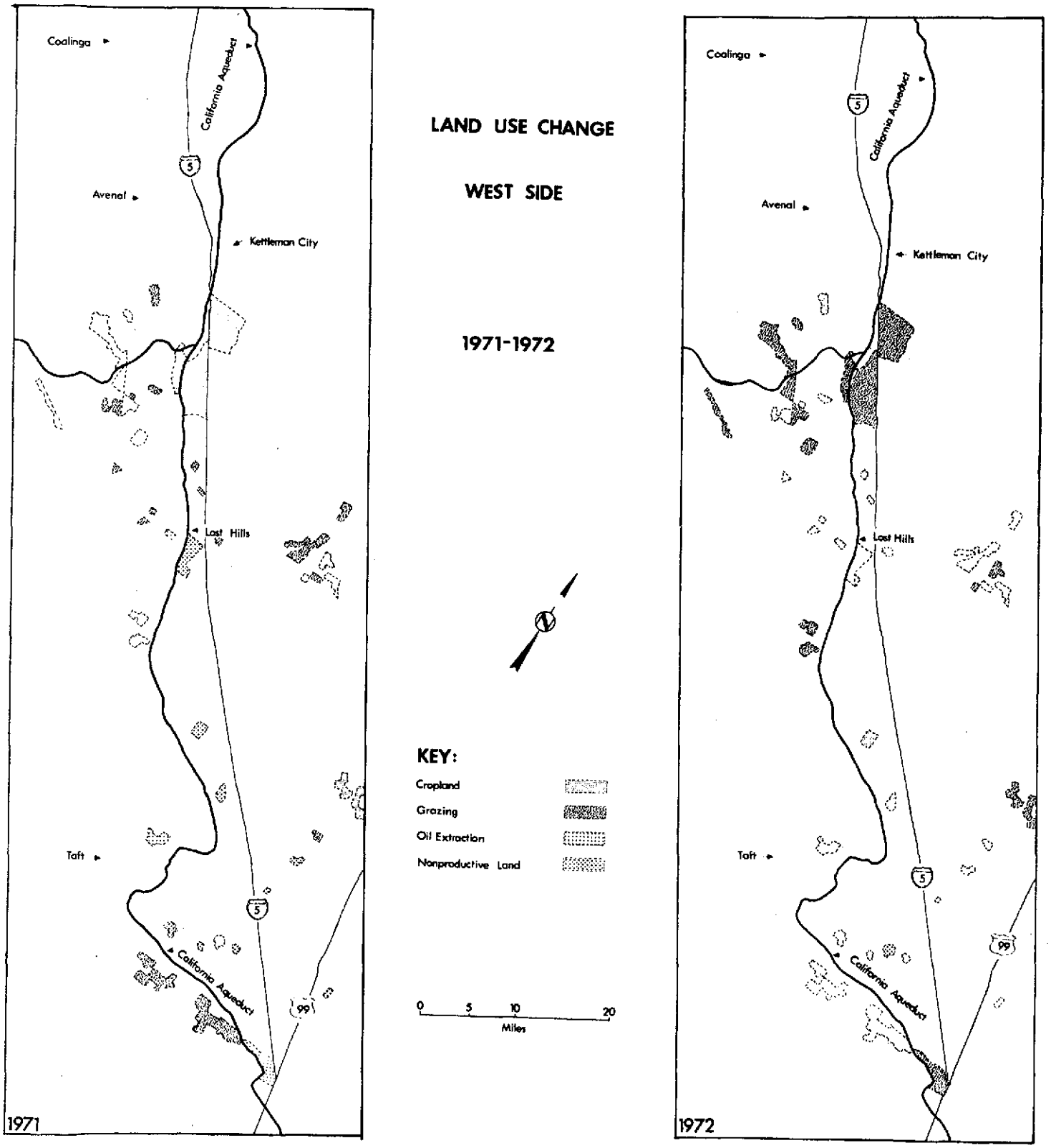

Figure 6.3. Map showing land use change from 1971 to 1972 in the West Side of the San Joaquin Valley, California.

TABLE 6.8. LAND USE CHANGES 1971 - 1972

1971	1972 LAND USE CHANGES (IN ACRES)				
	CROPLAND	GRAZING	OIL EXTRACTION	NON-PRODUCTIVE	TOTAL
CROPLAND		49,152		896	50,048
GRAZING	22,258				22,258
OIL EXTRACTION	2,074				2,074
NON-PRODUCTIVE	7,163				7,163
TOTAL CHANGE IN LAND USE ACREAGE	31,495	49,152		896	81,543

NET CHANGE IN LAND USE CATEGORIES (ACRES)

CROPLAND	GRAZING	OIL EXTRACTION	NON-PRODUCTIVE
Loss: 50,048	Loss: 22,258	Loss: 2,074	Loss: 7,163
Gain: 31,494	Gain: 49,152	Gain: N/A	Gain: 896
Change: -18,553	Change: +26,894	Change: -2,074	Change: -6,267

providing water to marginal holdings, agriculturalists have resorted to: (1) taking marginal land out of crop production and converting it to grazing land; (2) postponing actual planting in fields which were already surveyed and graded for production (in anticipation of water availability); or, (3) initiating a program of "shifting" cultivation, in which established fields are allowed to go fallow and new fields are opened for production, when individual water quota limitations do not permit full irrigation of all available arable land.

The interpretation of the four land use categories was accomplished with little difficulty from ERTS-1 data. Tonal and textural signatures for cropland and grazing were readily identifiable owing to field boundary outlines, distinct patterning, and/or pronounced contrasts with adjacent land uses. Non-productive and oil extraction areas were more difficult to identify owing to the similarity of their signatures (usually, due to lack of extensive vegetative cover and poor contrast). However, oil extraction could be consistently identified where extensive access road networks were visible. In cases where the roads were not detectable (owing to insufficient resolution), it was necessary to supplement ERTS-1 data with high altitude supporting photography and limited ground truth.

The results of this evaluation of ERTS-1, as a data source for monitoring land use change, show a definite potential for the use of satellite imagery in monitoring and mapping the macro-scale changes discussed above. Few interpretation problems were experienced, and the overall maps constructed (e.g., the 1972 maps found in Figures 6.2 and 6.3) correspond closely to: (1) ground truth data collected for the area; and, (2) coincident NASA high altitude photography imaged in 1972.

6.1.4 Summary

Based on the research which has been accomplished, ERTS-1 data will have useful applications for the identification and measurement of land use features at a macro-level. While not lending itself to micro-analysis and identification of very small features (i.e., urban residences), ERTS-1 does offer valuable potential as a tool for land use planning based on regional analyses of gross features (i.e., urban areal extent, transportation features, agricultural acreage, etc.).

The potential value for regional planning purpose of the synoptic view afforded by ERTS, is evident. This is illustrated by the Central Region Land Use Data Base Map, both in the extent (52,213 square kilometers) and the nature (transcending artificially created political boundaries) of the coverage which is provided. Land use information is essential for determining present levels of land development and evaluating future directions that development should take. These considerations are becoming increasingly regional in scope, and ERTS provides a mechanism whereby regional planning efforts can be coordinated

on a large scale. As this trend becomes more firmly established, ERTS-1 type data for land use should play a more substantial role in the planning process and facilitate regional level decision-making activities.

6.2 CROP IDENTIFICATION

The difficulty in consistently identifying crop types with any degree of accuracy from single date satellite imagery is widely recognized. However, it has been determined that vegetated/non-vegetated field conditions can be accurately identified from ERTS-1 data. Since non-vegetated (bare soil) conditions signal the beginning and end of any given growing season, it was hypothesized that this information could be extracted from ERTS-1 data and correlated with a conventional crop calendar to generate crop acreage statistics.

The methodology to evaluate this concept consisted of three (3) proposed phases. The first phase would involve the collection of vegetated/non-vegetated data on a field-by-field basis over a year-long growing cycle. These data would be extracted from ERTS-1 imagery solely on the basis of tonal changes in fields. In the second phase, these data would be examined to determine the discrete periods during the year when a field is in a vegetated condition. The third phase would involve the correlation of these discrete temporal tonal patterns (for vegetated conditions) with a conventional crop calendar to identify characteristic tonal signature patterns that may be directly associated with the growing season of a specific crop type.

At the completion of this investigation, it was anticipated that it would be possible to make some but not all pertinent conclusions concerning: (1) the types of crops for which this technique is particularly suitable; (2) the amount of error which might be anticipated if the technique is made operational; (3) any peculiarities of crops or field conditions that restrict the use of the technique; and, (4) the times of the year when it may be expected that image acquisition will be difficult to accomplish.

The last consideration mentioned above precluded completion of the investigation beyond the first phase. It proved possible to document the vegetated/non-vegetated condition of individual fields from ERTS-1 data with a high degree of accuracy (nearly 100 percent). However, a problem of unforeseen magnitude developed in the area of ERTS-1 image acquisition. It was anticipated that atmospheric conditions might preclude acquisition of usable data for a few months of the year, particularly during the rainy season. In the case of our Central Valley study area, such conditions prevailed for approximately six (6) consecutive months for most of the sites. The time period extended from late September through early March, and represented one-half of

the annual growing season for which no data could be obtained. The major cause of the problem was extensive and complete cloud cover, although for January the difficulty could be attributed to processing (imagery was too dark to be usable).

Because of the lack of sufficient data for long and critical time periods during the growing season, we found it impossible to complete the proposed study. However, the portion of the investigation which was completed (phase one) did produce two significant findings. The first of these relates to the fact that vegetated/non-vegetated field conditions could be accurately identified from ERTS-1 data. Since these data are the most critical inputs to the technique under investigation, it is expected that such data collected over a larger part of the annual growing season would validate the technique. The second finding concerns the problems encountered in data acquisition. If the problem reflects an unfortunate series of coincidences, then its magnitude might be expected to be of significantly less importance for future data acquisition missions. If such is not the situation, then more study will be required to attempt to optimize the actual timing of data acquisition. In either case, closer investigation of this problem will be required before the technique suggested in this section can be scientifically validated and put into operational use.

6.3 DRAINAGE AND LANDFORM MAPPING

As elements in the data base approach being utilized to more fully evaluate the potential of ERTS-1 data, drainage and landform characteristics of the Central Coastal Zone and San Joaquin Valley are being mapped. These phenomena are significant for several reasons including the following: (1) watershed management; (2) determination of potentially hazardous areas; (3) identification of possibly unique environmental features or habitats; and, (4) assessing the potentials and limitations for planned area development.

6.3.1 Drainage Networks and Basins

As stated in prior reports, preliminary analysis of ERTS-1 data indicated a definite potential for compiling drainage network and basin maps. In order to more fully evaluate this potential, drainage characteristics of the Central Region were mapped from ERTS-1 data and then compared to 1:250,000 U.S.G.S. topographic maps to determine the accuracy of mapping and the feasibility of using ERTS-1 data to update existing small scale drainage maps.

The methodology for mapping drainage characteristics consisted of four basic steps: (1) tracing all clearly defined stream flowlines on the ERTS-1 images; (2) delimiting drainage basins on the basis of the stream flowlines and topographic characteristics; (3) delimiting drainage basins on 1:250,000 U.S.G.S. topographic maps; and, (4) comparing the

ERTS-derived drainage data with data determined from the topographic maps. Mapping was performed at actual ERTS-1 scale, using acetate overlays. Interpretation was facilitated by utilizing different dates of ERTS-1 imagery for the same area, since this procedure provides a capability for stereoscopic viewing.

The accuracy of identifying drainage networks and basins from ERTS-1 data was determined by comparing three selected areas on 1:250,000 topographic maps with corresponding areas on the completed ERTS-1 Central Region Drainage Data Base map (see Figure 6.4). The comparison indicated that major streams (third order or greater) could be identified with 100 percent accuracy, while the accuracy for minor streams (second order or smaller) dropped to approximately 77 percent. There were no problems in accurately identifying drainage basins for the areas compared; stereoscopic viewing made it a simple task to delimit these features from ERTS-1 data.

The major difficulties in interpreting drainage data from ERTS-1 imagery were encountered in areas of: (1) arid environments; (2) valley bottoms; and, (3) slopes where a larger number of streams flow into a higher order stream system. Arid environments presented the problem of deciding the proper flowline to trace. Water flow is so intermittent that the course of a given stream channel may vary considerably, depending upon the amount of rainfall received in a particular season. In the case of valley bottoms (such as may be found in the San Joaquin Valley), field patterns associated with agricultural land usage exhibit a tendency to mask natural lines of water flow; inferrences must be made in these situations. Finally, certain areas (particularly steep-sloped ones) posed problems related to storm conditions. Heavy water flow during storms causes stream channels to vary their courses, and it is often difficult to establish what the proper flowline should be.

Despite the problems cited, ERTS-1 imagery appears to be a very useful source for mapping drainage networks and basins. Major stream courses could be delimited with 100 percent accuracy and, in several instances, flowlines could be identified on ERTS-1 imagery that did not appear on 1:250,000 topographic maps. Drainage basins could be delimited with no problems. Consequently, it should be feasible to employ ERTS-1 data for the construction of new drainage maps or to update existing ones. This would be an invaluable aid to government agencies charged with this responsibility, and to those groups involved in watershed management and planning.

6.3.2 Landform Mapping

Previous analysis of ERTS-1 data had indicated a definite potential for use in regional landform mapping. In order to evaluate this potential, a landform data base map for the Central Region was prepared directly from ERTS-1 imagery (see Figure 6.5). Review of the specific difficulties involved in the preparation of this map provides a perspective

Central Region Drainage Data Base

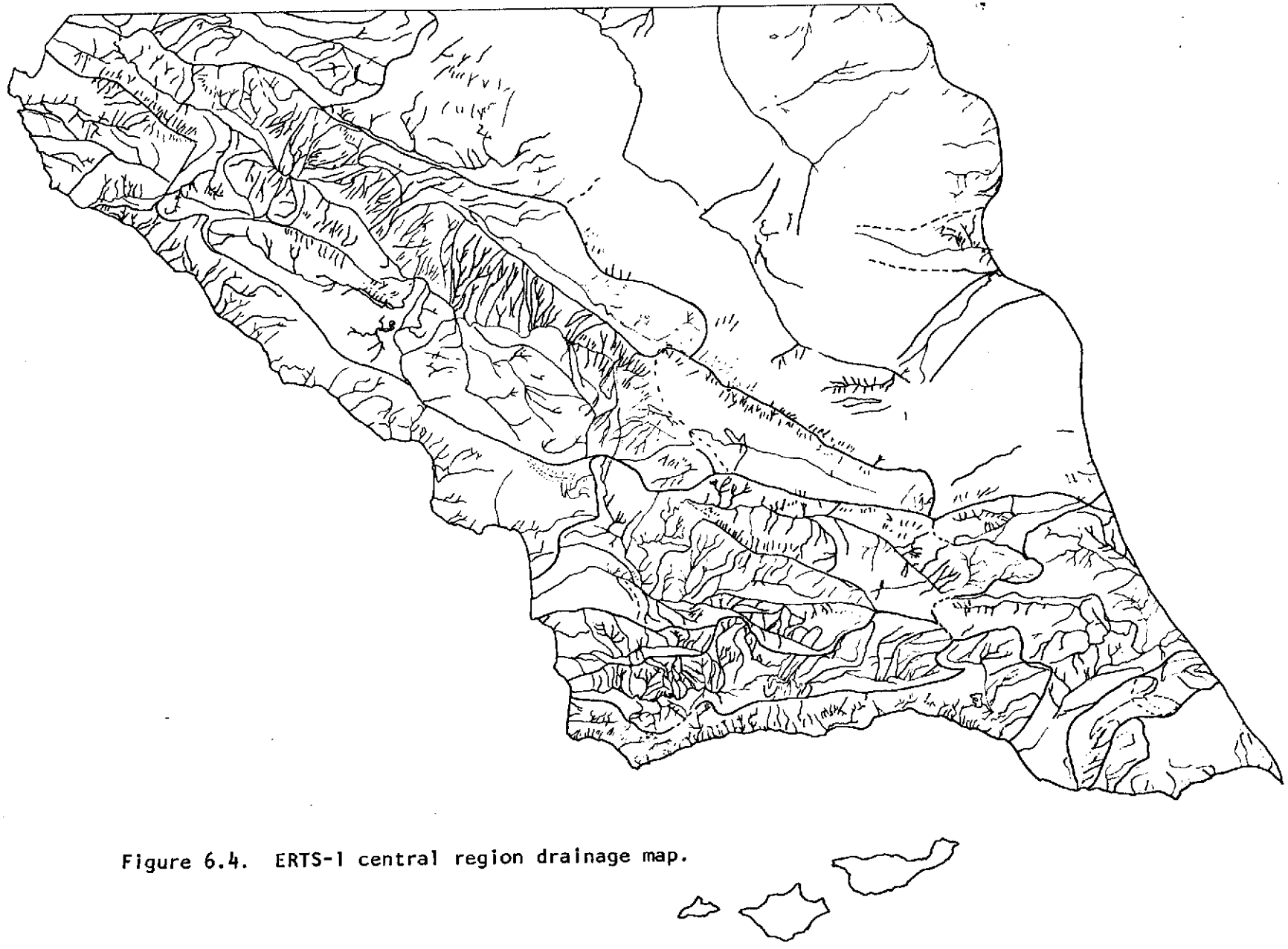

Figure 6.4. ERTS-1 central region drainage map.

CENTRAL REGION LANDFORM DATA BASE

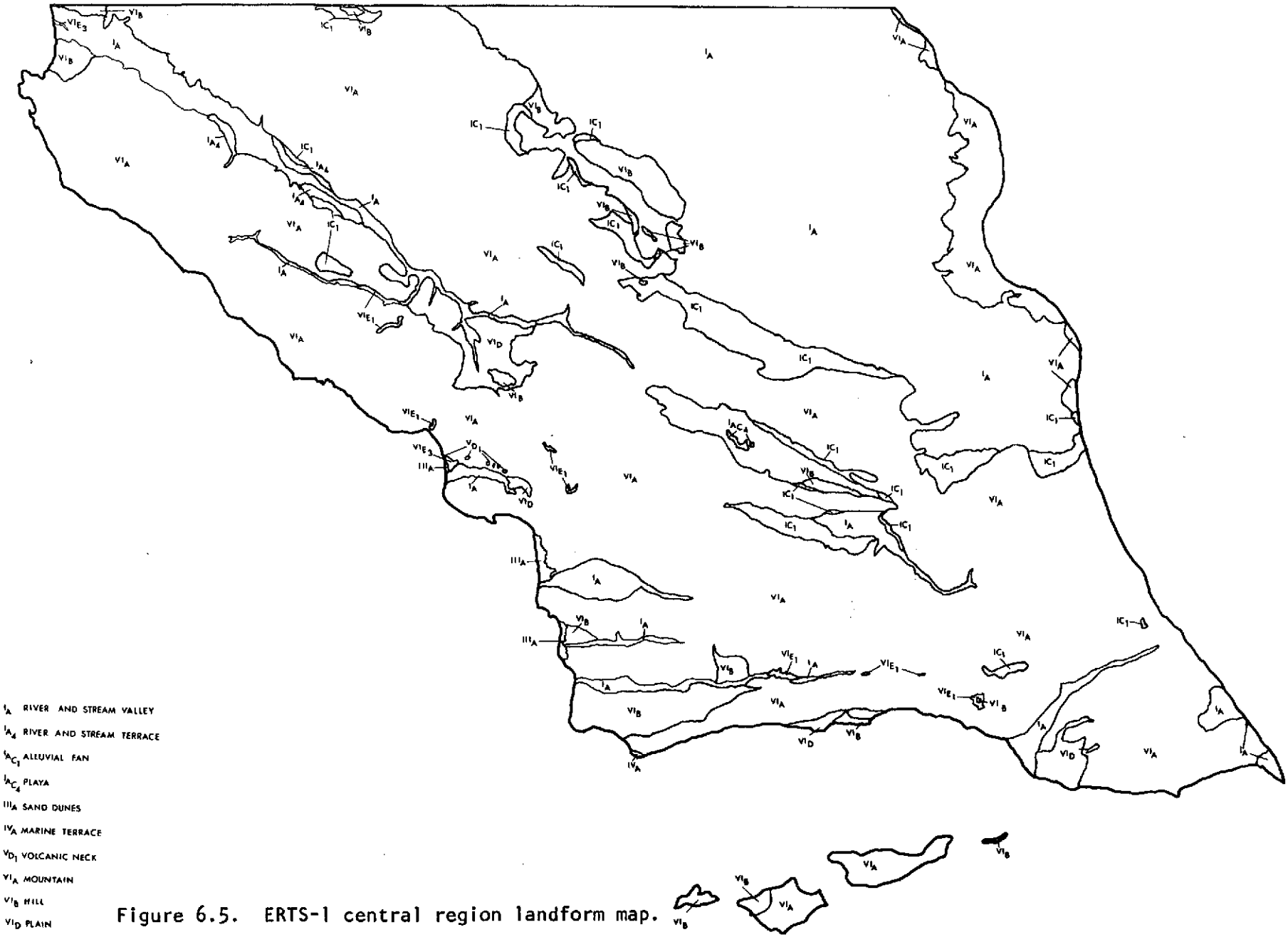

I_A RIVER AND STREAM VALLEY
I_{A_4} RIVER AND STREAM TERRACE
$I_{A_{C_1}}$ ALLUVIAL FAN
$I_{A_{C_4}}$ PLAYA
III_A SAND DUNES
IV_A MARINE TERRACE
V_{D_1} VOLCANIC NECK
VI_A MOUNTAIN
VI_B HILL
VI_D PLAIN
VI_E LAKE
VI_{E_3} ESTUARY

Figure 6.5. ERTS-1 central region landform map.

concerning the feasibility of constructing actual landform maps or revising existing maps using ERTS-type data.

ERTS-1 landform mapping procedures involved several basic steps. These included the choice of area to provide for a wide variety of landforms and to correspond with existing landform map coverage. The latter was desired to facilitate evaluation. Once mapping locations were chosen, a landform classification scheme was organized. This is shown in Figure 6.5. Actual mapping was performed on cellulose acetate overlays to ERTS-1 9.5 x 9.5-inch positive transparencies. The interpretation of specific landform categories was accomplished from several ERTS-1 images taken on different dates. This procedure provided a capability for stereoscopic viewing, which is necessary for specific landform identification.

Some of the more significant problems encountered during mapping included occasional difficulty in locating boundaries between categories, delimiting narrow beaches and terraces and partial obscuring of features by vegetation cover or urban areas. In addition, some misclassification resulted from the inability to recognize certain subtle differences between similar appearing features, which might give clues regarding the exact nature of the landform. For example, some volcanic landforms were classified as "hill" simply because ERTS-1 imagery did not provide sufficient resolution capability to determine any significant difference between the two. This type of error reflects the fact that the classification scheme which was used is probably too specific for ERTS-type data. The greatest difficulty was experienced in relation to the problem of locating certain category boundaries. It was very difficult to draw a precise line separating low hills from fan categories, and fans from valley classes. This problem was most commonly encountered along areas in the West Side of the San Joaquin Valley. The hill-fan-valley floor relationship may change in the course of a single storm, and is consequently too variable to be accurately identified from ERTS-1 imagery.

These problems do not greatly detract from the potential use of ERTS data for large scale regional mapping, however. The problems cited are, for the most part, local and can be resolved with minimum ground truth operations. All major landform categories were identified with a high degree of accuracy, and without a need for supporting ground truth information. The inability to map very specific categories in the landform classification scheme would probably have little importance to users of macro-scale regional maps (state, national, or global levels).

6.4 INVENTORIES OF SEA KELP (MACROCYSTIS) OFF THE COAST OF CALIFORNIA

Studies of ERTS-1 MSS imagery have indicated that it may be of value for the assessment and monitoring of kelp concentrations off the coast of California.

The role of kelp (Macrocystis) in the Coastal marine ecology is significant. Kelp beds provide habitats and a source of nutrients for marine flora and fauna. It is also important that the occurrence and growth of kelp is related to many environmental factors such as water temperature, depth, sub-strata, turbidity, currents, meteorological conditions, and waste disposal.

The resource potential of kelp and associated fauna has been recognized for many years. The utilization of kelp resources by harvesting, sport, and fishing industries is a multimillion dollar market operation.

Several environmental problems related to the distribution and depletion of kelp include: (1) the effects of waste disposal from sewage outfalls; and, (2) the effects of kelp cutting by commercial and pleasure craft.

Increased kelp harvesting activities and the utilization of coastal waters for waste disposal have demonstrated a need for proper inventories and management of existing kelp resources. The problems of inventorying kelp have been studied using both ERTS-1 imagery and conventional color infrared aerial photography. The purpose of this study was to: (1) evaluate the interpreter's ability to locate, delimit, and conduct areal estimations of Macrocystis, using ERTS-1 imagery; and, (2) determine if ERTS-1 can provide reliable input for the monitoring of coastal kelp on a regular basis.

6.4.1 Methodology

ERTS-1 imagery was analyzed for an area off the California coast from the Monterey Peninsula in the north to Morro Bay in the south. Optimum contrast between kelp and the background water was obtained using ERTS-1 MSS image number 1002-18140, band 6 (0.7 - 0.8 micrometers). Maps were constructed from positive and negative transparencies (scale = 1:1,000,000) enlarged by projection to a scale of 1:290,000. Conventional color infrared aerial photographic coverage of the same area was obtained by NASA in April 1971 at scales of 1:60,000 and 1:120,000. Maps of the kelp were constructed using the CIR 9" x 9" transparencies. These maps were then compared with the maps prepared from the ERTS-1 imagery to determine the usefulness of the ERTS-1 data.

Discrimination of kelp was based on uniform light tonal signatures (on band 6) of the kelp canopy; for the purposes of interpretation, three general classes of kelp concentration were selected: (1) continuous cover; (2) mottled cover; and, (3) sparse cover.

All contiguous concentrations of kelp were delineated, and artificial breaks in beds resulting from extreme boat traffic were also considered. Each discrete kelp concentration ("kelp island") was assigned an

identification number and measured in areal extent. Measurements of the total surface area (km^2) were made with a compensating polar planimeter and a millimeter square grid. Excellent correlation between the two systems provided a dependable check of measurement accuracy.

Using maps constructed from ERTS-1 imagery, and employing a similar system of classification and quantification of surface features, one should find it possible to monitor coastal kelp beds on a regular 18-day basis.

6.4.2 Analysis

The map in Figure 6.6 shows the individual kelp beds that were mapped along the coast of California. Figures for the quantitative estimations of the surface area of the kelp are found in Table 6.9.

Initial analysis of areal estimations reveal that the relative surface area of each kelp bed is small. Only one of the individually delimited areas exceeded an estimate of 5.0 square kilometers. The majority of the areas measured were between 0.7 and 5.0 square kilometers. These results, when converted to a total estimated surface area of 34.44 square kilometers, reveal the relative discontinuity of coastal kelp beds along the California coast. This figure may also have bearing on the difficulty encountered by harvesting activities and the fact that only 5 percent of the total biomass is harvested annually. There also seemed to be some correlation between the size of kelp beds and their location relative to the littoral zone. In certain areas (e.g., 34-40 on Figure 6.6) kelp cutting from non-commercial marine traffic has contributed to the separation of individual concentrations from the main body.

In the analysis of the surface cover of the individual beds, no apparent attenuation of kelp from south to north is revealed. A general clumping of individual beds was observed for most locations along the coast. A breaking up of individuals (e.g., 53-57) was noted along the Monterey Peninsula.

Apart from the effect of cutting on the surface area of kelp, many of the changes observed between individual concentrations may be attributed to storms, wave action, surface winds, or currents. The effects of sewage disposal were not observed in this study owing to the location of the test site.

Some of the complications inherent in the monitoring of coastal kelp from ERTS-1 MSS imagery include the above mentioned effects of environmental forces. While quantitative estimations of kelp biomass considered observable surface coverage, a large portion of the kelp biomass remains submerged and undetected by remote sensing techniques. The value of systems using ERTS-1 imagery rests in the ability to locate and map surface features on a regular basis, thus, providing a system that can

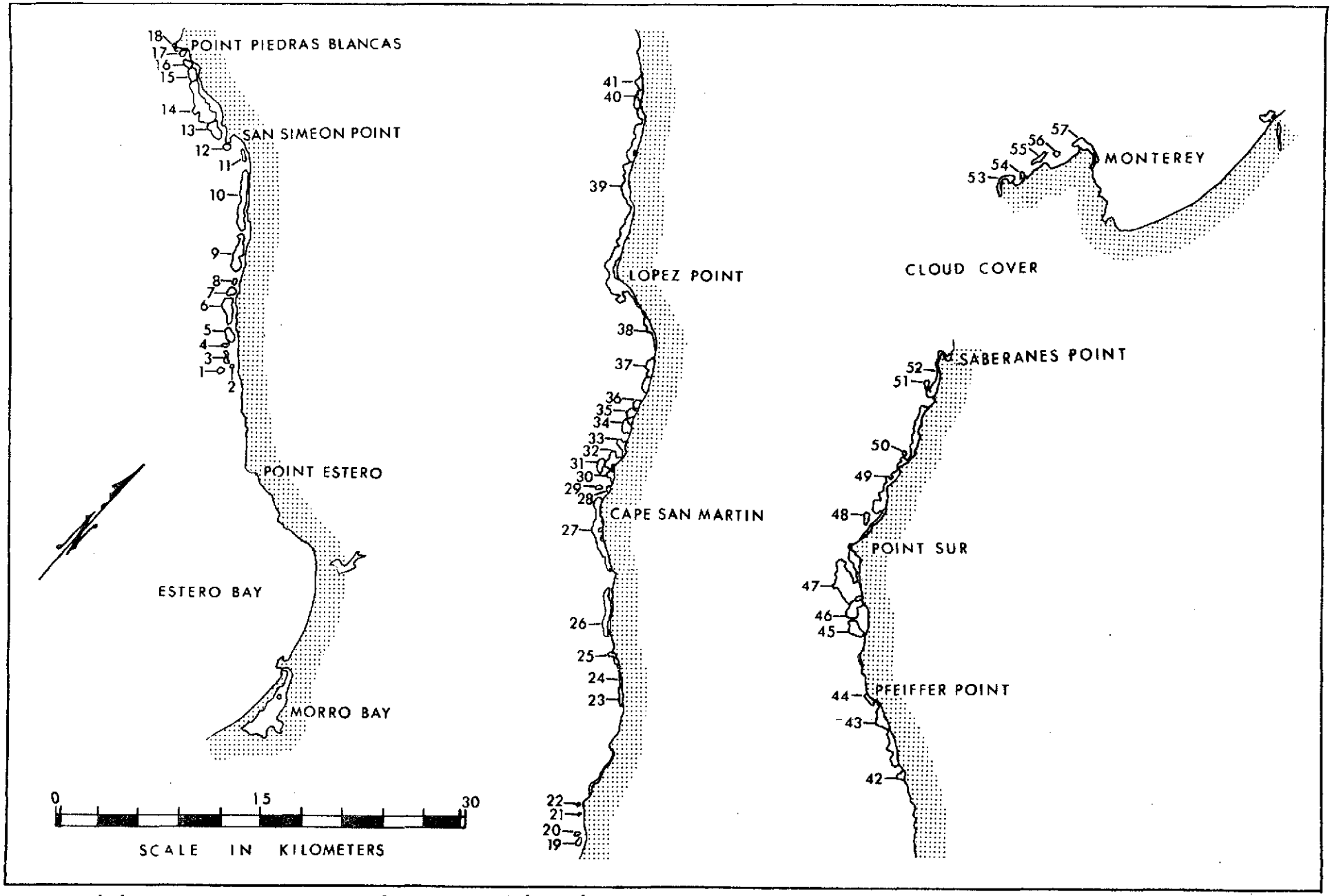

Figure 6.6. Map showing the areal extent and location of Kelp beds (Macrocystis) along the California coast from Morro Bay north to the Monterey Peninsula. Land area is shown by stippled pattern, while individual kelp concentrations are indicated by number (1-57). Data for the map was derived from ERTS-1 MSS image number 1002-18140, band 6 (July, 1972).

TABLE 6.9. QUANTITATIVE ESTIMATES OF SURFACE AREA OF INDIVIDUAL KELP BEDS FROM MORRO BAY TO MONTEREY PENINSULA, CALIFORNIA FROM ERTS-1 MSS BAND 6 IMAGERY

Numerical Designation	Kelp (Macrocystis) Area Km^2	Numerical Designation	Kelp (Macrocystis) Area Km^2
1	.1282	31	.2860
2	.0673	32	.7500
3	.0013	33	.2940
4	.1002	34	.4370
5	.4205	35	.3280
6	.8831	36	.1680
7	.2520	37	.8490
8	.0841	38	.3780
9	.9672	39	6.510
10	1.261	40	.1770
11	.1282	41	.2350
12	.1282	42	.2270
13	.6308	43	.1250
14	2.712	44	.1850
15	.3364	45	.5720
16	.1513	46	.6810
17	.1010	47	3.458
18	.1282	48	.1680
19	.0757	49	2.882
20	.0421	50	.0674
21	.0421	51	.1090
22	.1682	52	.7460
23	.2607	53	.5130
24	.0873	54	.0841
25	.2103	55	.2020
26	.8831	56	.9250
27	1.808	57	.6900
28	.0925		
29	.0757		
30	.1700		
		TOTAL KELP AREA	34.4432

monitor the movement and fluctuations of kelp boundaries. Eventually, it may be possible to relate the total surface area, as delimited on ERTS-1 imagery, to the total kelp biomass.

6.4.3 Summary

Data obtained from maps and quantitative measurements indicate that accurate delimitation of kelp may be done using ERTS-1 MSS band 6 imagery. The use of descriptive categories based on uniform tone responses may prove to be a reliable indicator of surface characteristics within kelp boundaries. Observable surface patterns and estimations of kelp area may be applicable to other environmental parameters such as canopy density, standing crop, and biomass availability. The ability to observe the behavior of sea kelp may provide a system to monitor the location and migration of offshore "kelp islands," while at the same time affording a basis for the assessment and management of the earth's total kelp resource.

6.5 DELIMITATION OF THE EXTENT OF FOREST FIRE DAMAGE

Investigations have been conducted to determine the effectiveness of delimiting fire damage areas on ERTS-1 imagery. Within the California Coastal Range area near Santa Barbara, there recently have been two extensive forest fires: (1) the "Romero Fire," just east of Santa Barbara in October, 1971 which burned an area of approximately 16,000 acres; and, (2) the "Bear Fire," just north of Santa Paula in August, 1972 which burned approximately 17,260 acres of scrubland and forest vegetation. Both fires offer excellent test sites for the study of fire damage and vegetation regeneration using ERTS-1 imagery.

It is a common practice of the U.S. Forest Service to delimit the area of each major fire using conventional aerial photography and ground reconnaissance techniques. These techniques have inherent limitations in that: (1) they require the preparation of large photo-mosaics; and, (2) the cost of the acquisition of such photography generally provides for only single date coverage, thus making time-dimensional studies difficult. Acquisition of ERTS-1 imagery in early August, 1972, afforded an opportunity to study the Bear Fire area before the fire, and two subsequent opportunities to study the extent of fire damage just after the fire and before the first major rains of the 1972 winter.

6.5.1 Analysis of ERTS-1 Data

In order to evaluate the ERTS-1 imagery, a data base was built up using: (1) conventional aerial photo-mosaics and already delimited U.S.G.S. topographic maps of the Romero Fire; and, (2) NASA high altitude color infrared photography (approximate scale 1:90,000) and topographic maps of the Bear Fire. Using these data sources, exact delineations of the fire areas were prepared and the areal extent for each

burn area was calculated.

Upon receipt of ERTS-1 imagery, it was determined that band 7 (0.8 - 1.1 micron band) provided excellent data for the identification and delimitation of the fire areas. Figure 6.7 shows an enlargement of MSS frame number 1054 - 18010, band 7, of the area of the Bear Fire. Analysis of the NASA high altitude imagery indicated that the boundary delineations and area estimations generated from ERTS-1 imagery are more accurate than the results obtained by the U.S. Forest Service, as are the areal estimates of unburned, vegetative "islands" within the fire boundaries.

In addition to the capability demonstrated for accurate delimitation of the extent of fire damage for the Bear Fire, it also proved feasible to utilize ERTS-1 imagery (band 7) for delimiting the extent of the Romero Fire (which had occurred almost a year prior to the acquisition of October ERTS-1 imagery). This ability to document the effects of a former burn indicates that 18-day repetitive ERTS-1 coverage is of considerable value for monitoring changes in an area which has been burned more than one year before. Such monitoring could have considerable utility for: (1) studying the rate of natural vegetation regeneration; (2) investigating the detrimental effects of a burn, such as increased erosion, flooding, mudslides, land slides, etc.; and, (3) monitoring the success of revegetation programs (the area burned by the Bear Fire has been aerially seeded with rye grass, as a deterrent to erosion).

6.5.2 Conclusions

In summary, the synoptic view and multi-date acquisition aspects of ERTS-1 imagery provide a means, with respect to forest fires, to: (1) clearly define the boundaries of the burned area; (2) allow for rapid calculation of the areal extent of the damage; (3) eliminate the need for preparing large aerial photo-mosaics; (4) supply a valuable temporal dimension to the study of the effects of large scale forest fires; and, (5) determine the extent of like vegetation remaining within a fire perimeter.

6.6 VEGETATION MAPPING

The objective of the vegetation mapping study was to determine the extent to which ERTS-type imagery might be used for the generation of base data concerning vegetation associations found in the Central Region of California. Attainment of this objective would be achieved by the construction and evaluation of a vegetation data base map for the entire region, based on ERTS-1 imagery obtained throughout the 1972-1973 growing season.

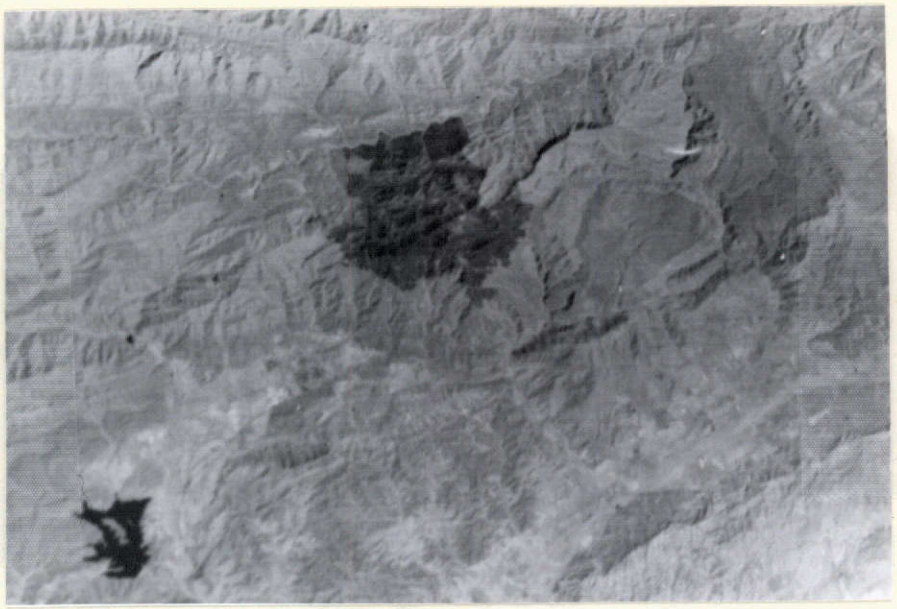

Figure 6.7. ERTS MSS band 7 (0.8 - 1.1 microns) image showing the Bear Fire area as a dark island (owing to low infrared reflectance) amidst the surrounding vegetation.

6.6.1 Approach

The evaluation of ERTS-1 imagery for purposes of vegetation mapping entailed nine interrelated phases: (1) formulation of a system for classifying the characteristic vegetation associations of the Central Region; (2) construction of a Central Region vegetation verification data base from ground truth and high altitude photographic data; (3) selection of sample test sites within the region; (4) familiarization with the image characteristics of ERTS-1 imagery; (5) preliminary interpretation of ERTS-1 imagery for the sample test sites; (6) evaluation of the preliminary maps; (7) selection of optimal dates of ERTS-1 images to be used in a multidate mapping approach; (8) interpretation of ERTS-1 imagery for the entire region and the completion of the vegetation data base map; and, (9) final analysis of the data base map and the utility of ERTS-1 imagery for vegetation mapping.

6.6.2 Formulation of a System of Vegetation Classification

Before a preliminary evaluation of the utility of ERTS imagery for vegetation mapping purposes could be performed, it was necessary to prepare a suitable vegetation classification scheme. The scheme was designed so that it: (1) included major plant communities found in the Central Region; and, (2) was flexible enough so that it could be expanded or contracted for use with variable photographic scales and/or resolutions.

In order to prepare such a classification scheme, a thorough examination of literature on California natural vegetation was carried out. The resultant scheme was derived, for the most part, from five sources (California Parks and Recreation, 1971; Critchfield, 1971; Kuchler, 1964; Munz and Keck, 1970; and, Nash, 1970). It consisted of a hierarchical classification of the natural vegetation associations of the Central Region and was divided into three basic levels (see Table 6.10). The first and most general level is divided into aquatic vegetation and terrestrial vegetation; the second level comprises major vegetation groups on a physiognomic basis (e.g., grassland, scrub vegetation, forest, etc.); and, the third level breaks down these general physiognomic classes into individual vegetation communities. (A fourth level is provided in some cases where characteristic species tend to be dominant in some associations.)

Symbols were developed for use on vegetation maps and indicate both the physiognomic and community affiliation of each vegetation type. The system is open-ended, thus making it feasible to add or subtract symbols depending upon the precision required for vegetation mapping.

6.6.3 Construction of a Verification Data Base

The information content of any remote sensing imagery can be effectively evaluated only if an accurate data base for the area under

TABLE 6.10. NATURAL VEGETATION CLASSIFICATION SCHEME

Plant Community	Code
I. Aquatic	
A. Marine (Aquatic)	M
1. Nearshore (Kelp and seaweed)	Mn
2. Intertidal	Mi
B. Freshwater (Aquatic)	Fw
C. Marsh	Ma
1. Salt Marsh	Ma_{sm}
2. Freshwater Marsh	Ma_{fm}
II. Terrestrial	
A. Barren	Ba
B. Strand	Sr
C. Grassland	G
1. Coastal Prairie	Gcp
2. Valley Grassland	Gvg
3. Meadows	Gme
D. Woodland-Savanna	Ws
E. Scrub	S
1. North Coast Shrub	Snc
2. Coastal Sagebrush (soft chaparral)	Scs
3. Cut-over Forest	Scf
4. Chaparral (hard chaparral)	Sc
5. Scrub-Hardwood	Shw
6. Desert Scrub	Sd
a. Mesquite	
b. Sagebrush	
c. Saltbush	
F. Forest	F
1. Hardwood	Fhw
2. Mixed Evergreen	Fme

TABLE 6.10. (Continued)

Plant Community	Code
3. Coniferous	Co
a. Redwood	Co_{rw}
b. North Coast	Co_{nc}
c. Douglas Fir	Co_{df}
d. Pine	Co_{pc}
G. Riparian	R
H. Agriculture	A

consideration is available. With this in mind, data base maps of the vegetation in the entire Central Region were prepared. The preparation of these maps entailed the use of 1:60,000 and 1:120,000 scale high-altitude color infrared photography taken in April, 1971. Stereo coverage was available in most cases and the overall quality of the imagery was excellent. The actual data base maps were constructed on cellulose acetate overlays. Site locations of representative plant communities were selected and ground truthed in order to evaluate interpretation accuracy. Herbarium specimens of dominant plant species within each community were also collected to relate physiognomic characteristics (e.g., leaf structure and plant geometry) to variations in tonal response apparent of the imagery.

6.6.4 Preliminary ERTS-1 Vegetation Mapping

Two representative test areas were selected within the Central Region for preliminary evaluation of ERTS-1 imagery for vegetation mapping purposes. One test area was situated along the coast (in the vicinity of Morro Bay), and the second was in the more arid San Joaquin Valley (northeast of Bakersfield). The test area near Morro Bay included a representative sample of most of the major vegetation associations characteristic of the coastal portions of the Central Region. The area near Bakersfield included a representative sample of most of the characteristic vegetation associations in the more arid portions of the Central Region.

A time period of approximately one week was allotted to the study of ERTS-1 imagery to permit familiarization with its unique tonal, textural, and scale qualities. All seven MSS and RBV bands and the bulk color composite for frame number 1002-18140 (Monterey area) were examined with the aim of selecting the most appropriate band for vegetation studies. The results indicated that, of the seven black-and-white bands, MSS band 5 was most suitable for vegetation mapping purposes.

Through the use of both the color composite and band 5 (imaging in the red portion of the spectrum from .6 - .7 microns), vegetation boundary delineations were drawn using cellulose acetate overlays. These maps were then compared with the 1:120,000 and 1:60,000 vegetation data base maps prepared from high altitude color infrared photography.

After the ERTS-1 imagery had been compared with the conventional photography and vegetation data base maps, it was possible to determine relevant tonal ranges, textural characteristics, shapes, and locational parameters for each vegetation community under consideration. From these data, a descriptive interpretation key was prepared (see Table 6.11), which was utilized for the preliminary interpretation of ERTS-1 data.

Preliminary interpretation and mapping for both sample test sites was performed utilizing photographic enlargements of ERTS-1 images

TABLE 6.11. VEGETATION INTERPRETATION KEYS

Classification	Symbol	Tone	Texture	Shape	Distribution	Community Characteristics
Barren	Ba	white to light grey	continuous		In man-induced and naturally disturbed areas.	Mostly lacking or devoid of vegetation.
Coastal Strand	Sr	light grey to grey	continuous to streaked		Dunes and sandy beaches dispersed along entire coast with community variability from north to south.	Consists of low prostrate vegetation, often succulent woody perennials. Genera include: Atriplex, Franseria, Lupinus, and Abronia.
Coastal Salt Marsh	Ma_{sm}	dark grey to black	continuous		Coastal habitats, sea level to 10 feet, most extensive on tidal flats and lagoons.	Lacking perennial grasses. Mostly succulents, herbs or shrubs and prostrate vegetation. Characteristic genera include Salicornia, Suaeda, and Distichlis.
Coastal Sagebrush (Soft Chaparral)	Scs	Grey	mottled		Transverse, peninsula and South Coast Ranges to Baja, California. Mostly below 3,000 feet between the ocean and chaparral communities.	Occurring on dry and semi-rocky moderate to steep south and west facing slopes. Shrubs 1-5 feet in height with fasciculate leaves. Fairly continuous ground cover although less dense than chaparral. Characteristic genera include Salvia, Artemesia, Baccharis, and Eriogonum.

TABLE 6.11. (Continued)

Classification	Symbol	Tone	Texture	Shape	Distribution	Community Characteristics
Chaparral	Sc	dark grey to black	mottled to patchy		Coast Ranges from southern California to Mexico, notably in San Luis Obispo and Santa Barbara counties. Occurring in dry, rocky slopes and ridges often north facing on lower altitudes and south facing on higher altitudes to 6,000 feet.	Pyrophytic and evergreen shrubs. Dense, broad-leaved, and sclerophyll vegetation, 3 to 15 feet in height. Occurring as a continuous, often impenetrable cover. Characteristic genera include: Adenostoma, Ceonothus, and Arctostaphylos.
Desert Scrub	Sd	light grey to grey	mottled	some fence-lines along edges.	Throughout the San Joaquin Valley in arid lowland environments; primarily in sites not suitable for agriculture.	Sparse low vegetation characterized by dominant shrubs such as Prosopis, Atriplex, Artemesia, Allenrolfia and Suaeda plus an understory of annual grasses such as Bromus, Schismus, etc.
Grass-land	G	light grey	continuous		Low hot valleys of coast ranges on clay soils from sea level to 3,000 feet.	Uncultivated grasses and low associated herbaceous plants. Characteristic genera include indigenous Stipa, Poa, and Aristida, and replacement genera including Bromus, Avena, Festuca.
Wood-land Savanna	WS	light grey to grey	mottled to patchy		Occurring in areas of mergent grass and woodland from sea level to 6,000 feet.	Open stands of broad-leaved trees and evergreen with intermittent grass and herbaceous vegetation. Refer to Forest Hardwood and Grassland.

TABLE 6.11. (Continued)

Classification	Symbol	Tone	Texture	Shape	Distribution	Community Characteristics
Scrub-Hardwood	Shw	dark grey to black	mottled		Refer to Hardwood Forest.	Open stands of broad-leaved trees with open spaces occupied by sagebrush, chaparral, and low herbaceous vegetation.
Forest Hardwood	Fhw	Black	continuous to mottled		Semi-rocky to clay soils on foothills and in valleys. Inner coast ranges from sea level to 4,000 feet.	Mixed or homogeneous stands of broad-leaved species 15 to 70 feet in height forming a closed or nearly closed canopy. Characteristic genera include: Quercus, Pinus, and Umbellularia
Forest-coniferous	Fco	Black	mottled		Coastal ranges from sea level to 12,000 feet.	Dense stands of homogeneous or mixed coniferous trees ranging from 10 to over 100 feet in height. Closed or nearly closed canopy. Characteristic species include Pinus muricata, P. radiata, and Cupressus sargentii.
Riparian	R	Dark grey to black	mottled to patchy	thin streamers, sometimes patchy	Species of trees and shrubs restricted to streambank environments from sea level to 6,000 feet.	Broad leaved trees 10 to 70 feet in height forming a dense crown cover. Understory consisting of low shrub and herbaceous growth (generally phreatophytic) along stream course. Characteristic genera include: Platanus, Acer, Alnus, Populus, and Salix.
Agriculture	Ag	dark grey to black	continuous	rectangular	Coastal and mountain regions.	Regularly cut hay lands, cultivated and irrigated fields.
Water body	WB	black	continuous		Marine and terrestrial.	

1002-18140 (July 25, 1972) of the Morro Bay area, and 1091-18064 (October 22, 1972) of the San Joaquin Valley area. The resultant scales were approximately 1:290,000 and 1:250,000 respectively.

Through use of the information contained in the photo interpretation key in Table 6.11, plus an a priori knowledge of the vegetation associations of these areas, complete vegetation maps for the two sample areas were prepared on acetate overlays.

After completion, the maps of the sample areas prepared from ERTS-1 data were compared to maps constructed from high altitude photography and ground truth data. The comparison and subsequent evaluation indicated that some vegetation categories were too detailed for interpretation from ERTS-1 data, while others were not identifiable with any reliable degree of consistency. Consequently, the initial vegetation classification system was modified preparatory to the construction of the Central Region Vegetation Data Base. The revised system comprised 17 categories (see Table 6.12), and reflected an assessment of what categories would be most compatible with ERTS-type data based on the preliminary mapping that was accomplished.

Coincident with the testing of the classification system, an evaluation of the optimum dates for interpretation of particular vegetation association categories from ERTS-1 data was performed. The purpose of the evaluation was to effectively utilize the opportunity for a multidate mapping approach afforded by ERTS-1 data. Five image dates, representative of seasonal variations, were selected for each vegetation association category. Each vegetation association was interpreted on band 5 for the five dates, and a final assessment was made as to the optimum time period for differentiating a particular vegetation association from its surrounding environment. The results of this testing can be seen in the Cross-Evaluation chart in Table 6.13. This table formed the basis for selecting particular images to be used in the construction of the Central Region Vegetation Data Base.

6.6.5 Central Region Vegetation Data Base

The actual interpretation and mapping of the vegetation in the Central Region was done by three skilled interpreters, who were familiar with the characteristic vegetation types in the area. The interpretation was done on the original black-and-white, 1:1,000,000 scale, 9.5 x 9.5-inch transparencies. For each scene or area imaged on a given frame, at least two bands (generally bands 5 and 7) were interpreted in concert to fully utilize the significant information from both the visible and infrared portions of the spectrum. Two or more dates were also utilized for each scene to exploit seasonal variations that might improve identification and delineation accuracy. The actual identification of the different vegetation associations was based solely on tonal differences, macrotextural differences, and locational data on the ERTS-1 imagery.

TABLE 6.12. VEGETATION CLASSIFICATION USED FOR VEGETATION DATA BASE MAPPING OF THE CENTRAL REGION TEST SITE

1. Barren
2. Strand
3. Marsh
4. Grassland
5. Soft Chaparral
6. Hard Chaparral
7. Scrub
8. Scrub Grassland
9. Scrub Hardwood
10. Woodland Savanna
11. Hardwood Forest
12. Coniferous Forest
13. Desert Scrub
14. Riparian
15. Agriculture
16. Urban
17. Waterbodies

TABLE 6.13. CROSS-EVALUATION CHART SHOWING OPTIMUM MONTHS FOR DIFFERENTIATING VEGETATION ASSOCIATIONS ON ERTS-1 IMAGERY

	Barren	Strand	Marsh	Grassland	Soft Chap.	Hard Chap.	Scrub	Scrub Gras.	Scrub Hrd.	Wild Sav.	Hrd. Forest	Riparian	Agriculture	Urban
Barren		5	5	10	10	10	10	10	10	10	10	5	5	5
Strand	8		8	8	8	8	8	8	8	8	8	8	8	8
Marsh	10	8		10	10	10	10	10	10	10	10	10	10	10
Grassland	10	10	10		3	10	8	8	3	3	1	5	8	N
Soft Chap.	10	8	10	3		8	3	3	3	10	10	5	5	5
Hard Chap.	10	8	10	10	8		3	3	3	8	1	8	8	8
Scrub	10	8	10	8	3	3		1	N	N	3	8	8	8
Scrub Gras.	10	8	10	8	3	3	1		3	3	1	8	8	8
Scrub Hrd.	10	8	10	3	3	3	N	3		3	8	8	8	8
Wdl. Sav.	10	8	10	3	10	8	N	3	3		1	8	8	8
Hrd. Forest	10	8	10	1	10	1	3	1	8	1		8	8	8
Riparian	5	8	10	5	5	8	8	8	8	8	8		8	8
Agriculture	5	8	10	8	5	8	8	8	8	8	8	8		8
Urban	5	8	10	N	5	8	8	8	8	8	8	8	8	

N - no optimum
1 - Jan.
3 - Mar.
5 - May
8 - Aug.
10 - Oct.

The interpretation was carried out utilizing hand magnifiers and Zeiss stereoscopes (when reinforcement and/or combination of images was desired, or when limited stereoscopic viewing was possible). The original mapping was completed on individual acetate overlays and later transferred to a single map base.

The minimum mapping unit, i.e., the smallest area that was classified as to given vegetation association, was 2.641 square kilometers. At a scale of 1:1,000,000, 2.641 square kilometers equals approximately 0.026 square centimeters on the image. Accordingly, it was felt that units smaller than 2.641 square kilometers would be comparatively insignificant, and unmappable, at a scale of 1:1,000,000. As a consequence of the selection of this minimum mapping unit, certain vegetational features (such as the kelp concentrations and areas of riparian vegetation) were too limited in areal extent to merit mapping at the ERTS-1 scale. However, it has been possible to map and determine the areal extent of these areas (as documented in section 6.4 and 6.5), using five to ten times (5x to 10x) enlargements of the ERTS-1 imagery.

Upon completion, the 1:1,000,000 data base map of the vegetation association of the Central Region test site (Figure 6.8) was evaluated by: (1) comparing the mapping accuracy (i.e., delineation of vegetation boundaries) with similar maps constructed utilizing 1972 NASA High Altitude photography; (2) viewing analagous areas on color and color infrared high altitude photography (at scales of 1:60,000, 1:120,000 and 1:390,000) on which a majority of the mapping categories could be consistently identified; and, (3) selectively ground truthing areas to determine variable species composition in the major associations throughout the region.

The major problem encountered in working with the ERTS-1 imagery was the difficulty in differentiating between woody and arborescent vegetation, such as hard chaparral, hardwood forests, and coniferous forest. Based on tonal variations alone, these associations tend to range from dark grey to black and are very difficult to differentiate. Nevertheless, some differentiations can be made based on geographical location (i.e., proximity to the coast or location in mountainous areas). The Cross-Evaluation chart (Table 6.14) shows the relative ease of differentiation between the vegetation associations. The ratings are based not only on tonal, macrotextural differences, and locational factors, but also on the use of the multidate and multiband aspects of ERTS-1 images. The ratings indicate that there is reasonably high accuracy for differentiating between some of the individual categories. However, in attempting to differentiate between a given category and all other possible categories, the identification accuracy is considerably reduced owing to the similar signature and geographic distributions of different vegetation association. Table 6.15 provides a list of vegetation associations, or groups of vegetation associations, which can be accurately differentiated from each other, but within each group

Figure 6.8. ERTS-1 central region vegetation map.

TABLE 6.15. VEGETATION ASSOCIATIONS OR GROUPS OF VEGETATION ASSOCIATIONS WHICH HAVE SIMILAR SPECTRAL SIGNATURES AND LOCATIONAL CHARACTERISTICS

The members within each group are generally very difficult to differentiate from one another.

I	VI
Barren	Woodland Savanna
	Scrub Grassland
II	
Strand	VII
	Soft Chaparral
III	Hard Chaparral
Marsh	Scrub
Waterbodies	Scrub Hardwood
	Hardwood Forest
IV	Conifer Forest
Grassland	
	VIII
V	Riparian
Desert Scrub	
	IX
VI	Agricultural
Woodland Savanna	
Scrub Grassland	X
	Urban

TABLE 6.14. CROSS-EVALUATION CHART SHOWING THE RELATIVE EASE OF DIFFERENTIATING BETWEEN VEGETATION ASSOCIATIONS ON ERTS-1 IMAGERY BASED ON INTERPRETATIONS PERFORMED USING MULTIBAND-MULTIDATE ERTS-1 DATA

	Barren	Strand	Marsh	Grassland	Soft Chaparral	Hard Chaparral	Scrub	Scrub Grassland	Scrub Hardwood	Woodland Savanna	Hardwood Forest	Coniferous Forest	Desert Scrub	Riparian	Agricultural	Urban	Waterbodies	Composite
Barren		+	++	++	++	++	++	++	++	++	++	++	+	++	++	++	++	++
Strand	+		++	++	++	++	++	++	++	++	++	++	++	++	++	+	++	++
Marsh	++	++		++	-	+	+	++	++	++	++	++	++	+	++	++	-	-
Grassland	++	++	++		++	++	++	-	++	+	++	++	+	++	+	++	++	++
Soft Chaparral	++	++	++	++	--	--	--	+	+	+	-	+	++	+	++	++	++	--
Hard Chaparral	++	++	+	++	--		--	+	--	++	--	-	++	+	++	++	++	--
Scrub	++	++	+	++	--	--		+	--	+	--	-	++	++	++	++	++	-
Scrub Grassland	++	++	++	-	+	+	+		+	--	++	++	-	++	++	++	++	-
Scrub Hardwood	++	++	++	++	+	--	--	+		+	--	--	++	-	++	++	++	+
Woodland Savanna	++	++	++	+	+	++	+	--	+		+	++	+	++	++	++	++	+
Hardwood Forest	++	++	++	++	-	--	--	++	--	+		--	++	-	++	++	++	--
Coniferous Forest	++	++	++	++	+	-	-	++	--	++	--		++	+	++	++	++	--
Desert Scrub	+	++	++	+	++	++	++	-	++	+	++	++		++	++	++	++	+
Riparian	++	++	+	++	+	+	++	++	-	++	-	+	++		-	++	++	-
Agricultural	++	++	++	+	++	++	++	++	++	++	++	++	++	-		+	++	++
Urban	++	+	++	++	++	++	++	++	++	++	++	++	++	++	+		++	++
Waterbodies	++	++	-	++	++	++	++	++	++	++	++	++	++	++	+	++		++

++ Excellent Differentiation (approximately 100%)
+ Good Differentiation (limited confusion)
- Limited Differentiation (often confused)
-- Poor Differentiation (undifferentiable in most cases)

correct identification is generally very difficult. The major difficulty is in differentiating between woody vegetation types (comprised of tree and woody shrubs). Grassland associations, or areas having relatively high concentrations of grass, can generally be easily differentiated from the more woody associations. Despite the difficulty of differentiating between woody vegetation associations, it should be emphasized that ten distinct vegetation categories can be identified with a relatively high degree of accuracy. The most significant of the results of the vegetation mapping using ERTS-1 imagery may be summarized as follows: (1) the realization of its value as a mapping base on which accurate, continuous boundaries of major vegetation units can be delineated; (2) the ability to improve identification and delineation results with multidate imagery received on a regular basis; and, (3) the use of ERTS-1 imagery for the selection of optimal areas for verification of interpretation results, either by utilizing limited conventional aerial photography or ground reconnaissance techniques.

6.6.6 Conclusions

The completion of the vegetation data base map for the entire 52,213 square kilometer Central Region area showed that the use of multidate, multiband ERTS-1 imagery permitted rapid and accurate delineation of major vegetation associations. An evaluation of the map (see Figure 6.8) indicated that most of the major physiognomic vegetation groupings (e.g., forest, scrubland, grassland, savanna, etc.) can be mapped with an accuracy comparable to that obtained using conventional high altitude photography. Through the use of ERTS-1 imagery, it should be possible to rapidly update valuable vegetation resource data on a regional basis. With varying degrees of accuracy, 17 different vegetation units could be identified (see Table 6.12). These 17 different vegetation units comprise the modified vegetation classification scheme, which resulted from the previously mentioned preliminary mapping studies. Each of these different vegetation units represents basic differences in site characteristics. In most cases these may indicate either the developmental potential of an area or the effect, favorable or unfavorable, that man has had on the area.

The time saving resulting from the interpreter's ability to continuously map large areas eliminates difficulties commonly encountered when utilizing conventional aerial photomosaics. The time required to map the entire 52,213 square kilometer area was approximately 10 man-days. A large proportion of this time included familiarization with the small scale imagery, the selection of optimal dates, and general familiarization with the variable tonal characteristics of the different vegetation types over time. Given present expertise, the completion of vegetation maps of similar size, scale, and areal extent should require no more than 3-5 man-days.

The major drawbacks of utilizing ERTS-1 data for vegetation mapping seem to be: (1) the broad classification systems used with ERTS imagery (i.e., grouping more specific units into more general categories) may be of only marginal use for land use planning purposes; and, (2) in order to achieve an acceptable level of identification accuracy, the mapping must be performed by interpreters who are well acquainted with the vegetation associations and their geographic distribution. An alternative would be the utilization of a well-coordinated program of high altitude photography and ground reconnaissance to verify identifications. There is still a need for some reliance on ground reconnaisance, selective use of coincident conventional aerial photography, or a priori knowledge of the vegetation in order to accurately identify the vegetation units that are detectable on ERTS-1 imagery.

6.7 CONCLUSIONS

The results of the investigations discussed in the preceding sections indicate that ERTS-1 type data can be a valuable source for environmental resource information needs. The resolution of ERTS-1 data places constraints upon the detail to which specific environmental phenomena can be investigated. Furthermore, the resolution limitations create certain problems for the investigation of environments where a high diversity of phenomena are localized in small areal units, such as the coastal portion of the Central Region of California. However, these limitations are mitigated to a large degree through the synoptic perspective afforded by ERTS-1. ERTS-1 data provide a capability to inventory resources over extremely extensive areas (e.g., the 52,213 square kilometer area of the Central Region), and generate data for these areas at essentially a single point in time. Although the detail of information may be insufficient for specialized user requirements, the advantage of this synoptic view is that large scale environmental resource information can be: (1) obtained within a standardized format for a single date; and, (2) monitored and updated with comparative ease and frequency to reflect changing resource conditions. This is not feasible utilizing conventional data collection methods.

With respect to the specific studies which the Geography Remote Sensing Unit has conducted, the following conclusions can be made:

Land Use

1. Urban areas can be differentiated best on MSS bands 4 and 5.

2. Transportation linkages (highways, roads, airports, canals) are most readily defined from MSS band 7.

3. Agricultural field boundaries are adequately identifiable on MSS bands 4 - 7, and most clearly defined on band 7.

4. Cultivated land can be mapped accurately (under 5 percent error) from MSS band 5. Fallow land identification explains the majority of error.

5. Land use is difficult to map in the California coastal environment because many individual use categories occupy very small areal units; land use mapping is easier and capable of more sophisticated refinements in the arid California Central Valley.

6. Macro-level land use change can be identified, mapped, and measured with a high degree of reliability.

Crop Identification

1. Non-vegetated (bare soil) field conditions are identifiable with almost 100 percent accuracy (negligible errors of omission or commission).

2. It is difficult to identify specific crops on a single date because of signature overlap.

3. Identification accuracies can be improved by a multidate analytical approach, since crop growth cycles are reflected in progressively changing tonal signatures on ERTS-1 imagery over time.

Drainage and Landform Mapping

1. Drainage networks and basins can be mapped with sufficient accuracy to permit updating of U.S.G.S. 1:250,000 topographic maps.

2. Macro-scale landform mapping is feasible.

Kelp (Macrocystis)

1. Kelp concentrations can be identified and located accurately.

2. Boundaries of kelp concentrations can be delimited accurately and good areal estimations made.

3. Internal variations within kelp concentrations are detectable (probably related to density) and may, in conjunction with estimates of areal extent, provide an indication of biomass.

Forest Fire Damage

1. The perimeter of forest fire damage can be accurately delimited.

2. "Islands," or pockets of unburned vegetation, can be identified and mapped.

3. Burn area of previous forest fires (at least one year in the past) can be identified and mapped.

Vegetation Mapping

1. Barren land, Coastal Strand, Coastal Salt Marsh, Grassland, Scrub Hardwood, and Agricultural vegetation exhibit good differentiation.

2. Coastal Sagebrush, Chaparral, Woodland-Savannah, Forest Hardwood, and Riparian vegetation exhibit limited differentiation.

3. Coniferous forest is difficult to differentiate.

4. Individuals, with comparatively minor training in photo interpretation and vegetation identification, can perform vegetation mapping at reasonable levels of accuracy; more specifically, at the association rather than the community level. This indicates that ERTS-1 type technology should be transferable into operational usage for this type of resource inventory.

5. Some problems in the interpretation of specific vegetation associations may be mitigated through selective use of ground or light aircraft reconnaissance.

The successes resulting from these specific investigations are primarily attributable to the multiband (opportunity to view phenomena that are highlighted in different bands) and multidate (certain phenomena are more observable during particular seasons of the year) aspects of ERTS-1 data. Perhaps most significantly, it is estimated that each of the Central Region data base maps (encompassing an area of approximately 52,213 square kilometers) could be constructed for a different time period in approximately one man-week. These considerations indicate that ERTS-1 type data should provide significant input to resource management and planning at regional, or larger, scales.

ERTS IMAGE DESCRIPTOR FORM

(See Instructions on Back)

NDPF USE ONLY
D _____
N _____
ID _____

DATE _____

PRINCIPAL INVESTIGATOR _____

GSFC _____

ORGANIZATION _____

PRODUCT ID (INCLUDE BAND AND PRODUCT)	FREQUENTLY USED DESCRIPTORS*			DESCRIPTORS
	Land-use	Veg.	Geology	
1251 17565M				Clouds
1256 18242M				Clouds, Bay
1287 17564M				Clouds
1269 17565M	X	X	X	
1291 18182M	X	X	X	Bay
1291 18184M	X	X	X	
1273 18183M	X	X	X	Bay
1273 18185M	X	X	X	
1289 18081M	X	X	X	Islands
1289 18072M	X	X	X	
1289 18074M	X	X	X	
1290 18124M	X	X	X	
1290 18130M	X	X	X	
1290 18133M	X	X	X	
1274 18241M	X	X	X	Bay
1305 17563M				Clouds, Haze
1252 18021	X	X	X	Clouds, Urban Area
1252 18023				Islands
1272 18131	X	X	X	
1272 18133	X	X	X	Sand Dunes
1272 18924	X	X	X	Snow, Urban Area, Sedimentation
1292 18240				Haze, Bay, Urban Area
1306 18015				Clouds, Haze
1306 18021				Clouds
1323 17562				Fog, Haze
1324 18014	X	X	X	Fog, Desert
1324 18020				Clouds

*FOR DESCRIPTORS WHICH WILL OCCUR FREQUENTLY, WRITE THE DESCRIPTOR TERMS IN THESE COLUMN HEADING SPACES NOW AND USE A CHECK (✓) MARK IN THE APPROPRIATE PRODUCT ID LINES. (FOR OTHER DESCRIPTORS, WRITE THE TERM UNDER THE DESCRIPTORS COLUMN).

MAIL TO ERTS USER SERVICES
CODE 563
BLDG 23 ROOM E413
NASA GSFC
GREENBELT, MD. 20771
301-982-5406

GSFC 37-2 (7/72)

Chapter 7

USE OF ERTS-1 DATA TO ASSESS AND MONITOR CHANGE IN THE SOUTHERN CALIFORNIA ENVIRONMENT (UN314)

Co-Investigator: Leonard W. Bowden

Contributors: J. Viellenave, C. Johnson, J. Bale, J. Huning, R. Pease, R. Petersen, R. Minnich, A. Sullivan, C. Hutchinson, K. Rozelle, G. Tapper, K. White, C. Arthur

Department of Geography, Riverside Campus

TABLE OF CONTENTS

7.1 INTRODUCTION

The research effort at UCR, associated with this integrated study, has consisted of attempts to determine the value of ERTS-1 and similar data for analysis of environmental problems in a variety of regions in Southern California. Initial investigations dealt mainly with general land use patterns and changes, but advanced methods of displaying and enhancing the imagery have made it possible to conduct more detailed studies of specific environments.

7.1.1 Data Acquisition

The latest ERTS-1 imagery which our group has received was that of May 5, 1973. Preliminary evaluations have been made of all frames, and some color combinations have been produced. Acquisition of a Mini-Addcol Viewer from International Systems Inc. (I^2S) has made it possible to perform color combinations to simulate true color and CIR images as well as a variety of other color combinations. The Mini-Addcol Viewer allows better image registration and a greater variety of color combinations than the Diazochrome method which we previously have used, though image and color qualities vary according to the phenomena under study.

The data from the U-2 flights were of significant value for detailed interpretation and verification of patterns extracted from ERTS-1 data. The detailed studies were limited, however, to the areas covered by U-2 flights. This restricted us to making a less detailed analysis of most of the desert areas, based primarily on ERTS-1 imagery, because very little U-2 imagery exists for coverage of the northern Mojave Desert in which these studies were made.

7.1.2 Relationship to Non-ERTS-1 Research and Science

7.1.2.1 Information and Application Assistance

The receipt of ERTS imagery has generated considerable interest throughout the public and scientific community in Southern California. The number of weekly visits by prospective users has doubled in the past six months. It is, of course, a major function of the University, in addition to research, to help disseminate new information and technology to the public and other scientific groups. The expertise and the data file that have been accumulated at Riverside over the past six years provide a natural attraction to researchers. Appendix A lists some of the universities, colleges, public agencies, and private industries which have been assisted within the last six months here at UCR. The list briefly describes the kinds of projects which have brought to us the research groups in question.

7.1.2.2 Integration with NASA NGL 05-003-404 Grant

The acquisition of ERTS-1 satellite and high altitude aircraft (U-2) data has assisted in the NASA funded "Integrated Study of Earth Resources in the State of California Using Remote Sensing Techniques." Two particular studies under this contract have been: (1) the development of an environmental data base for Southern California, and (2) a study of urban-regional land use in the Riverside-San Bernardino-Ontario standard metropolitan statistical area.

Environmental Data Base

The major objective is to generate a data base reflective of the conditions, processes and important features present within the coastal environment. The development of an information base requires that two functions be performed: (1) image (data) interpretation, and (2) interfacing of data with a geographic information system. The interpretation function is currently being undertaken in the area of Orange and northern San Diego Counties. (See Section 7.2.2.)

The initial data source used in this study was the high altitude imagery from NASA Mission 164. Since the receipt of the recent U-2 imagery, secondary interpretation and sequential analysis have proved useful in verifying and modifying previous evaluations.

Urban Regional Land Use

The metropolitan area of which Riverside and San Bernardino form the core, has been selected by USGS as one of 26 sites for study of urban land use under the Urban Atlas Project. The basic data gathering system, of mapping land use information on USGS 1:24,000 sheets, is being continued until its completion. Computer maps are being prepared from the base data. Five quadrangles have been finished and are mosaiced together (Figure 7.1).

This large scale data base, while useful in its present condition, also allows rapid and useful correlation with ERTS-1 and ERTS-B imagery. The sequential nature of ERTS-1 imagery fits in well with the requirements of the project, including those of monitoring urban and regional land use changes. The conversion of conventionally mapped data into a format for computer storage and manipulation allows quick comparisons of several dates, and thus rapid assessment and calculation of urban changes.

Present plans include the production of a technical report summarizing all the work of the project at UCR. It will include details on the methodology and techniques as well as analysis of data from selected sites in the study area. This paper will provide local county and city planners with quantitative data and adaptable techniques for their use

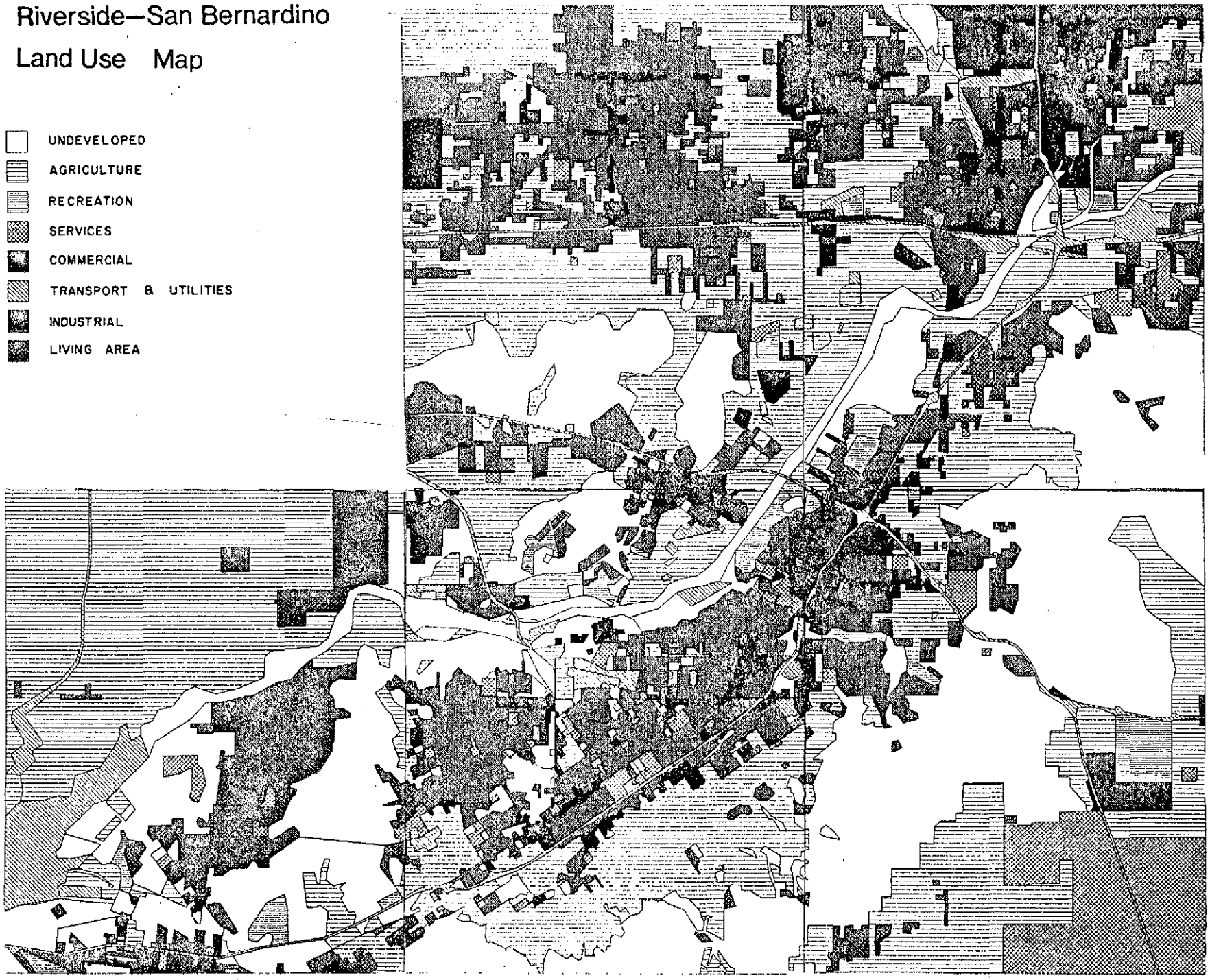

Figure 7.1. Riverside-San Bernardino land use map.

in evaluating land use changes and processes occurring in the area. It also reflects the ability and intention of this research program to go beyond the limited objectives stipulated by USGS and make information available for practical, local agency utilization.

7.2 ACCOMPLISHMENTS

The general objectives of the investigations conducted by UCR under the ERTS-1 program are listed as: (1) mapping of general land use patterns in rural and urban regions of Southern California; (2) monitoring of changes in land use, particularly in urban and rural/urban locations and with additional emphasis placed upon analysis of wildland areas coming under urban and/or agricultural pressures; (3) monitoring environmental pollution in Southern California basins; and, (4) developing models defining "environmental quality."

Out of these goals have grown a series of specific studies. In some cases, the concepts of these individual studies are included under more than one of the four prescribed goals, lending greater importance to the studies and demonstrating greater utility of ERTS-1 data.

The synopses of three studies are described first in the following three sub-sections. The studies represent the kind and scope of effort initiated during the first part of the contract year and consequently are the three studies which are closer to completion. The first is the monitoring of cyclic crop production with the objective to develop a semi-automated system of identification of specific crop types in the Imperial Valley. The second study was designed to create a vegetation classification system, functional with ERTS-1 data, and to produce a map of the floral distributions of Orange County. The last study focuses upon land use changes in the Coachella Valley.

Included also in this section are reports of projects presently underway which require not only high altitude imagery (U-2), but also good quality ERTS-1 imagery as well. The lack of a refined method of multi-spectral color combination and enhancement forced a delay in the research efforts for these studies. These summaries represent the extent of significant results gained from the research conducted thus far. These projects vary widely in subject matter and location, although most are contained within the Desert regions.

7.2.1 Monitoring Crop Changes in the Imperial Valley from ERTS-1 Data

Based on our studies to date, sequential satellite imagery can provide sufficient data to determine specific field conditions with 97 percent accuracy, and specific crop identification for any one field can be achieved with a 92 percent accuracy. Techniques being developed at the University of California, Riverside, utilize the color infrared returns from an ERTS-1 color combined image of multispectral bands 4,

5, and 7 (Figure 7.2a). Combining the interpretation procedures of the imagery with a computerized program that compares the data to the actual crop calendar of the region, each field of 20 acres or more can be monitored over a minimum of four sequential 36 day cycles and subsequently identified by the computer as to the most probable crop that is growing within that field.

ERTS-1 images of 1972 of 26 August, 1 October, 6 November, and 12 December were interpreted for the experiment and results compared to approximately 10 percent of the total field population (biased sample) that had been ground surveyed. The results discussed in this report are based on this comparison. Although the ground survey fields were biased by accessibility to hard surfaced roads, the percentage breakdown by total number of crops by field and by acreage are almost identical to the Imperial Irrigation Report percentage breakdown of crops growing as of December 31, 1972.

Initial interpretation of the first complete ERTS-1 image of the Imperial Valley (26 August 1972; 1015-17440M) showed that the quality and resolution of the image is better than that of Apollo 9. Superimposition of the color combined ERTS image onto a base map controlled by USGS topographic maps (Figure 7.2b) enables field conditions to be interpreted for fields as small as ten acres and a few even smaller five acre plots. However, because of the uncertainty of detection (or identification) of all fields below twenty acres the project was limited to monitoring fields of twenty acres and greater. Preliminary computer processing of the data from the first image indicates the objectives of the research will be attained successfully. The primary objective is to develop a semi-automated system that will enable the identification of specific crops in each field and subsequently produce thematic computer maps for the Imperial Valley on a regular basis. A valuable and anticipated "spin-off" has already resulted from the analysis. The original categorization of field conditions into fields with growing crops, wet fields, plowed fields, and dry fields makes it possible to assess the irrigation requirements both currently and for the next two or three weeks. The assessment may be made within one to two days after receipt of the imagery.

The first thing noted on the imagery was the existence of four distinct colors within agricultural fields (Figure 7.2c). Growing crops with good ground cover are readily identifiable by the red color. Completely bare (fallow) fields present a distinctive white or "sand" color. Two other colors show a deep purple and a very light purple. The darker color proved to be irrigated or wet bare fields that have just been seeded. The lighter lavender color is an indication that the field has been freshly plowed. To these four categories it soon became obvious that a "no data" category was required for those instances where it is impossible to distinguish the field condition due to imperfections, cloud cover, or other causes. We have found that further refinements

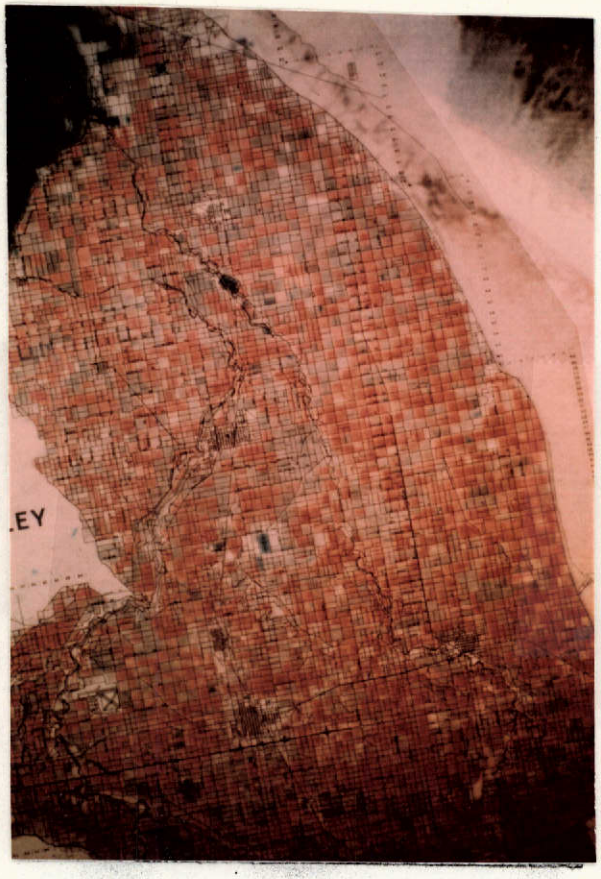

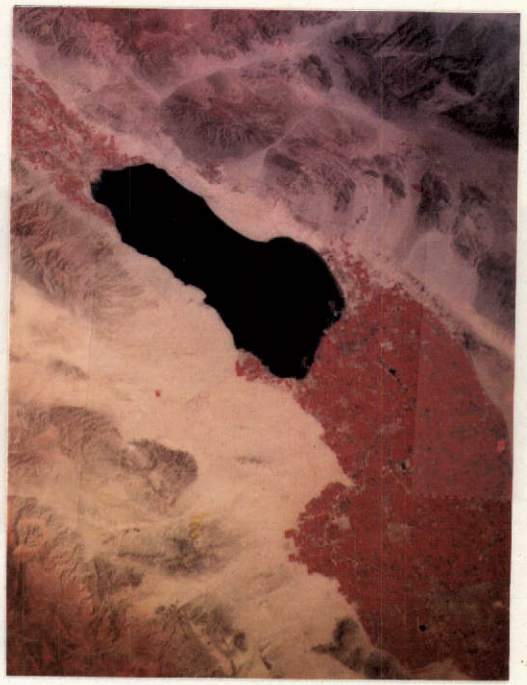

A B C

Figure 7.2. Color infrared images of the Imperial Valley, California. Figure 7.2A (October 1, 1972) shows the relatively small number of growing crops indicated by the red return (33 percent). Figure 7.2B is a combined image of December 12, 1972, with a super-imposed grid map for locating each of the more than 8,000 fields. Figure 7.2C is the image of March 30, 1973, indicating almost 85 percent crop cover within the fields.

can be added in late spring or summer due to the bronze color of mature small grains, the yellow color of grain stubble and the black color of burned grain stubble. These later indicators will be categorized as harvested crops. Within the boundaries of the study area are a variety of "permanent" crops (e.g., asparagus and citrus) as well as beef feeder lots. As these areas are identified by ground survey they will be located and eliminated from the interpretation process. Urban areas and the changes in their boundaries are detectable and excluded from the total agricultural acreage. Experience has shown that within the legal survey limits of each field approximately 10 percent of the area is devoted to off-site improvements which includes highways, roads, field access roads, canals, and farm equipment and hay lots. Therefore, in the compilation of the statistics an automatic 10 percent is deducted from each field. It is anticipated that ten categories will be sufficient to provide data input for the automatic identification system.

To facilitate the interpretation process as well as the computer mapping process, the valley was subdivided into seven arbitrary regions. These divisions were separated by boundaries that more or less divided the valley into regionalized agriculture. Regions 1 and 2 are primarily vegetable crops with most of the asparagus grown in region 1 and carrots in region 2. Regions 3 and 4 act as a transition from vegetable crops to field crops. The other three regions (5, 6, and 7) are predominantly large acreages (160 acres) of field crops. Crop regionalization will be one factor used in the automatic identification system.

Table 7.1 summarizes the field conditions interpreted from the 26 August ERTS-1 image. Approximately six man hours was required to determine the condition of the 8,861 fields of the Imperial Valley. Considerably more time was involved in transferring the data to machine cards. Future research will concentrate on making this process more automatic. The total of 464,496 agricultural acres agrees to within 1 percent with the farmable acres reported by the Imperial Irrigation District annual summary. Some difference is found in the decision to eliminate fields of less than twenty acres. Another point of difference may be found in the method of computing the acreage (e.g., different percentage used to compute off-site improvements). The total acreage of growing crops (154,429) representing one third of the farmable lands is expected for the month of August when daily temperatures rise above 110° almost every day of the month. Reference again to the Imperial Irrigation District Report of July 1972 and the crop calendar shows that the three major crops growing in August are: (1) alfalfa (over 100,000 acres); (2) cotton (30,000 acres); and, (3) sorghum (over 20,000 acres). Other minor crops (no more than 2,000 acres) which are in production on 26 August are: Sudan grass, Bermuda grass, onions, and fall melons. Although there are only seven crops to consider at this time of year it is still impossible to distinguish specific crops from a single image.

TABLE 7.1. IMPERIAL VALLEY -- FIELD CONDITIONS AUGUST 26, 1972.

REGION	TOTAL ACRES	NO DATA	GROWING CROPS	WET BARE FIELD	PLOWED BARE FIELDS	DRY BARE FIELD	HARVESTED CROPS	PERM CROP	FEED LOTS	AGRICUL OFFSITE	URBAN
1	58,255	2,047	23,211	4,846	11,371	9,180	342	27	243	5,698	1,290
2	54,455	968	19,014	4,361	8,327	13,367	1,300	324	720	5,379	695
3	111,771	2,380	33,087	1,728	28,233	26,876		288	562	10,352	8,265
4	119,629	1,390	37,603	3,510	37,048	22,461	220		301	11,396	5,700
5	74,203	689	22,599	805	17,415	24,627			287	7,381	400
6	78,131	594	15,503	1,075	28,364	23,877			309	7,749	660
7	38,047	1,189	3,412	99	5,089	23,228				3,670	1,360
TOTAL	534,491	9,257	154,429	16,424	135,847	143,616	1,862	639	2,422	51,625	18,370
Less URBAN	18,370										3.45%
	516,121										
Less OFFSITE	51,625									10%	
TOTAL AGRI ACREAGE	464,496	2.0%	33.3%	3.5%	29.2%	30.9%	0.4%	0.14%	0.5%		

Initial work with specific crop identification involved field condition data from four 36 day cycles between August 26 and December 12, 1972. Table 7.2 summarizes these findings. From the 8,000 plus fields in the Imperial Valley, 1,164 fields were studied, and their data used to test different approaches to crop identification. The 1,164 fields used were specifically selected because ground truth surveys were available for these fields, thus making it possible to check tentative conclusions about the crop growing in any one field, and facilitating perfection of the crop identification process. A computer card was made for each field, and each time more imagery was received, the condition of each field was coded and punched on the card.

The Imperial Valley Crop Calendar was used as a guide; however, it was found that the field condition code sequences obtained from ERTS-1 imagery differed from the idealized crop calendar because of the extremely wet fall and winter in the Imperial Valley in 1972. Therefore, it was necessary to depart from the idealized crop calendar. In order to devise a system for crop identification applicable to the time period in question, we examined carefully the code sequences of the sample fields, and recorded them. Then, we matched each field's code sequence, ground truth, and acreage. This allowed us to note several trends in the data, and to determine which crops would fit any particular sequence. Two significant things were noted at this time: (1) for any one sequence, crops varied if the field in question was over 80 acres or 80 acres or less, because field crops are more common in fields of over 80 acres, and (2) some crops could not be positively identified from only four periods because of similar code sequences and acreage sizes as other crops.

Steps were taken to incorporate the above two findings into a computer program designed to automatically identify crops from the input data. The first step was to divide fields with a certain sequence into fields with over 80 acres and fields with 80 acres or less. The second step was to establish "weights" relating to the probability of a particular crop growing under any code sequence. The weights were obtained by computing percentages of different crops in each code sequence. For example, a very common code is 1 1 1 1, indicating that the crop in that field was identified on ERTS-1 imagery as growing during each of the four periods considered. We determined that, for fields of over 80 acres and for that code sequence, the weighted values are:

Alfalfa 92 Sugar Beets 3 Cotton 3 Barley 2

Using only four cycles, uncertainty of identification for some sequences results. For example if the sequence is 1 1 1 2, with 80 acres or less, the identification and weights are:

Alfalfa 40 Cotton 38 Sorghum 13 Sudan Grass 6 Lettuce 3

TABLE 7.2. SUMMARY OF IMPERIAL VALLEY FIELD CONDITIONS DETECTED FROM ERTS-1.

Field Condition / ERTS Color Code	GROWING CROPS (Red) (1)	WET PLANTED (Purple) (2)	DAMP PLOWED (Lavender) (3)	DRY BARE (White) (4)	HARVESTED STUBBLE (Yellow) (5)	PERMENENT AGRICULTURAL (8)	NO DATA (0)
	(Acres) (%)	(Acres) (%)	(Acres) (%)	(Acres) (%)	(Acres) (%)	(Acres) (%)	(Acres) (%)
August 26	153,528 (33.3)	40,374 (8.8)	128,219 (27.8)	123,025 (26.7)	2,636 (0.6)	3,640 (0.8)	9,599 (2.1)
October 1	142,047 (30.9)	69,115 (15.0)	150,351 (32.7)	83,642 (18.2)	787 (0.2)	3,640 (0.8)	10,470 (2.3)
November 6	199,197 (43.3)	120,330 (26.2)	48,736 (10.6)	80,221 (17.4)	315 (0.1)	3,640 (0.8)	7,627 (1.7)
December 12	213,233 (46.3)	116,426 (25.2)	55,542 (12.0)	62,262 (13.5)	1,075 (0.2)	3,640 (0.8)	8,270 (1.7)

	TOTAL PRODUCING ACRES	FEED LOTS	FARM ASSOCIATED	OFFSITES (Roads, Canals)	TOTAL AGRICULTURAL	URBAN	TOTAL ACRES
	(Acres)	(Acres)	(Acres)	(Acres)	(Acres)	(Acres)	(Acres)
August 26	461,021	2,698	180	51,508	515,407	14,640	530,047
October 1	460,052	2,703	184	51,467	514,406	15,140	520,546
November 6	460,066	2,747	463	51,442	514,718	15,350	530,068
December 12	460,448	2,734	486	51,489	515,157	14,850	530,007

In this case, the addition of more code sequences would permit definite identification of the crop.

In the process of reviewing the fields and determining the weights, it became apparent that some codes fit no known crops. We designed the computer program to note all the fields with code sequences other than those of known crops. The irregular code sequences can then be checked to determine if human error in initial interpretation of the imagery occurred. If so, the error can be corrected, and the code identified. Another possibility with an irregular crop code is that a new crop is being grown, such as was the case with Alicia grass. In a few cases, data were not obtainable from the imagery for certain fields. The crops in these fields, obviously, could not be identified.

With the system outlined above, using only four periods, accuracy of specific crop identification varies. It is not usually possible to state for certain that one particular crop is growing in a field because several crops may have the same code sequence, and four time periods are enough for only preliminary identification of the crop growing in any one field. Our findings suggest that overall, an 81 percent accuracy can be expected if one accepts the two highest weights of any code sequence. With more sequential imagery interpretation, more accurate identification of a crop can be anticipated.

Conclusions

The system being developed shows great promise of achieving the objective of more than 90 percent accuracy of crop inventory for a given agricultural region. The experiment utilized only four 36 day cycles. Many more fields could have been identified if the cycles were extended to at least 6 time frames. More importantly, the system operating throughout the entire year would have the advantage of knowing the previous crop. In the Imperial Valley the previous crop is a great aid to identification and inventory procedures because there are restraints on crop rotation. Sugar beets for example must be planted before cotton has been picked. Therefore, sugar beets cannot follow a cotton crop. Watermelons cannot be planted in the same field for a five year period. Factors such as the above can be very useful in developing an automated crop inventory system. Future investigations should consider performing the task on a year around basis.

7.2.2 Mapping Vegetation in Orange County from ERTS-1 Data

Vegetation mapping from high flight U-2 imagery at small scales (1:131,000) can be accomplished with proper methodological procedures. These same techniques can be applied to the ERTS-1 imagery for interpretation of (generalized) vegetation patterns of the landscape. However, the greater perspective gained from ERTS-1 at greater altitudes can both aid and hinder investigation and accuracy.

Through the use of U-2, RC-10 high flight color infrared imagery, Orange County was mapped for vegetation and wildlife patterns. Development of a functional classification scheme is of primary importance. It must be coordinated with the capability of the imagery to record information as well as with the needs of the investigation. It was felt that the best accuracy could be achieved using ten vegetation classifications (Grassland, Coastal Sage, Chaparral, Oak Woodland, Pine Woodland, Riparian, Fresh Water Marsh and Salt Water Marsh) and five wildlife associations (large animals, small animals, upland birds, waterfowl, and saltwater birds) (Figure 7.3).

In formulating the classification system an intensive study of ERTS-1 imagery (band 7) and the U-2, RC-10 CIR imagery was required to determine patterns of specific tonal and texture registration. Careful attention was given to locational relationships such as slope orientation, drainage patterns, accessibility of wind systems and moisture, and elevation. Broad general patterns can be determined in the ERTS-1 photos and more specific and accurate delimitations made with the U-2 imagery.

Field checking was required to identify the specific signature pattern and determine the vegetative type characteristic of that registration. After a signature has been identified it can be applied to the entire study to delineate the vegetation type.

In this systematic development a functional classification system can be formulated based on observable data and geared to the photography. The methodology can be applied to any region for mapping vegetation and will yield accurate, comprehensive results.

Mapping of vegetation can provide a useful data base for planning, especially when introduced into a computer format with land use, landform, and hydrological data. Digital plotting of boundaries recorded from air photos can enable quantification of, heretofore, arbitrary information and quickly provide accurate, usable data.

7.2.3 Land Use in the Northern Coachella Valley

The initial design of this research concerned the qualitative evaluation of ERTS-1 imagery's utility as an information source for the detection of land use change. A by product, however, namely the regional perspective and relatively exact spatial relations provided by the imagery is potentially significant for regional planning and management decisions. Open space desert resources, in California, are under severe pressure to serve as a source for recreational gratification to individuals living in the heavily populated southern coastal plain. Concern for these sensitive arid environments (the Colorado and Mojave Deserts) has been expressed by both federal and state agencies. The northern half of the Coachella Valley, part of the Colorado Desert natural province, has long served

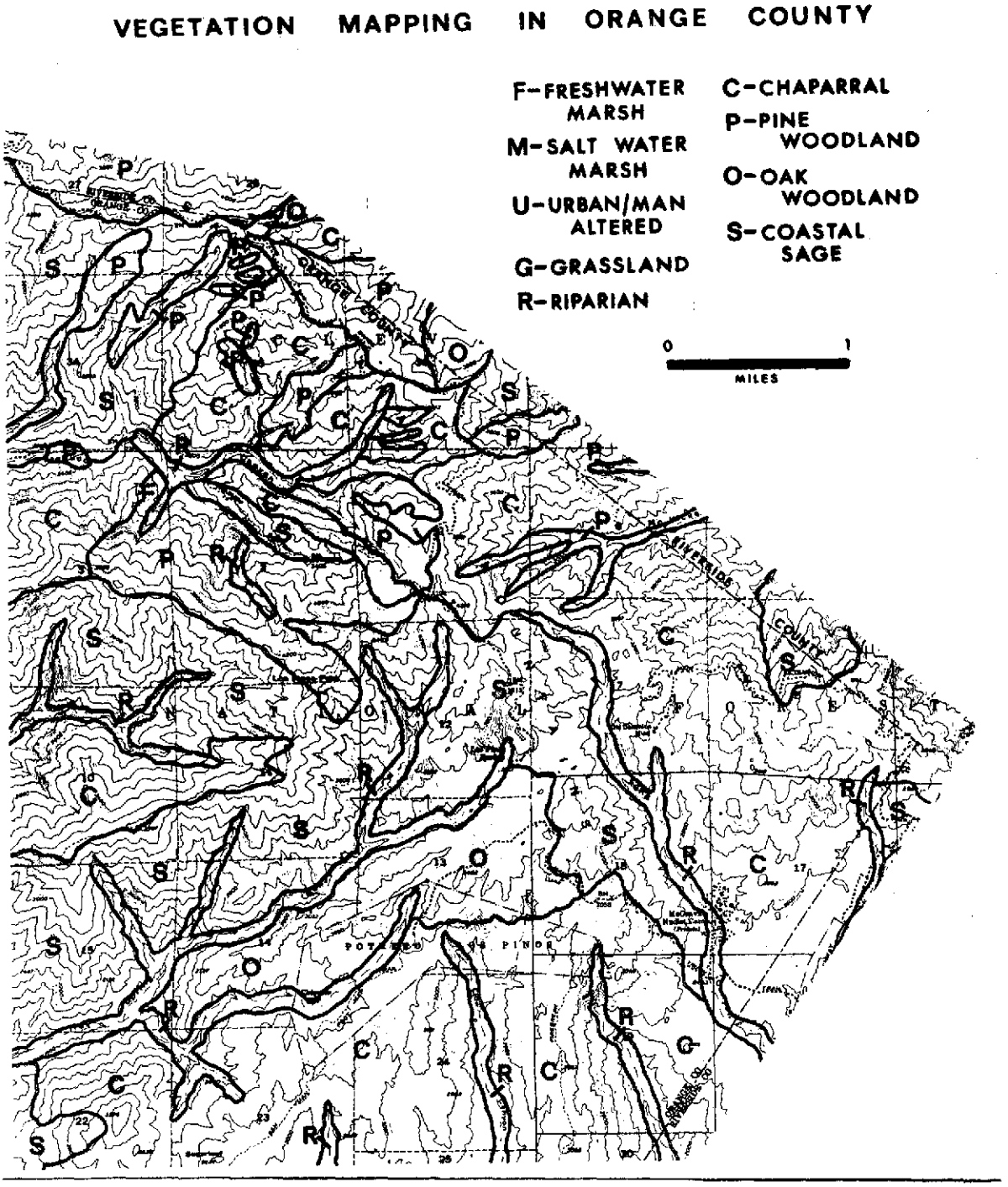

Figure 7.3. Vegetation mapping in Orange County.

as a focal point for weekend and seasonal (winter) recreational activity.

Area

The Coachella Valley is the northernmost extension of the Salton-Imperial Trough (Figure 7.4). Land use has traditionally been a contrast between agriculture and recreation. The valley is approximately 50 miles (80.5 km) long and averages less than 15 miles (24 km) in width. As a structural trough, it is bounded on both the north and southwest by the highest mountain ranges in Southern California. It terminates in the south at the Salton Sea and narrows to the north to form San Gorgonio Pass. If one wished to delimit geographic regions solely on physical characteristics, the Coachella would qualify. Dominant land use types dictate that the valley be divided into two regions (Glendinning, 1949). The northern half of the valley possesses a recreational economic base while the southern half from Indio to the Salton Sea depends primarily on an agricultural economic base. The investigation has been limited to the northern half of the valley where recent residential and recreation oriented building occurs at rates far above county averages.

Research Design

Research objectives involve the qualitative testing of ERTS-1 imagery as a data source for land use monitoring at the urban-rural fringe in the desert environment. Base land use information was obtained in 1966 and 1969. This information was then compared with the record obtained from ERTS-1 to produce a map of change. Analysis of the change, where it is concentrated, and how quickly it is occurring will provide insight into potential regional problems.

Data Sources

Although ERTS-1 imagery served as the primary data source, both U-2 and RB-57 photographs were also used. Field surveys and the aforementioned high altitude imagery allowed the information interpreted from ERTS-1 to be verified and more precisely located.

Two formats of ERTS-1 imagery were used with an I^2S Mini-Addcol Color Viewer to produce interpretable false color representations. 70 mm positives were used in their entirety, while only a portion of reproduced 9 x 9 inch (22.9 x 22.9 cm) positives were used. Diazochrome black-and-white positive transparencies were prepared from 9 x 9 inch (22.9 x 22.9 cm) ERTS positives. These were then cut to fit the 2-3/4 x 2-3/4 inch (6 x 6 cm) yoke format of the color viewer. The resulting scale, as visible on the ground glass view plate of the color viewer, was approximately 1:150,000. This technique provided more enlargement,

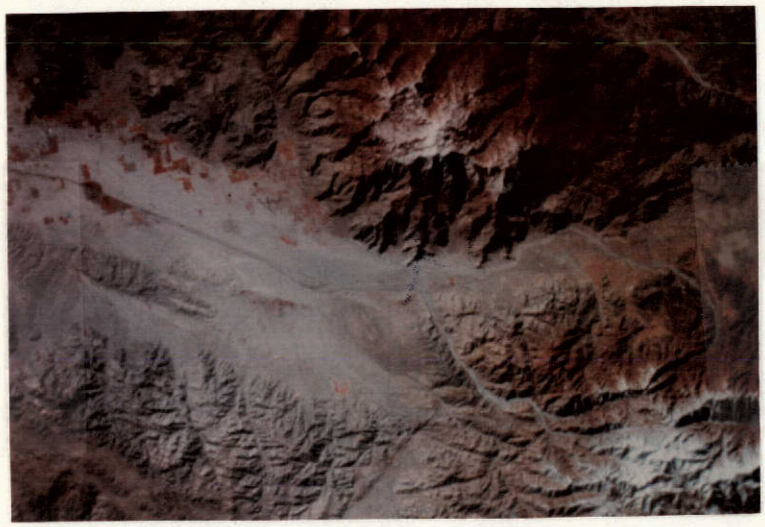

Figure 7.4. A portion of an ERTS-1 image showing the northern Coachella Valley. (Note: north is at bottom of photograph).

but less resolution than the enlarged 70 mm positive transparencies. MSS bands 4, 5 and 7 were used in three of the four channels of the color viewer. In order to reconstruct a false color infrared image, band 4 was projected through a blue filter, band 5 through a green filter and band 7 through a red filter. In order to enhance the image record of commercial activities along main thoroughfares the filters used for bands 5 and 7 were switched and a false color image, with green in place of red, was created.

Mapping Procedures

The largest portion of the mapping was accomplished from enlarged positives or projected slides taken off a portion of the reconstructed 70 mm image on the color viewer view plate. Projected images were worked at scales no larger than 1:62,500. Resolution usually extended to eighty-acre sections. Better resolution occurred where intense signatures associated with specific uses could be found in isolated parts of the valley. Linear features and land use arrays appeared to be more visible than other features of equal area. Such findings were expected and not in themselves surprising.

Strict procedures were established, and followed, during the mapping process. One interpreter accomplished all the mapping. Factors which influence the quality and resolution of land use information gleaned during this study include the scale of the imagery, the scale of the final map product, the availability of secondary data sources, the expertise of the interpreter, and finally, how well the interpreter knows the subject area. In evaluating the usefulness of a remote sensing system, there is no justification for faulting a mapping procedure because one interpreter, through his own knowledge of the area, is more proficient at correctly identifying land use than another equally skilled individual who does not know the area.

During this study more land use information could be extracted from the imagery because the interpreter "knew" the region, than would have been possible otherwise. Familiar areas where residential and commercial urban uses are fixed, because of high capital investment, served as a base for identifying uses in less well known areas and in areas where change had taken place. Members of any regional planning organization should be as knowledgeable about areas under their jurisdiction as was our interpreter in the Coachella Valley.

Previous land use mapping in 1966 by R. Van Curen served as a base for change comparison. An intermediate set of information was obtained in 1969 through the work of J.B. Bale and W.G. Brooner for Palm Springs. The land use classification used for ERTS-1 derived information (see table on following page) is a modification of the one used in 1966. This, of course, is necessary to maintain consistency and allow land use change identification. In most areas, the classification scheme allows more detail to be recorded than is actually visible from the imagery -- the 1966 survey was based on both a low altitude large scale photographic record and detailed field work. A less detailed classification system would inhibit interpretation processes where additional information is available on the photo.

Techniques developed in previous agricultural surveys at the University of California, Riverside and elsewhere facilitate identification of agricultural uses. Crop calendars, dependence on false color infrared film where various shades of red facilitate interpretation, and the fact that agricultural fields usually cover large areas, allow interpreters to obtain greater detail (even to the identification of specific crops) in an agricultural area than in urban areas. In the Coachella Valley, however, certain urban associated recreation uses, specifically golf courses and fairway side housing, can be easily identified (Tamarisk, Bermuda Dunes, La Quinta, Canyon Country Club, Thunderbird, etc.). This combination of residential and recreational use has its own category in the land use classification scheme.

Ground Truth

All areas where positive change was mapped within the city limits of Palm Springs were ground checked February 18, 1973. In every instance some form of positive change had taken place in or adjacent to the boundaries drawn on the map. In no instance were the boundaries which were drawn on the map exact representations of the actual area where the change occurred. Although no attempt was made to identify the new land uses as they were being mapped, it was noted in the field that all change identified consisted of residential structures or subdivisions except for one park in section 34 at the north end of town. All areas of change 1/8 section or larger were recorded. Change did occur which was not recorded, but it was from one use other than open space to another or it occurred over an area which was too small to be recorded (Figure 7.5).

East of Palm Springs in the unincorporated portion of the test site, land use change was monitored with similar accuracy to that which was achieved in the more densely occupied city area. Identification of land

TABLE 7.3. COACHELLA VALLEY LAND USE CLASSIFICATION (1972).

A. AGRICULTURAL LAND USES
- 1. Field Crops
  - a. grains
  - b. feed
  - c. vegetables
  - d. truck crops
  - e. other
  - f. pasture
- 2. Row Crops
  - a. vegetables
  - b. maize
  - c. other
- 3. Tree Crops
  - a. citrus
    - (1) oranges
    - (2) lemons
    - (3) grapefruit
    - (4) limes
    - (5) other
  - b. vineyards
  - c. palm orchards
    - (1) date
    - (2) ornamental
  - d. other (i.e., pecans)
  - a/c. palms with citrus
- 4. Rural Housing and Agricultural Services
- 5. Unidentified or Unknown
- 6. Miscellaneous Agriculture
  - a. nursery
  - b. feed lot
  - c. other agriculture (experiment station)
  - p_p. packing plant

B. URBAN LAND USES
- 1. Residential
  - a. single
  - b. multiple
  - c. transient
  - l. lot subdivisions
  - m. mobile
  - r. recreation
- 2. Commercial
  - a. sales and service
  - b. recreation
- 3. Industrial
- 4. Institutional and Governmental
- 5. Unknown

C. UNDEVELOPED AND UNUSED
- 1. Vacant
- 2. Abandoned
  - a. agriculture
  - b. urban

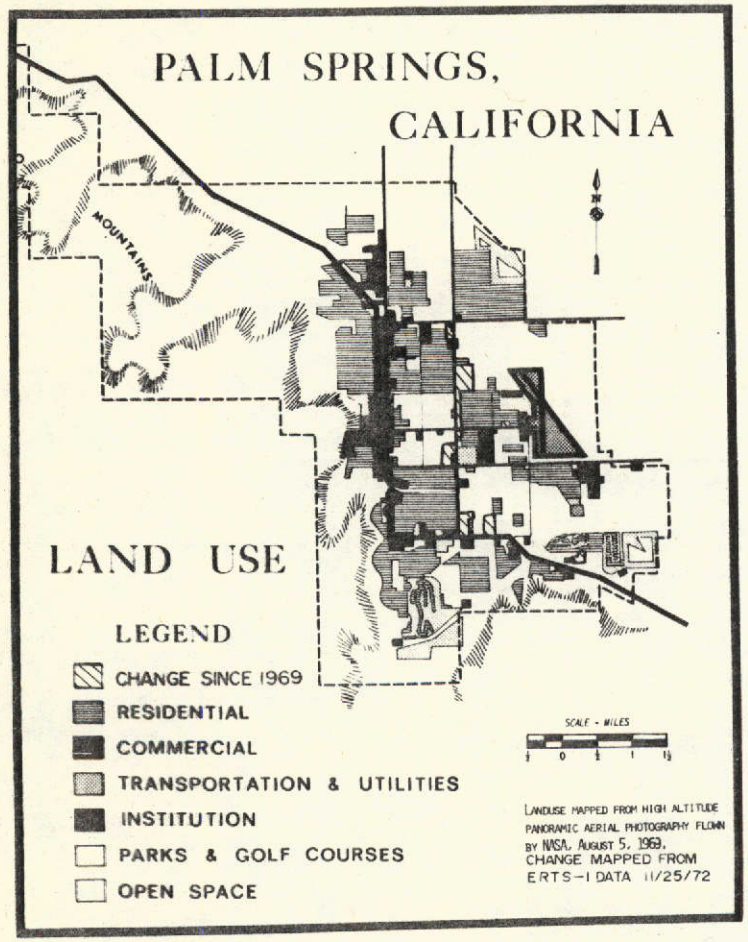

Figure 7.5. Palm Springs, California.

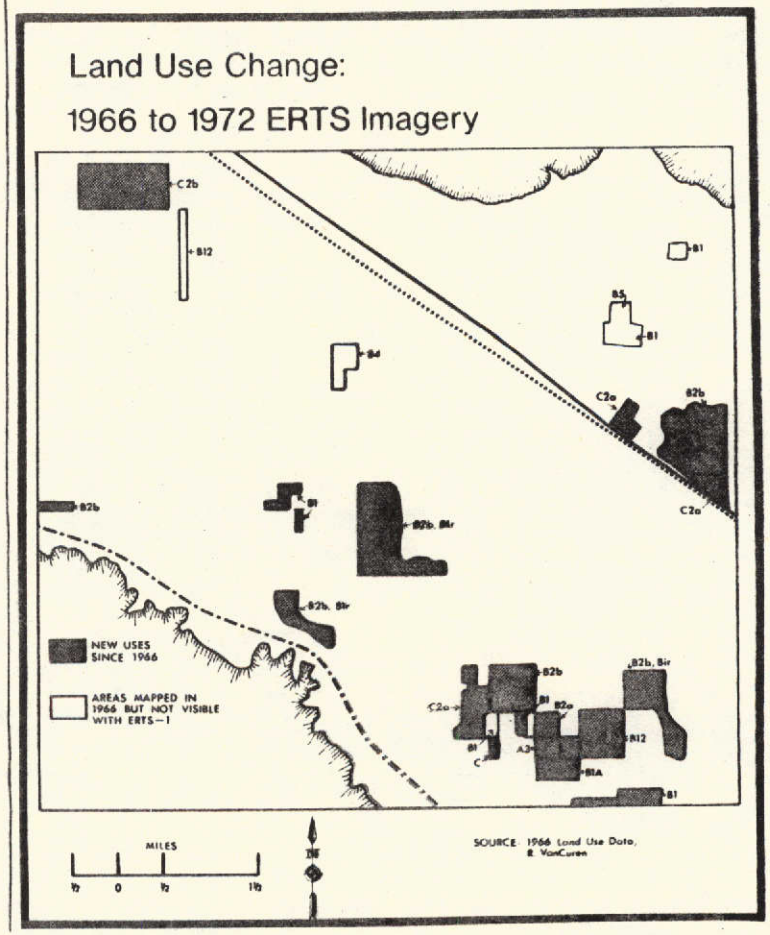

Figure 7.6. Land use change.

use type as well as land use change was attempted. Boundaries again could not be placed exactly, but in only two instances were land uses misinterpreted. The first case was a locational problem involving the improper postioning of a small area of abandoned vineyards in the south central part of Figure 7.6. Secondly, at Thousand Palms recreational residential use involving mobile homes around a golf course was not identified. Less critical problems involved the category of agricultural abandonment (C2a in Figure 7.6). Here, no distinction could be made between actual removal of orchards or groves, and their complete removal. The difference between active agriculture, and abandonment or disinvestment was always apparent.

Results

From both maps and the ERTS-1 imagery, it is obvious that much of the urban development has occurred on the various alluvial fan surfaces that emanate from the San Jacinto Mountains. These areas, somewhat protected by spur ridges from the winds which are strongest along the axis of the valley, were developed first and still contain the most diversified urban uses (residential, parks, commercial). More recent residential development has occurred on the upper portion of some fans (Deep Canyon Fan for example) or along the south center axis of the valley at the expense of open space or agricultural uses. All agriculture will be gone from the north half of the valley within the next few years.

Change in the Palm Springs area consists primarily of the filling in of an already urban environment. Alternate sections within the city limits belonging to the Agua Caliente Indian Reservation are now being transformed from open spaces to urban uses. Problems were encountered while working in this more complex urban environment. With the present system of combining and projecting reconstructed imagery, land use boundaries within the city could not accurately be drawn. Furthermore, except for most single family residential areas, parks, golf courses, and some, specific commercial uses, a full range of urban uses including most commercial areas, multi-family residential, governmental, and other institutional uses were not discernible. Positive change however was visible where other forms of use have replaced open space.

Farther to the southeast, in what was originally a less complicated agricultural landscape, change occurs in the center of the valley. This area, originally a "blow-sand" environment, is undergoing a transformation from open space and agriculture to recreational and residential uses. What exists is perhaps the heaviest concentration of golfing facilities in any area of this size in the world. In situations where direct conversion from agriculture does not occur, fields are abandoned, left fallow or trees (either citrus or date palm) are maintained as ornamentals to residential uses. Agricultural abandonment is one form of factor disinvestment common to the rural-urban fringe

in Southern California (Goehring, 1971).

Analysis

If they existed, information systems featuring rapid updating procedures and utilizing statistical data sources such as census returns, assessor's data or building permit totals could provide more accurate information concerning land use change than is available from ERTS-1 imagery. However, information developed from such sources, even if graphically arrayed (in map form) can approximate an areal perspective of the landscape or accurately convey regional spatial relationships like ERTS-1 imagery. Perspectives available from ERTS-1 imagery allow regionwide views containing information in quantities not available from composite sources (maps or photo mosaics). The sequential nature of the imagery adds to potential utility although biannual collection instead of every 18 days would suffice to monitor urban land use change in the northern Coachella Valley.

Although no regional planning agency with responsibilities in the Coachella Valley has yet to integrate ERTS-1 imagery into its resource management procedures, various members of the planning departments of Riverside County and Palm Springs City have made casual use of reconstructed images. Individuals from both organizations have, from other sources, already been made aware of problems illustrated by ERTS-1 imagery. Alarmed by what appears to be a loss of amenities in a primarily recreational urban environment, officials in Palm Springs have called a temporary building moratorium, and proposed revolutionary measures to maintain open space within the city (personal communication, Department of Planning and Development, City of Palm Springs and Proposed Open Space and Conservation Element, Palm Springs General Plan). County officials have expressed little concern over loss of open space but have been confronted by numerous local conservation organizations that have expressed concern over a number of related topics ranging from a loss of wildlife habitat to deteriorating ground water quality.

Additional building and subsequent increases of human activity will jeopardize numerous specialized natural habitats in surrounding areas. Most recent land use change suggests a loss of unique natural habitats, including fan surfaces emanating from the San Jacinto Mountains, the sand dune habitat that extends along the axis of the valley, and the Bighorn sheep habitats in the mountain slopes surrounding the valley bottom. Continued residential construction has also reduced the habitat value of the valley to man. Increased environmental pollution (air pollution, noise and visual pollution) threaten the area's economic base. Amenity loss stemming from the lack of attention to concepts of environmental design and consequent impacts of continuing development can be inferred. Sequential ERTS-1 imagery has recorded the most recent chapter of the Coachella Valley's continuing environmental alteration.

References

Bale, J. B. and W. G. Brooner (June, 1970), "Experimental Land Use Mapping from High Altitude Panoramic Photography," Paper Presented at APCG Meeting, Santa Cruz, California.

Glendinning, Robert M. (1949), "Desert Contrasts, Illustrated by the Coachella," Geographical Review, 39:221-228.

Goehring, Darryl R. (1971), Monitoring the Evolving Land Use Pattern on the Los Angeles Metropolitan Fringe Using Remote Sensing, Technical Report T-71-5, Contract No. N00014-69-A-0200-5001, NR 387-047 and NASA NGL 05-003-404, Department of Geography, University of California, Riverside.

Roos, Marvin (January 1973), Assistant Planner, Department of Planning and Development, Palm Springs, California, Personal Communication.

Van Curen, R. (1966), "Land Use Maps of the Coachella Valley," Unpublished, University of California, Riverside.

7.2.4 Southern California Compression Zone

The Los Angeles Basin and its several sub-basins have been blocked out by the intersections of the northwest-trending Peninsular fault structures of the San Andreas system with the east-west or Transverse structures related to the Murray Fracture Zone. Local seismic interest has been focused upon faults related to the two tectonic alignments. ERTS-1 imagery of Southern California clearly indicates a third tectonic lineation which appears more closely related to recent seismic activity than the traditionally recognized structures (Figures 7.7 and 7.8).

The ERTS-recognized lineations appear as a broad zone, some 50 miles in width, which intersects the Transverse Ranges at about a 15° angle or with an azimuth of 70°. Although a limited number of landform features appear to be solely the products of the forces responsible for this sub-transverse zone, extensive evidence is also to be found in elements of the larger structures of the Transverse Ranges. Ridges that form the northwestern edge of the San Gabriel Mountains, for example, are properly oriented and in turn align with Oak Ridge which extends in a west-by-southwest direction toward the Pacific Ocean to impart the same orientation to the Santa Clara River Valley. North of the valley, the prominent ridge of the Topatopa Mountains, similarly set obliquely to the Transverse Ranges of which it is part, delineates the approximate northern edge of the zone.

The southern edge follows a line of recognized faults which for the most part are buried under alluvial fill of the Los Angeles Basin

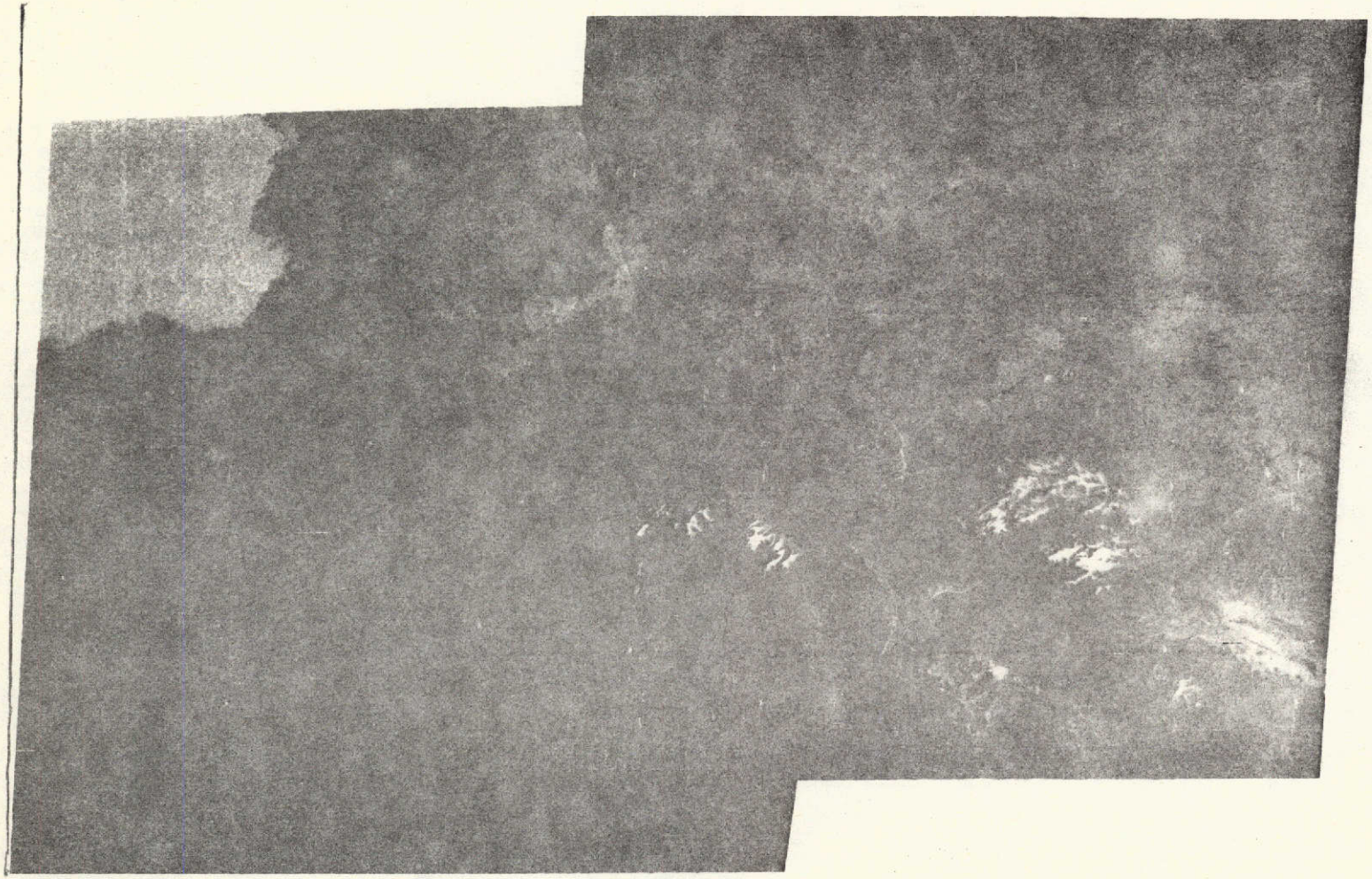

Figure 7.7. A mosaic of ERTS images of November 25 (RH) and November 26 (LH) showing the Los Angeles Basin, Transverse Ranges, and Mojave Desert. The zone of tectonic lineations with the 70° azimuth is located in the accompanying map.

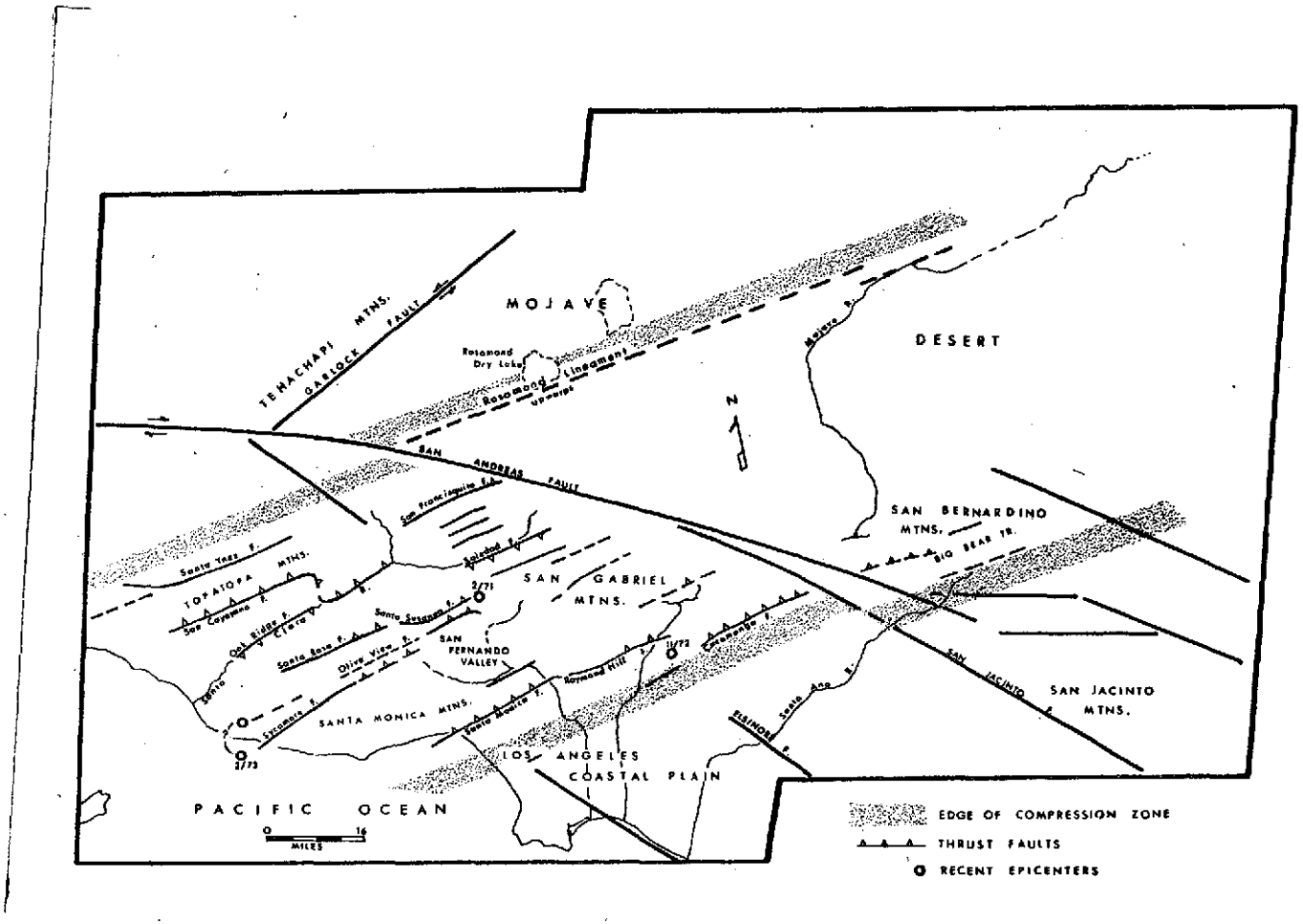

Figure 7.8. Zone of tectonic lineations.

(Geologic Atlas of California). At the western end of this alignment is the Santa Monica Fault while to the east the Cucamonga Fault facets the southeastern corner of the San Gabriel Mountains near the point where the San Andreas system bisects the Transverse Ranges at Cajon Pass. It is significant to note that at this point the ERTS-recognized alignment crosses the San Andreas Fault with less than a mile of right-lateral offset which may give some clue to its age. The tectonic trend has affected the San Bernardino Mountains east of Cajon Pass by giving landform orientations that are cross-grained to the trend of the mountain range. These include a major indentation on the southern mountain front, the trend of the Big Bear-Baldwin lakes trough, and the general trend of the Santa Ana River canyon. Although the lineation just described is taken as the southern edge of the zone, ridge orientations and recognized faults in the San Jose Hills south of the San Gabriel Mountains may indicate a slightly wider zone, but evidences on ERTS imagery for this are not definitive.

The most prominent single indicator, both for the existence of the zone as well as its orientation, is a single tectonic line that extends across the Mojave Desert along the zone's northern edge and about halfway between the San Andreas and Garlock faults. On the imagery, it is particularly conspicuous along the southern edge of Rosamond Dry Lake (Figure 7.9) where desert-floor alluvium has been upwarped into low knolls with sufficient drainage to permit heavy stands of trees yucca (Yucca brevifolia) to form dark patches on the scans (Figures 7.10 and 7.11). To the east, the tectonic line extends along the northern edge of several low domes on the desert floor to be eventually occupied by a portion of the course of the Mojave River.

The alluvium knolls south of Rosamond playa, as well as the dome landforms, suggest that the desert tectonic line has been subjected to lateral pressure from the southeast. A number of faults with the sub-transverse orientation are known to be thrust faults and the San Fernando earthquake of 1971 indicated that those buried by alluvium may well be. Recognized as thrust faults are the Santa Susanna-Santa Rosa Fault, the San Cayetano Fault, the Cucamonga Fault, and, in all probability, the Santa Monica Fault. This combination of evidence strongly suggests that the sub-transverse zone here described is a zone of active crustal compression which is absorbing much of the compressional stress being exerted by the northwestward-moving blocks of the peninsula of Baja California which intrude into Southern California.

It is of particular interest to relate the tectonics of the San Fernando earthquake of February 9, 1971, to the zone of lineations observed on ERTS imagery. Surface breaks related to the Olive View Fault (Youd, 1971) were thrust plates with strikes close to the 70° azimuth of the ERTS-recognized zone. Several feet of crustal compression occurred. The compressional component of earth movement lifted

Figure 7.9. Rosamand dry lake and lineament. Band 5, 26 November 1972.

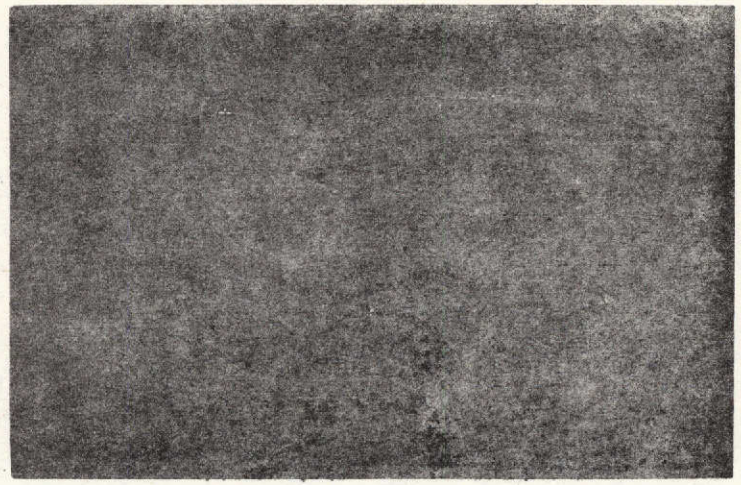

Figure 7.10. An oblique view of Rosamond playa showing groves of tree yucca along lineament.

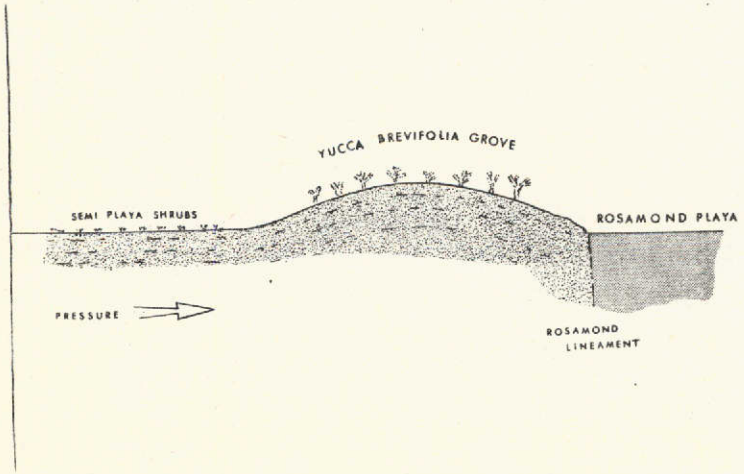

Figure 7.11. Cross-section diagram of knolls along the Rosamond Lineament which appear to be upwarped from desert-floor alluvium.

Figure 7.12. The lineament of olive view fault connecting two recent earthquake epicenters.

the surface north of the break approximately three feet and in so doing demonstrated that forces associated with the zone may well be responsible for much of the mountain-building in and around the Los Angeles Basin. The cause of the left-lateral movement associated with the quake can also be conjectured since the wedging of the shattered crustal block against the San Andreas Fault backed by the more intact Mojave block should eject the coastal structures westward. The indication provided by the Rosamond lineation that the Mojave block is absorbing some of the crustal stress may also indicate a lessened chance that severe slippage will occur along the San Andreas Fault adjacent to the Los Angeles Basin.

An epilogue to the San Fernando movements occurred on February 21, 1973, with a sizable tremor centered near the western end of the Santa Monica Mountains (Figure 7.12). An extension of the Olive View Fault southwest along the Simi Hills at an azimuth of 70° joins the Sycamore Fault which is believed to have caused the recent quake. This again demonstrates that the compressional zone is active. On November 28, 1972, a swarm of small tremors occurred, centered under the alluvium near Pomona, California. This is a location which does not fit the traditional fault network of Southern California but which would act like on a westward extension of the Cucamonga segment of the compression zone system.

In summary, ERTS-1 imagery in concert with previously recognized evidence delineates a zone of crustal compression across Southern California which is responsible for mountain building, landform orientations, and current seismic activity. The orientation of the zone can be considered "sub-gransverse". The zone thus intersects both the San Andreas system and traditional transverse structures obliquely. The existence of the broad zone of compression strongly suggests that Southern California seismic activity may be as much related to the zone as to specific faults. In other words, earthquake-producing compressions may occur anywhere within the zone and may not be related to known faults.

References

Geologic Atlas of California. California. Department of Natural Resources. Division of Mines. Scale: 1:250,000. Los Angeles, 1969; San Bernardino, 1967; Long Beach, 1962; and Santa Ana, 1965 sheets.

Youd, T. L., "Landsliding in the Vicinity of Van Norman Lakes," The San Fernando, California, Earthquake of February 9, 1971. U.S. Geological Survey Professional Paper 733, U.S. Government Printing Office, Washington, D.C., 1971.

7.2.5 A Remotely Sensed Examination of the Tectonic Framework of the Mojave Desert North of San Bernadino, California

The area selected for examination encompasses that portion of the Mojave Desert represented on the 1:250,000 USGS topographic sheet of San Bernardino, California. The Mojave Desert, being a distinct structural and physiographic unit was studied by itself, and only the adjacent borders of the Transverse Ranges to the south were included in the study. Thus tectonic homogeneity was preserved during the study. Because of lack of sufficient high altitude imagery for the entire Mojave region, only the south-central portion, with its complete air photo coverage, was studied.

A map showing the tectonic framework of the region was prepared using the San Bernardino sheet as a base map. The structural data were compiled from color and CIR imagery from Mission 164, recent U-2 CIR imagery, and from continuous black-and-white and color composite ERTS-1 imagery. The map records all faults, folds, volcanic features, joint systems, and surface fractures visible on the imagery. Mapping proceeded through the spring of 1973 (Figure 7.13).

The Tectonic Framework

The predominant trend of faulting in the area is northwest. These faults are for the most part rifts with right-lateral strike-slip displacement. These rifts display an average trend of N39°W. They are more numerous and better displayed at the surface in the eastern half of the area. The traces of many of them are striking, even when observed upon ERTS-1 imagery (Figure 7.14). The faults in the western half of the area are much more subtle in their surface expression and must be traced from Mission 164 and recent U-2 imagery. Very poorly developed wrench faults with an average trend of N8°E may be found in the eastern half of the area. Two were significant enough to be mapped. Others appeared with the same approximate trend in complex fault zones in the Bullion, Bristol, and Cady Mountains. These faults may represent a left-lateral set of a conjugate system composed of the northwest and northeast trending faults. Another set of better developed wrench faults with left-lateral strike-slip displacement and an average trend of N78°E occurs throughout the area, but with more frequency and longer traces in the eastern half. The best developed of these are the Cady fault, the Rainbow Canyon fault zone, and the Pinto Mountain fault.

The folds in the area are poorly developed. Most of them strike northwest, with an average axial trend of N43°W. Half of the observed folds plunge to the northwest. No plunge was observed for the others. The best developed fold is the Lenwood anticline. The Bullion Basin anticline has an axial trend of N85°W.

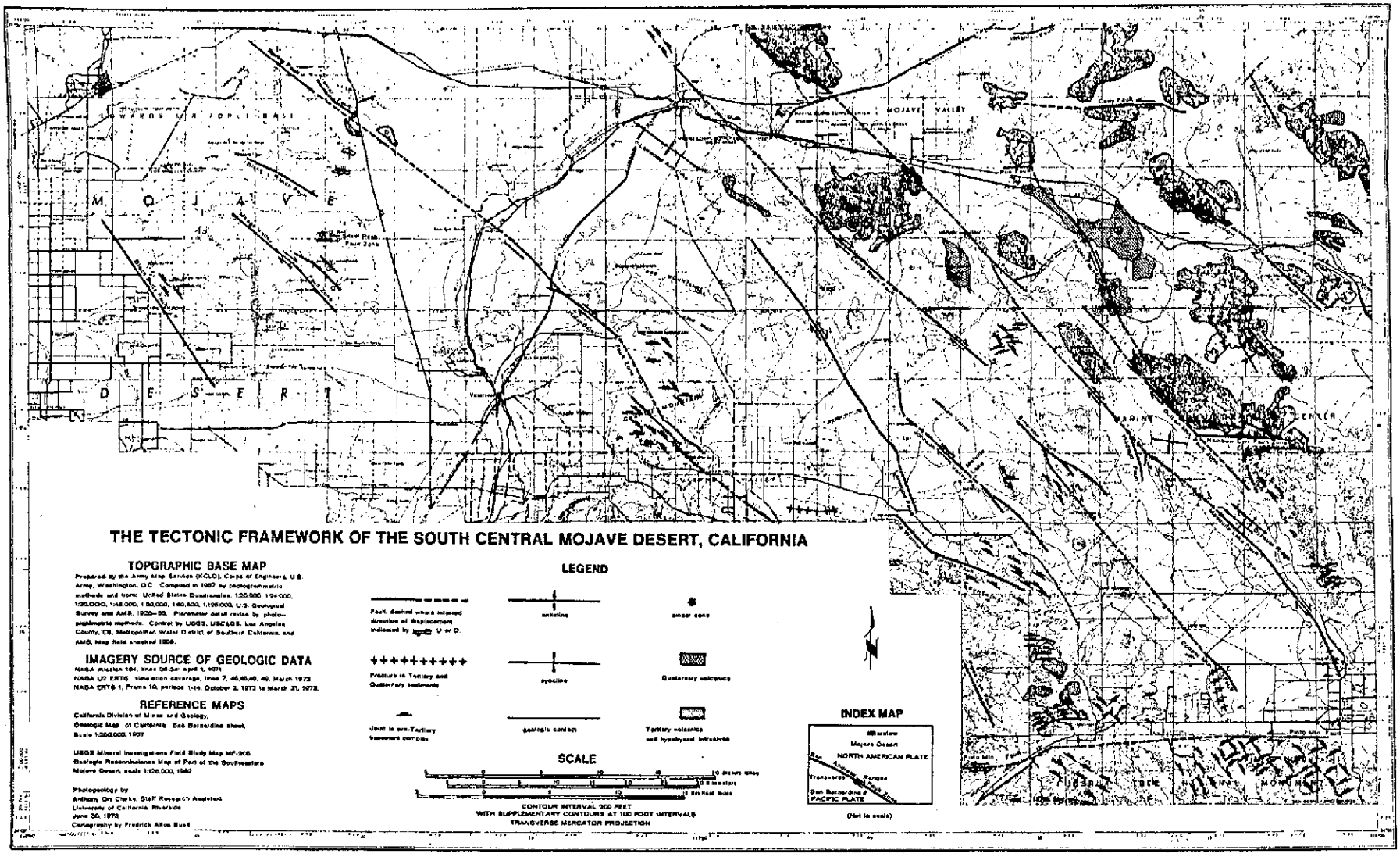

Figure 7.13. The tectonic framework of the south central Mojave Desert, California.

Figure 7.14. ERTS-1 photo (25 November 1972), 1:1,000,000. The Mojave Desert lies in the northern half of the photograph, bordered on the south by the Transverse Ranges. The Los Angeles Basin and San Bernardino Valley occupy the lower portion of the photo. Many structural lineaments are visible on satellite imagery, those which may be seen on this frame have been outlined in black.

Quaternary volcanic action has been extensive in the eastern half of the area, and is non-existent in the western half. Cinder cones possess a high degree of alignment with the rifts. Three of the five cones are within the Pisgah fault zone, and the other two are approximately three miles from exposed surface faulting. Pisgah Crater is a fairly recent feature and is remarkably well preserved. Its lava flows are by far the largest. Tertiary volcanics and hypobyssal intrusives are frequently found exposed in the eastern half of the area. These Tertiary volcanics display dominant northwest alignment and may be related to deep-seated Tertiary rifting. The most common extrusive rock in the area is basalt.

Two joint systems occur in the area. The system in the southeast corner is composed of two intersecting sets of joints, one striking northwest and the other striking northeast; both sets dip toward each other and appear to be conjugate shear joints. This system presents an imposing appearance in both Mission 164 and U-2 imagery, and is best observed in the vicinity of Joshua Tree National Monument. The second joint system is less dominant but easily observable. This system may be seen throughout the northern and central portions of the area. It is made up of two intersecting sets of joints, one striking northwest and the other striking east-west. The origin of the second set is not as clear as the first. Both systems occur in the pre-Tertiary basement complex and are best developed in the Mesozoic granitic rocks.

Surface fractures are observable in unconsolidated Quaternary deposits at two locations, an east-west trending fracture in the alluvium at the base of the Transverse Ranges north of Baldwin Lake, and two parallel northwest trending fractures in the lake bed sediments immediately west of Copper Mountain fault. These fractures or fissures may be related to dislocations in the bedrock at depth or they may be the result of surface subsidence caused by a recompaction of unconsolidated sediments following some seismic event.

The northwest trending mountain ranges of the area are low-lying and much more eroded than those of the Basin and Range to the north and east. For these reasons they must be much older. They consist primarily of folded and faulted Mesozoic volcanics, Mesozoic granitic rocks, and Paleozoic and pre-Cambrian metamorphic rocks. Locally they are intruded and overlain by Tertiary volcanics. They are for the most part fault-block mountains. Many appear to have been uplifted by rotational movement along strike-slip faults rather than by gravity faulting, creating the current rift topography. Rifting, uplift, and vulcanism occurred mutually during the Tertiary and some rifting and vulcanism continued into the Quaternary.

Stress - Strain Analysis

In the area studied, the structural fabric fits the conjugate

faulting model remarkably (Figure 7.15). When the trends of the right-lateral rift faults are averaged, a mean shear fault trace with a trend of N39°W is computed. The rifts have a median trend of N40°W, and a mode of N45°W. In the following stress analysis the mean value of N39°W is used. Using the stress ellipsoid, the greatest principal stress axis P and the least principal stress axis R may be assumed to be perpendicular to each other, and both lying in the same near horizontal plane, somewhere at depth. The intermediate principal stress axis Q is perpendicular to P and R, and is nearly vertical. This stress arrangement will produce strike-slip faulting. Shear fractures f_1 and f_2 should develop at 30° left and right respectively to P and lie in the same plane as Q: f_1 will experience right-lateral displacement and f_2 will experience left-lateral displacement. N39°W may be assigned as the trend of f_1. This will orient the stress ellipsoid in space, and give the same approximate stress distribution as must have been present to produce the tectonic pattern observed in the area of study.

With this orientation we might expect to find left-lateral shear fractures developing parallel to the f_2 plane at N21°E. Several small faults with a mean trend of N8°E are found in the area. This is only a 13° deviation from the expected trend, and suggests a conjugate system of faults. Such a stress distribution also predicts second order left-lateral wrench faults trending N66°E. The mean trend of the ENE left-lateral wrench faults found in the area is N78°E which is a deviation of 12° from the predicted. Some of these may be thrust faults, particularly the Pinto Mountain fault. If they are thrust faults rather than second order wrench faults, there is only a 3° deviation from the predicted trend of N81°E for thrust faulting. The folds, exclusive of the Bullion Basin anticline, have a mean axial trend of N43°W. The predicted trend for second order folding is N54°W, and the deviation is 11°. The Bullion Basin anticline has an axial trend of N85°W, and the predicted trend for first order folding is N81°E; the deviation is 14°.

In all cases, the greatest deviation between observed and predicted lineaments is 14°, which is close enough to make a valid suggestion of conjugate faulting. The above analysis may also be performed using the strain ellipsoid. In this case, the greatest principal stress axis P becomes the least strain axis C, the least principal stress axis R becomes the greatest strain axis A, and the intermediate principal stress axis Q equals the intermediate strain axis B. The shear fractures f_1 and f_2 remain the same. Simultaneous shear faulting and thrust faulting may be explained by the rotation of the B axis in a vertical plane from its vertical position at depth (where, because of the greater lithostatic load, strike-slip faulting would be produced), to a horizontal B axis at a shallow position, (where, because of the decreased lithostatic load, thrust faulting would be produced).

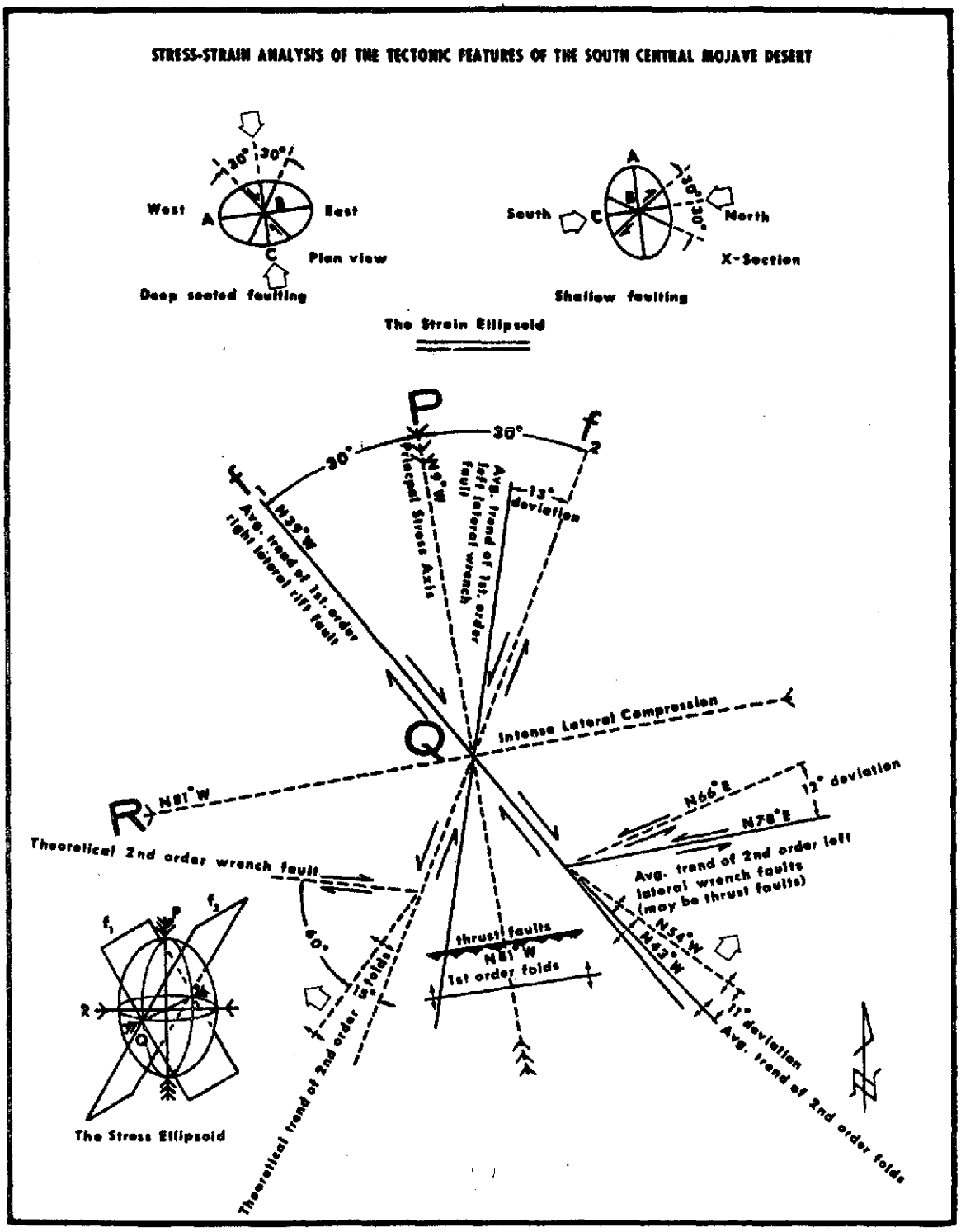

Figure 7.15. Stress-strain analysis.

Conclusion

The stress and strain orientations suggest severe compressive forces having an axis of greatest principal stress trending approximately N9°W and causing intense lateral compression in a belt of easiest relief trending approximately N81°E conforming with the least principal stress axis. This near north-south compression culminated in the uplifting of the Transverse Ranges south of the area in the late Tertiary and Quaternary. These mountains have been uplifted by late Cenozoic thrust faulting along their base and have been thrown into folds possessing dominant trends oriented approximately east-west.

References

Badgley, Peter C., 1959, Structural Methods for the Exploration Geologist, New York: Haryper & Bros.

Billings, Marland P., 1954, Structural Geology, Englewood Cliffs: Prentice-Hall.

Kedar, Ervin Y., 1969, Geomorphotectonic Inferences from Earth Photographs: A Case Study of the Western and Southwestern United States, a presentation at the annual meeting of the Pacific Coast Geographers.

Kupfer, D. H. and A. M. Bassett, 1962, Geologic Reconnaissance Map of Part of the Southeastern Mojave Desert, California, Scale 1:125,000, U.S. Geological Survey Mineral Investigations Field Studies Map, MF-205

Lowman, Paul D., 1969, Apollo 9 Multispectral Photography: Geologic Analysis, Greenbelt, Maryland, Goddard Space Flight Center, X-644-69-423.

Oakshott, Gordon B., 1971, California's Changing Landscapes, New York: McGraw-Hill.

Pease, Robert W., 1969, "Normal Faulting and Lateral Shear in Northeastern California," Geological Society of America Bulletin, 80: 715-720.

Pease, Robert W. and Claude W. Johnson, 1973, New Fault Lineament in Southern California, Symposium on Significant Results Obtained from ERTS-1, Greenbelt, Maryland, Goddard Space Flight Center.

Rogers, Thomas H., 1960, San Bernardino Sheet of the Geologic Map of California, Scale 1:250,000, California Division of Mines and Geology Map Sheet.

7.2.6 Regional Monitoring of Atmospheric Circulation and Atmospheric Pollution

Conventional aerial photographs or small scale formats of weather satellite images seldom provide information at intermediate scales useful for monitoring atmospheric circulation in a region the size of Southern California. Research for this project is designed to visually monitor and record atmospheric pollution if possible and to record and help explain the delicate energy transfers that occur at the interfaces of dissimilar desert and marine air masses.

A system for collecting recorded atmospheric data from all stations in Southern California is now under development. Standard information including temperature, humidity and air pressure, as well as synoptic maps, can be gathered each date when there is an overflight. This information will then be compared to the ERTS-1 photography once it arrives. If pollution monitoring is possible, there will be the interesting potential of matching a visual record with measurements of ground stations. Because of sensor characteristics and atmospheric conditions, little synoptic information concerning either regional atmospheric circulation or pollutant dispersal patterns has been available from extant ERTS-1 imagery.

7.2.7 Impact of Off-Road Vehicles

The recreational use of off-road vehicles, especially in the arid regions of the western United States, has become an important and rewarding leisure time activity. As a result, off-road vehicular traffic, especially motorcycle traffic, has already caused considerable damage to these delicate desert environments, and this damage will certainly become more widespread unless regulatory action is taken promptly to prevent overuse and destructive uses of the terrain.

Location of damaged areas and the study of their proliferation would aid greatly in efforts to minimize the impact of this vehicular traffic. Such a study would also provide a rational basis upon which to establish regulatory policy for off-road vehicles. In this study the utility of remote sensing techniques for the dual purposes of location and study of damaged area is explored.

Through the use of imagery of California's northern San Gabriel bajada, spanning nearly three years from July 1968 to July 1972, all major areas of off-road vehicular damage within the study region were located (Figure 7.16). Growth of areas subject to damage, for the time period in question, was also mapped for specific locations.

Small scale imagery, particularly from the U-2 aircraft and NASA Mission 164, was found to be most desirable for purposes of initial

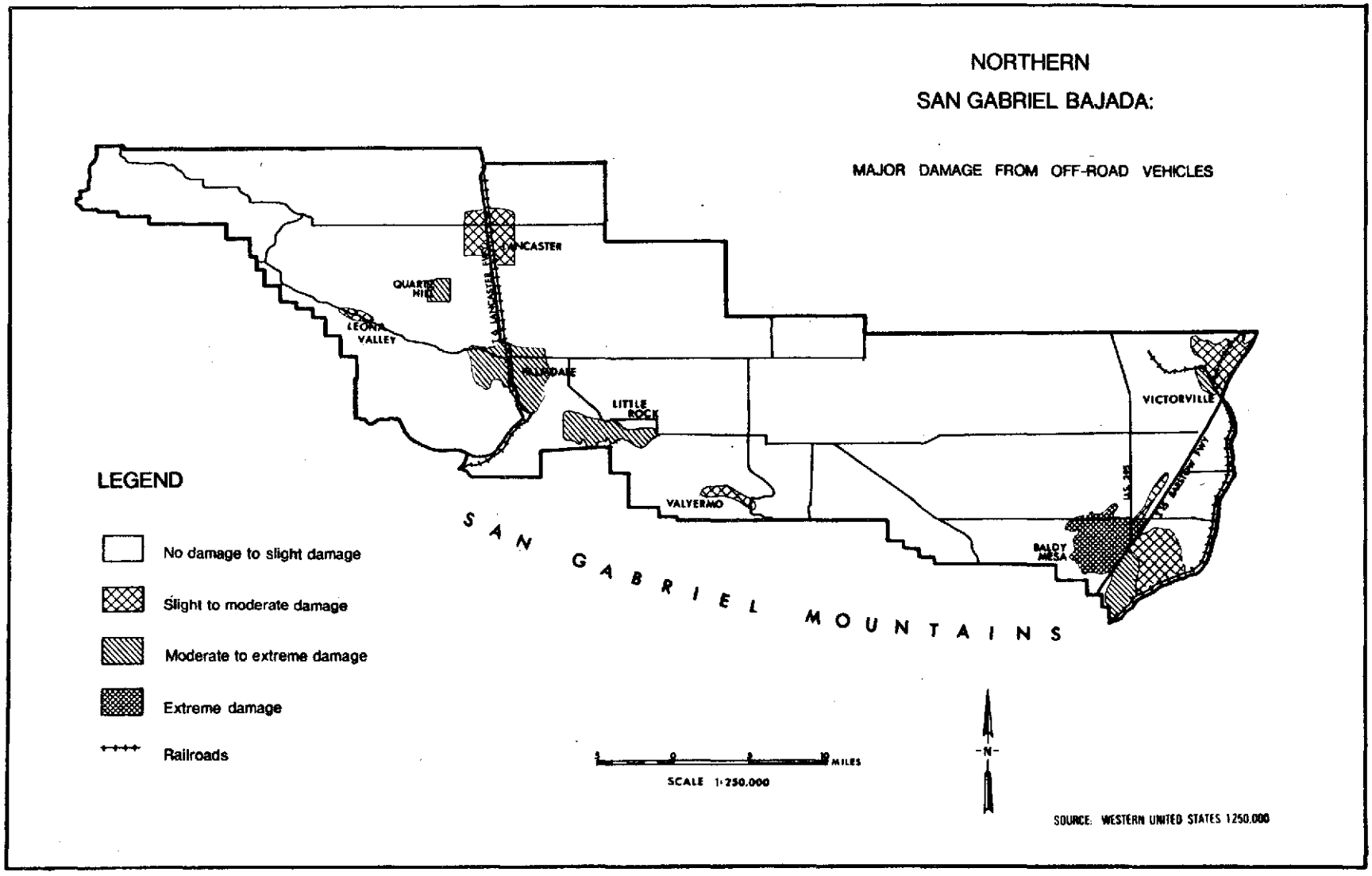

Figure 7.16. Northern San Gabriel Bajada.

location of damaged areas. Larger scale photography (1:24,000 to 1:30,000) was found to be more appropriate for more intensive study once damaged areas had been located. CIR imagery, particularly under a stereoscope, was found to be especially valuable in this investigation. Imagery of damaged areas from more than one date is, of course, requisite for a temporal comparison to determine expansion of damage.

Remote sensing techniques have direct application to the tasks of locating and studying off-road vehicle damage. Aerial survey is clearly superior to ground survey for these purposes for several reasons. First, the use of aerial photographs allows vast areas to be rapidly examined. Second, the perspective offered by aerial photographs allows the interpreter easily to see spatial patterns not readily visible from the ground. Finally, the number of man hours required for ground survey and mapping of damaged areas probably renders that method prohibitively expensive.

7.2.8 Impact of the Barstow to Las Vegas Motorcycle Race -- An Update

Off-road-vehicle (ORV) use in the desert is becoming an ever increasing activity for a large number of people, especially in Southern California. The impact of ORV operation has led to significant environmental change of the desert, often to its detriment. Initially, our study evaluated the use of U-2 underflight imagery for detecting the effects of ORV's. The annual Barstow to Las Vegas Motorcycle Race was chosen for analysis, primarily because the Bureau of Land Management (BLM) was considering suspension of approval to hold the race in future years if damage proved excessive. Damage was defined as any change that resulted in a dimunition of any of the factors that serve to make the desert environment unique (i.e. desert surfaces, soils, vegetative cover and air quality). We cooperated with the BLM in analyzing this race with our input focusing on the use of remotely sensed imagery for evaluating damage. The race was an organized event and the race route traversed a narrow and pre-determined path. Consequently, the amount of damage which the desert sustained proved minimal, especially in view of the large number of people who derived pleasure from the event (15,000 to 20,000). However, those areas which did sustain damage could have been spared if the race had been more carefully routed. The effects of this event and the results of the more common, extensive, random ORV operation in other areas of the Mojave were compared on U-2 imagery. Damage resulting from random usage was found to be the most serious and also the most easily detected on the U-2 imagery.

Ground reconnaissance both before and after the race showed that certain desert surfaces were much more able to withstand intensive ORV activity than others. For example, playa surfaces represent the local base level so that they are not susceptible to severe water erosion. Once the compacted playa surface is broken, however, dust becomes and and continues to be a major problem. In addition, many archaeological

sites exist near the playa shores. Washes represent a type of ephemeral surface that is most adaptable to ORV activity; they consist of coarse and non-compactable material so that any indication of change which they incur disappears with the next significant rainstorm. Fan surfaces consist of sorted material and thus the head, consisting of the coarsest and least compactable material, is more adaptable to ORV operation than the foot of the fan, which consists of finely sorted material. The most vulnerable of all the surfaces to ORV activity are (natural) pavement surfaces. Different grades of pavement exist, varying in degree of development and particle size, and they are often somewhat indurated. Once the pavement surface is broken, it is susceptible to severe erosion by both wind and water (Figure 7.17).

In the attempt to determine textural composition of the various desert surfaces, ERTS-1 images were pre-enhanced and mapping done from the resultant image. The objective was to map the desert surfaces which texturally are most adaptable to ORV operation from a small scale image such as ERTS-1 (1:1,000,000). This information will provide a planning input to agencies, such as the Bureau of Land Management, concerned with recreational planning of the desert.

Unenhanced ERTS-1 images have poorly defined boundaries separating different desert features (Figure 7.18). Through use of the unenhanced image, it would be impossible to determine surface texture in any precise manner. One of the major problems encountered is that changes in parent material tend to greatly blur any boundaries. The technique of density slicing, reported in another ERTS-1 study, allowed for more precise boundary determination. The technique was used in order to enhance the boundary between different textural surfaces. The enhanced frame (Figure 7.19) showed pronounced breaks where different textural/slope conditions prevailed. The topographic sheet onto which the information was mapped (Figure 7.20) showed a relatively close correlation between the small scale ERTS-1 enhanced image and the large scale topographic sheet. A large degree of generalization was required, due to scale differences. Finer definition is discernible on the enhanced image so that it will be possible for us to draft a much more detailed map. The two most easily definable changes are in rock outcrops and playa bottoms. Often when a distinct break appeared, it proved, upon field checking, to correspond with a break in slope (Figure 7.21).

Perhaps more significantly, the "break" also corresponded with significant textural differences, determined later by laboratory analysis. For example, transects down an alluvial fan bordering Roach Dry Lake, and another bordering Mesquite Dry Lake, revealed the following textural differences:

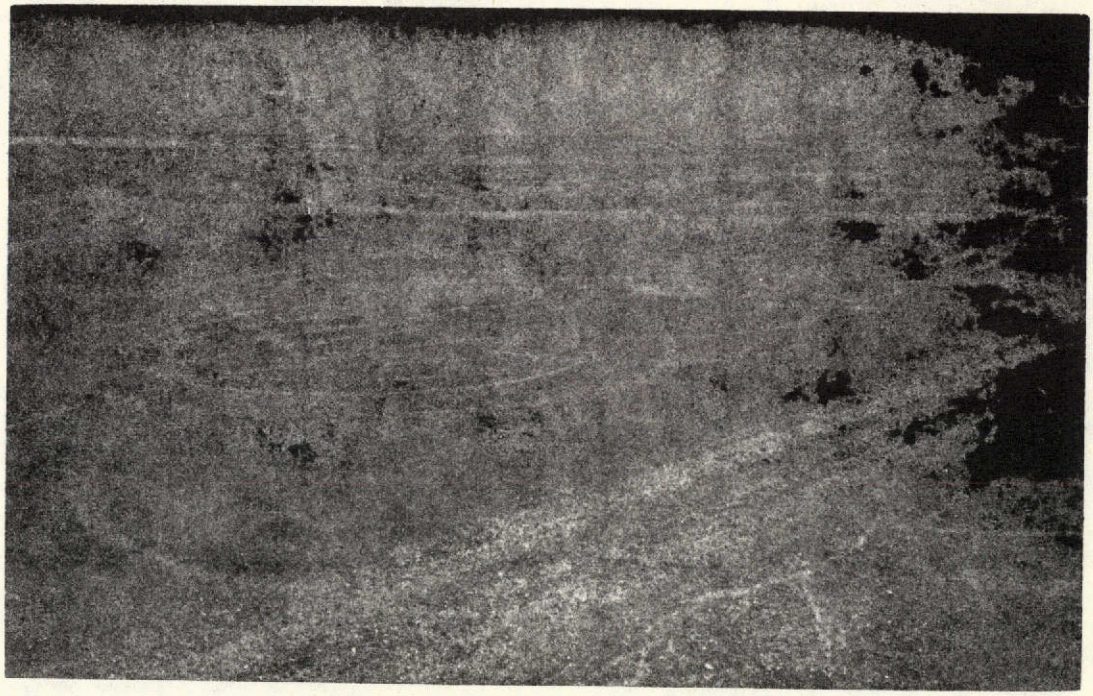

Figure 7.17. Broken desert pavement surface near Barstow, California. The surface is now susceptible to both wind and water erosion. Dust can also be a minor problem.

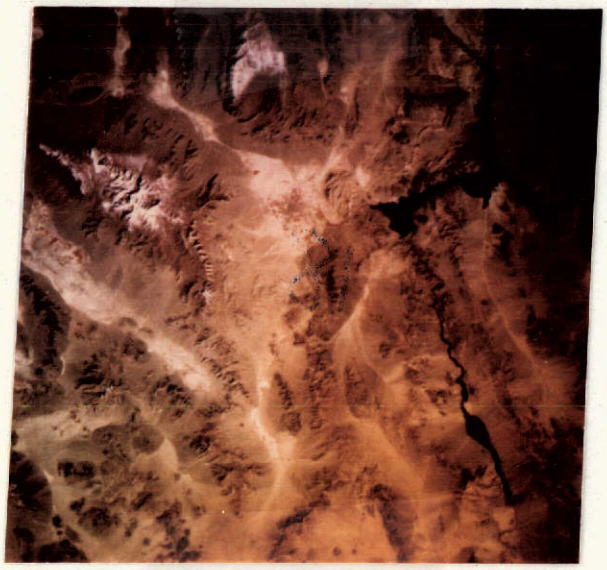

Figure 7.18. Unenhanced CIR simulation made from an ERTS-1 frame of Las Vegas.

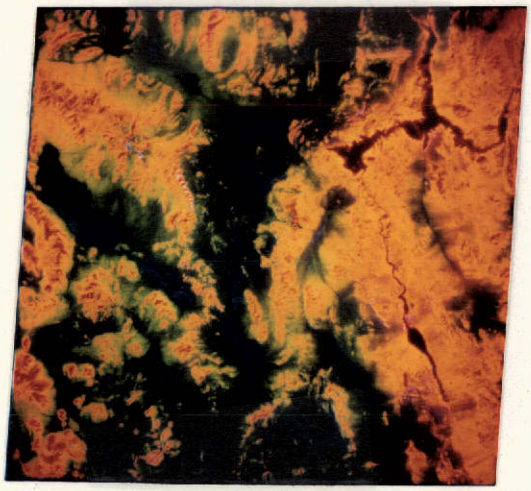

Figure 7.19. Density slice of the same ERTS-1 frame of Las Vegas. Textural/slope boundaries are much more easily determined.

Figure 7.20. Mapped information placed onto a topographic map.

Figure 7.21. Photograph near Ivanpah Dry Lake. Break in slope occurs where IR signature changes from the darker red (front) to a lighter red (rear).

ROACH DRY LAKE

Size	Above "Break" Line Percent	Near "Break" Line Percent	Playa Bottom Percent
1/4"	21.40	2.70	0.00
Mesh 10	22.12	14.20	1.62
Mesh 30	10.76	27.48	8.39
Mesh 70	6.88	23.77	28.74
Mesh 230	17.78	22.21	47.50
pan	21.06	9.64	13.75

MESQUITE DRY LAKE

Size	Above "Break" Line Percent	Near "Break" Line Percent	Near Playa Percent
1/4"	21.70	7.72	2.10
Mesh 10	19.47	12.01	3.59
Mesh 30	18.13	12.12	5.53
Mesh 70	19.61	16.34	25.45
Mesh 230	10.55	20.39	41.73
pan	10.54	30.88	21.60

As expected, the coarsest materials are found on the highest part of the fan surface. Still, the most significant result is the fact that these changes in surface texture can be detected from ERTS-1 imagery.

The recreational planning potential of this study for the desert is great. Not only do textures have a direct relation to the adaptability of desert surfaces to withstand ORV operation, but the importance of texture in the distribution of desert vegetation is receiving increasing attention.

7.2.9 Use of Yucca Brevifolia as a Surrogate for Detection of Near Surface Moisture Retention

For this investigation, ERTS-1 imagery proved useful, albeit not conclusive. ERTS-1 imagery supplemented both low altitude (1:20,000) color infrared imagery and field/laboratory analysis. It also provided a regional photo mosaic of the Mojave Desert from which to work. By examination of false color Diazo transparencies made from such imagery one can detect the signature of Yucca core areas and associated vegetation.

It was our intention to isolate the major controls which govern Yucca distribution. For the purpose of this preliminary investigation, we focused upon core areas of Y. brevifolia which were within two hours driving time of Riverside, California and chose for detailed examination only those sites which appeared to have the most dense and healthy stands of Yucca. Thus, the sites studied probably possess optimal physical conditions for the Yucca's survival. The discussion centers on climatic and edaphic parameters, parameters which are felt to be of primary importance, at least within the area studied.

The primary factor governing Yucca distribution is the availability of moisture during the season of seed germination: summer. (Temperature factors are considered only secondary since the Yucca seed will germinate at warm/hot temperatures, a condition satisfied throughout the desert in summer). Precipitation, although in meager amounts, comes to the Mojave (high) Desert in both winter and summer. The Gulf of Mexico and the Gulf of California are both source regions of maritime tropical air which influences the Mojave Desert in summer. Circulation patterns and the thermal low pressure system developed over the Mojave-Colorado Deserts in summer initiate influx of this maritime tropical air. In contrast to the Colorado (low) Desert, the Mojave (high) Desert receives a greater percentage of its total precipitation during the summer season. The overall greater elevation of the Mojave complements the convective processes triggered over the strongly heated desert area in summer. Areas with the highest elevations will thus likely have more summer precipitation, usually in the form of thundershowers. This is seen in the areas of Joshua Tree National Monument and the environs of Mountain Pass-Cima Dome, for example. Consequently many stations in the Mojave exhibit a degree of bimodality in their precipitation curves, with maxima in late summer and winter.

Not all areas in the Mojave which receive summer precipitation (and would thus appear to have Yucca) do, in fact, possess Yucca. Conversely, several areas which receive a relatively small percentage of their precipitation in summer do have Yucca. In order to understand these situations, a detailed examination of soil conditions is needed,

especially with reference to the moisture-retentive capability of the soil.

In the Mojave, it was assumed that the surface and near-surface soil samples were reasonably representative of soil characteristics as deep as Yucca root penetration, at least in terms of the soil parameters examined. This assumption is considered valid since no significant caliche or claypan horizons were detected in any accessible stratigraphic sections.

Within the broad ranges of pH tolerance of the Yucca, which includes the span 6.8 to 8.2, soil pH does not seem to be a critical factor governing Yucca distribution. Similarly, available soil nutrients also seem not to be significant relative to Yucca distribution. Textural analysis of soils, however, proved to be very useful and enable the determination of the edaphic factors regarding Yucca growth.

Yucca supporting soils are bimodal, with maxima in the medium-coarse sand and silty clay fractions, (.75Ø and 4ØØØ). The textural composition is highly moisture-retentive. This is understandable as Yucca-supporting (as opposed to the well-sorted soils) if the upper Mojave Desert is accepted as a climatically tense environment in which Y. brevifolia is able to survive only where there is available sufficient soil moisture. Soil moisture, thus, becomes the limiting factor governing Yucca distribution which, in turn, is controlled by soil texture, given a certain minimum of precipitation.

The significance of optimal soil conditions for moisture retention is additionally confirmed by the fact that Y. brevifolia tends not to occur on pedimented surfaces, the depth to bedrock on which very rarely exceeds one meter. There simply is insufficient groundwater to support Yucca.

Although species identification is not possible from ERTS-1 imagery, since it is now known that Y. brevifolia occurs in the moistest areas in the high desert, which can be predicted from physiography, (i.e. non-pedimented surfaces, alluvial fans, wadis), these secondary physiographic surrogates, easily detectable from ERTS-1 imagery, can be used to ascertain the general distribution of Y. brevifolia and, therefore, the regions in the high desert with the greatest potential for near-surface moisture retention.

7.2.10 Disjunct Fluvial Transport Patterns in the Colorado River Delta as Interpreted from ERTS-1 Imagery

Cursory examination of ERTS-1 imagery of the Colorado Delta for two dates, September 12 and December 29, 1972 (Figures 7.22 and 7.23) reveals differences in sediment transport patterns in the waters of

Figure 7.22. Colorado delta.

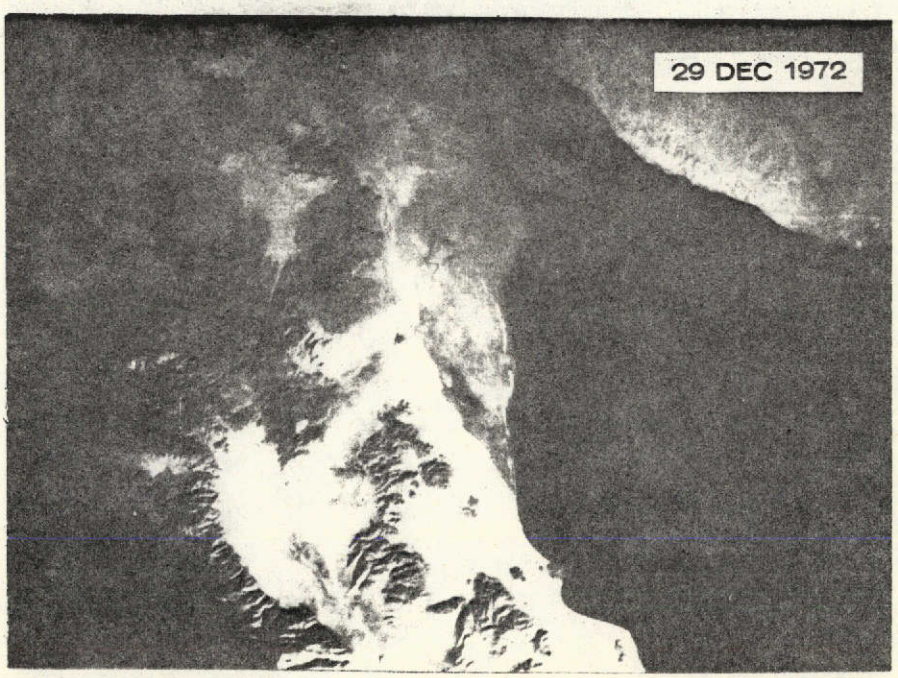

Figure 7.23. Colorado delta.

the Northern Gulf of the California Delta region. Initial impression of these differences leads one to believe that what is seen is either surface phenomena or the bottom configuration of the Colorado River Delta. The discontinuities might be attributed to any one or a combination of variables. These variables could conceivably be: (1) local storm activity and related precipitation; (2) agricultural activity; (3) tidal flow or stage; (4) currents in the gulf; (5) thermal mixing of the fresh and saline water at the delta.

Such examination of ERTS-1 imagery of the Colorado Delta and Gulf of California coastal region leads to certain possible generalizations about agricultural activity and, in turn, some inference can be made about relative amounts of precipitation for that region. These elements combine to modify fluvial transport patterns in the delta region significantly. Examination of sequential imagery of the delta could be used to substantiate any interpretation of agricultural activity made from ERTS imagery of the Lower Colorado River. At this time more intensive research into the variables affecting the delta sedimentation system is necessary before any extensive application of the imagery is made. Lack of access to tidal information and to data regarding temperatures of the Colorado River and the Gulf of California, and likewise to scant data available on mixing rates in the delta, makes any conclusions or statements unsupportable. Initial impressions realized from the imagery are encouraging, however, and it is felt that further research on this aspect of the Colorado River water system is warranted.

7.2.11 Land Evaluation Based on ERTS and High Altitude Imagery

The vital environmental economy of "Spaceship Earth" has become today's immediate concern for both layman and earth scientist. To properly manage these natural resources and to compile the necessary resource information in a speedy and comprehensive manner, has become a formidable task. The solution for this problem is now under investigation by various organizations (federal, state and private) each in harmony with two immediate goals: (1) to provide assistance to earth resource managers and (2) to develop and test inventory techniques applicable to developing areas of the world. To benefit most from a resource inventory one should apply a holistic method: a purely holistic method implies that the environment should be studied in its entirety attuning more to remote sensing techniques in the modern sense, rather than photo interpretation which was designed as a tool used for separate evaluations of land attributes.

The assessment of the world's resources through the use of both satellite (ERTS-1) and high altitude (U-2) imagery leans naturally toward the broad perspective, thus obtaining the holistic impression of the region. Some authorities, however, believe that the retrieval of environmental information can best be accomplished by means of

aerial photography (Katz, 1967). The value of combining both satellite and high altitude imagery, however, will probably reveal maximum utility in large environmental surveys. Consider for a moment the land attribute of relief which usually is not great enough to be stereoscopically visible on ERTS-1 photography, but is on the high altitude imagery. This single characteristic of land relief is an essential asset in a holistic survey.

Recognizing that the compilation of all the environmental attributes necessary to properly evaluate the usefulness of satellite and high altitude images in a holistic survey is still being made, certain preliminary observations and conclusions have been compiled and grouped into three sections: (1) the practical application of ERTS-1 in a holistic survey, (2) the evaluation of the (MSS) bands in detection of land units and, (3) the advantages of their compatibility.

Explanation of Holistic Method

The holistic survey of the environment involves an assessment of the total characteristics of the landscape, including relief, vegetation, geology, and soils, remembering to account for the technological, sociological and economic considerations as well (note land classification in Figure 7.24). The divergence from a separate survey which is aimed at a specific land attribute can be seen in Figure 7.25.

The classification of individual land units is constructed upon the converging evidence of individual attributes which appear as homogenous areas (Zonneveld, 1971). The observable units can then reveal a comprehensive view of information to scientists who have knowledge of the land.

Application of ERTS for a Holistic Survey

The need for practical evaluations of large areas of land, especially in remote underdeveloped nations, has become extremely important in the assessment of world resources. The acquisition of this information prior to ERTS-1 was usually costly because of its scale, requiring large numbers of photographs and personnel. In a holistic method of evaluation, small scales present few problems and in fact scales smaller than 1 to 100,000 in areas where little knowledge is usually known, require a holistic approach. Both ERTS-1 and high altitude images are above this scale, thereby permitting this method optimum usage. The direct advantages in doing so are: (1) more direct integration of knowledge, (2) saving in logistics, (3) less need for personnel, if team leaders are experienced and, (4) the basic data result in an integrated basis for assessment of the land.

Furthermore, the final product provides a useful data base for specific studies, when certain resources are needed in detail.

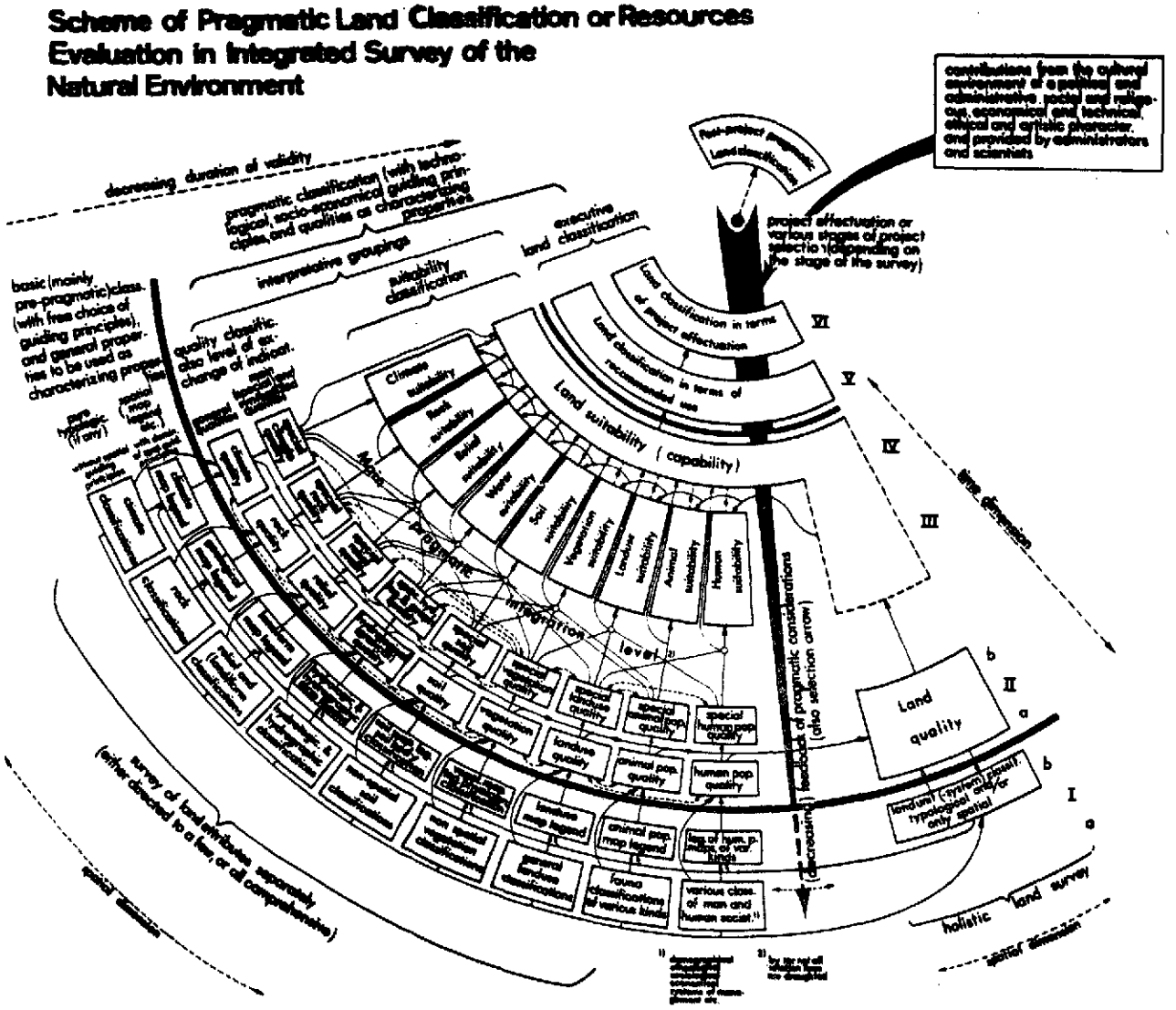

Figure 7.24. Land classification (source: Zonneveld, 1971).

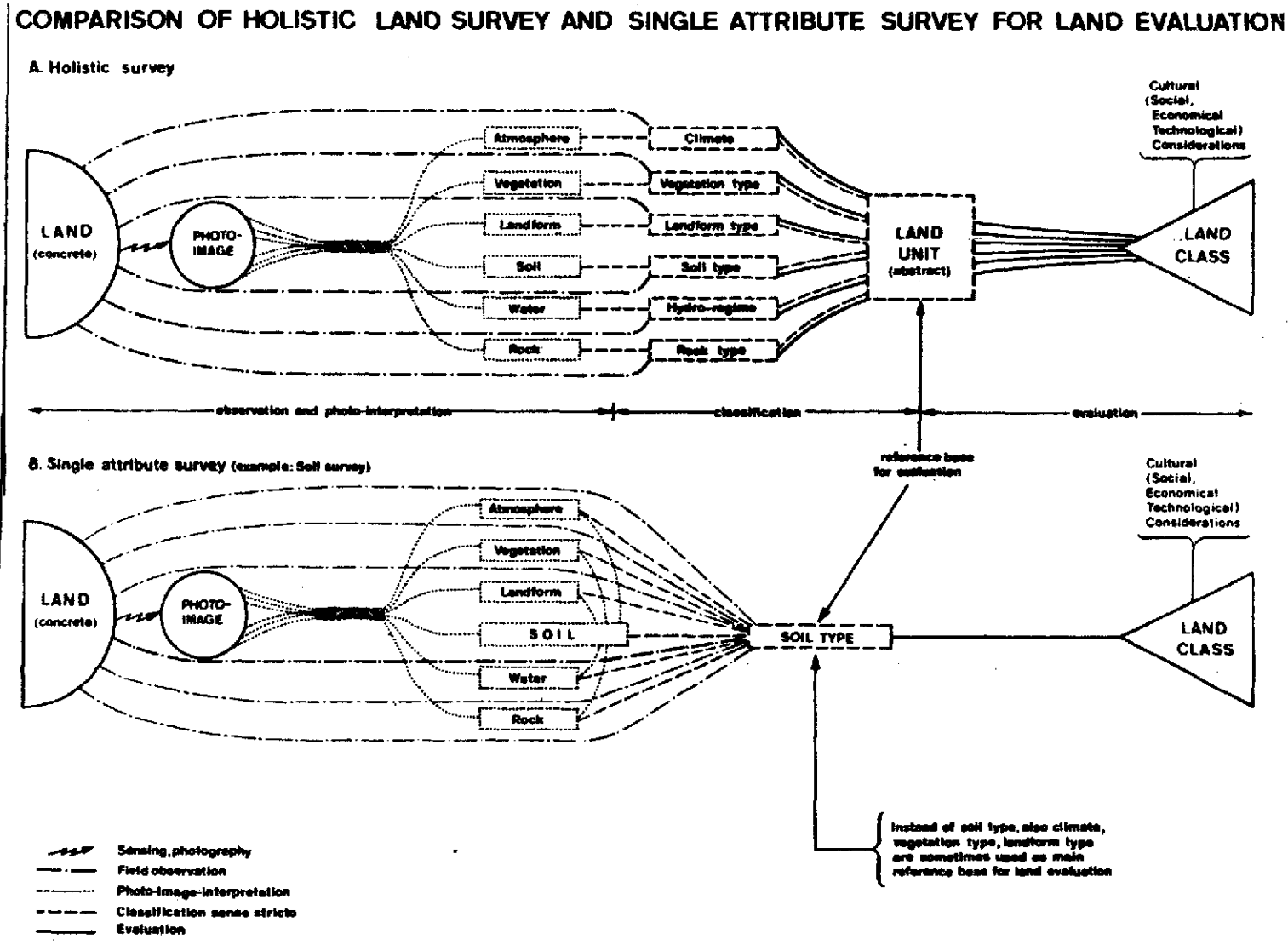

Figure 7.25. Single attribute survey.

Imagery and Scale

The primary set of imagery analyzed in this preliminary investigation was small scale satellite (ERTS-1) and high altitude (U-2) frames, recorded in September of 1972 and March of 1971, respectively. Analysis of the ERTS-1 imagery frame 1053-17551 generated by the Multispectral Scanner (MSS) Bands (channels 4 to 7) provided the satellite base. The high altitude photography, recorded on color infrared film because of its optimum quality in small scale interpretation, provided the aerial imagery in this interpretation.

As previously stated, survey scales smaller than 1 to 100,000 usually demand a holistic approach. Therefore, both ERTS-1 imagery having a scale of 1:1,000,000 (on 9 x 9 inched frames) and the high altitude imagery approximately 1:100,000 are acceptable in this holistic approach. However, other qualities necessitate their combined efforts in a land evaluation study.

The utility of ERTS-1 is curtailed by its lack of systematic overlapping coverage within the line of flight and consequently by the monoscopic view, thereby not permitting total reliance in a holistic survey. Numerous authors have announced that the mapping of land use categories is feasible, which is true in separate surveys concerned with one attribute. To map the total environment as a entity, however, requires an appreciation of all attributes of the landscape. Therefore to comprehensively investigate a region in a holistic method requires the sum of satellite and high altitude imagery.

Study Area

The landscape under this preliminary study is located in Perris Valley, California. This study area constitutes a surrogate for a larger regional investigation in Southern California. However, the geographic significance of this area is important due to the fact that the newly constructed Perris Dam represents the end of the California Water Project in Southern California. The area (Figure 7.26) geographically commences at the summit of the Box Springs grade near the intersection of Highways 395 and 60, and from there trends in a southerly direction. The end of the valley is located near Menifee Valley, approximately 25 miles distant. The western boundary parallels and is near to Highway 395, while the eastern limit is artifically delineated and extends from a point near the city of Hemet to Black Mountain.

The general topography of the area is one of denudational hills surrounding a lower peneplain which contains an occasional noticeable granitic remnant. The agriculture of this area can be divided into three categories: (1) irrigated crops, (2) non-irrigated crops and, (3) dry farmed crops. Predominantly the area is known for its

Figure 7.26. Preliminary study site. A portion of a U-2 frame of the Perris Valley (north at top).

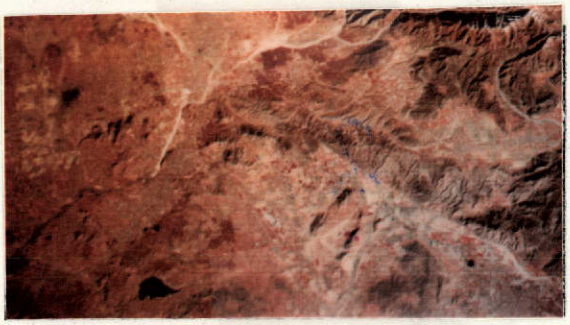

Figure 7.27. A portion of an enlarged ERTS-1 frame of the same area (north at top).

production of potatoes, sugar beets, onions, carrots, alfalfa, navel oranges and wheat or barley.

Interpretation

The preliminary interpretations of ERTS-1 and high altitude imagery concentrated upon the task of delineating holistic land units. The original scale of the ERTS photography was 1:1,000,000. Early observations made at this scale were achieved by using an Agafa 8X magnification loupe over a light table. Each individual MSS band was scanned in this process as well as the simulated CIR combined image. These observations allowed familiarization with the spectral characteristics which were later enhanced in an effort to delineate homogeneous land units.

The initial analysis of the 9 x 9 inches CIR high altitude imagery (Mission 164, 3/71) having a scale of 1:120,000 was accomplished on a Bausch and Lomb stereoscope which has the capability of scanning in both x and y directions. The only warranted discontent in using this device was in its limited free space beneath the lens, which caused difficulty in production of the overlays when viewing the image.

The technique of photographically enlarging a section of the ERTS image to recognize and delineate areas having homogeneous color tone was employed. The area photographed was taken from the I^2S color combiner and was enlarged to a scale of 1:125,000 (Figure 7.27). The emphasis upon this foremat in crop identification and other detailed investigations is still under quantitative testing but preliminary results published by various authors indicate future success (Estes, 1972).

During the preliminary investigation the four bands (channels 4 to 7) were examined manually so as to determine the attributes indicative of land use. These individual categories of urban, agriculture, rangeland, water bodies and barren land were delineated in order to evaluate the optimum band or bands for interpretation.

The urban areas of the investigation were mainly small service centers, except for the City of Riverside. The small cities of Perris and Sunnymead were difficult to interpret because the street patterns could not be observed (visible breaks or sudden bends in the transportation lines proved to be useful criteria). The larger City of Riverside is easily detectable due to the street complex and coarse texture.

Agricultural areas provide detectable signatures because of their distinct geometric shapes and spectral signatures, especially in the color combined image.

Rangeland vegetation, interpreted on band 5, was possible to differentiate, although the identification of particular communities

was sometimes difficult. Chaparral had a grey to grey-black tone signature as opposed to the usually lighter grey grassland communities.

Water bodies of large proportion could always be detected owing to their low reflectance in the red band (0.6 to 0.7 microns). However, the smaller reservoirs near the agricultural fields, owing to their similar geometric shapes and tonal characteristics, were difficult to identify.

Barren land, having a light grey signature, can usually be easily distinguished. The features which cause possible confusion are large construction areas (e.g., Perris Dam) and fallow land, if not distinguishable by their geometric shape.

The preliminary observations of the MSS bands presented some problems in that the spatial resolution and tonal ranges were poor. The same areas, however, when viewed on the simulated CIR combined composite, permitted substantial information in delineating vegetation communities, a quality especially useful in a holistic evaluation.

In short, the preliminary results of the interpretation show that bands 4 and 7 allowed the greatest differentiation in urban areas. Transportation routes and agricultural areas were best observed using band 7. Convergence of evidence, necessary in the delineation of homogeneous land units, was best accomplished from the simulated CIR combined image. This fact results primarily from the sharper vegetation boundaries visible on that image.

It should be noted that in this preliminary interpetation only a single land attribute (land use) was delineated using ERTS-1 and high altitude imagery. To properly benefit from a holistic land survey all the land attributes should be known. This then would permit the convergence of evidence necessary in delineation of land units.

Conclusion

Evidence available at this time demonstrates that both ERTS-1 and high altitude imagery can be useful in a holistic approach, especially over large areas where little prior knowledge is known. To recapitulate, the advantages of a holistic survey are as follows: (1) adapted to small scale imagery; (2) provides a better integration of knowledge; (3) lowers total survey costs; (4) requires fewer experienced personnel; and (5) facilitates presenting the results in an evaluation format.

Preliminary conclusions of this study obviously point out the useful application of a holistic land evaluation. Based upon both ERTS-1 and high altitude photography, a holistic resource evaluation, whether on a regional, national or global basis, can be an asset to a resource manager in any country.

References

Estes, John E., 1972, Use of ERTS-1 Data to Assess and Monitor Change in the West Side of the San Joaquin Valley and Central Coastal Zone, NASA Technical Report No. NAS-5-21827.

Katz, A. H., 1967, Reflections on Satellites for Earth Resource Surveys, Rand Corporation P-3753, 28 p.

Zonneveld, I. S., 1971, Land Evaluation and Land(scape) Science, International Institute for Aerial Survey and Earth Sciences Press, Enschede, The Netherlands.

7.2.12 Impact of Linear Features

It has been accepted among geographers that linear human constructions (roads, railroad, aqueducts) have had more than local environmental impact. The question is especially timely because of the present debate over the Trans-Alaska pipeline.

ERTS and high altitude U-2 images have proven valuable as monitoring devices for the study of such impact. Moreover, such images reveal patterns of change which are not readily visible from the ground. The arid areas of the western United States provide an excellent environment within which to demonstrate the capacities of this imagery for such purposes. First, vegetation in this environment tends to be constant; therefore lithic and soil changes are readily discernible there. Second, the imagery allows for the interpretation of groundwater flow. The properties of this simulated CIR imagery are especially useful for the detection of vegetation; where groundwater is trapped and pushed nearer the surface, fluorescence of vegetation results and can be detected on the imagery. Moreover, the variability of arid basin-and-range landscapes like the Mojave Desert provides many different environments in which the effects of these linear features can be observed. Mountain passes and playa surfaces, for example, are two of the many environments common to the Mojave which show the marked impacts of road construction. Several examples of the impacts of linear features are available. Figure 7.28 shows, for example, the influence of road construction upon the surface of Ivanpah Dry Lake. The road at the south of the lake is of special interest because it has become the southern boundary of that playa.

Figures 7.29A and B are ground photographs taken on either side of a road near the margin of Lucerne Dry Lake. The effect of this road on vegetation is clear; such effects are visible on ERTS imagery.

Other influences on vegetation, soil, and other physical features are also visible on ERTS imagery. Many influences can be located and their progression studied through ERTS and U-2 sequential photographs,

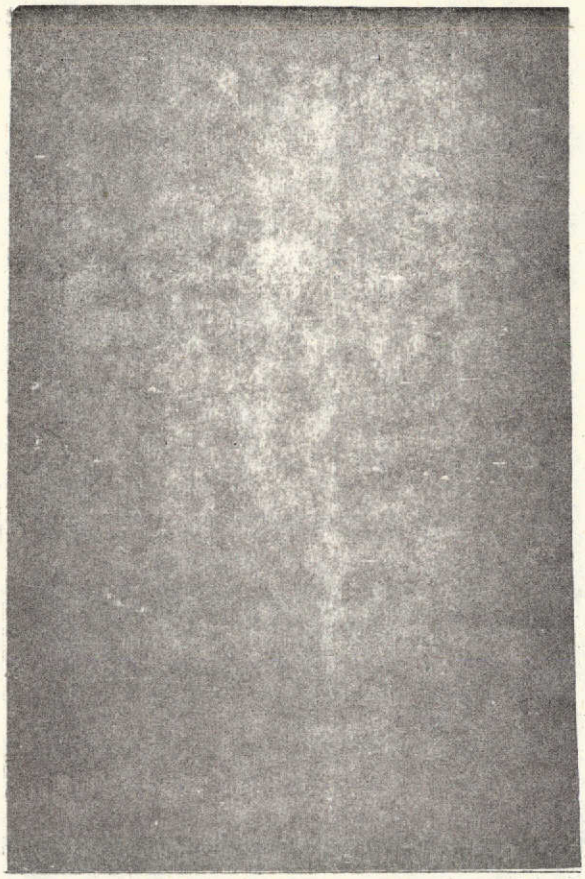

Figure 7.28. Enlargement of a portion of an ERTS frame of Las Vegas. Shown are Roach (top) and Ivanpah dry lakes. Note influence of highway construction.

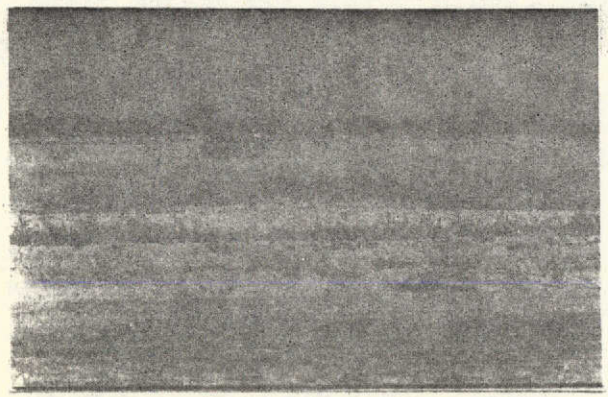

Figure 7.29A

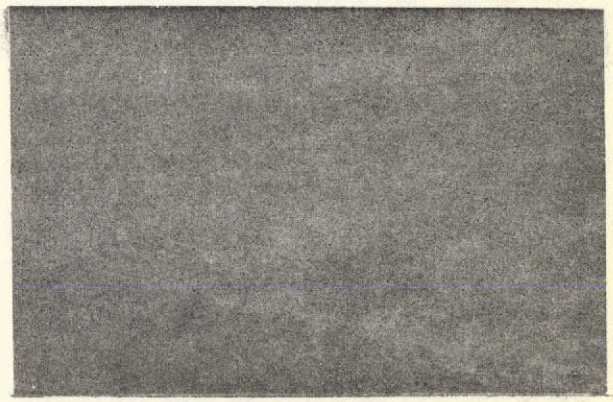

Figure 7.29B

given the regularity with which these kinds of imagery become available. Lower altitude imagery with greater resolution would be appropriate for more detailed study of the resultant environmental impact.

Because ERTS band number 4 has proven best for the location of linear features it has special application for the study of the environmental impact caused by roads, aqueducts, and other similar features. Band number 7, however, reflects vegetation patterns most clearly and is, therefore, also especially valuable for these purposes. Vegetation patterns are the ones most often altered by the linear constructions.

Finally, it should be noted that the broad vegetation boundaries which are often clearly discernible on ERTS imagery are not always easily observed on the surface or at low altitude. Thus, for example, the boundary effects of linear human construction are frequently more easily seen on small scale ERTS imagery than they are on the ground.

7.2.13 Archaeological Findings in Hidden Valley, Nevada

While observing U-2 imagery of Las Vegas, Nevada (CIR, RF 1:131,000) to gain another view of the environmental impact of linear human construction in that area, the researcher observed several odd lines around the margin of Hidden Valley, south of Las Vegas. ERTS imagery was inspected carefully for evidence of these lines but scan line and resolution problems made them impossible to see at that smaller scale.

The lines have several interesting characteristics and present indications are that they represent a major archaeological find. First, the lines, overall, extend for more than four miles, mainly on the west side of Hidden Valley, but they can also be faintly seen in the southeast. There are at least 18 lines in the best preserved series. In addition, they are evenly spaced, curving, and parallel as if they were created by design. They do not, however, follow lines of equal elevation as recessional shorelines of the lake which once filled Hidden Valley would have to do. Moreover, they can be seen to have deflected drainage in several areas. There is no natural mechanism by which these lines could have been created.

Further observation indicates that these lines end abruptly at the edges of several alluvial fans and then resume on the other side. There are only three possible ways in which this situation could have developed. The first possibility is that they never existed on these several fans, but did exist on either side thereof. This is extremely unlikely however. Ground observation has shown that these fans have not been disturbed in an extremely long time; they are covered with a deeply patinated desert pavement, indicating that they have not been disturbed for a considerable length of time. Thus, the second possibility, viz. that these lines underlie and are older than the fans, seems most likely. It is a generally held opinion among geomorphologists

that fans of this type have not been growing in the southwest since the end of the Pleistocene Epoch, some ten to thirteen thousand years ago. Rather, since that time, fans in the area have been subjected to erosion. Thus, there is a considerable chance that these lines are at least ten thousand years old.

Ground observations strengthen this possibility. A stone circle which apparently was a fire ring has been found, as have several madatis. These features are patinated in such a way as to suggest great age. The lines themselves are extremely obscure, and disconnected (Figure 7.30). Yet they can be seen as stone lines, perhaps ten feet wide and one or two feet high at the present time. Because these stone lines are a preferred environment for certain types of vegetation, they often correspond with linear plant formations (Figure 7.31). They are clearly human constructions and are quite old. The lines, in fact, are much more obvious on the imagery than they are on the surface. One might make an analogy with a pointillistic painting. One must get a removed perspective before the lines become apparent. Initial observations indicate that these stone lines were part of a water conservation system the size of which is unequalled at any archaeological site in North America.

Much more work needs to be done in Hidden Valley to determine the origin and purpose of these stone lines. Nevertheless a purely speculative explanation of their origin is offered here. It may be that these lines date from the last filling of the lake which once occupied Hidden Valley; presumably the last time the lake was filled to overflowing was at the end of the Pleistocene. A relatively dense population could have developed which was economically dependent upon that lake. When the lake began to dry, however, a new food source presumably had to be found. Because wild grasses with edible seeds are presently found in the valley, these may have become the new source of food for this population. Even today, the floor of Hidden Valley supports a lush growth of flowers each spring; the valley contains fertile soil, weathered from the basalts which comprise the regolith of the area. One must assume that in times past, when the soils were not as saline, that Hidden Valley provided a rich environment for the growth of wild grasses. Moreover, the lack of salinity in the valley floor made its center a natural catchment basin where plant growth was probably lush, at least initially, after the drying of the lake.

Nevertheless subsequent partial fillings and evaporation would have increased salinity on the floor to a point where grasses would no longer grow there. It is at this point that the stone lines in question may have been constructed. Their function, if this theory is correct, would have been to retard sheetwash and other runoff so as to encourage the growth of grasses with edible seeds on the less saline slopes. Hopefully the origins of these lines will be more certainly established by further field work by the author in Hidden Valley.

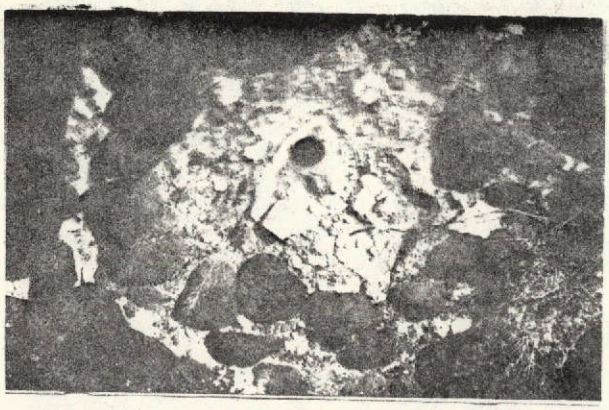

A

B

C

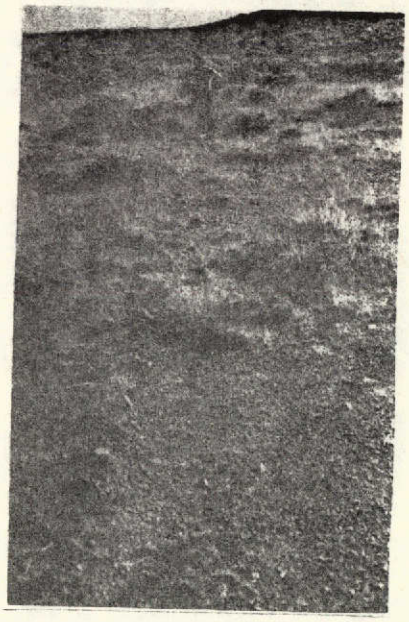

D

A -- Fire Ring
B -- Matadi
C -- Stone Line
D -- Stone Line

Figure 7.30. Archaeological findings in Hidden Valley, Nevada.

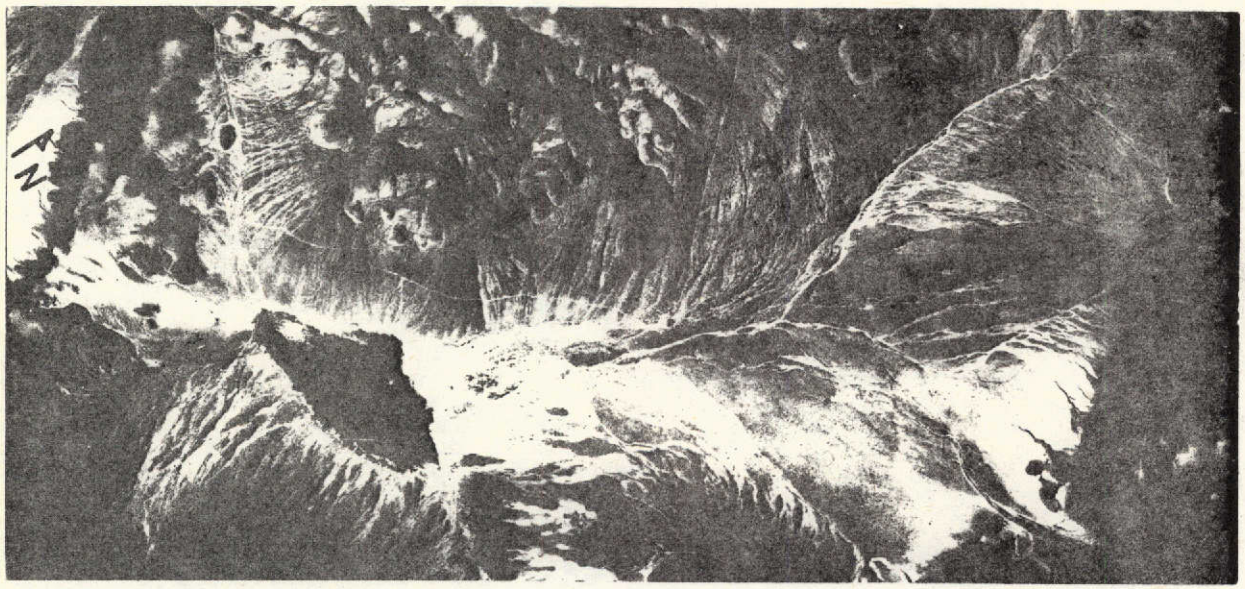

Figure 7.31. Enlargement of a portion of a U-2 frame of Hidden Valley, Nevada (21 November 1972). The stone lines appear as white curves.

7.3 NEW TECHNOLOGIES

7.3.1 A Recipe for "Do-It-Yourself" Color Composites of ERTS-1 Imagery: The Poor Person's Guide to Everlasting Color

Due to the shortage of color composite prints and the denseness of 70 mm bulk negatives available from early ERTS-1 imagery, the investigators at the University of California (Davis, Berkeley, and Riverside) sought alternate methods of producing "true" and "false" color images suitable for preliminary research and investigation. Several expensive "darkroom" techniques were attempted but a parallel system was developed that is cheap, practical and universally applicable. The simple, but practical, idea is presented here because any present or potential user can do it!

All you do is follow a few easy steps:

1. Use Diazochrome color proofing film. Diazochrome is purchased from most audio-visual stores as a product of Tecnifax (a subsidiary of Scott Graphics) and is supplied in fifteen colors of Pastel (P) and Dense (K).

2. Acquire 9 x 9 inch black-and-white positive transparencies in bands, 4, 5, 6, and 7 from the Sioux Falls or NASA-Goddard data processing facilities.

3. We prefer the dense (K) for the following combinations:

a. Band 7, use Cyan (KCY)
b. Band 5, use Magenta (KMG)
c. Band 4, use Yellow (KYL)
d. For edge enhancement, buy Black (KBK) and use with Band 7.

The cost is only about twenty-five cents per sheet.

4. Expose each band to the corresponding color (a subtractive process) with an ultraviolet light, i.e. a #4 photo-flood lamp, overhead projector, or use an Ozalid, Bruning or Diazo machine. Exposure times of one to three minutes are required. The longer the exposure, the less dense the image. (At Riverside, we are using a Sears Photo Lamp, over a glass plate, cooled by an office fan.)

5. Acquire a one gallon "pickle jar" to develop the Diazo image in a closed bottle. The process requires ammonia vapors and we are using a 1/2 inch "sponge" covered with a plastic sheet at the bottom of the jar with 1/3 inch of #26 blue print ammonia. (Film may also be developed in a Diazo machine.)

6. For variety you may want to experiment with various colors and change the number of layers. As a final product, sandwich the desired

layers together with double-stick tape. Use a magnifier to align and recheck the registration marks. The cost per color composite printed is usually less than $1.00.

Figure 7.32 shows a color composite of ERTS-1 on September 4, 1972, made by using blue in band 7 and red in band 5 for a simulated false-color image of the San Diego area of Southern California. Figure 7.33 shows a simulated CIR image of the same region produced on the I^{2}S Mini-Addcol Viewer.

7.3.2 Density Slicing to Enhance ERTS-1 Imagery

The technique of density slicing using a photographic film, and its application for pre-enhancing ERTS-1 imagery in preliminary testing, appears to be an effective one for mapping variegated areal phenomena. Furthermore, it provides a useful supplement to the I^{2}S Mini-Addcol viewing system. The test presently to be described involved enhancement of selected ERTS-1 imagery (November 1972), showing the Las Vegas, Nevada region, eastern Mojave Desert, and the Los Angeles Basin. Early difficulties in obtaining high resolution enhancements from ERTS-1 MSS imagery by use of Diazochrome composites, and initial interpretation from the 70 mm MSS chips in the viewer (Figure 7.34), led to experimentation with an equidensity film, Agfacontour Professional, to pre-enhance the selected ERTS-1 MSS bands.

Equidensity Film

Briefly, Agfacontour equidensity film is a black-and-white copy film, which at a specific combination of exposure and development becomes transparent, creating a band or line of isodensity (Ranz, 1970) (Figure 7.35). The underexposed and overexposed areas of the film adjacent to the transparent sector essentially remain black or opaque. The transparent portions of the image relate to a specific band of density on the negative and an areal representation of that density manifests itself on the positive equidensity film. The emulsion is blue sensitive, and the width of this band (i.e., the thickness of the density slice) can be varied by increasing or decreasing the amount of yellow-filtration used during the exposure process. Only first generation equidensities of the ERTS-1 imagery were used in this study. Subsequent experiments with this enhancement technique should include second generation density slicing.

The above implies a procedure whereby the first generation density slice is contacted onto a litho film and a subsequent density slice is taken from that negative. Perhaps third generation density slices might be required to further enhance the image. Initial results indicate that this technique of density slicing, using accesible darkroom facilities and procedures, allows rapid, accurate, and facile interpretation of certain areal phenomena. As seen in Figure 7.36, the distribution of the Joshua Tree or Tree Yucca, Yucca brevifolia (Jaeger variation; Jaeger 1968) in the Eastern Mojave Desert of Southern California and Southern

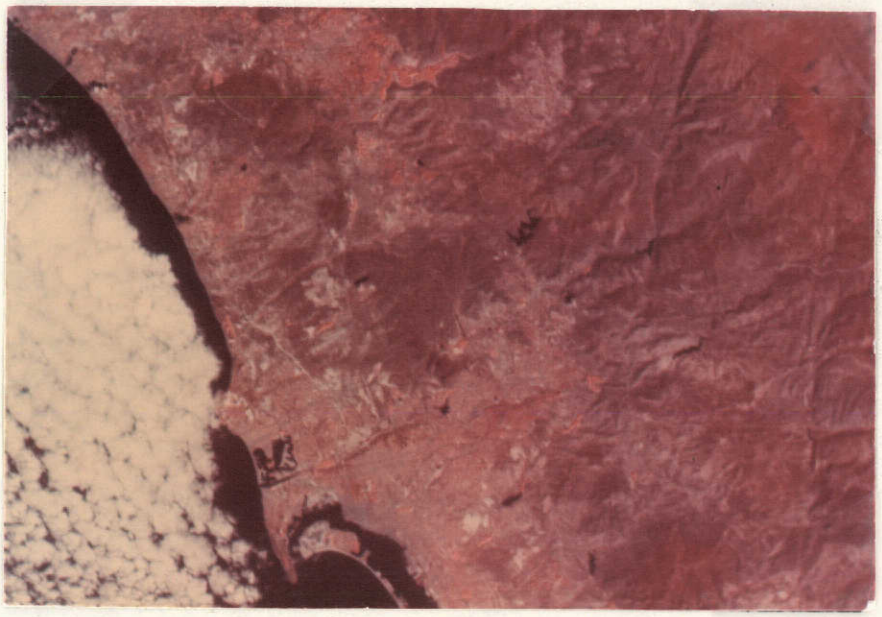

Figure 7.32. Simulated color infrared ERTS-1 image of the San Diego area; produced by the diazochrome technique.

Figure 7.33. Simulated color infrared ERTS-1 image using the I^2S Mini-Addcol Viewer.

Figure 7.34. Unenhanced ERTS frame of Las Vegas.

Figure 7.35. Density slice of the same ERTS Las Vegas frame.

Figure 7.36. Yucca brevifolia (Jaeger variation).

Nevada was used as an example to test the technique in terms of accurately mapping a minor element of the desert's environment. Because of difficulties experienced in obtaining the contour film no extensive experiments have as yet been conducted in the Los Angeles Basin Region.

Mapping of Yucca Brevifolia Jaegeriana

The negatives of MSS bands 5 (0.6-0.7 micrometers) and 7 (0.8-1.1 micrometers) of the Las Vegas Region were used to produce various density slices on the equidensity film. The first step in this process was to determine the negative density for a predetermined concentration of Y. brevifolia Jaegeriana (Joshua Tree). Teutonia Peak or Cima Dome, a well-known geomorphic feature in the Eastern Mojave, which is covered by a dense stand of Tree Yucca was used (Huning and Petersen, 1973). Once its image density had been determined using a densitometer with a suitably small sensing spot, the equidensity film was exposed to isolate this preselected area. A series of different density slices were also extracted from the same ERTS negatives bracketing the above key density. The resultant density slices were then viewed in the combiner using various filter combinations. The results are an enhanced and mappable signature for an environment in which the Tree Yucca is dominant (Figure 7.37). The enhanced density slice specifically depicting this environment was viewed through a green filter. The other three density slices used for the combination were projected through red and blue filters. It is felt that the green signature was most easily accommodated by human eyes for proper interpretive purposes. The areal expression of this environment was then mapped from the combined enhanced imagery (Figure 7.38).

Field Check of Yucca Environment

Over a three-day period the mapped distribution of Y. brevifolia Jaegeriana was field checked by the author. This field check of the mapped data revealed a high correlation with the environment's distribution. The field check also involved keying the vegetative community associated with it. This was done to determine more accurately the basis for the recorded signature. With the exception of two sites, the mapped signature from the enhanced imagery was a location containing Yucca. The exceptions were in areas where extremely high concentrations of another Yucca, Mojave Yucca or Yucca shidigera, were found in combination with a dense stand of Creosote Bush, Larrea divaricata. The morphology of mature Mojave Yucca (which is quite similar to the Y. brevifolia in its juvenile form) when found in a vegetative community having a high density of the Creosote Bush records as a similar signature on the imagery.

The mapped locations were all indicative of Yucca and its related community (Figure 7.39) but an inaccuracy was noted for the boundaries of each location. In all instances interpreter error on the boundary may result from the interaction of several related elements. Foremost of these is a change in topography from a low local relief fan surface

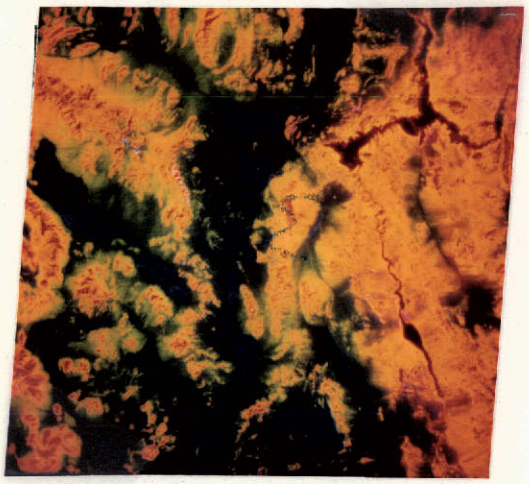

Figure 7.37. Density slice of the Las Vegas frame from which the Tree Yucca environment was mapped.

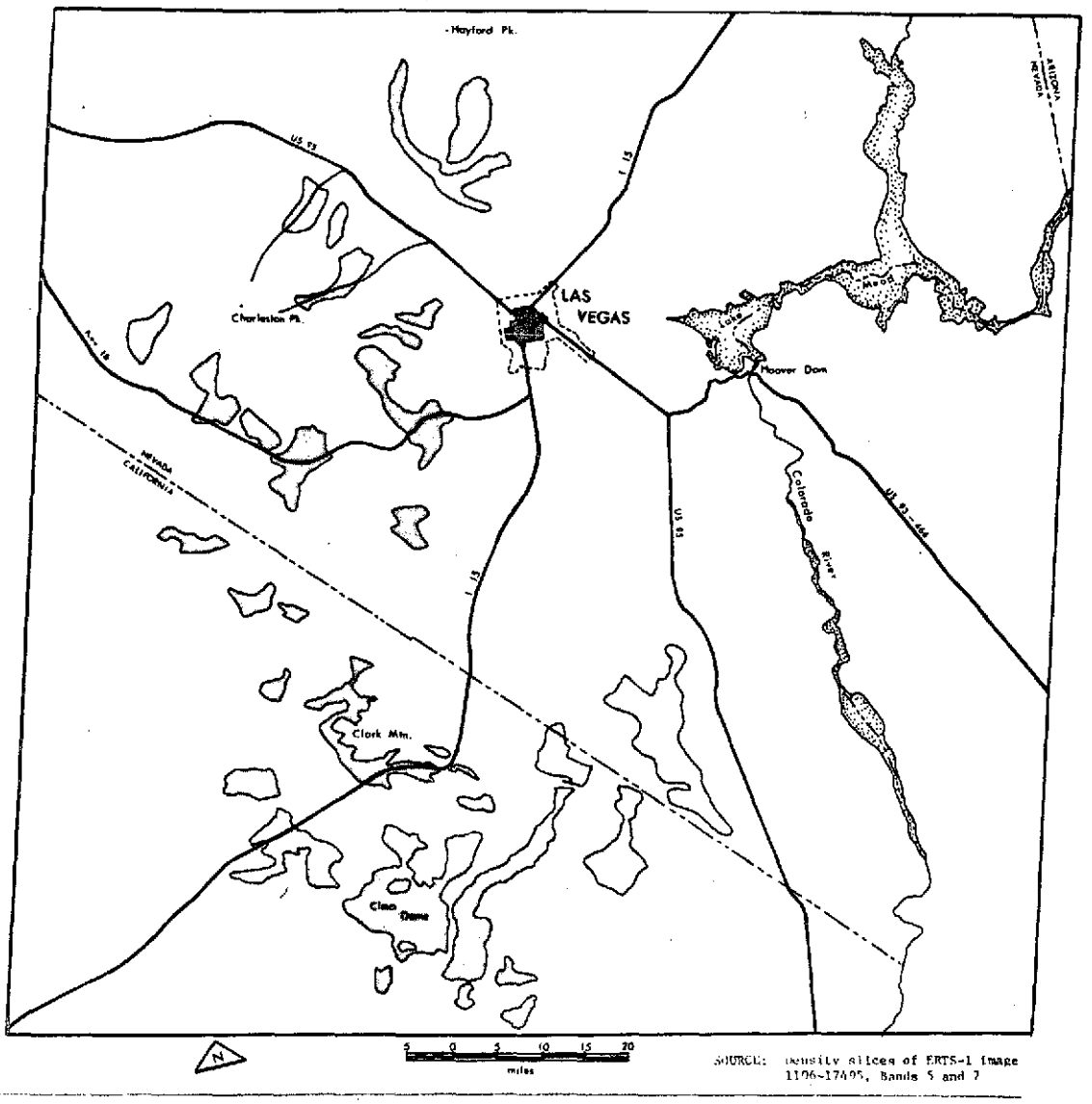

Figure 7.38. Distribution of Yucca brevifolia jaegeriana.

Figure 7.39. Type of environment mapped in the Eastern Mojave Desert.

to one of more rugged topography and high local relief. The key area, for example, Cima Dome, where the initial sample density was determined, is a feature of low surface relief on the Mojave landscape. The density of the community as isolated on Cima Dome would apply only to other low relief features where the environment is present (e.g., upper portions of alluvial fans, old pediment surfaces, and some high elevation alluvial-filled valleys). These types of surfaces where the Tree Yucca community is present would provide similar physical characteristics of albedo, texture, slope, and exposure to the sensor. Thus, they would present a similar density on the density slice. Another group of factors influencing the determination of the boundary of the community is the transition between environments of different plant communities.

Examination of Figure 7.40 reveals that the signature mapped there belongs to a vegetative community dominated by Joshua Tree, Y. brevifolia; Blackbush, Coleogyne ramosissima; and Burrograss, Scleropogon brevifolius. A group of minor species also are nearly always found in association with the above dominants. These are Mormon Tea, Ephedra spp.; and Cheesebush, Hymenoclea salsola. Also, in certain sites, at lower elevations of ±1,000 meters, Mojave Yucca, Y. shidigera, becomes codominant. Further tests need to be made to determine the degree to which plant associates other than the Tree Yucca contribute to the imagery signature.

Los Angeles Basin Slices

The Los Angeles Basin density slices were exposed to no specific density. They are the result of early experiments with the equidensity film to determine proper exposures. Filter packs were then combined to determine the value of the equidensity film to enhance urban phenomena.

Though no attempt was made to isolate specific densities, enhancement of certain features on the imagery results. The normal ERTS image of the Los Angeles Basin is highly interpretable and many elements of the urban environment may be discerned. Examination of comparable density slices reveals that certain features not visible on the normal false color image are readily apparent and more easily delineated. The density slice technique greatly enhances topography. The San Gabriels, Santa Monicas, Santa Susannas, Topatopas and the Simi Hills and Verdugo Hills are especially apparent. Other elements of alpine environments also become enhanced. Note, for example, the white enclosed ring pattern. This pattern is believed to closely delimit the extent of conifer vegetation in the San Gabriels, especially in the vicinity of Mt. Wilson. Re-examination of an enlarged portion of the ERTS combination of the Los Angeles Basin (Figure 7.41) reveals excellent information about the detail of the street and freeway network of the city. The density slice of the same scale (Figure 7.42) shows an obliteration of certain details of the above pattern. Harbor and coastal features, however, are greatly enhanced. The turbidity pattern of coastal waters is enhanced on the density slice. This pattern is scarcely visible on the original imagery.

Evaluation of the density slices for the Los Angeles Basin reveals

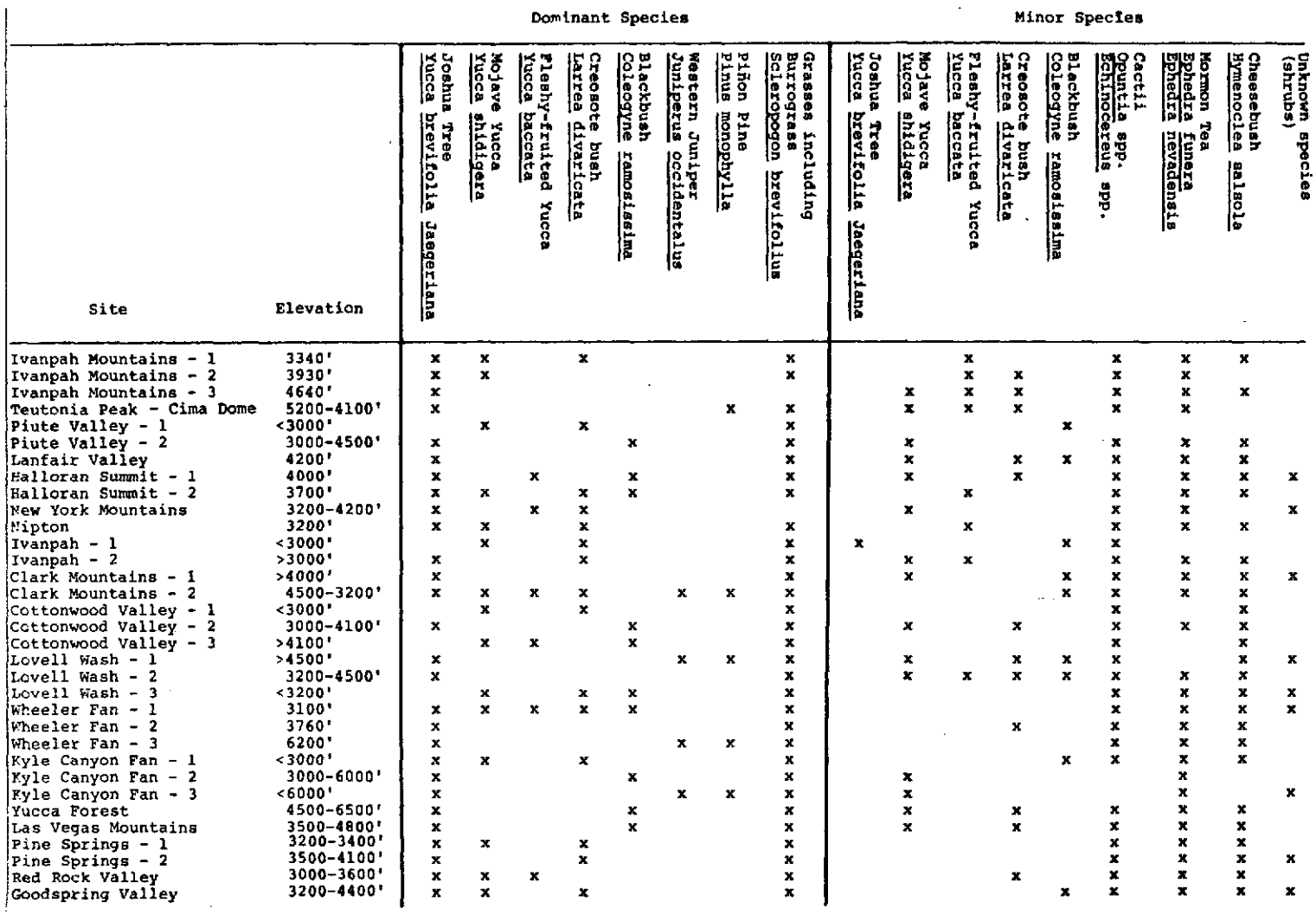

Site	Elevation	Dominant Species: Joshua Tree *Yucca brevifolia jaegeriana*	Mojave Yucca *Yucca schidigera*	Fleshy-fruited Yucca *Yucca baccata*	Creosote bush *Larrea divaricata*	Blackbush *Coleogyne ramosissima*	Western Juniper *Juniperus occidentalus*	Pinon Pine *Pinus monophylla*	Grasses including Burrograss *Scleropogon brevifolius*	Minor Species: Joshua Tree *Yucca brevifolia jaegeriana*	Mojave Yucca *Yucca schidigera*	Fleshy-fruited Yucca *Yucca baccata*	Creosote bush *Larrea divaricata*	Blackbush *Coleogyne ramosissima*	Cactii *Opuntia* spp. *Echinocereus* spp.	Mormon Tea *Ephedra funera* *Ephedra nevadensis*	Cheesebush *Hymenoclea salsola*	Unknown species (shrubs)
Ivanpah Mountains - 1	3340'	x	x		x				x			x			x	x	x	
Ivanpah Mountains - 2	3930'	x	x						x			x	x		x	x		
Ivanpah Mountains - 3	4640'	x									x	x	x		x	x	x	
Teutonia Peak - Cima Dome	5200-4100'	x						x	x		x	x	x		x	x		
Piute Valley - 1	<3000'		x		x				x					x				
Piute Valley - 2	3000-4500'	x				x			x		x				x	x	x	
Lanfair Valley	4200'	x							x		x		x	x	x	x	x	
Halloran Summit - 1	4000'	x		x		x			x		x		x		x	x	x	x
Halloran Summit - 2	3700'	x	x		x	x			x			x			x	x	x	
New York Mountains	3200-4200'	x		x	x						x				x	x		x
Nipton	3200'	x	x		x				x			x			x	x	x	
Ivanpah - 1	<3000'		x		x				x	x				x	x			
Ivanpah - 2	>3000'	x			x				x		x	x			x	x	x	
Clark Mountains - 1	>4000'	x							x		x			x	x	x	x	x
Clark Mountains - 2	4500-3200'	x	x	x	x		x	x	x					x	x	x	x	
Cottonwood Valley - 1	<3000'		x		x				x						x		x	
Cottonwood Valley - 2	3000-4100'	x				x			x		x		x		x	x	x	
Cottonwood Valley - 3	>4100'		x	x		x			x						x		x	
Lovell Wash - 1	>4500'	x					x	x	x		x		x	x	x		x	x
Lovell Wash - 2	3200-4500'	x							x		x	x	x	x	x	x	x	
Lovell Wash - 3	<3200'		x		x	x			x						x	x	x	x
Wheeler Fan - 1	3100'	x	x	x	x	x			x						x	x	x	x
Wheeler Fan - 2	3760'	x							x				x		x	x	x	
Wheeler Fan - 3	6200'	x					x	x	x						x	x	x	
Kyle Canyon Fan - 1	<3000'	x	x		x				x					x	x	x	x	
Kyle Canyon Fan - 2	3000-6000'	x				x			x		x					x		
Kyle Canyon Fan - 3	<6000'	x					x	x	x		x					x		x
Yucca Forest	4500-6500'	x				x			x		x		x		x	x	x	
Las Vegas Mountains	3500-4800'	x				x			x		x		x		x	x	x	
Pine Springs - 1	3200-3400'	x	x		x				x						x	x	x	
Pine Springs - 2	3500-4100'	x			x				x						x	x	x	x
Red Rock Valley	3000-3600'	x	x	x					x				x		x	x	x	
Goodspring Valley	3200-4400'	x	x		x				x					x	x	x	x	x

Figure 7.40. *Yucca brevifolia jaegeriana* and its associated vegetation.

Figure 7.41. An enlarged color infrared ERTS-1 image of the Los Angeles Basin.

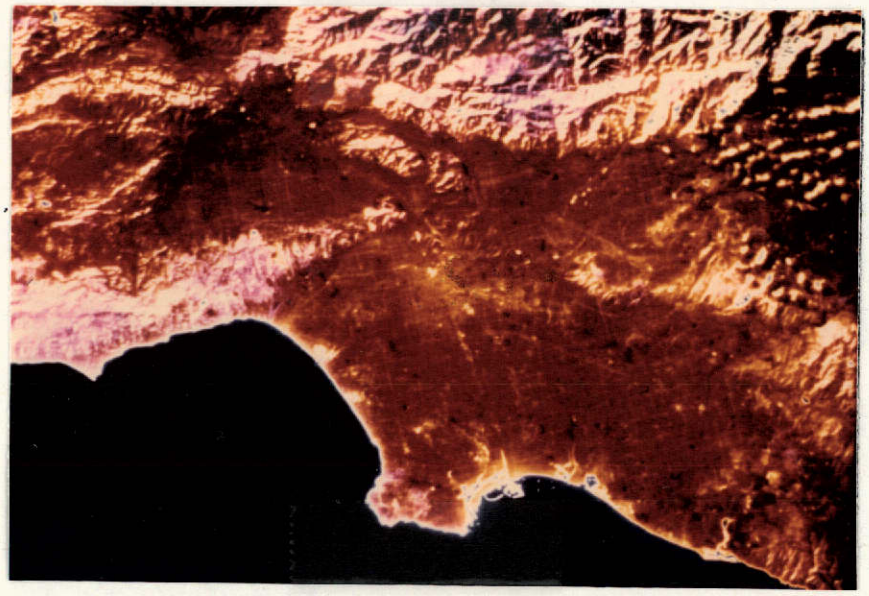

Figure 7.42. Density slice of the same ERTS-1 image of the Los Angeles Basin.

that certain elements of this landscape were greatly enhanced. The enhanced image is, for many sectors of this coastal basin, highly interpretable. Further experiments with the density slices could allow enhancement of any desired phenomenon in the Basin.

Conclusions

To reiterate, the technique of pre-enhancing ERTS-1 MSS 70 mm chips with an equidensity film has greatly increased the utility and application of the imagery. The density slicing technique also provides a useful supplement to the I^{2}S Mini-Addcol Viewing System.

The technique should not be viewed as final, however, since its full potential has not yet been realized. A further test of the technique might include mapping all the various vegetation environments in the Mojave, something which, considering the facility with which Y. brevifolia was mapped, could be done with small inputs of interpretation time. The technique can also be applied to the delimitation of specific urban environments as outlined for the Los Angeles Basin.

Density slicing of ERTS-1 imagery as realized from this technique has the potential for increasing the interpretability and use of the imagery and can provide the user with environmental data not easily obtained with other technology. The technique can contribute to studying various physical and cultural environments, and can be used to map their areal signatures at a high level of confidence.

References

Ranz, E. and E. Schneider, 1970, "Der Aquidensitenfilm als Hilfsmittel bei der Photointerpretation," Bildmessung und Luftbildwesen, 2: 123-134.

Jaeger, Edmund C, 1968, Desert Wild Flowers, Stanford; Stanford University Press.

Huning, J.R. and R.M. Petersen, 1973, "Use of Yucca brevifolia as a Surrogate for Detection of Near-Surface Moisture Retention," NASA Technical Report N-71-1, Department of Geography, University of California, Riverside.

7.4 SUMMARY

Our position as we near the end of the present contract may be summarized as follows: Imagery has been late in coming, and therefore much of the work was delayed. The first few weeks were primarily involved in developing a crude, color enhancement technique and determining the best ways of utilizing ERTS-1 data. Refinement of enhancement techniques, receipt of better imagery, and acquisition of the I^{2}S Mini-Addcol Viewer have allowed significant and rapid progress toward the fulfillment of the program objectives and have stimulated additional, unsupported research

within the department.

Our research objectives have been generally achieved. Development of the semi-automatic crop inventory system is well on its way to fulfillment.

ERTS-1 has provided a needed regional overview of Southern California, revealing previously unrecognized physical phenomena (such as the compression zone, described in Section 7.2.4). In addition, the sequential coverage of ERTS lends itself to the detection of dynamic environmental change (Coachella Valley, Section 7.2.3). Overall, research conducted under ERTS-1 has been most rewarding.

Appendix A provides an indication of the very extensive effort made by our group during the period covered by this report in providing information to interested groups and agencies about ERTS-1 imagery and its potential applications.

7.5 APPENDIX A -- INFORMATION AND APPLICATIONS ASSISTANCE

1. Origin of Visitor
    A. Academic
        1. Faculty
            (a) University of Montana
            (b) University of California, Riverside
            (c) University of Wisconsin
            (d) University of Southern California
            (e) California State University, Fullerton
            (f) California State University, San Diego
            (g) University of California, Los Angeles
            (h) Cal Poly, Pomona
            (i) University of California, Santa Barbara
            (j) Rio Hondo Junior College
            (k) San Bernadino Valley College
            (l) Riverside City College
            (m) Pierce Junior College
            (n) California Institute of Technology, Jet Propulsion Lab
            (o) California State University, Hayward
        2. Students
            (a) University of California, Riverside
                (1) Anthropology

(2) Geology
(3) Business Administration
(4) Sociology
(5) Political Science
(6) Urban Studies
(7) Dry Lands Institute
(8) Biology
(9) Agriculture
(10) Soils

(b) University of California, Los Angeles
(1) Geography
(2) Meteorology
(3) Hydrology

B. Government Agencies

1. City
(a) Department of Water and Power, Los Angeles
(b) Department of Parks and Recreation, Los Angeles
(c) Riverside City Planning Department

2. County
(a) Los Angeles County Planning Department
(b) Los Angeles County Parks and Recreation
(c) Riverside County Planning Department
(d) San Bernadino County Planning Department
(e) Orange County Planning Department
(f) San Diego County Planning Department

3. State
(a) Department of Water Resources
(b) Department of Highways
(c) Department of Parks and Recreation

4. Federal
(a) Bureau of Land Management
(b) NASA (Goddard)
(c) Bureau of Reclamation
(d) U.S. Department of Agriculture

(e) NSF Institute

(f) U.S. Department of State

C. Private

1. Southern California Testing Labs, San Diego
2. Davidson Engineering, Riverside
3. Doubleday and Company, La Habra
4. Los Angeles Times

II. Types of Assistance

A. Philosophy and Uses

B. Introduction to Remote Sensing Technology

C. Sensors and Processing

D. Techniques and Methods

E. Automated Interpretation and Mapping

F. Classroom and Instructional Aids

G. Bibliographic Aid

III. Subjects Analyzed

A. Land Use

B. Natural Vegetation and Wildlife Habitats

C. Geomorphology

D. Urban Growth

E. Environmental Impact Studies

F. Real Estate Development

G. Recreation

H. Statistics on Newcastle Disease

I. Regional Planning

J. Environmental Hazards

K. Environmental Perception

IV. Coordination on Projects

Chapter 8

DIGITAL HANDLING AND PROCESSING OF REMOTE SENSING DATA (UN645)

Co-Investigator: R. Algazi

Contributors: D. J. Sakrison, J. Schreibman, W. Dere
B. Romberger, A. Samulon

Department of Electrical Engineering and Computer Sciences,
Davis and Berkeley Campuses

TABLE OF CONTENTS

8.1 INTRODUCTION

An important part of the integrated study of Earth Resources carried out by the University of California is the combined use of all available sensing devices which provide information of interest to earth resource scientists. The data collected in each of several different bands on each of several different dates need to be analyzed in various combinations. Thus a significant component of our work is the efficient or optimal use of the large amount of ERTS-1 data available which has bearing on the study of specific earth resources. Three approaches are used in the analysts of the available data:

Human Photo Interpretation

Electronic Image Enhancement

Automatic Data Processing

These three approaches complement one another and are all pursued within our study. In order to articulate and understand these different approaches we show in Figure 8.1 a block diagram of the acquisition, analysis, and enhancement of remote sensing imagery. For each of the features of interest a set of attributes, $\underline{Y}$, makes it possible to study this feature from remote sensing imagery. By the time the attributes of the feature of interest have been recorded, in block 3, as spectral images or scans, these attributes have been modified by several partially known or unknown adverse effects. These effects include, for instance, the mixing of features due to insufficient image resolution, the variations of sunlight illumination, and degradation due to atmospheric scattering and turbidity. The analysis of the resulting imagery is affected to various degrees by all of these poorly known effects. In some cases, such as the mapping of rangeland resources, the task can be done conveniently by considering a single spectral image or standard color combination of spectral images. In other cases, such as monitoring water quality, the task is sufficiently more difficult so that more sophisticated analysis techniques are needed. In its generality, the study of ground features from remote sening data falls within the framework of statistical decision and estimation theory. The study of spectral and other properties of surfaces is one phase in the acquisition of *a priori* information. The transformation of the attributes of the feature of interest into attributes of the images or scan entails probabilistic mapping. Thus, for a given feature of interest the recorded attributes have a statistical distribution which has to be taken into account in studying this feature. The number of images or scans is large, and the number of observed attributes can be even larger. Thus the intelligent exploitation of the relevant information requires the ability to handle large amounts of data in a con-

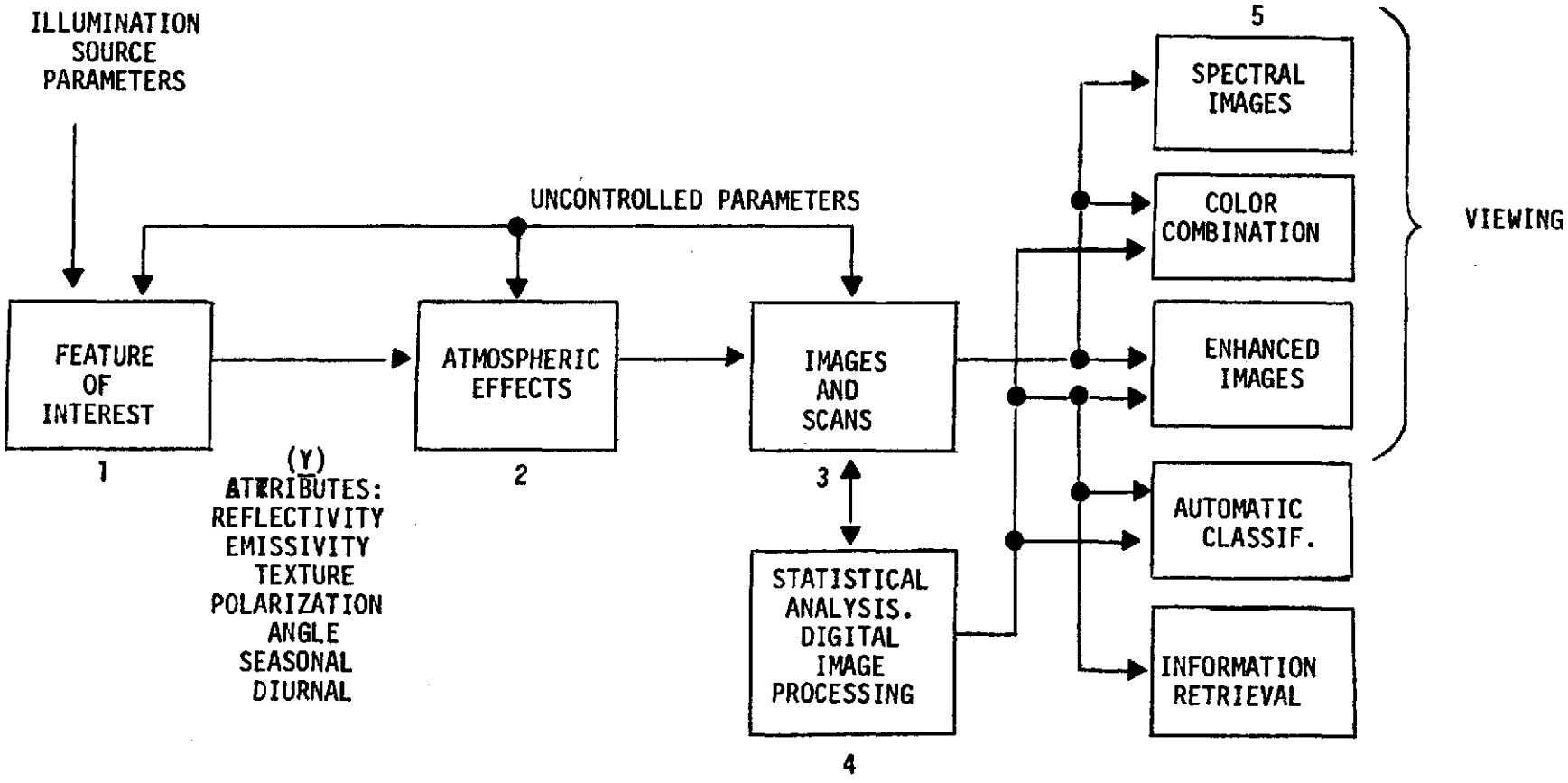

Figure 8.1. Flow diagram of the acquisition, analysis and enhancement of remote sensing images.

certed fashion. Our group, shown as block 4 in the diagram of Figure 8.1, brings to the integrated study both the experimental facility and personnel with the knowledge and background needed to perform the systematic exploitation of the available information. Such elaborate methods are most pertinent for tasks which cannot be done by direct observation of conventional black-and-white or color combined imagery. For this work the data processing facility established as part of the University of California program emphasizes man-machine interaction rather than bulk processing of data. It uses as a central processing element a digital computer; thus the development and use of data processing algorithms becomes principally a computer software problem.

Our facility and programs allow us to answer among others the following questions for the various investigations in our integrated study:

1. Which spectral bands and what spatial resolution capabilities are needed in a specific discrimination problem?

2. How should spectral bands be combined to perform feature enhancement?

3. How well can a priori information (e.g., signature analysis) be relied upon to design enhancement algorithms?

To handle these questions our approach is to rely both upon ground truth and the images transmitted in digital form from ERTS-1. For digitized images a quantitative analysis is conducted of the effect on spectral components as well as on texture of images due to the features of interest. The results of this analysis in the form of one and multi-dimensional histograms, Fourier spectra, etc., allow us to eliminate irrelevant data, rank the usefullness of relevant data to a specific enhancement task, and guide the design of enhancement programs. Our approach is to perform the steps of the analysis rapidly using a small data array, observe intermediate results in color display, and make use of and try to quantify all clues available to a trained observer. This approach is being used with very promising results on ERTS-1 data, as we described later in this report.

8.2 WORK PERFORMED DURING THE PERIOD COVERED BY THIS REPORT

The progress to date on our part of the integrated study can be divided into the following broad categories:

1. Development of a very flexible programming system for interactive image handling and display.

2. Development of a systematic image enhancement procedure

applicable to a variety of problems as well as to remote sensing.

3. Nonlinear equalization and calibration of the ERTS-1 MSS sensors.

4. Preliminary work on the combination of multispectral data for the study of Earth Resources.

5. Application of the procedure of 3) to ERTS-1 data and enhancement of imagery of interest to several participants of our integrated study.

6. Articulation and investigation of some of the basic issues which underlie the interacting enhancement of remote sensing data by digital computers. We shall avoid repetition of the major results reported in the Type 1 and Type 2 progress reports and elaborate primarily on the results obtained since January 1973.

8.2.1 Digital Processing Facility

The facility is shown in Figure 8.2 and is now operational. Minor modifications of the Image Processing Facility are still underway.

8.2.2 Picture Processing Programming System*

General Description

Due to the large number of specific operations of interest in our work it is necessary to provide a framework for the organization of user oriented image processing programs. To this end an image processing system has been developed.

The programming system can best be understood by considering a typical 'experiment'. The investigator has an idea of what operations are necessary on the data to get the results he wants but is not usually sure of the exact parameters. He takes a sample data block and performs the series of steps necessary to get the results using his estimates of the parameters. Based on the results, the steps are performed again with altered parameters or possibly even an altered procedure to see the effect of the results. After a number of such tries, a procedure is developed which gives the best results. This procedure is then used on other data blocks.

Without some sort of programming system, each step in the above procedure requires one to start execution of the proper program and

---

*The material contained in this section has been contributed by J. Schriebman and B. Romberger.

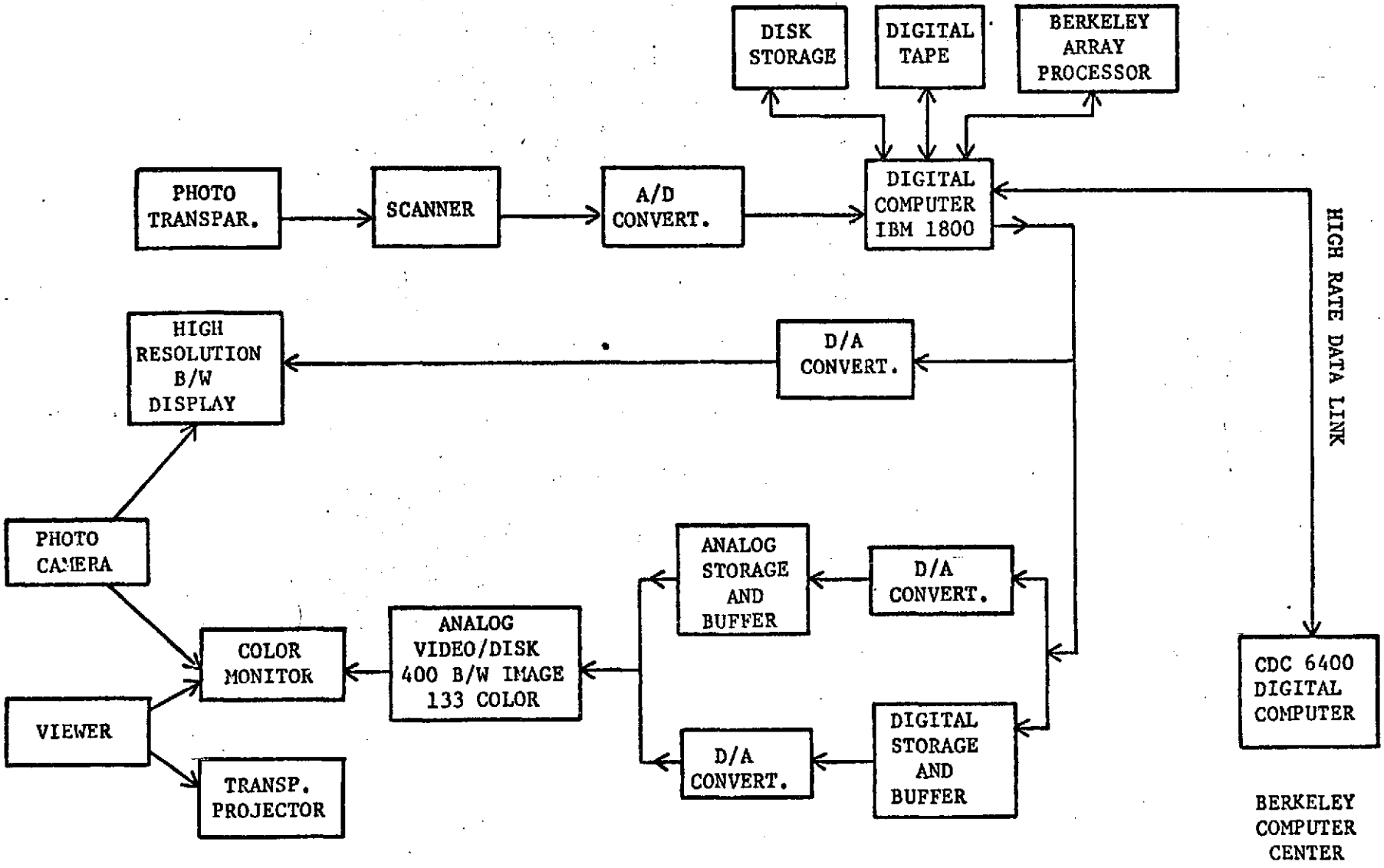

Figure 8.2. Digital Image Processing Facility

enter the data and parameters. It also requires one to keep track of intermediate results that are needed later and to set up his own data storage. The system was developed to eliminate much of the work involved with these manual operations.

The basic objective of the system is interactive usage. During the trial phase, each step is performed as the user presents it to the system with intermediate results readily available so that he can tell how well the procedure is working. He then runs through the entire procedure to look at the results. The procedure can be repeated with modifications or changes in the parameters to see the effect on the results. Once a procedure is finalized, it is possible to repeat it on a series of data.

A second objective of the system is that it be easy to use. The user is able to sit at the console and type in the commands that tell the system what parameters to use. The syntax is fairly easy to understand without being overly restrictive or hard to expand.

A number of secondary user objectives are also met by the present system:

1. Parameters with a commonly used value have default values so that they do not have to be entered every time.

2. Parameters with restricted values are checked for validity.

3. Results (such as max or min) from one step are usable in further steps without requiring the user to remember and enter them.

4. The user is able to interrogate the system as to what programs are available, what data are presently accessible, what the values are for the various parameters, and what parameters are required for each program.

5. Once the user determines a procedure, he is able to set up a whole series of commands which the system can execute without requiring his intervention at every step.

6. The system handles data storage space allocation unless the user wants to intervene.

A third objective of the system is that new processing programs can be added easily. This requires an easy procedure for telling the system what new programs have been added, what the program parameters are and the restrictions of each, how to set up data files or where to find input files, and what comments to give the user if he requests information on the program or its parameters.

A fourth objective is that the system be easy to implement. A balance must be reached between features wanted and difficulty of implementation. The system is designed in such a way as to make check-out convenient, but is also flexible enough to make modifications and additions fairly easy.

System components, system user language, functions and commands, and an example of system use are described in the Type 2 report of January 1973.

8.2.3 A Systematic Image Enhancement Procedure

A systematic approach to the enhancement of images has been developed. This approach exploits two principal features involved in the observation of images: the properties of human vision and the statistics of the images being observed. A fairly detailed exposition of the technique has been presented in Appendix 1 of the Type 2 progress report. The rationale of the enhancement procedure is reasonably simple: In the observation of some features of interest in an image, the range of objective luminance-chrominance values being displayed is generally limited and does not use the whole perceptual range of vision of the observer. The purpose of the enhancement technique presented is to expand and distort in a systematic way the grey scale values of each of the multispectral bands making up a color composite, to enhance the differential visibility of the features being observed. Thus, the enhancement is feature dependent and the work proceeds in the following steps:

1. Extraction of a geographic area of interest from NASA CCT and reformating for subsequent work.

2. Display on a color television monitor of standard color composites, to check for misregistration and to select subareas with features of interest.

3. Generation of histograms in each of the spectral bands for subareas of the image which include features of interest. For instance we may wish to obtain maximum visibility in the water to monitor water quality and various types of water pollution.

4. Production on the color television monitor of a color composite based on a systematic expansion of the histogram values obtained for each band so as to exploit the full perceptual range of the observer.

A slightly revised and expanded version of this work entitled "Digital Image Enhancement by Grey Scale Mapping" has been submitted for publication.

8.2.4 Nonlinear Equalization and Calibration of ERTS-1 MSS Sensors

In some of the images distributed by NASA the stripping effect, due to different responses of the sensors in the Multispectral Scanner, is quite apparent. This effect is greatly magnified as one tries to enhance the images digitally for visibility in the water, since the range of useful sensor outputs is then quite narrow and data errors are more significant. It is possible to bring about some improvement on image quality by equalizing the sensors response on the basis of the statistics of the received data.

Our preliminary work, which equalizes offset and gain of the sensors, has not been too successful. The technique we currently use determines a non-linear compensation curve for each of the sensors and is somewhat more successful. This technique is described in Appendix 1.

8.2.5 Multispectral Data Combination

A problem of continuing interest in Remote Sensing is the rational use of multispectral data. The problem is inherently related to the limitation of a human observer to comprehend and correlate the information provided by a large number of sensors. This problem is already apparent with ERTS-1 data recorded in 4 spectral bands. The conventional solution used by NASA is to provide color composites of either MSS bands 4, 5, and 6 or MSS bands 4, 5, and 7. We have undertaken a fairly long range, systematic study of this problem by considering in turn the following two important points:

1. The redundancy of data and the correlation of data from one spectral band to another.

2. The combined limitation of the reproduction media and of the human observer to discriminate information presented in image form.

The second point is related to our study of perceptual scales. Work is continuing in this area, but we are currently limited in our ability to obtain quantitative, reproducible color reproductions.

At this time we shall report some preliminary results on the correlation and similarity in the ERTS-1 MSS data, and on dimensionality reduction.

8.2.5.1 Correlation and Similarity of ERTS-1 Data

In the determination of the spectral bands of interest in specific applications of remote sensing, one measure of the addi-

tional information contributed by each spectral band is the degree of correlation of this spectral band to all others. An alternative viewpoint is to consider how predictable is each spectral band, given that all others are known. If, for instance, we were to find that MSS band 7 is completely predictable from the knowledge of MSS bands 4, 5 and 6, there would be no merit in processing and displaying MSS band 7 in addition to the other three bands.

These ideas can be formalized, using the framework statistics and estimation theory.

One traditional measure of similarity between two random variables, x and y, is the covariance given by

$$\mu_{xy} = E[(x - m_x)(y - m_y)] \tag{1}$$

$$= E(xy) - m_x m_y$$

in which

$$m_x = E[x] = \int \alpha f_x(\alpha) d\alpha \tag{2}$$

$$E(xy) = \iint \alpha\beta f_{xy}(\alpha,\beta) d\alpha d\alpha \tag{3}$$

where $f_x(\ )$ and $f_{xy}(\ ,\ )$ are the first and second order probability density functions of the random variables x and y.

Here x, y, etc., stand for the radiometric values in each of the spectral bands. We shall designate these random variables as I_4, I_5, I_6, I_7 to match the MSS band designations.

The probability density functions are obtained empirically from the data by forming one and two dimensional histograms.

Let

$$m_i = E[I_i] \tag{4}$$

$$\sigma_i^2 = E[I_i^2] - m_i^2 \tag{5}$$

$$\mu_{ij} = E[I_i I_j] - m_i m_j \tag{6}$$

$$\rho_{ij} = \frac{ij}{\sigma_i \sigma_j} \tag{7}$$

since i, j = 1, 2, 3, 4 the $\{\mu_{ij}\}$ form a 4 x 4 symetric matrix,

examples of which will be given later on.

The knowledge of the μ matrix allows the determination of the best linear estimate $\hat{I}_i$, of component I_i, given all other spectral components. The estimate takes the form

$$\hat{I}_i = \sum_{j \neq i} \alpha_j I_j + c_i \tag{8}$$

in which c_i is a constant.

If the estimate $\hat{I}_i$ is obtained only from one other spectral component I_j, then it can be shown that the resulting normalized mean-square error is given by

$$\varepsilon_{ij}^2 = \frac{E[(\hat{I}_i - I_i)^2]}{\sigma_i^2} = 1 - \rho_i^2 \tag{9}$$

clearly, this residual error measures the content of image I_i which is not predictable from I_j.

The ε_{ij}^2 form also constitutes a 4 x 4 matrix and $\varepsilon_{ii}^2 = 0$. Another approach to measuring the similarity between spectral components again considers mean-square estimation of one spectral component from another, but in this instance does not require the form of the estimator be linear. Given the observation of spectral component I_j we now write

$$\hat{I}_i = g(I_j) \tag{10}$$

in which $g(I_j)$ is chosen in such a way that

$$E[I_i - g(I_j))^2] \tag{11}$$

is a minimum. It is known that we have then

$$\hat{I}_i = E[I_i | I_j] \tag{12}$$

$$\hat{I}_i(I_j) = \int \alpha f_{i/j}(\alpha/I_j) d\alpha \tag{13}$$

in which $f_{i/j}(\alpha/\beta)$ is the conditional probability density of I_i given that I_j has value $I_j = \beta$. These are classical results from estimation theory.

Because of the additional freedom allowed in the form of the estimator, the nonlinear estimate will always outperform a linear estimate in the sense that the resulting normalized mean-square

error $\eta_{ij}^2 < \varepsilon_{ij}^2$, in which

$$\eta_{ij}^2 = \frac{E[(I_i - g(I_j))^2]}{\sigma 2_i} \qquad (14)$$

and ε_{ij}^2 is as given by equation (9).

Our interest in the result of equation (14) is that in the visual observation of spectral components, a human observer will conclude that no additional information is provided by spectral component I_i, if I_j is known, whenever $\eta_{ij}^2 = 0$, although ε_{ij}^2 may be different from zero. In other words, a human observer is not limited to perceiving linear relations between spectral components. To illustrate the idea, we show the results for two geographic regions in California.

Table 8.4 shows the covariance matrix $\{\mu_{ij}\}$, the linear error matrix $\{\varepsilon_{ij}\}$, and the nonlinear error matrix $\{\eta_{ij}\}$ for the data for Bucks Lake (1002-10125).

The μ matrix shows on its main diagonal, the variance of each spectral band. MSS band 4 has a small variance and generally gives a very flat image when it is reproduced without enhancement. High entries off the main diagonal in the μ matrix indicate correlation between the corresponding spectral components. The error matrices are more informative from that standpoint. All entries are now normalized to 1 so that an entry $\varepsilon_{ij} = 0$ means I_i is perfectly predictable in terms of I_j, and $\varepsilon_{ij} = 1$ means that knowing I_j does not help at all in predicting I_j. Obviously we have $\varepsilon_{ii} = \eta_{ii} = 0$. We observe that MSS bands 6 and 7 are the most correlated and thus justify the common choice of discarding either MSS band 6 or MSS band 7 in color composition. Note however that MSS bands 4 and 5 are nearly as correlated and that almost as good a choice for the Bucks Lake area would be to discard either MSS band 4 or MSS band 5 and color combine the rest.

The comparison of the linear error matrix $\{\varepsilon_{ij}\}$ and the nonlinear error matrix $\{\eta_{ij}\}$ shows no significant differences.

Table 8.5 shows similar results for the farm land south of Isleton (1003-18175).

The interpretation of the results is generally as for Table 8.4

TABLE 8.4. BUCK'S LAKE
(1002 - 10125)

3.1	4.7	4.1	1.7
4.7	8.1	5.7	2.1
4.1	5.7	22.3	14.0
1.7	2.1	14.0	9.5

Covariance Matrix

$\mu = [\mu_{ij}]$

0	.35	.87	.95
.35	0	.90	.97
.87	.90	0	.28
.95	.97	.28	0

Linear Error Matrix

$\epsilon = [\epsilon_{ij}]$

0	.35	.81	.87
.36	0	.88	.93
.77	.79	0	.30
.85	.86	.30	0

Nonlinear Error Matrix

$\eta = [\eta_{ij}]$

TABLE 8.5. FARM LAND SOUTH OF ISLETON
(1003 - 18175)

7.18	13.0	4.5	.34
13.0	26.86	4.6	2.27
4.5	4.6	52.2	33.2
.34	2.27	33.2	27.1

Covariance Matrix

$\mu = [\mu_{ij}]$

0	.335	.97	.9997
.335	0	.992	.996
.97	.992	0	.468
.9997	.996	.468	0

Linear Error Matrix

$\varepsilon = [\varepsilon_{ij}]$

0	.32	.91	.88
.31	0	.92	.86
.96	.92	0	.29
.98	.90	.30	0

Nonlinear Error Matrix

$\eta = [\eta_{ij}]$

with some significant differences.

Note first that the data are considerably more active as indicated by the variances on the main diagonal of μ. Based on the linear error matrix one would conclude that MSS bands 4 and 5 are most correlated and thus a "best" color composite is obtained from MSS band 4 or 5 and MSS bands 6 and 7. Given that the variance of MSS band 5 is considerably larger than that of band 4 for a composite without enhancement the obvious choice would be bands 5, 6 and 7.

The nonlinear error matrix changes these conclusions because the entries are significantly different from the entries on the linear error matrix. In particular, bands 6 and 7 are now most correlated (correlated is a somewhat improper word and codependent would be more suitable).

The nonlinear dependence between spectral components is shown in Figure 8.6 in which are graphed the nonlinear estimates

$$\hat{I}_2 = g_{2,3}(I_3) \tag{15}$$

$$\hat{I}_2 = g_{2,4}(I_4) \tag{16}$$

$$\hat{I}_3 = g_{3,4}(I_4) \tag{17}$$

corresponding to equation (13).

These curves are quite nonlinear, even within the active range of the data. The random fluctuations at the top of the range are not significant and are due to the insufficient data, a factor which makes the estimator curve quite inaccurate.

Note that these results, based on correlation and similarity by pairs of spectral components, are subject to revision whenever all spectral components are considered jointly.

8.2.5.2 Multispectral Data Combination: Dimensionality Reduction

The motivation for extracting the most significant three spectral components from the 4 spectral MSS bands of ERTS-1 is that the space used for display, the perceptual space, has only 3 dimensions corresponding to the 3 primary colors.

The discussion on correlation and similarity of ERTS-1 data, presented in 8.2.5.1 is used to determine, on objective grounds, which one of the 4 spectral components should be discarded. The

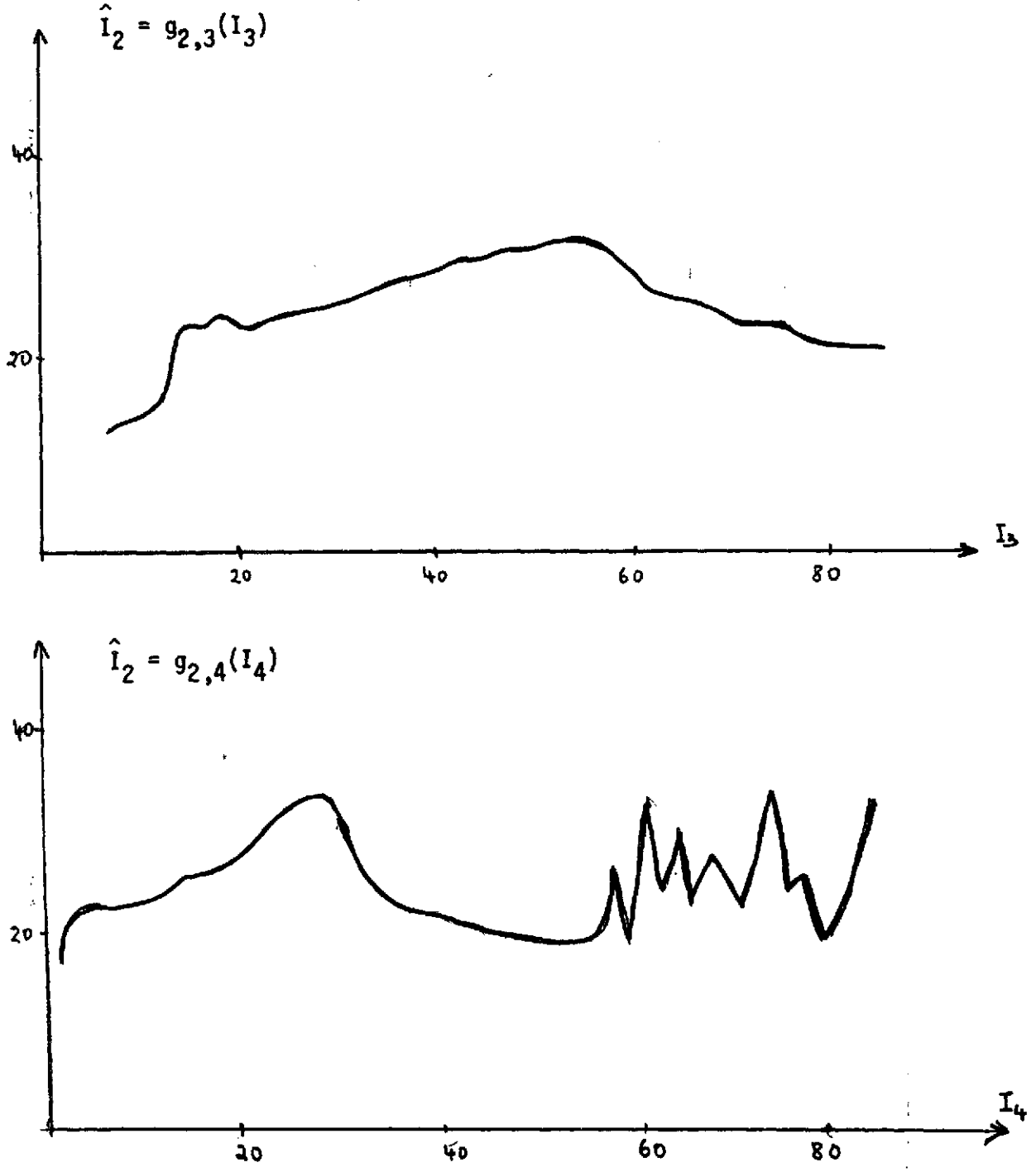

Figure 8.6. Nonlinear estimates of spectral components.

common assumption is that the preserved components are then displayed as standard color composites.

More generally, the problem of processing and display of multispectral data is to map a set of N spectral components $\{I_k\}$ into a 3-dimensional perceptual space. The approach of 8.2.5.1 is to choose the "best" three I_k's out of N possibilities.

Another approach, described briefly here, is to apply a set of invertible transformations to the multispectral data and then to choose the best subset of transformed components.

Let $\underline{I}'$ be the set of transformed spectral component.

We write

$$\underline{I} = [A]\underline{I}' \tag{18}$$

in which [A] is an N x N matrix, corresponding to a linear transformation of $\underline{I}'$ into $\underline{I}$. The columns of [A] are taken to be orthonormal vectors.

Assume that $L < N$ components of $\underline{I}'$ are used and the others discarded. By entering N-L zero components into $\underline{I}'$ we form a new vector $\underline{I}''$ which generates by (18)

$$\hat{\underline{I}} = [A]\underline{I}'' \tag{19}$$

$\hat{\underline{I}}$ is an approximation to $\underline{I}$. The goodness of the approximation can be measured in a mean-square sense.

$$\varepsilon_L = E[||\underline{I} - \underline{I}||^2] = E[\Sigma_k (I_k - \hat{I}_k)^2] \tag{20}$$

For a given L, a question of interest is the optimum choice of the set of transformed components $\underline{I}'$ and therefore of the transformation matrix [A]. The solution to this problem for the criterion of (20) is well known in the fields of communications and pattern recognition as the decomposition into principal components or as the Karhunen-Loeve representation of $\underline{I}$[1,2]. It has been applied to automatic classification in remote sensing by Haralick (3) at Kansas and by personnel of LARS at Purdue.

As before, let [μ] be the covariance matrix of the data, then the vectors $\underline{e}_k$, k=1,...N columns of the matrix A are obtained by solving the matrix equation

$$[\mu]\underline{e}_k = \lambda_k \underline{e}_k \tag{21}$$

in which the λ_k's are positive numbers, also to be determined.

Equation 21 is the formulation of a classical mathematical problem with known solution [4]. The λ_k's and $\underline{e}_k$'s are denoted eigenvalues and eigenvectors of matrix [μ]respectively.

Once the λ_k's and the $\underline{e}_k$'s are obtained, the transformed coefficients $\{I'_k\}$ are obtained by the matrix operation

$$\underline{I}' = [A]^T \underline{I} \tag{22}$$

From $\underline{I}'$, one obtains $\underline{I}$ back by the use of equation (20) since

$$[A]^T[A] = [I] \tag{23}$$

in which [I] is the identity matrix.

The mean-square error approximation of equation (20) is expressed easily in terms of the λ_k's. It can be shown that

$$\varepsilon_L = E(\Sigma_k (I_k - \hat{I}_k)^2) = \sum_{k=1}^{N} \lambda_k \tag{24}$$

Since $\hat{\underline{I}}$ is obtained by retaining only L of N transformed components $\{I'_k\}$, one can readily determine, from the λ_k's, the mean-square error incurred by discarding N-L components.

We have applied the approach just outlined to ERTS-1 data, and the results are interesting, both in terms of the small mean-square error caused by the dimensionality reduction, and in terms of the quality of the enhanced images we have obtained.

We first examine the mean-square error caused by the dimensionality reduction for 3 areas of California: The Bucks Lake region, which is almost entirely a wildland area; the farmland south of Isleton; and the East Bay cities which include part of San Francisco Bay and some woodlands. The two questions of interest are: What is the percent mean-square error introduced by a dimensionality reduction? What are the corresponding eigenvectors and thus the corresponding spectral combination used?

The answers to these questions can be obtained from Tables 8.7, 8.8 and 8.9.

The normalized covariance matrix (correlation coefficient matrix) indicates the pairwise linear similarity and correlation of the data for the 4 spectral components. As noted earlier, MSS bands 4 and 5 and MSS bands 6 and 7 are highly correlated in all cases. The covariance matrix is shown and indicates, on its diagonal, the relative ranking of the variances of spectral components (the absolute scale has no meaning). Ratios of

TABLE 8.7. RESULTS OF DIMENSIONALITY REDUCTION FOR THE BUCK'S LAKE AREA (1002 - 10125)

1.0000	.9356	.5097	.3341
.9356	1.0000	.4317	.2429
.5097	.4317	1.0000	.9633
.3341	.2429	.9633	1.0000

$[\rho]$ Normalized Covariance Matrix

109.7	165.0	150.2	85.72
165.0	283.5	204.5	100.2
150.2	204.5	791.6	663.9
85.72	100.2	663.9	600.0

$[\mu]$ Covariance Matrix

.8685	-.4939	-.03927	.001917
.07850	.1941	-.6708	.7114
.4659	.8220	-.05041	-.3232
.1492	.2060	.7388	.6240

$[A]^T$ Rows are Eigenvectors

9.278	10.79	325.1	1439.

$\{\lambda_k\}$ Eigenvalues

	Blue	Green	Red

Assigned color primaries

TABLE 8.8: RESULTS OF DIMENSIONALITY REDUCTION FOR THE EAST BAY CITIES

1.0000	.8610	.3586	.1821
.8610	1.0000	.5765	.4125
.3586	.5765	1.0000	.9583
.1821	.4125	.9583	1.0000

$[\rho]$ Normalized Covariance Matrix

300.9	253.9	.80.0	103.3
253.9	289.0	283.6	229.4
180.0	283.6	837.4	907.1
103.3	229.4	907.1	1070.

$[\mu]$ Covariance Matrix

-.01146	-.2830	.7559	-.5901
-.6717	.7085	.1100	-.1859
.7259	.6052	-.01705	-.3262
.1471	.2268	.6450	.7146

$[A]^T$ Rows are eigenvectors

20.32	32.11	462.0	1983.

$\{\lambda_k\}$ Eigenvalues

Blue	Green	Red

Assigned Color Primaries

TABLE 8.9. RESULTS OF DIMENSIONALITY REDUCTION FOR THE FARMLAND SOUTH OF ISLETON (1003 - 18175)

1.0000	.9537	.2323	.0187
.9537	1.0000	.1226	-.0881
.2323	.1226	1.0000	.9629
.0187	-.0881	.9629	1.0000

$[\rho]$ Normalized Covariance Matrix

467.6	634.9	147.3	8.21
634.9	947.8	110.7	-54.99
147.3	110.7	860.1	572.5
8.21	-54.99	572.5	411.0

(μ) Covariance Matrix

.1515	.0120	-.5699	.8074
.8118	-.5689	.0208	-.1292
-.2358	-.4330	.6859	.5349
.5120	.6990	.4517	.2123

$[A]^T$ Rows are Eigenvectors

7.548	25.16	1186.	1467.

$\{\lambda_k\}$ Eigenvalues

Blue	Red	Green	

Assigned Color Primaries

variance range from 3 to 1 to 8 to 1.

Turning now to the eigenvalues and using (24) we have the following table for percent mean-square error due to dimensionality reduction:

	Bucks Lake	Isleton	East Bay
1 component discarded	0.52	0.28	0.81
2 components discarded	1.13	1.21	2.1

We see that in all cases, by linear transformation, it is possible to generate 3 equivalent components which represent the 4 spectral MSS bands with less than one percent error.

There are some interesting remarks to be made with regard to the eigenvectors. The eigenvector associated with the largest eigenvalue, thus the spectral combination which carries most of the energy, has components which all have roughly the same magnitude. They thus correspond approximately to a panchromatic image over the whole spectral range of the ERTS-1 sensors. The second eigenvalue is associated to an eigenvector with combine MSS bands 4 and 5 with one sign and 6 and 7 with the opposite sign. Thus, roughtly speaking, the difference between total responses in spectral band 0.5 - 0.7 nm and spectral band 0.7 - 1.1 nm seems most useful in the presentation of the data. The last two eigenvectors, associated with small eigenvalues cannot be assessed easily. Haralick (3) has made similar observation for a 12 band-airborne MSS.

In the following we show some examples of enhanced images which combine from the 3 most significant components, obtained after transformation. In all cases we enhance each of 3 components following the procedure of 8.2.3.

For each area we have 2 enhanced images, the first one is for the best 3 of the original MSS bands, these are MSS band 4, 5 and 7. The second image is obtained by enhancing the three most significant transformed components. The assignment to color primaries is indicated in Tables 8.7, 8.8 and 8.9. These enhanced images are shown in figures 8.11, 8.12 and 8.13.

In all cases these are are a definite improvement in the visual discrimination of areas with different features if all 4 spectral bands are combined. The most apparent one is probably in the farm land south of Isleton in which color discrimination between a significantly larger number of individual fields appears possible after data combination.

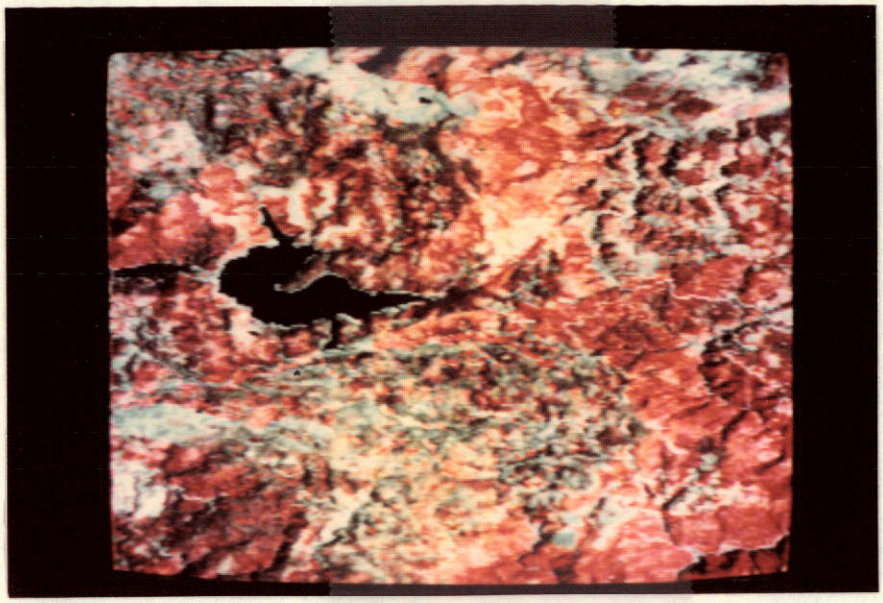

a. Enhanced bands 4, 5 and 7

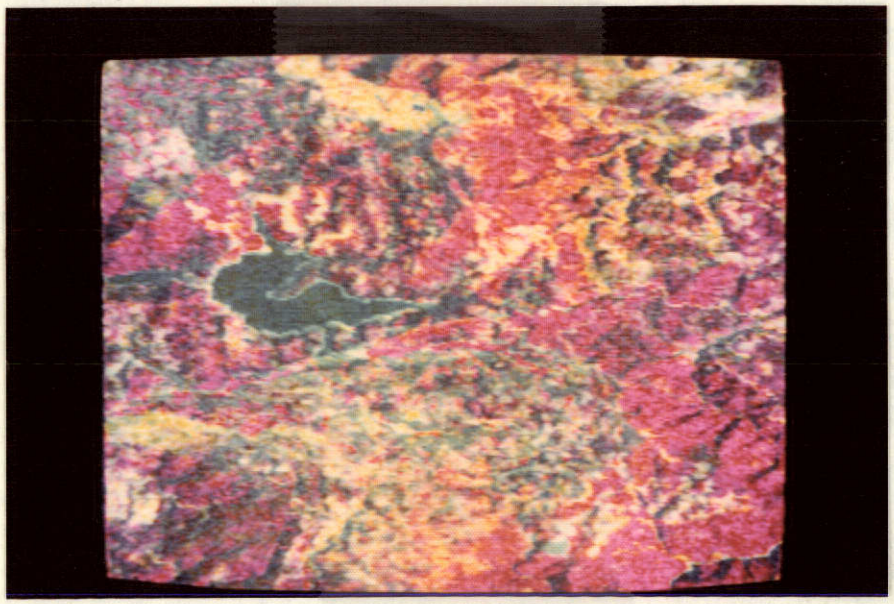

b. Enhanced combined bands (see Table 8.7)

Figure 8.11. Buck's Lake, (1002 - 10125).

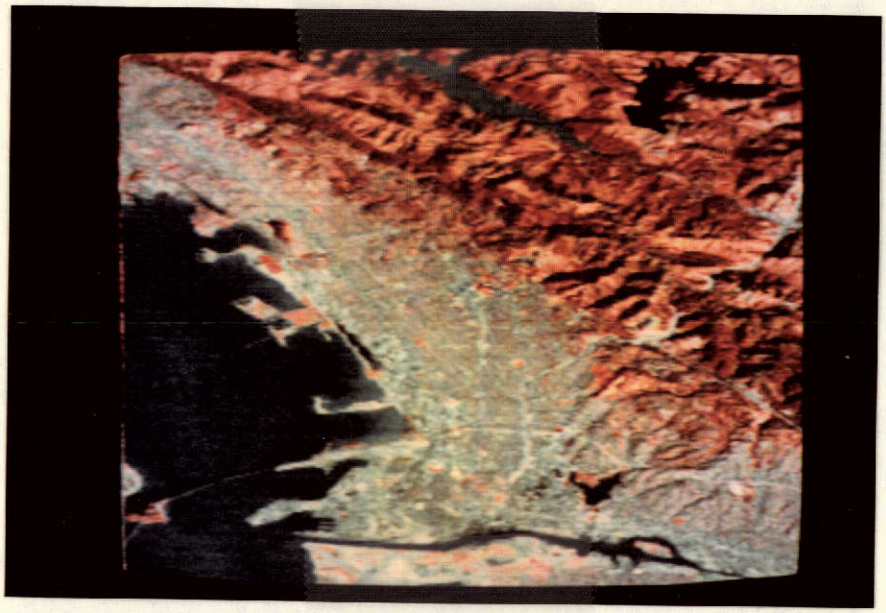

a. Enhanced bands 4, 5 and 7

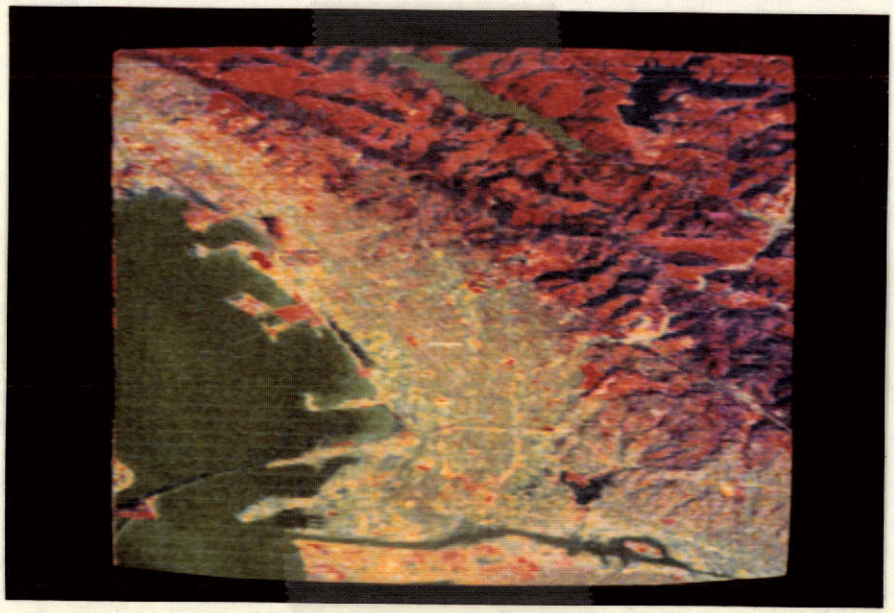

b. Enhanced combined bands (see Table 8.8)

Figure 8.12. East Bay cities, (1165 - 18175).

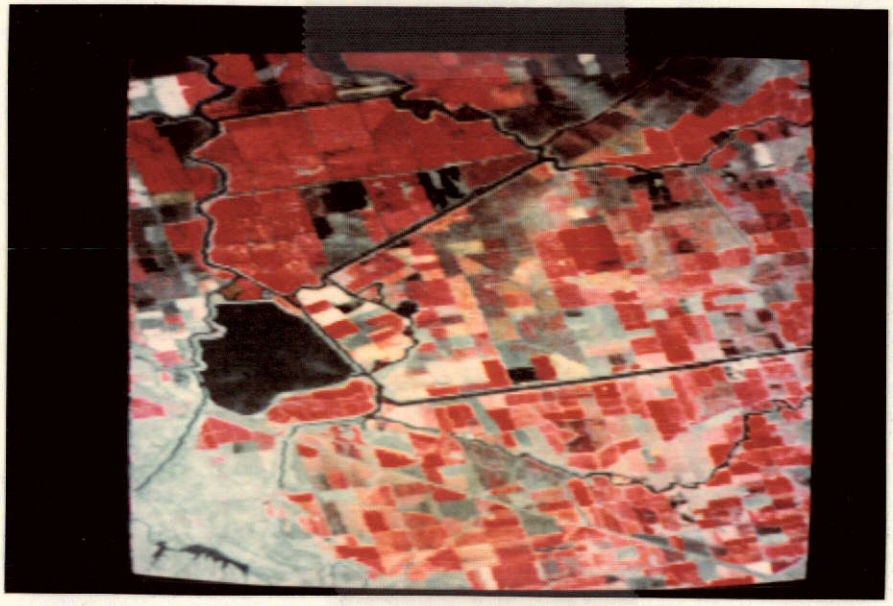

a. Enhanced bands 4, 5 and 7

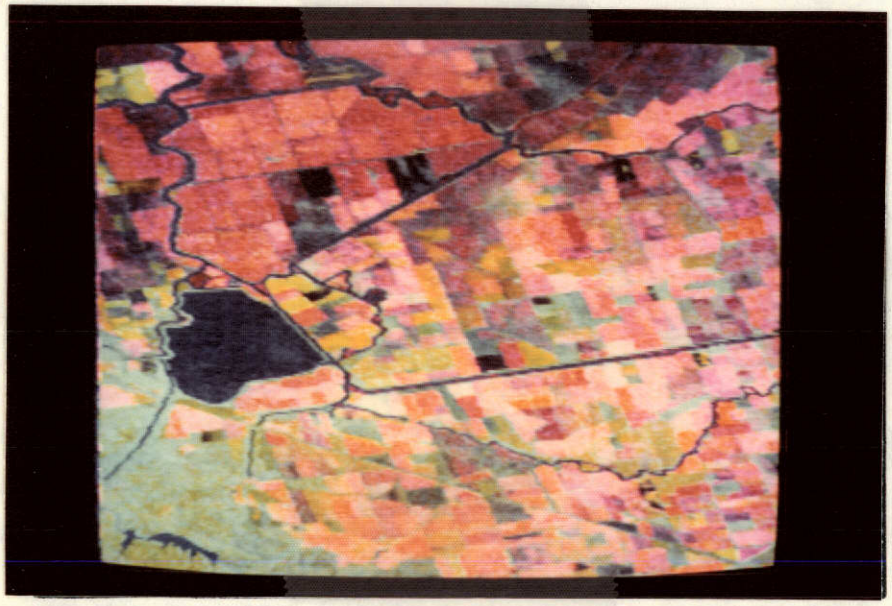

b. Enhanced combined bands (see Table 8.9)

Figure 8.13. Farmland south of Isleton, (1003 - 18175).

One can also display in black and white the 4^{th} transformed component, which has not been displayed in the color composite. This 4^{th} component gives a noiselike image with very little apparent visual information. Although the method seems promising, there is still a shortcoming in the way the images have been displayed. For several reasons, the assignment of 3 data components, either original MSS bands, or combined bands to Red, Blue, and Green color primaries is not necessarily a good choice of color assignments. This is an area of study we are currently pursuing.

8.2.6 Support Activities and Image Enhancement for Other Participants of the Integrated Study

A substantial part of our activities this year has been in support of the research and studies carried out by other participants of the Integrated Study of the State of California using Remote Sensing techniques.

Although a more substantial description of the studies is given in the appropriate chapters of this report we shall list briefly the investigators and the type of work considered.

1. Enhancement of ERTS-1 imagery to improve the visibility and mapping of frost damage eucalyptus trees in the Berkeley Hills. This work is of prime interest to Dr. Robert N. Colwell, the principal investigator of the study.

2. Enhancement and Processing of ERTS-1 data to improve the visibility of sediments, pollutants and other indicators of water quality. This fairly extensive work, of interest to Dr. Robert Burgy, was carried out in consultation and cooperation with Jean Malingreau, also of the Department of Water Sciences and Engineering at the University of California, Davis.

3. Enhancement of ERTS-1 imagery to assist in the delineation and inventory of Earth Resources in wildlands and agricultural area of Northern California. This work was done to assist Don Lauer and Dr. Bill Draeger of the Forestry Remote Sensing Laboratory.

4. Scanning, digitization, processing and enhancement of imagery to assess the potential contributions of polarization information to the inventory and discrimination of Earth Resources. This substantial effort was carried out for Dr. Kinsell Coulson of the Davis Campus.

Enhanced ERTS Imagery was also supplied to Dr. John Tremor of the NASA Ames Research Center, at his own request, to illustrate the information available in ERTS data and the capabilities of digital image enhancement to extract this information.

8.3 REFERENCES

1. Davenport and Root: "Random Signals and Noise", McGraw Hill, 1958.
2. See for instance: H.C. Andrews "Introduction to Mathematical Techniques in Pattern Recognition", Wiley-Interscience-1972.
3. R.M. Haralick and I. Dinstein "An Iterative Clustering Procedure", IEEE Transactions on Systems, Man and Cybernetics, Vol. SMC-1, No. 3, July 1971, pp. 275-289.
4. See for instance: Hildebrand "Methods of Applied Mathematics", Prentice Hall, 1952.

Appendix 1
Nonlinear Equalization and Calibration
of MSS Sensors Response
(V.R. Algazi)

Introduction

The ERTS-1 data provided to users by NASA in the form of single spectral images, standard color composites or computer compatible tapes can be marred by data errors which, in some cases, seriously limit the usefulness of the data. In this appendix we describe and analyze the technique we have used during the past several months to correct a recurrent type of error known as "stripping". This type of error is caused by the differences in radiometric response and in calibration of the six sensors used in each spectral band of the Multispectral Scanner.

After a ground calibration of the sensors, NASA had planned an in-flight calibration procedure consisting of internal calibration using a calibrated lamp and a calibration wedge and of external sun calibration using all the optical paths used in the remote sening of earth radiance. (The NASA ERTS-1 User Manual contains a complete description of the calibration procedure). The external sun calibration procedure is not being used on ERTS-1. The internal calibration procedure is being used consistently but it yields data which are obviously in error. Ever since this problem became apparent we have tried to use the digital data provided by NASA to determine and equalize the response of the sensors from which the data originated. Since we have succeeded to a large extent in that task and since we are aware that it is a problem of concern to a large number of data users, we shall describe the rationale and the exact steps followed in our procedure.

Model of the Sensor Responses

In each spectral band the six sensor channels sweep across adjacent narrow zones of the ground scene. As shown in Figure A.1.1., $X_i(x,y)$ denotes the input radiance, and $V_i(x,y)$ the corresponding output voltage.

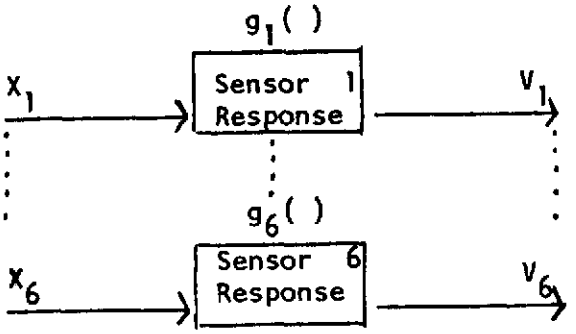

Figure A.1.1

Various models can be used for the response curve of the sensors, $g_i(\ )$. NASA, in its calibration procedure, uses a linear model which thus requires only 2 parameters for its complete specification. We have found that allowing $g_i(\ )$ to be an arbitrary monotonic function leads to more satisfactory results.

Assuming that the response curves, $g_i(\ )$ and $g_j(\ )$ $j \neq i$ do differ after all of the calibration has been performed by NASA, the question for the user is then how to use the available data $V_i(x,y)$, $i=1=6$ to correct these differences or to perform the processing or quantitative analysis of the earth resources of interest. In the case of automatic classification or image enhancement one can process independently the response of each sensor, that is to say, one can devise different algorithms for V_i and V_j, $i \neq j$. This approach works quite well for image enhancement* but requires a large amount of additional processing for each pass through the data since no correction of the data is done. A second approach, whenever only one of the 6 sensors is at fault, is to discard the data as useless and to replace such data by the average of adjacent lines, presumed good. This method obviously breaks down if 2 or more sensors out of 6 have unsatisfactory responses. Correction, or at least equalization, of the data is possible and can be done once and for all independently of the subsequent processing to be performed.

Note that since x_i is not available to the user, we shall not determine the sensor response curves $g_i(\ )$ but instead the sensor equalization curves $g_{ij}(\ )$ which relate the ouput of sensor i to the ouput of sensor j. This mathematical curve is shown in Figure A.1.2 and defined in terms of $g_i(\ )$ and $g_j(\ )$.

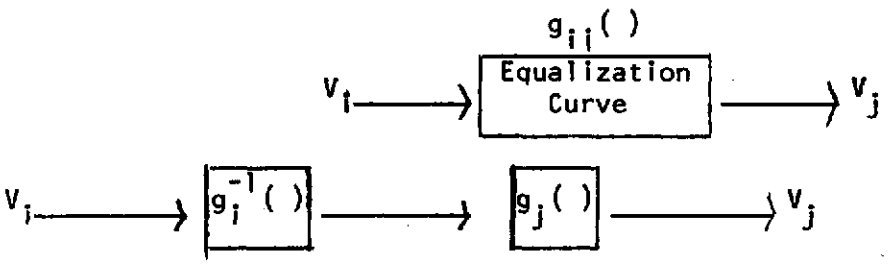

Figure A.1.2
Model for the Equalization Curve

*Using the technique described in the body of the report.

We denote by $g_i^{-1}(\ )$ the inverse of the curve $g_i(\ )$, which is well defined since $g_i(\ )$ is monotonic. Note that $g_{ij}(\ )$ is also a monotonic function.

Estimation of $g_{ij}(\ )$ from the Measured Output Statistics

The ouput data for different sensors can be obtained from exactly the same geographic area within a single NASA image. Hence, we shall assume that the statistics at the output of each sensor would be identical if it were not for the difference in sensor response and for statistical fluctuations due to the finite sample size on which the statistics are based. We shall assign all measured differences in statistics to the equalization curve $g_{ij}(\ )$. A statistical analysis would be needed to determine the accuracy in the determination of $g_{ij}(\ )$ due to a finite data sample size. The basic relation which determines $g_{ij}(\ )$ is extremely simple.

A classical problem of Probability Theory [1] is to determine the probability density at the output of a known nonlinear device when the input probability density function is known. The problem here is to infer the nonlinear relation from the input and output probability density or distribution functions. The following relation holds between the input probability density function $f_i(\ )$, the output probability density function, $f_j(\ )$ and the nonlinear function $g_{ij}(\ )$

$$\int_{\infty}^{\alpha} f_i(\beta)\,d\beta = \int_{-\infty}^{g_{ij}(\alpha)} f_j(\beta)\,d\beta \qquad \text{(A.1.1)}$$

see for instance Papoulis [1].

In equation A.1.1, the probability densities functions are estimated by forming histograms of the ouput of each sensor. The left hand side of A.1.1 is evaluated for a given value . The right hand side is then evaluated for increasing values of $g_{ij}(\ )$ until equation A.1.1 is satisfied thus giving one point $\hat{g}_{ij}(\ )$ on the estimate of the equalization curve $\hat{g}_{ij}(\ )$.

Since operations are performed digitally on a discrete grid of values it is convenient to restate A.1.1 for discrete random variables.

$$\sum_{k=0}^{k_0} f_i(V_k) = \sum_{l=0}^{l_0 = g_{ij}(V_{k0})} f_j(V_l) \qquad \text{(A.1.2)}$$

In A.1.2 it is possible that no discrete value l_0 exists such that the right side sum is equal to the left side sum.

To allow for interpolation we write

$$\sum_{k=0}^{k_0} f_i(V_k) = \sum_{l=0}^{l_0} f_j(V_j) + \Delta l_0 \, f_j(V_{l_0+1}) \qquad \text{(A.1.3)}$$

and

$$l_0 + l_0 = g_{ij}(V_{k0}) \qquad \text{(A.1.4)}$$

Example of Application

We illustrate the application of this technique to image 1021 - 18165 MSS 4. We shall only obtain here the statistics and equalization curves for the data. An example of corrected imagery has been given in a previous report.

The first step in the correction of the data is the determination of the 6 histograms for each of the sensors. From these histograms the mean and standard deviation at the ouput of sensors are obtained.* This information yields the values shown in Table A.1.3.

Table A.1.3

STATISTICS AT THE OUTPUT OF SENSORS

Sensor No.	1	2	3	4	5	6
Mean	21.49	28.14	28.23	28.38	28.22	27.54
Standard Deviation	4.17	5.77	5.52	5.94	5.72	5.75

*Note that a linear equalization curve can be obtained from the mean and standard deviation.

The numbering of sensors is arbitrary. From Table A.1.3, we note that sensor 1 is in error and possibly sensor 6 is also. All other sensors seem equally good. We then choose one sensor that we shall use as a target to equalize all sensors. The corresponding target histogram is used on the left hand side of (A.1.3). Here we use sensor 5 as a target.

We then proceed to determine the equalization curves $g_{5j}(\ )$ for each of the sensors using (A.1.3) and (A.1.4). Histograms and correction curves for sensors 1, 3 and 5 are shown in figures (A.1.4), (A.1.5) and (A.1.6). We note that the histograms are substantially different for the 3 sensors shown. For sensor 5 the equalization curve is a straight line with slope unity, as expected. For sensor 1 the average slope is higher than one and there are some small non-linearities (probably due to statistical fluctuations) and a global curvature of the equalization curve. Note that the behavior of the equalization curve for data ranges with small probability is somewhat erratic. This has no operational significance in the correction of the data.

An underlying assumption of the technique is that the sensor response curve does not vary significantly for the data over which the statistics are gathered. NASA's dynamic calibration procedure could in fact produce such variations and invalidate the technique. We have read the calibration block on computer compatible rate and have found that the linear corrections coefficients used on the data are essentially constant, with a variation of only 1 percent across an image.

The method described here for equalization can also be used for calibration. Let us assume that we take the global histogram at the output of sensors 2,3,4,5 as representative of the input radiance. The equalization curves $g_{ij}(\ )$ now become calibration curves for each of the sensors.

References

[1] See for instance A. Papoulis: "Probability Random Variables and Stochastic Processes", McGraw-Hill, 1965.

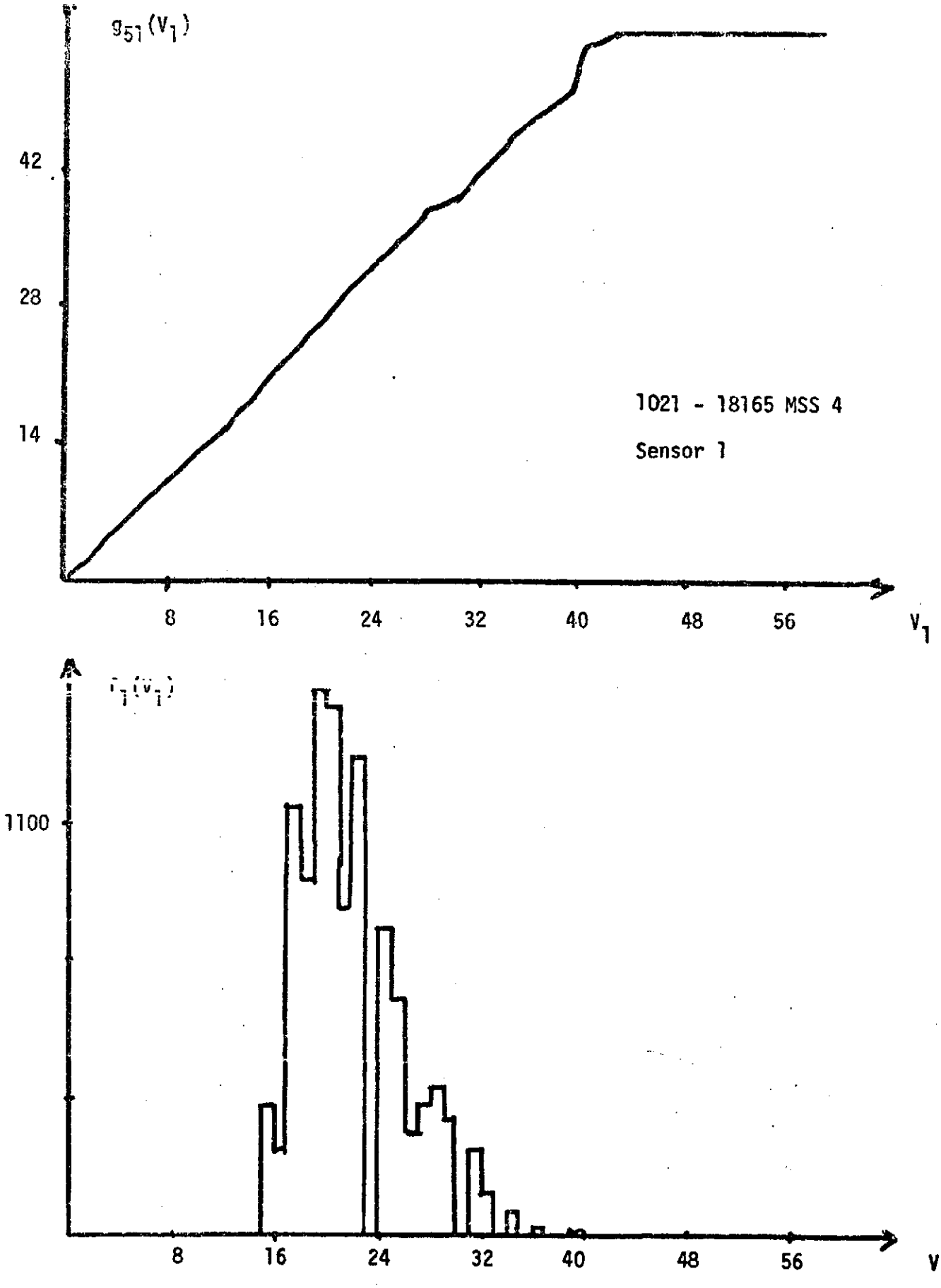

Figure A.1.4. Equalization of Sensor 1.

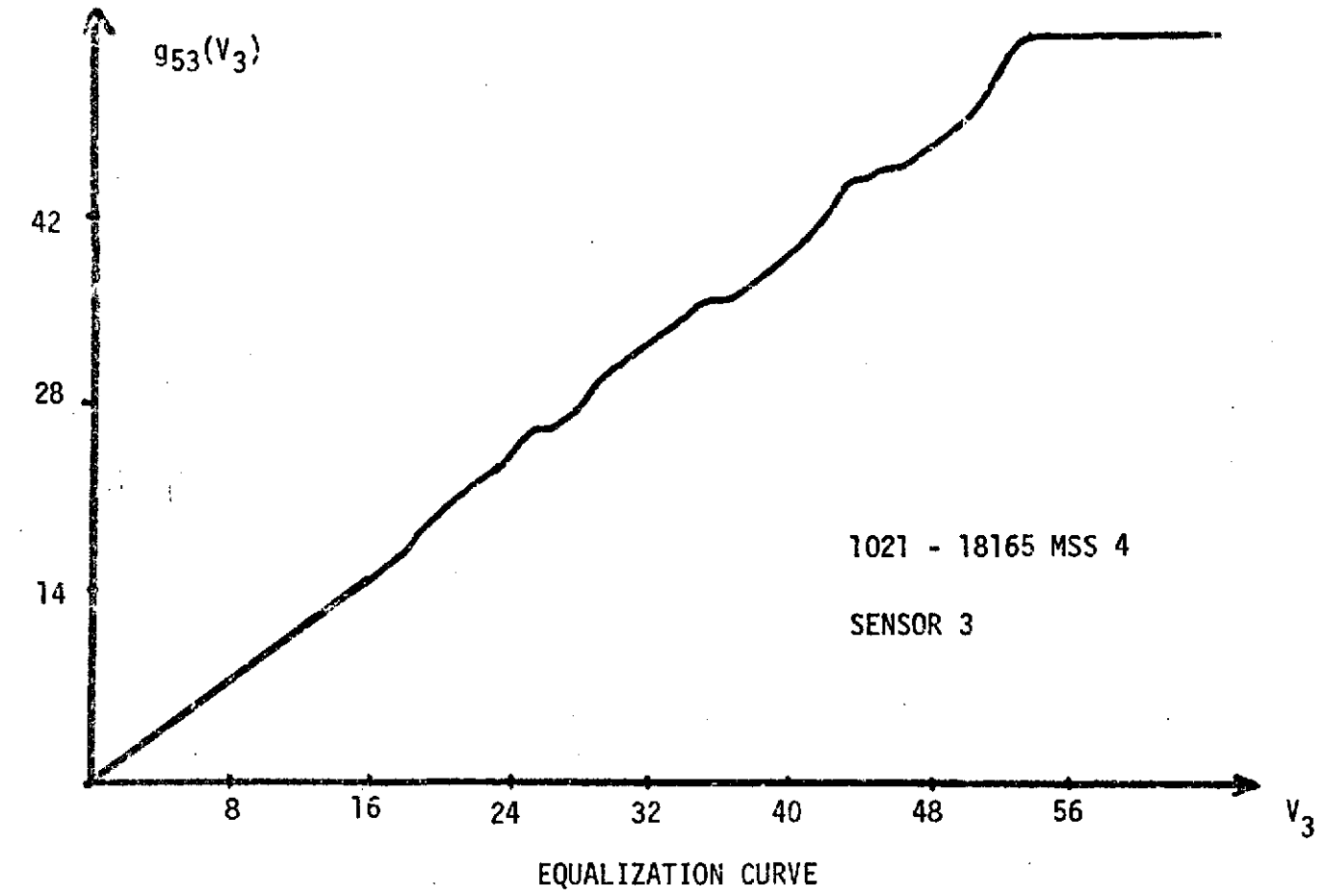

EQUALIZATION CURVE

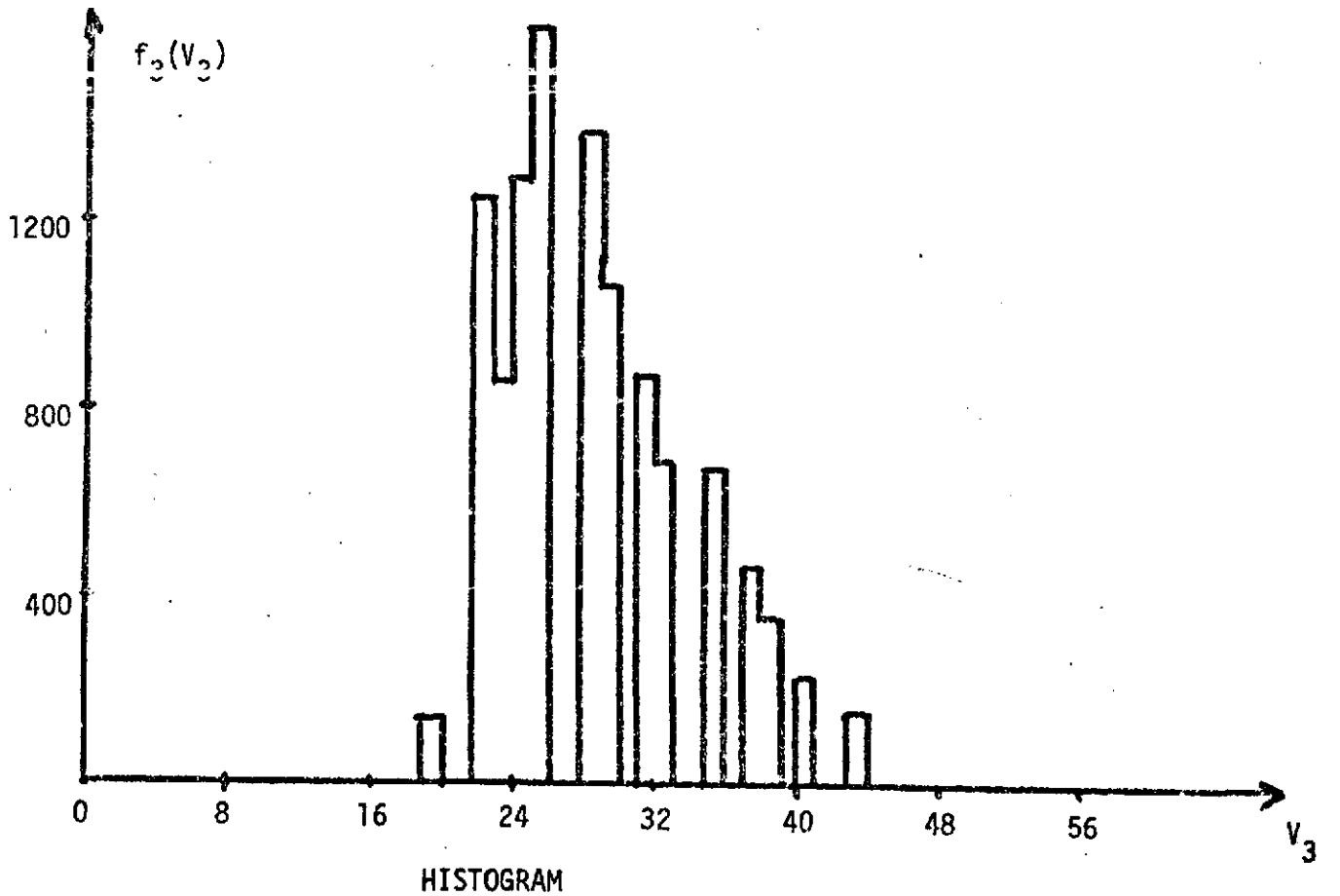

HISTOGRAM

Figure A.1.5. Equalization of Sensor 3.

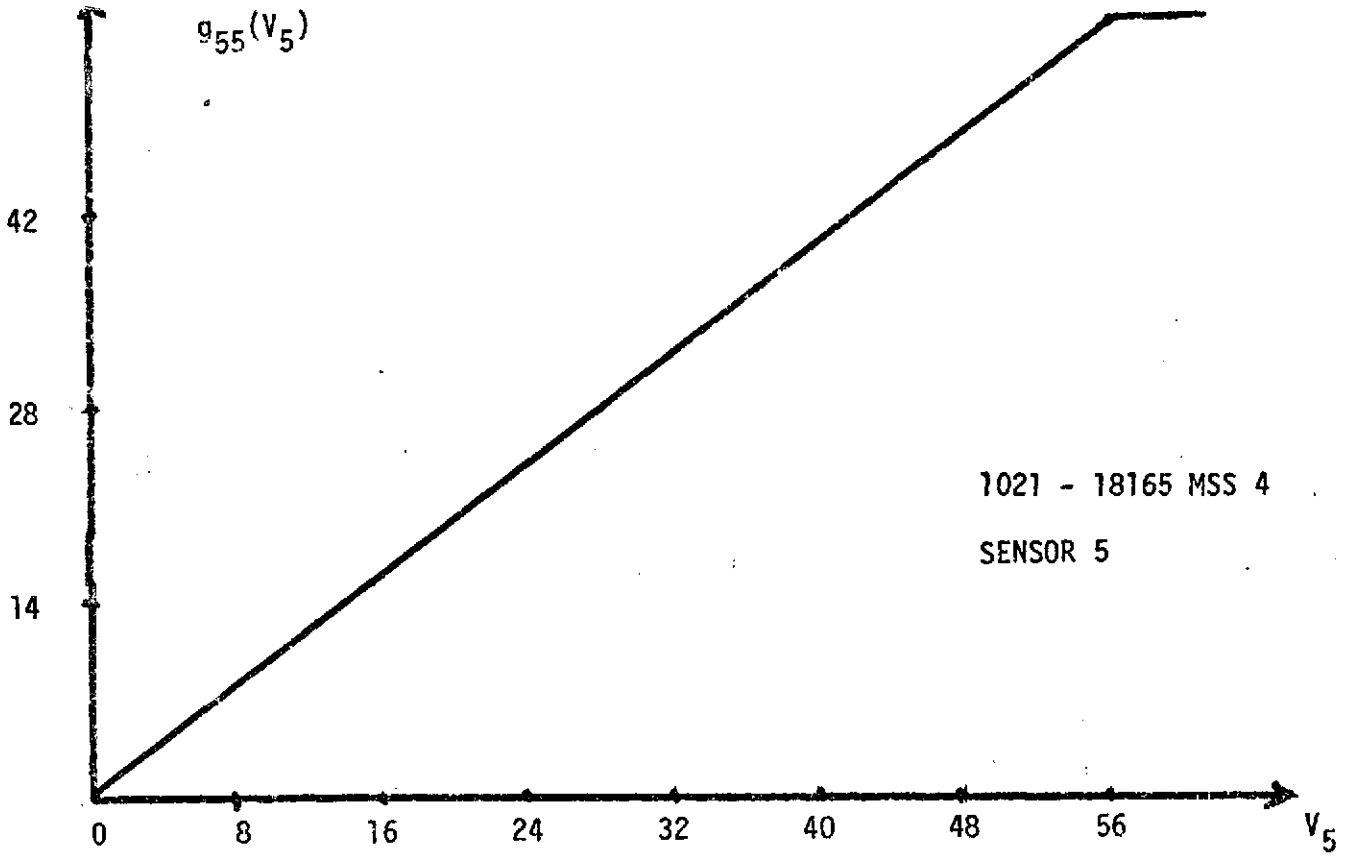

EQUALIZATION CURVE

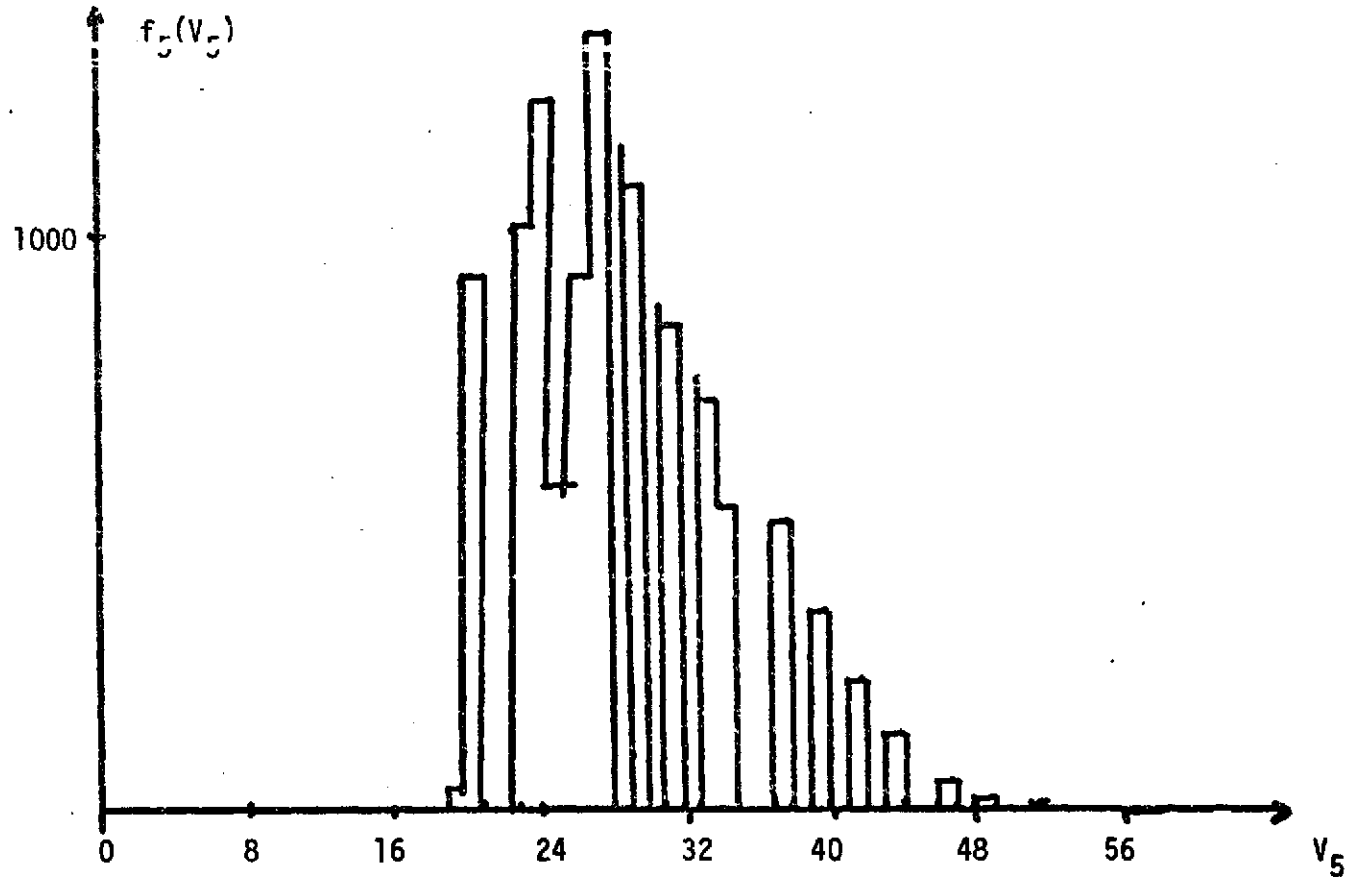

Figure A,1,6. Equalization of Sensor 5.

Appendix 2
Separation of Manmade and Natural Patterns in High Altitude Imagery to Emphasize Salt Patterns in the Earth
(A. Samulon)

An important application of high altitude photography to studies of earth resources is the determination of salinity concentration in soils of agricultural areas. The techniques of digital picture processing can be fruitfully applied to this problem. The use of high altitude imagery for salinity studies is being worked on by scientist at U.C. Davis in conjunction with the ERTS program, while at U.C. Berkelev the relevant digital processing techniques are being investigated. This progress report discusses the motivation and philosophy behind the work being done in Berkeley on this problem. Also included are some enhanced ERTS images. One area of particular interest was selected by Professor Huntington of the Soil Science Department at U.C. Davis. ERTS images of the area were enhanced. The results were then shown to Professor Huntington. By comparing the enhanced images with soil maps Professor Huntington concluded that contours of soil salinity were more easilv discernible in the enhanced images than in the original.

In the process of enhancing the images, field boundaries are located. A multispectral method for determining field boundaries has been developed and an illustration of the results is given below.

Finally, while the overall enhancement method is here applied to the problem of soil salinity determination, natural patterns such as drainage patterns can be expected to be enhanced as well, and consequently the enhancement method should be useful in a number of areas of study.

The Problem

Knowledge of the salinitv condition of the soil is important in agricultural regions because of the restrictions which salty soil puts on the tvpe of crop that can be grown. In addition the salinity of the soil in any particular location can vary over a period of several years. In irrigated areas salinity is particularly variable because of irrigation's effect on the water table and the salinitv of irrigation water itself. Since various measures can be taken to reduce the salt concentration in the soil or to prevent further increase, it is important that changes in soil salinitv be detected.

The Value of High Altitude Synoptic Imagery

In order to detect changing salt conditions, regular monitoring is necessary. For several reasons high altitude photography is especially

suited to provide the soil scientist with raw data with which he can estimate soil salinity. These include the following:

1. Determination of sizes of areas with high salt concentration to within a quarter of a square mile is sufficient for many purpose. This accuracy is well within the capability of the ERTS and Skylab sensors.

2. Saline soil reduces the vigor of plants growing in it. This reduction in vigor causes a decrease in reflectivity of the vegetation, particularly in the near infrared portion of the electromagnetic spectrum. Thus contours of salt concentration in the earth tend to show up as contours in imagery taken of the earth from above. Consequently, high altitude imagery contains information pertinent to the determination of salt concentrations.

3. High altitude photography provides the soil scientist with synoptic views of large areas. This capability is valuable because knowledge of soil salinity is required for vast areas.

4. Satellite photography of the same geographic area can be performed on a regular basis. This permits the soil scientist to observe changing patterns.

Soil Scientist's Approach to Photo Interpretation of Salt Concentrations

In general terms the method used by soil scientists to analyze high altitude imagery consists of two steps. The first is the separation of image patterns into two classes: manmade (e.g. fields), and non-manmade (e.g. contours caused by salt concentrations). In the second step, the non-manmade patterns are analyzed to see which ones indicate high soil salinity and which are due to other factors such as furrows made in bare soil by wind.

The problem of classifying non-manmade patterns is a formidable one and is based on a great many factors. Among other things the soil scientist must know something of the history and geology of the area represented in the image. Digital data processing does not seem applicable to this step.

Application of Digital Processing

Unlike subsequent steps, the first step in the analysis, the separation of manmade and non-manmade patterns, is particularly suited to digital processing. In agricultural areas the manmade patterns visible with high altitude synoptic photography are primarily fields. Depending on the crop in each field, the reflectance varies greatly from field to field. Any variations in reflectance due to non-manmade features such as salt concentration are superimposed

on the reflectance due to crops in individual fields. The variations in reflectance due to the crops tend to obscure the non-manmade patterns. By digital processing we can emphasize the non-manmade patterns and deemphasize the manmade patterns. This enhancement should very much simplify the first step in the analysis of imagery and also should be of value in the second step.

Substantial strides have been made toward the solution of the enhancement problem. A physical model of the relevant image properties and a corresponding mathematical representation have been developed and experimentally justified. A framework has been chosen by which to determine the best processing method. The optimum processing method within this framework has been mathematically derived and a near optimum method implemented using the Berkeley image processing facility. An ERTS image contining an area of interest to Professor Huntington of U.C. Davis has been enhanced and the results are favorable when compared with ground truth information. In the process a method for using multispectral information to determine field boundaries has been developed.

Figures A.2.1 and A.2.2 illustrate the results discussed above. Figure A.2.1 is taken from ERTS tape 1002-18134 reel 4 and is from spectral component MSS 4 (lines 1329 to 1585, elements 179 to 435). The region represented in the image is near Firebaugh, California. Professor Huntington of U.C. Davis has been interested in the salinity problems of this area. The grey levels in the image have been linearly extended to occupy the full range of the display monitor. Figure A.2.2 is a color composite created as follows: The image in Figure A.2.1 was displayed in blue. The edges found by the field boundary locating routine were displayed in green. The natural portion of the image, obtained by applying to the original image the near optimum processing method discussed above, was displayed in red. Not only has the detail of the natural patterns been enhanced in Figure A.2.2, but also contours can be followed across field boundaries more easily in Figure A.2.2. In particular the large trapezoidal group of fields just to the right and below the center of the image should be noted. Because the natural contribution to the original image does not contain the large variations in brightness that the manmade contribution contains, many slight variations are nearly invisible in Figure A.2.1 but appear clearly in the enhancement, Figure A.2.2.

Physical Model

The physical model explains how the reflectivity at each point on earth is related to the manmade feature and the non-manmade feature at that point. It further contains a number of assumptions about manmade patterns and non-manmade patterns. Through the use of these assumptions a method can be derived for separating the patterns

Figure A.2.1. Salt affected agricultural land near Firebaugh, California, (1002 - 18134 MSS 4)

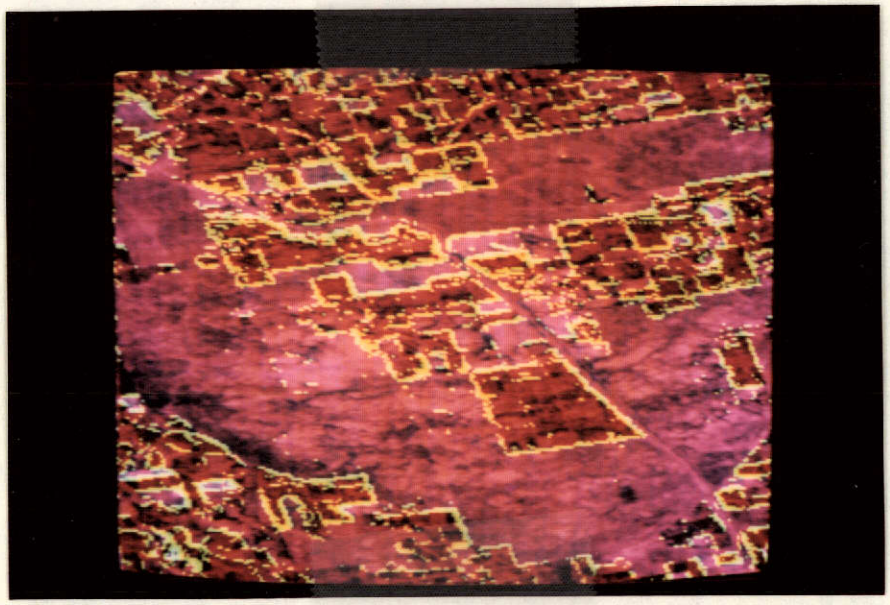

Figure A.2.2. Processed image 1002 - 18134 to enhance visibility of salt affected soils.

in an image. The main assumptions in the model are the following:

1. At the scale of synoptic high altitude photography, the primary manmade features visible in agricultural areas are the fields.

2. Over any given field, the reflectivity tends to be constant at the resolution available where it is not for non-manmade features underlying the field.

3. Soil salinity tends to be distributed with no preferred direction.

4. Soil salinity tends to vary gradually over areas of size comparable to that of a field.

5. Reflectance of a particular crop is proportional to the "vigor" of the crop. This should be interpreted as follows: Consider two different plants. The ratio of the reflectivity of the two plants is constant as long as the vigor of the two plants is equal (i.e. it is independent of the actual vigor of the plants). Preliminary experimentation indicates this assumption is sufficiently good for the purpose of separating manmade and non-manmade patterns.

Mathematical Representation

The foregoing assumptions can be represented in a mathematical form. The image is viewed as a function, $f(x,y)$, from the two dimensional spatial domain into a range of grey levels. The assumption which relates the reflectivity to the manmade and non-manmade features then can be expressed mathematically as:

$$f(x,y) = g(x,y)e(x,y) + n(x,y)$$

where g and e are non-negative, g representing the manmade component of the picture, e the non-manmade portion, and n noise in the recording and transmission process. Then

$$\log f(x,y) \cong \log g(x,y) + \log e(x,y) + \frac{n(x,y)}{g(xy,y)e(x,y)}$$

for n sufficiently small.

Let $\phi(x,y) = \log f(x,y)$
$\gamma(x,y) = \log g(x,y)$
$\theta(x,y) = \log e(x,y)$

$$\eta(x,y) = \frac{n(x,y)}{g(x,y)e(x,y)}$$

Then $$\phi(x,y) \approx \gamma(x,y) + \theta(x,y) + \eta(x,y)$$

We take as the object of the enhancement, estimation of $\theta(x,y)$ given $\gamma(x,y)$. Our approach is to find the best (in the mean square sense) linear, spatially varying, noncausal filter, h, to apply to γ. That is, our estimate, $\hat{\theta}(x,y)$, is given by

$$\hat{\theta}(x,y) = \sum_{\gamma=0}^{n-1} \sum_{\tau=0}^{n-1} h(x,y,\tau,\gamma)\gamma(\tau,\gamma)$$

where h is chosen such that $E[(\theta(x,y) - \hat{\theta}(x,y))^2]$ is minimized.

Summary and Conclusion

We have discussed the motivation behind a particular application of digital image enhancement. A model has been developed and an optimum enhancement derived. An area of interest to soil scientists has been chosen and enhancement of salinity conditions in this area has been accomplished. As an offshoot of this work, a multispectral method for finding field boundaries has been devised.

Chapter 9

USE OF ERTS-1 DATA IN THE EDUCATIONAL AND APPLIED RESEARCH PROGRAMS OF AGRICULTURAL EXTENSION (UN326)

Co-investigator: William E. Wildman

Contributors: Jack Clark, Hays Fisher, Richard Pelton, James Thayer

Department of Soils and Plant Nutrition, Agricultural Extension, Davis Campus

TABLE OF CONTENTS

9.1 INTRODUCTION

The University of California Agricultural Extension maintains educational and applied research programs in agricultural production, environmental management, home economics and nutrition, and youth development. It operates through a staff of 408 farm and home advisors in offices serving 56 of the 58 counties in California, and 165 program leaders, subject matter specialists and administrative staff located mainly at the Berkeley, Davis, and Riverside campuses of the University. The scope of activities ranges widely and is directed toward such problem areas as crop production, range management, economics, waste disposal, water quality, land use, climate, low income nutrition and money management. Before ERTS-1 was launched, it was anticipated that satellite photos might be useful in a number of ways in most of these areas. It was felt that a broad photographic view of a county's agriculture and land use patterns would prove useful in educational presentations to commodity or environmentally oriented groups. Some County Extension Directors saw in ERTS images a possibility of mapping land use or cover in remote county areas as a means of improving county general plans.

A nonfunded project was proposed and accepted in which the project leader, a soils specialist with U.C. Agricultural Extension, would receive ERTS-1 imagery of the entire state of California at quarterly intervals. This imagery would be reproduced in the Visual Aids Unit of Agricultural Extension, and distributed to the county farm advisors and statewide specialists. Training sessions would be held to educate these staff members in the fundamentals of remote sensing, and to explore with them the possible applications of ERTS-1 data to practical problems of agriculture and the environment. This report describes the educational and investigative accomplishments during the first year of ERTS-1.

The ERTS-1 investigation of the University of California Agricultural Extension has three primary aims. These are:

1. To provide reproductions of ERTS-1 Imagery for Extension staff as an aid to their educational programs, whatever they may be.

2. To train Extension personnel in the fundamentals of remote sensing and to help them in applying high, intermediate and low altitude remote sensing to their work in crop production and land management.

3. To interpret to the general public the practical significance of the ERTS-1 investigations in public meetings and displays.

Each of these aims has been accomplished to a considerable degree. A great deal more might have been done if the project leader and various county staff members had been able to spend full time studying the uses of ERTS.

About 150 Agricultural Extension workers representing all areas of the state and many crop specialties received training in the principles and applications of remote sensing in 15 one-day workshops. Another 650 agriculturally-oriented persons were directly reached in 8 public lectures by the project leader. The multiplier effect of farm advisor contacts with the public is unknown but has probably contributed significantly to the increased public awareness of the University of California's participation in the ERTS-1 program. Finally, displays of ERTS and aircraft remote sensing at two agricultural fairs and at UC-Davis' annual Picnic Day exposed large numbers of people to remote sensing as a new and useful technique.

9.2 WORK PERFORMED DURING PERIOD COVERED BY THIS REPORT.

9.2.1 Image Reproduction, Black-and-White

Our original plan was to furnish each county office with a 1:1,000,000 scale black-and-white print and a 35 mm slide of a color composite of their county for each cycle we received. We have received the entire state in two consecutive 18-day cycles each three months. In addition, for those counties in the Central Valley of California, we can furnish these same products for the cycles we do not receive by making use of the imagery received every 18 days by Co-investigator Gordon Huntington.

We have completed distribution of black-and-white 1:1,000,000 scale prints to all the counties for the imagery received through October 1972. Imagery received in January 1973 was of lesser usefulness because of cloud cover, extremely dark images (because of low sun angle) and few growing crops. For this reason, it was decided not to routinely distribute this imagery but to leave it to the counties to order it if it appeared to be useful to them. The April 1973 coverage is much better and will be reproduced as soon as it all comes through.

9.2.2 Use of Quartz Lamp to Improve Enlargements

Many of the ERTS-1 70 mm negatives have been very dense and impossible to use with ordinary enlarging equipment. We have been able to improve the quality and efficiency of making prints by use of a quartz projection lamp in our enlarger. The following paragraph written by Agricultural Extension Photographer Jack Clark describes the process.

In order to facilitate the production of black-and-white prints from ERTS negatives, a Durst S-45 enlarger was modified for an increased level of illumination. To do this, an adapter was built that would allow the use of a General Electric DVY quartz lamp in the enlarger head in place of the conventional enlarger bulb. The advantages are twofold. First, because the DVY quartz lamp has almost twice the light

output of a #302 enlarger lamp, printing times are reduced substantially. Second, because of its very small size, the quartz lamp becomes, in effect, a point-source type illumination. This results in an overall increase in definition, due mainly to increased contrast (note the graininess in Figure 9.2a). But at the same time edge sharpness, between densities that represent detail in the scene, is also enhanced. Tables 9.1 and 9.2 may be of help in interpreting Figures 9.1, 9.2a and 9.2b.

TABLE 9.1. COMPARISON OF ENLARGER LAMPS

Lamp	Wattage	Rated Lumens	Bulb Diameter (inches)
302 (conventional)	500	11,000	3-3/4
DVY (quartz)	650	20,000	7/8

TABLE 9.2. ENLARGING DATA FOR FIGURES 9.1, 9.2

Fig.	Scale	Lamp	Lens Opening	Exposure Time (seconds)	Contrast Filter
9.1	1:1,000,000	quartz	f 5.6	1-1/2	2.5
9.2a	1:250,000	quartz	f 5.6	18	2.5
9.2b	1:250,000	conventional	f 5.6	120	2.5

9.2.3 Diazochrome Color Composites

Shortly after ERTS-1 was launched, NASA announced that three color composites (simulating infrared ektachrome photography) would be available only on a limited basis by retrospective order. Due to the slow delivery time, it appeared that we should try to make our own color infrared simulations. Our visual Aids Specialist, Hays Fisher, developed a quick, inexpensive and very effective means of producing color enhancements directly from 70 mm or 9.5 inch bulk black-and-white positives. A

Figure 9.1 Image 1075-18173-5 (1:1,000,000) printed by use of the quartz lamp method.

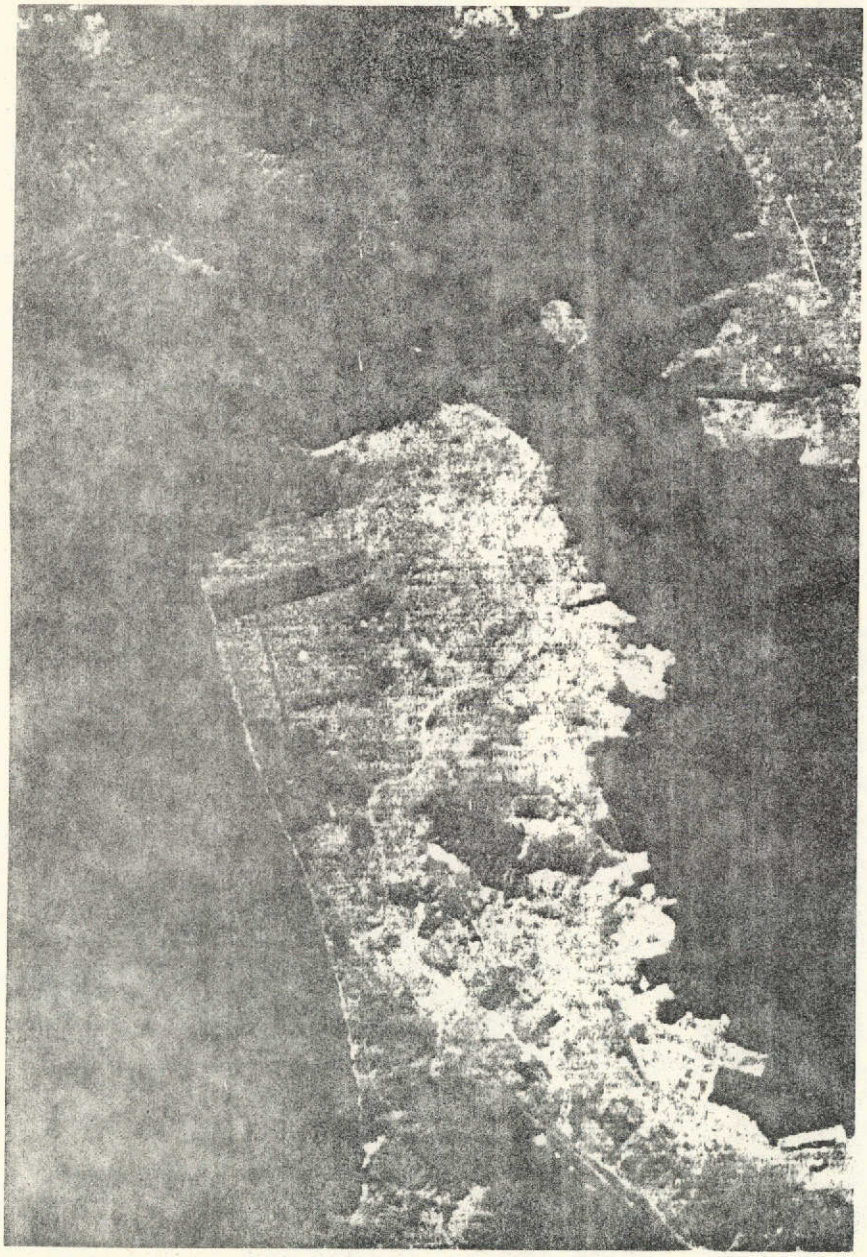

Figure 9.2a. Closeup of the San Francisco Bay area from image 1075-18173-5 (1:250,000), printed using quartz lamp.

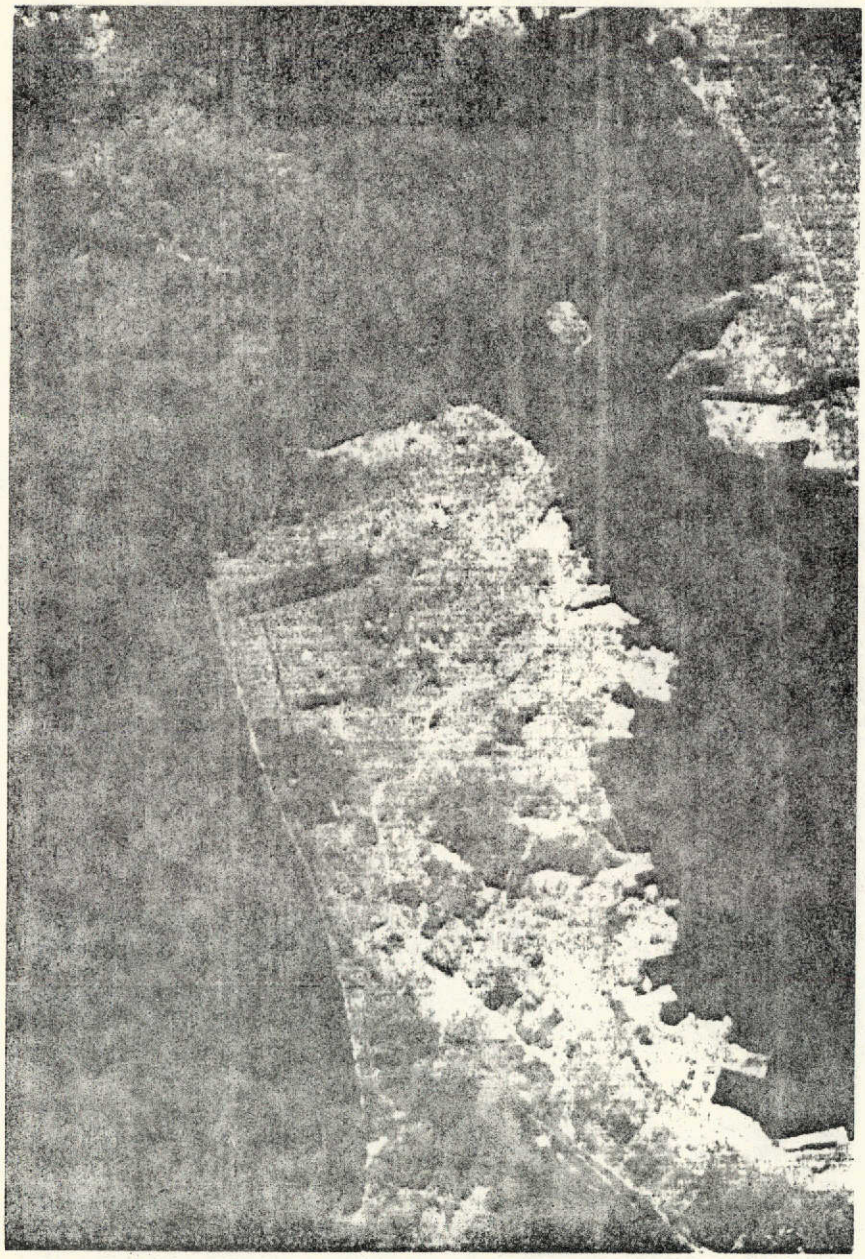

Figure 9.2b. Closeup of the San Francisco Bay area from image 1075-18173-5 (1:250,000) printed using No. 302 enlarger lamp.

diazo machine is used to make monochromatic colored positives from the green, red, and infrared wave bands, respectively. The three clear acetate positives, each in a different color, are then taped to a cardboard overhead transparency mount, in common register, to make a simulated false color infrared image. The image can then be studied directly, viewed with an overhead projector, or photographed to make slides.

A wide range of colors is available in acetate stock. For the first attempts at preparing color enhancements, we made 9.5 inch positives of yellow, magenta, cyan for the 4 (green), 5 (red), and 7 (infrared) bands of the MSS, respectively. The resulting enhancements were dull and somewhat disappointing in range of color tones discernible. Next, we tried red positives for the red band and blue for the infrared band, retaining yellow for the green band. After some experimentation to determine proper density, we arrived at settings which gave satisfactory color balance and detail. These settings allowed us to see about 10 shades on the gray scale for the red and blue positives, and 7 to 8 shades for the yellow positives.

The advantages of this color enhancement method are several. The most important is the faithfulness of reproduction of the original imagery. Since it is a contact process, much better detail is retained than in a process requiring projection. In addition, registering of the color separations is easy as long as the original transparencies register properly. (We have found one case, image 1004-18221, in which the 5 and 7 bands do not register).

The process is rapid and inexpensive. A color enhancement can be prepared in a few minutes from stock costing a few cents a sheet. Considerable flexibility in use of different colors for special false color effects is possible.

We have had some difficulty in standardizing the exposure and development times. We have found it necessary to place a voltage regulator in the line supplying the dizao machine to prevent voltage fluctuations which caused variations in exposure and development times using the same image. To get best results with our diazo machine, we have to treat each image separately, and arrive at the proper density by trial and error. Use of a densitometer on the original positives might facilitate proper exposure of the diazo sheets. In addition, more sophisticated diazo machines than our relatively inexpensive model may have better control of these factors.

Diazochrome composites have been made from good images of the whole state to use for slide making on county order. Diazochromes have also been made on special order for counties wishing to study the original composite.

Figure 9.3a is a print of a diazochrome three layer transparency made by our Visual Aids unit. Although the color balance is somewhat different, the detail compares favorably with a composite made of the same image (1004-18221) by NASA using a projection technique (see Figure 9.3b).

9.2.4 High Altitude Aircraft Imagery

We have also made 35 mm slide copies of 9 x 9" U-2 and RB-57 high altitude aircraft photos of each county. These have been distributed to county Agricultural Extension offices as examples of the imagery they can order through the EROS Data Center if they desire more detailed images for special uses. We have a catalog library from which they may request information on flights and frame numbers.

9.2.5 Aerial Photography Service for Farm Advisors

Complimentary to the ERTS-1 investigation, a low altitude aerial photography service was instituted to give farm advisors and other Extension personnel another educational tool and a means of evaluating crop growth from a more detailed perspective than offered by ERTS-1.

Four days each month Co-investigator Wildman, Visual Aids Photographer Jack Clark, and a data recorder fly a photo route covering all of California except the Owens Valley and Colorado Desert. Photo sites, previously requested on order forms by Extension personnel, are photographed using two 35 mm cameras mounted on a pistol grip frame (Figure 9.4) and activated simultaneously by a double cable release. One camera contains Ektachrome X film, the second Ektachrome Infrared. All sites are photographed using these films, and some sites in addition with Tri-X panchromatic, or black-and-white infrared film.

Individual sites vary from full sections down to plots less than one acre in size. Correspondingly, flight altitudes over sites range from 9,000 feet down to about 500 feet. Most photos are vertical shots taken with hand held cameras out the window of the Cessna 172 aircraft while in a banked attitude. An example of paired color and infrared pictures is shown in Figures 9.5a and b.

The purpose of the service is not to map large land areas but rather to be as flexible as possible in photographing particular sites of interest to the farm advisors in their educational and applied research programs. So far, the following crops and land uses have been photographed:

Oranges, grapefurit, lemons, avocados, pears, walnuts, almonds, olives, peaches, grapes, prunes;

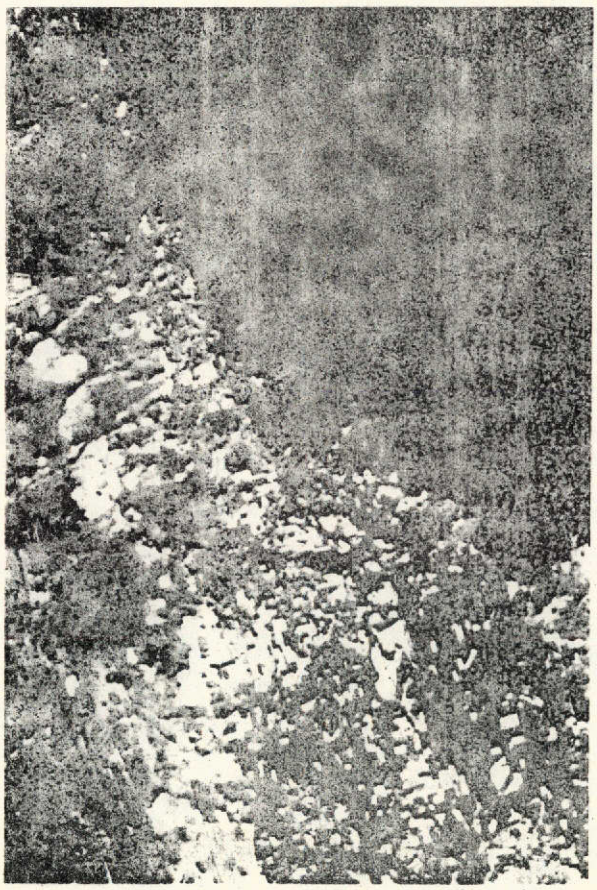

Figure 9.3a. Print made fro diazochrome three layer transparency (1004-18221) made by Agricultural Extension Visual Aids.

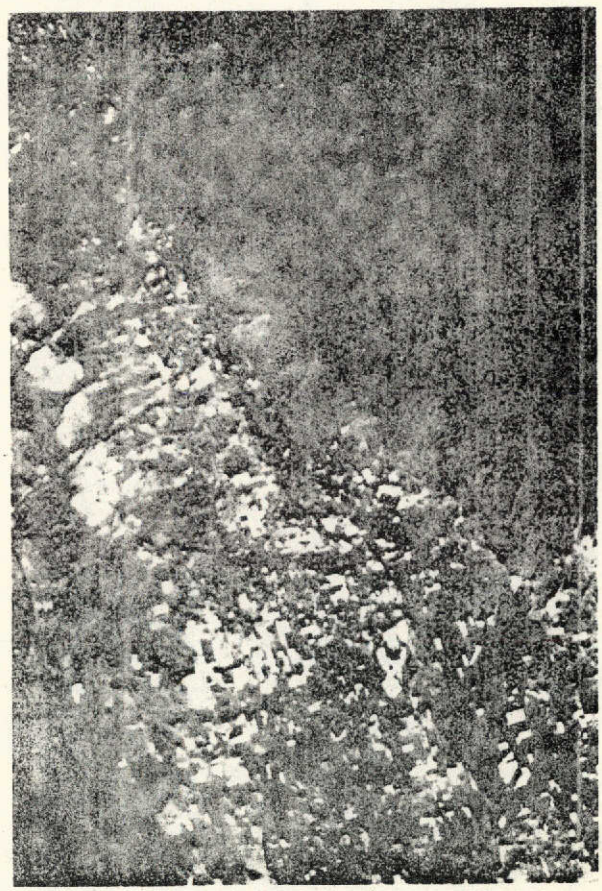

Figure 9.3b. Print made from NASA three color composite (1004-18221).

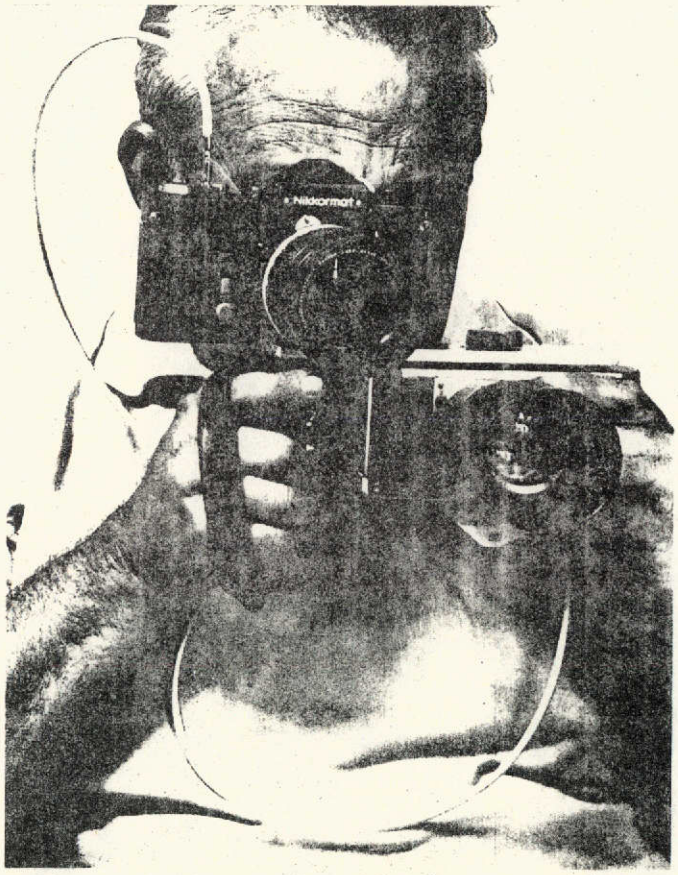

Figure 9.4. Two 35 mm cameras are mounted on a pistol grip frame with a double cable release to take simultaneous low altitude aerial photos with Ektachrome and Ektachrome Infrared film.

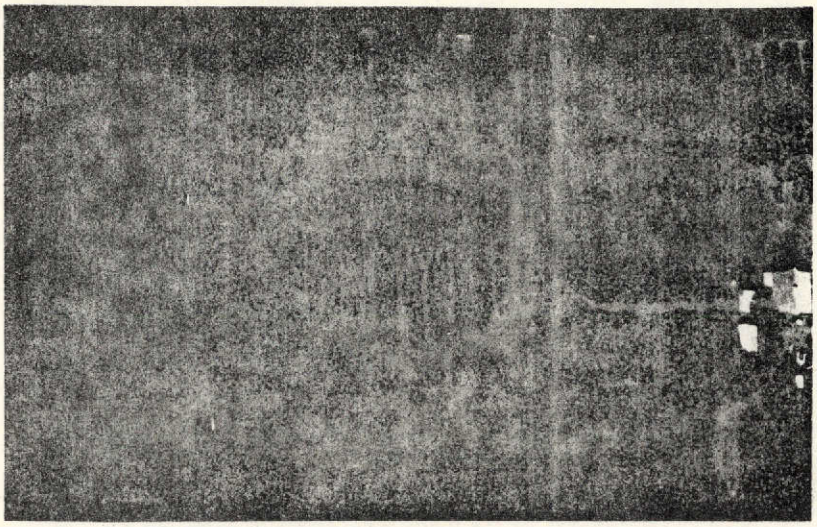

Figure 9.5a. Near vertical Ektachrome photo of almond orchard with oak root fungus infection spreading out in a widening circle. Walnut trees, more resistant to the disease, have been planted in the center as the almond trees die.

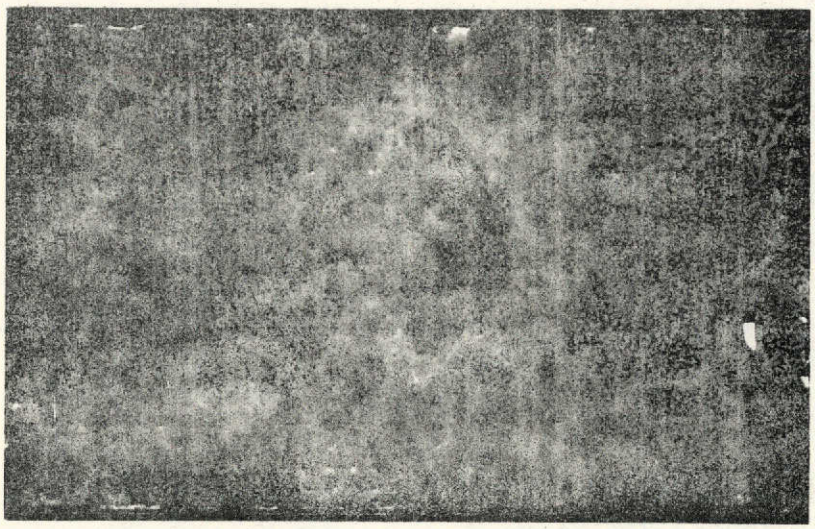

Figure 9.5b. Infrared Ektachrome photo taken simultaneously with Figure 9.5a. Weak almond trees around ring and scattered throughout orchard are much more evident than on the Ektachrome picture. Photos like these are useful not only for detection but also for Farm Advisor educational programs.

Barley, sugar beets, cotton, safflower, alfalfa, rice irrigated pasture, onions, tomatoes, beans, carrots, potatoes, corn, range fertilization, range brush conversion, timber disease, Eucalyptus freeze damage;

Central cities, high income residential areas, low income areas, nuclear power plants, industries, freeways, recreational subdivisions, airports, University field stations, dams and reservoirs, golf courses;

Erosion, water pollution, smog, geologic features, soil landscapes.

9.2.6 Remote Sensing Workshops

A series of 16 workshops was held in County Extension offices to inform Agricultural Extension personnel about the techniques and uses of remote sensing. The workshops covered the following subjects:

Energy and the Electromagnetic Spectrum
Plant Absorption and Reflectance
Visible Light
Photographic Infrared
Thermal Infrared
Optical Mechanical Scanners
The Three Sensitive Layers of Color Film
The Three Sensitive Layers of Color Infrared Film
False Color Enhancement in Multispectral Photography
Applications of Infrared Photography
Examples of Ground and Low Level Aerial Photography
Films and Filters
High Altitude Aerial Photography
ERTS-1 Sensors and Orbits
ERTS-1 Prints and Color Composites

1:1,000,000 black-and-white prints of ERTS-1 images were distributed to each county represented at a workshop. 35 mm slides of ERTS color composites and high flight photos were also distributed.

To enable Farm Advisors and Extension Specialists to quickly determine the ERTS-1 coverage and dates available, a map, a calendar, and an index were prepared. The map shows the flight lines covering California, numbered in succession from the easternmost. On the flight lines are plotted the approximate centers of the repeating images. These line up in an easterly-westerly manner and are assigned row numbers. A template is included which, when centered over a dot on a flight line, shows the approximate coverage by county on the map. Reference to the calendar shows the date when each flight line was imaged or will be imaged in the future. Application of the flight line and row number to the index gives the availability of a 9 x 9" positive of any scene in the state in

our image library. If we have the scene, the image identifier is given in the index. If we do not have the scene, but Co-investigator Gordon Huntington does, the identifier is listed in brackets, and the image is available for making prints or color composites.

Table 9.3 on the following page shows that about 1/3 of the total Agricultural Extension personnel, representing 44 of the 56 counties served, attended one of the workshops.

9.2.7 Public Presentations of ERTS-1 Images

ERTS-1 images have been used in a series of water quality meetings by Extension Soil and Water Specialist Robert Ayers to illustrate watersheds. They are much more detailed and graphic than topographic or relief maps.

ERTS-1 images have been shown in two meetings introducing new soil surveys by Extension Soils Specialist William Wildman. They have served to illustrate topographic features which account for differences in soil formation, and broad crop patterns which occur in response to differing soil types.

A description of low and high altitude remote sensing was presented to 200 growers at the annual Almond Institute in Durham in January, 1973. ERTS-1 images and close-ups of the northern Sacramento Valley were shown to illustrate rice areas in poorly drained basin soils contrasted with the orchard areas in the well drained medium-textured soils on recent alluvial fans and natural levees along the Feather River.

Another illustrated public talk was given by Co-investigator William Wildman to a group of 90 citrus growers at Corona. It was a part of the Tri-County (Riverside, Orange, Los Angeles) Citrus School under the direction of Riverside County Farm Advisor Leonard Francis. The talk was a general one on the functioning of ERTS-1 and the possible uses of data in agricultural management.

A similar lecture was given to the Kiwanis Club at Exeter, California. About 75 people were present, and the invitation to talk was through Tulare County Farm Advisor John Pehrson.

At the request of Plumas County Extension Director Arthur Scarlett, a mini version of our remote sensing workshop was presented for a small but intensely interested group including the County Planning Director and assistant, a forester for the California Division of Forestry, and a staff member of the U.C. Forestry Summer Camp. This half day session led to a full day workshop for the same group at the Forestry Remote Sensing Laboratory at Berkeley. Plumas County is in the throes of revising its general plan to cope with the onrush of recreationists

TABLE 9.3 Remote Sensing Workshops

Date	City	Counties Represented	Attendance Total	Non Extension
September				
17	Ukiah	Mendocino, Lake, Humboldt	6	1 UC Ag Field Station Staff
18	Susanville	Lassen, Plumas, Sierra	3	
20	Yuba City	Sutter, Yuba, Butte, Placer	9	
23	Woodland	Yolo, Sacramento, Solano, Glenn, UCD	11	
24	Modesto	Stanislaus, San Joaquin, Tuolumne, Calaveras, Mariposa, Merced, Amador	13	
25	Hayward	Alameda, Contra Costa, Santa Clara	4	
26	Salinas	Monterey, Santa Cruz, San Benito	14	1 Ag Commissioner
27	Redding	Shasta, Tehama, Siskiyou	6	
December				
14	Solvang	Santa Barbara, Ventura, San Luis Obispo	10	1 Cal Dept Agr
20	Bakersfield	Kern	14	4 USDA Shafter Field Station
21	Fresno	Fresno, Madera, Tulare, Kings	26	6 Cal Dept Agr
March				
12	Davis	Glenn, UC Davis	12	
20	El Centro	Imperial	10	5 USDA Brawley Field Station
21	Riverside	Riverside, Orange, Los Angeles, San Diego, San Bernardino	18	
28	Visalia	Tulare	12	
		TOTAL:	168	

which more than triples the county population in the summertime. The county is in a favored position, however, being a part of the long term remote sensing test site of the Forestry Remote Sensing Laboratory.

Another mini workshop was held for sales representatives of Occidental Chemical Company, makers of Best fertilizers. These men use ground photography to record crop appearance in various fertilizer treatments, but have not yet utilized aerial photography. They may soon, as their president wants to cut a hole in the floor of the company Piper Navajo.

TABLE 9.4. PUBLIC LECTURES BY CO-INVESTIGATOR WILDMAN

Date	City	Type of Group	Attendance
Jan. 17	Santa Maria	New Soil Report Meeting	100
26	Durham	Almond Growers Institute	200
29	Woodland	New Soil Report Meeting	150
Feb. 20	Corona	Citrus Short Course	90
23	Bakersfield	Boxwell Farming Company	5
Mar. 28	Exeter	Kiwanis Club	75
Apr. 12	Quincy	Plumas County Planning Department	5
June 25	Lathrop	Occidental Chemical Co. Fertilizer Sales Reps.	20
		TOTAL:	645

9.2.8 Public Displays at Colusa Orchard Fair and Tulare Agricultural Equipment Fair

These two fairs, held each year a week apart in February, each draw an attendance of 50 to 100 thousand agriculturally-oriented persons. Each year the University of California Agricultural Extension provides an educational program along with the exhibits of commercial interests. This year the University program at each fair was centered around a University-owned display bus. The bus has five display windows and a projection screen. Visual Aids Specialist Hays Fisher, Artist Harry Thoughton, and Communications Specialist Terry Jay Schnitter spent a great deal of time and effort to prepare the displays and the continuous slide show. The five displays were:

a. Remote Sensing -- An Important Agricultural Tool.
b. What? Eat Cotton Seed?

c. History -- A Measure of Agricultural Technological Progress.
d. Overhead Multiple-Use Sprinkler.
e. Research to "Meet" California Needs.

The remote sensing display (Figure 9.6) featured a model of the earth with an ERTS model (graciously loaned to us by General Electric Company) suspended above it. A ring of tiny light bulbs, representing an orbit across California, flashed on and off. In the upper right corner, two ERTS color infrared diazochrome composites were mounted on light boxes. One showed the Sacramento Valley (1003-18173) with a county overlay, the other the southern half of the San Joaquin Valley (1055-18062), with county overlay.

The display illustrated multistage sensing by showing suspended RB-57 and Cessna 180 aircraft, to represent high and low altitude aircraft photography. Beneath the suspended RB-57 model, light boxes illuminated color infrared U-2 and RB-57 10 x 10" photos of the Colusa area and Tulare Lake basins, respectively. Beneath the Cessna 180 model, light boxes showed low level shots comparing Ektachrome and Infrared Ektachrome of a diseased orchard for the Colusa display, and the same films showing cotton verticillium wilt test plots for the Tulare display.

In addition to the display windows, each display feature was illustrated by a four-minute slide show which was repeated each twenty minutes on the continuous projection unit. A narrative on continuous tape accompanied the slide show. The 16 slides and narrative on remote sensing illustrated the same theme -- the agricultural potential of remote sensing -- as the window display, but in greater detail. Close-ups of small portions of the aforementioned ERTS images were shown to illustrate the appearance of vineyard areas as contrasted with cotton, and rice areas contrasted with fruit and nut orchards.

No accurate estimate could be made of the number of persons who actually saw the display, but observers felt that the display bus was viewed with interest by a great many people. Local newspaper articles also called attention to the University's work in the fields of study illustrated by the displays.

The same display was removed from the bus and used as an exhibit in the Department of Soils and Plant Nutrition, U.C. Davis, during the annual Picnic Day. Out of 50,000 visitors on campus, several hundred, at least, viewed the display, and saw the accompnaying slide show.

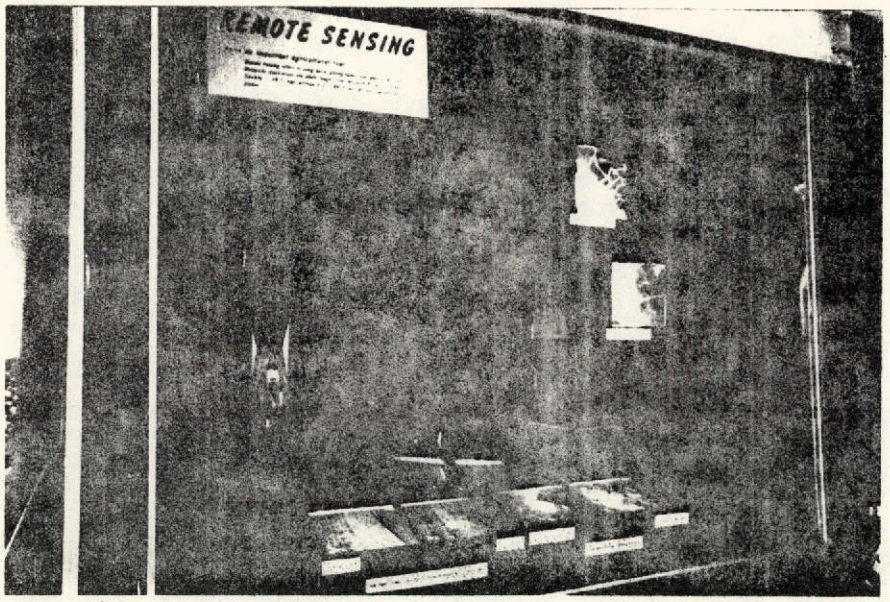

Figure 9.6. Display bus window showing ERTS model and images, along with high and low altitude aircraft photos, attracted considerable attention at both the Colusa Orchard Fair and the Tulare Agricultural Equipment Fair.

9.3 CONCLUSIONS

Our participation in the ERTS-1 investigation has resulted in increased understanding of the uses of remote sensing, not only by our own Agricultural Extension staff, but by a significant audience of the general public. We expect to continue reproducing and studying the imagery from the first year of ERTS-1. The imagery we already have will continue to provide benefits for Agricultural Extension educational programs for years to come.

Chapter 10

USE OF ERTS-1 DATA IN IDENTIFICATION, CLASSIFICATION AND MAPPING OF SALT-AFFECTED SOILS IN CALIFORNIA (UN327)

Co-Investigator: Gordon L. Huntington

Contributors: James Thayer, Eugene L. Begg, Fred W. Herbert
Jack K. Clark, William E. Wildman, Hays Fisher

Department of Soils and Plant Nutrition, Davis Campus

TABLE OF CONTENTS

10.1 INTRODUCTION

The pressure of an increasing population has brought about a diversion of much of the better land in the state from farm use to urban, suburban, or industrial use. The economics of land value under these conditions and the geography of the state have forced agriculture in many areas to move to poorer lands, including those affected by salts or alkali. In spite of this, California agriculture has continued to grow, and successful reclamation of salt-affected soils has been accomplished in many areas through the application of present knowledge.

Over 70 percent of the salt affected soils mapped in the state are located in the Great Valley of California -- the combined Sacramento and San Joaquin Valleys. A wide variety of these soils exists here under varying conditions of climate and land use. For these reasons, this centrally located region was selected for preliminary studies with ERTS-1 imagery.

Most of the salt-affected soils are located in the drier San Joaquin Valley. Very generally speaking, saline-alkali and alkali soils exist east of the axial trough of the San Joaquin Valley, while saline soils are more prevalent in the trough and on the west side of the Valley. In the Sacramento Valley, nearly all salt affected soils are west of the Valley trough and are saline-alkali in character. Extensive development of cropland in both valleys in recent years has drastically and extensively altered the concentration of salts and the character of thousands of acres of soils previously mapped as salt-affected. Examples of such areas lie in the naturally saline soils west of the Valley trough, which have been partially or wholly reclaimed within the past 30 years. In places, some of these soils are again becoming saline as a result of rising local water tables from increased irrigation on higher parts of the alluvial fans.

Over many years, soil surveys of segments of the state have laboriously gathered information concerning the nature, location, and extent of a large portion of the salt affected soils in California. However, due to the time-variable nature of these soils there is no current reliable record on the present status of saline and alkali soils in California. This has focused attention on the need for a more rapid means of inventory and evaluation of these soils for both short and long-range land use planning and management. The potential of satellite imagery as a means of extensive, periodic monitoring of these soils is being investigated in this project. ERTS-1 imagery is being used to evaluate the potential.

The object of this investigation, then, is to explore the effectiveness of ERTS-1 imagery as a means for extensively identifying and delineating salt-affected lands within California. The work entails a photo-interpretive study of imagery received for each 18 day period covering the Great Valley of California. A search is being made for distinctive patterns and tonal differences that would reliably identify imaged areas of salt-affected soils on either black-and-white transparencies or infrared color composites.

Studies to this point are encouraging, but indicate the need for at least an entire cropping season's imagery to select the best time, or times, to identify the distinctive features. The vernal period is thought to be the most sensitive period for identifying saline soils in uncultivated areas. Inconclusive results with color infrared images, thus far, suggest a lack of resolution of tonal patterns that otherwise would be useful to distinguish certain areas of salt-affected soils.

10.2 PROCEDURE

ERTS imagery in all 4 bands of the MSS was requested to cover the Great Valley throughout the year. All images as received are immediately inventoried, catalogued, and filed to be made available to other co-investigators of the University ERTS-Project. Eighteen day cycle maps showing the location and extent of coverage of each 4 band set of images are prepared and keyed by their observation ID. The 9 x 9 inches positive transparencies are used to make Diazochrome color composites, the principal imagery used in this investigation.

Intensive study has been focused on 4 selected locations known for their saline-alkali conditions.

1. Willows-Colusa region. Rice lands and game refuge areas in the westside basin lands of the central Sacramento Valley.

2. The Dozier area. Salt-affected grasslands on the westside basin rim of the lower Sacramento Valley northwest of Rio Vista and east of Travis AFB.

3. Firebaugh-Mendota region. East and westside basin rim lands and basin lands of the central San Joaquin Valley, west and northwest of Fresno.

4. Tulare Lake-Lost Hills region. Basin and basin rim lands in the southern San Joaquin Valley, northwest of Bakersfield.

Imagery taken in late summer and early fall of '72 and in late spring of '73 has been studied in the laboratory, in the field and in flight. We have compared visible features on the images with

selected aerial photography and recent soil maps of the chosen areas, and drawn upon our past experience of the surface appearances of salt-affected soils. Only a very few images between early October and late March have been useful due to the excessive cloud and/or fog cover in that part of the state. Those images which are free of clouds and fog during this period were found to be of only limited value due to darkness of the positives, presumably a function of low sun angle. During this period the greatest contrasts were found on band 7 whereas in the dry summer and fall, band 5 was the most useful for field inspections.

10.3 FINDINGS

The most notable pattern signatures of the ERTS imagery indicative of salt-affected soils are the contrasting, light colored, irregular clusters of small, barren soil areas. These are normally very characteristic of the surface appearance of alkali and saline-alkali soils as discussed in the Type I reports of this project on September 30 and November 30, 1972. The "scald spots", "slick spots", or "puff spots" are best identified on band 5 images on unreclaimed areas of salt-affected soils but they also are recognizable on partially reclaimed and cropped lands.

The scald spots are important surface features to use in determining the extent of affected areas, particularly saline-alkali soils. These spots are areas on the surface too saline or saline-alkali to support significant plant growth. On the ground, these blemishes range in diameter from 1 to 2 feet up to as much as 400 to 500 feet, occuring singly or in clusters. The limit of visibility of single blemishes or clusters on ERTS imagery is about 300 feet. In clusters, about 50 percent of the area is barren soil and the remainder is covered with sparse vegetation. Verification of these patterns on the ERTS imagery has been accomplished by low oblique photos in color and color IR, taken from approximately 5,000 feet, and on-site field investigations. The most extensive areas of these spots are observed in the basin-rim land on the east side of the San Joaquin Valley in Fresno, Merced and Madera counties.

In the Dozier area, south of Dixon and east of Travis Air Force Base, somewhat rounded, barren areas are associated with the irregular clusters. These are small playas. They range in size from less than an acre to about 80 acres and are slightly depressed areas on the landscape, seasonally collecting shallow bodies of water that evaporate eventually. On the 9 x 9 inches Diazochrome composites one large spot (approximately 80 acres) is visible without magnification and spots down to about 5 acres appear as individual entities under low power magnification.

Diazochrome infrared color composites prepared in the laboratory

and ERTS infrared color composites received on special order have been studied. To date no consistent detection has been made of reduced infrared reflectance from fields of irrigated crop plants growing in known areas of salt-affected soils in comparison to the same kinds of crops growing in soils known to be non-salt affected. As earlier reported, slight inconsistent variations in the tonal character of the infrared reflectance signatures are detectable on rice in the Sacramento Valley, but another year's imagery will be required to determine whether these variations are soil borne, or due primarily to varietal or crop maturation differences.

10.4 LIMITATIONS AND PROBLEMS

Imagery received thus far suggests the need for at least an entire cropping season or longer study of the variation in infrared reflectance from common, salt-tolerant crops growing on both salt-affected and unaffected soils. This guide line imagery is necessary for basic interpretative aids and would suggest the best time, or times, of the year to select imagery for future periodic surveys.

Under natural vegetation, the best time for detection and delineation of salt-affected soils is thought to be in the spring, near the end of the vernal period, before the natural drying of annual grasses and forbs. Correlation of ground truth information secured from low altitude flights and on-site observations with the ERTS imagery is critical during this period. It has been delayed and hampered this spring by an excessive lag period between the ERTS overpass and the actual receipt of imagery.

As stated in the Type 2 Progress Report of this project, infrared color composites from present ERTS imagery have less than the needed resolution for consistent detection of salt-affected soil patterns, particularly for those saline soils and classes of alkali or saline-alkali soils that are only affected in their subsoils or do not have scald spots. Complex patterns created by salt-affected and unaffected surface soils within very short distances constitute the basis for class differences of the soils in question. The associated vegetation reflects these conditions in its type and vigor. The variability of strong and weak infrared reflectance of such a pattern is not likely to be clearly resolved on the ERTS imagery. Seven general vegetation cover class patterns for both affected and unaffected soils have been defined. They reflect the kinds of patterns seen on the land.

1. Full cover -- healthy plants only.

2. Full cover -- healthy and stressed plants.

3. Full cover -- stressed plants only.

4. Partial cover -- healthy plants and bare ground.

5. Partial cover -- healthy plants, stressed plants, and bare ground.

6. Partial cover -- stressed plants and bare ground.

7. Barren -- bare ground only.

Geometric and random number controlled patterns have been prepared in the laboratory to resemble, on a small scale, cropping patterns such as plant settings in orchards or vineyards and diverse agricultural cropping practices. These geometric and random patterns have been applied to each of the seven vegetation cover classes. Optically degraded images of each have been prepared for comparison with areas on Diazochrome color composites in an attempt to predict the actual stressed vegetation patterns of the selected areas. At this time further study is needed to verify this procedure.

Two examples of these patterns are given in Figure 10.1. Both have about 50 percent red on blue, or vice versa. Figure 10.1(a) is one of several geometric patterns approximating open plantings in vineyards or orchards. This would be placed in vegetation cover class 4 showing only healthy plants and bare ground. Figure 10.1(b) has been defocused to simulate a lowering of resolution. Note the paler appearance of the "tree" rows. This is similar to the pale reddish appearance of most healthy orchards or vineyards observed on ERTS color infrared imagery at hand. The paler color in Figure 10.1(b) may be due in part to the effect of the thin white borders around each red square.

Figure 10.1(c) also represents a vegetation class 4 pattern, but a random one of healthy vegetation and bare ground. At lower resolution (Figure 10.1(a)) there appears to be an increase in the proportion of bare ground, and the appearance of a class 5 cover is suggested.

Mr. Samulson and Dr. Sakrison (UN 645) prepared a trial electronic enhancement of a large area of saline-alkali soils in Madera County, including lands that had been recently reclaimed and developed. Cultural patterns were tending to confound scald spot detection on the ERTS imagery. The enhancement, which deemphasized straight-line patterns, recreated an image strikingly similar to 1950 aerial photography of the same area taken long before its current stage of development. Identification of existing scald spots was improved and a better interpretive evaluation could be made of reclamation changes in the salt-affected soils.

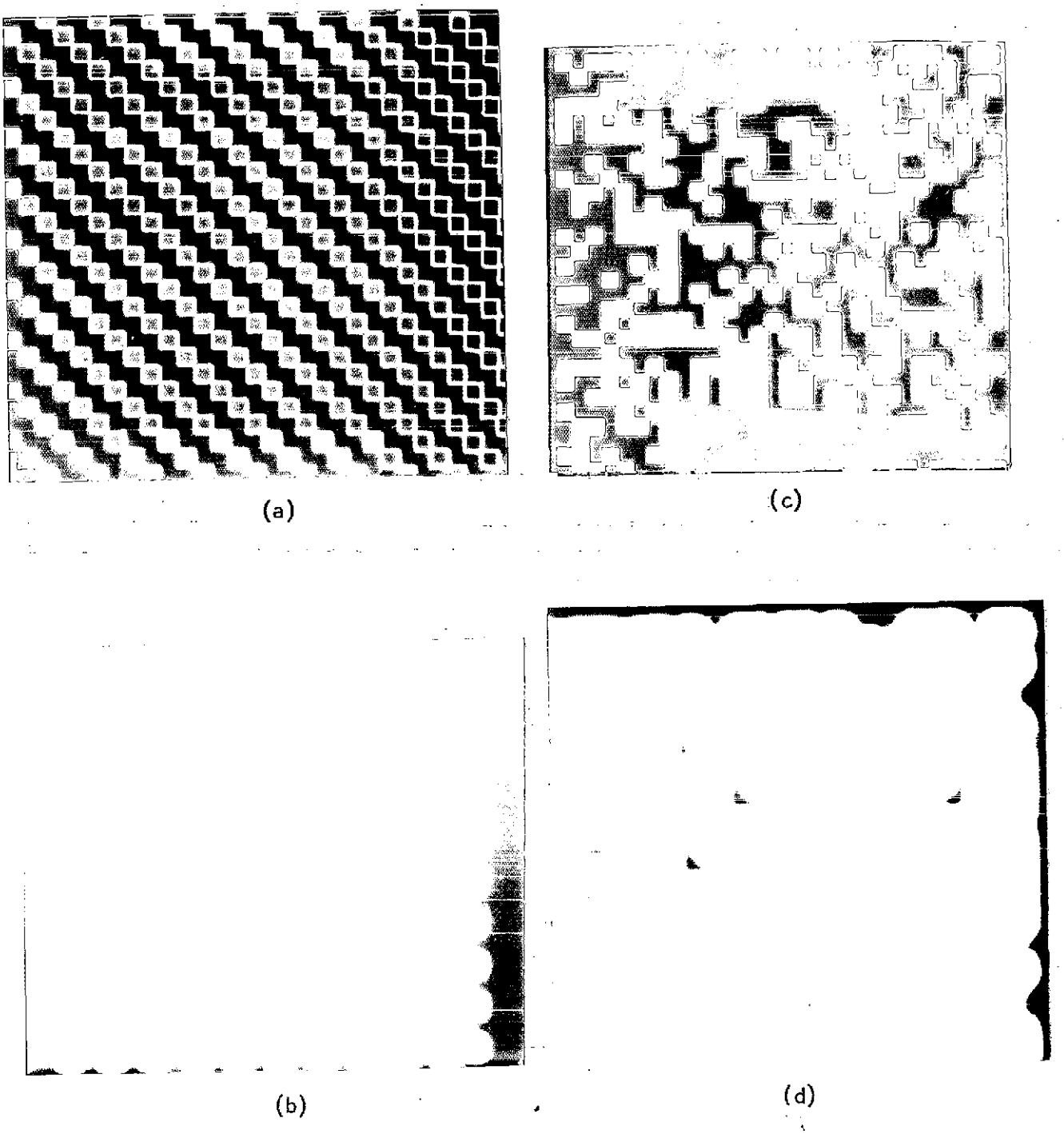

Figure 10.1. Examples of vegetation cover class patterns prepared to study the effect on color infrared imagery of complex, contrasting ground patterns with dimensions less than the limit of resolution of the imagery.

10.5 PROGRAM FOR CONTINUED STUDY

Investigations will be directed toward examination and correlation of infrared imagery from the Dozier area, Tulare Lake-Lost Hills, and the Firebaugh-Mendota regions, with ground truth information secured from natural vegetation areas during the vernal period of April and early May. With the receipt of summer imagery, attention will be redirected towards the cultivated lands of the Sacramento and San Joaquin Valleys. Through coordination with Dr. Wildman's investigation, low altitude color and color infrared photography will continue to be secured to maintain "ground truth" coverage. Laboratory studies will concentrate on further development and interpretation of the vegetation cover class patterns and development of other possible positive-negative combinations of bands 4, 5, and 7 for maximizing contrasts on Diazochrome composites.